

THESIS

Submitted to fulfil the requirements for achievement of the degree of

Doctor of the University of Strasbourg

Discipline: Life Sciences

Special Field: Plant Molecular and Cellular Biology

**Role of the *Arabidopsis* LIM proteins in the
regulation of the actin cytoskeleton
organisation and dynamics**

Jessica PAPUGA

Public PhD defense February 28th 2011

Dr. André STEINMETZ

DIRECTEUR DE THESE

Prof. Marleen VAN TROYS

RAPPORTEUR EXTERNE

Dr. Mario GIMONA

RAPPORTEUR EXTERNE

Prof. Mario KELLER

EXAMINATEUR INTERNE

Dr. Clément THOMAS

EXAMINATEUR INTERNE

Remerciements

Je tiens tout d'abord à remercier André Steinmetz pour m'avoir accueillie dans son laboratoire afin de me permettre de réaliser ma thèse dans d'excellentes conditions, aussi bien matérielles qu'humaines.

Je remercie Clément Thomas pour m'avoir supervisée tout au long des ces années. J'espère qu'il est aussi fier de moi que moi je le suis d'avoir été son apprentie.

Je remercie également Marleen Van Troys, Mario Gimona ainsi que Mario Keller pour avoir accepté de juger ce travail de thèse.

Je remercie en conséquence Christophe Ritzenthaler pour m'avoir montré la voie.

Je remercie très chaleureusement tous les membres du Laboratoire de Biologie Moléculaire Végétale du CRP-Santé (Luxembourg) :

Merci à Monika Dieterle pour ce précieux don de plantes transgéniques, sans qui, peu de choses auraient été possibles,

Merci à Céline Hoffmann pour m'avoir dévoilé les mystères de la microscopie,

Merci à Danièle Moes pour tous ses conseils, en particulier sur les cellules,

Merci à Flora Moreau pour toutes ces co-sédimentations qu'elle adore tant,

Merci à Katrin Neumann pour son aide et en particulier pour les clonages,

Merci à Stéphane Tholl pour avoir été un si bon et gentil compagnon de route,

Merci à Ning Wang pour son soutien dans les moments difficiles,

Merci à Tania Bour et WeiHong Li pour toute leur sympathie.

Au fil du temps, chacun d'entre vous est devenu bien plus qu'un collègue, un ami. Je vous suis reconnaissante pour bien plus de choses que les quelques phrases énumérées ci-dessus et je ne saurai dire d'autre que : merci, Danke schön, thank you, xièxie !

Je remercie tout particulièrement Natacha Ralainirina pour son amitié et son soutien incommensurable.

Je remercie ma petite Fredo pour toutes ces années inoubliables ainsi que Céline Charlot pour ces discussions interminables.

Je remercie également mes compagnons du bureau flexible : Stéphanie Kler pour ses précieux conseils concernant le magnésium, Maud Thérésine pour son magnifique pull yoda-like et « dans l'absolu » Delphine Lentz pour ses « à priori ».

Je remercie aussi toutes les belles rencontres que j'ai pu faire tout au long de cette thèse : Kamel Hammani, Emmanuel Boutant, Christina Hoffmann, Nadia Beaupain, Sabrina Gatti, Christelle Ghoneim, Nathalie Nicot, et tout ceux que je ne nomme pas.

Finalement, je remercie mes parents pour leur soutien tout au long de ces années. Olivier, Aurélie et tout particulièrement Sébastien pour avoir réussi à me supporter pendant tout ce temps !

J'ajouterai simplement qu'être ou ne pas être, telle est la question sinusoïdale de l'anachorète hypochondriaque...

Table of contents

Table of content

Abbreviations

Chapter 1: From the Actin Cytoskeleton to the Plant LIM Proteins

Introduction	1
From the Actin Cytoskeleton to the Plant LIM Proteins	2
I. Generalities	2
II. Actin cytoskeleton organisation and dynamics in plant cells	3
1. Structure and assembly of the actin filaments	3
1.1. Actin monomers	3
1.2. Assembly of actin filaments	4
2. Regulation of the actin cytoskeleton organisation and dynamics by actin-binding proteins (ABPs)	5
III. Actin bundling in plants	9
1. Review article "Actin-Bundling in Plants"	10
2. Last developments in plant actin-bundling	29
IV. Plant LIM proteins	31
1. Generalities	31
2. Two differentially expressed subfamilies of plant <i>LIM</i> genes	32
3. Subcellular localisation of LIM proteins	33
4. Nuclear functions of plant LIMs	34
5. Cytoplasmic functions of plant LIMs	35

Chapter 2: Comparative study of the actin cytoskeleton regulatory activities of the *Arabidopsis* LIM protein family members

37

I. Introduction	37
II. The six <i>Arabidopsis</i> LIMs are actin-binding proteins	38
1. Production and characterisation of GFP-fused LIM expressing <i>Arabidopsis</i> lines	38
2. Subcellular localisation of GFP-fused LIMs	40
2.1 GFP-fused LIMs interact with a filamentous network	

resembling the actin cytoskeleton	40
2.2. GFP-fused LIMs interact with the actin cytoskeleton	41
3. <i>Arabidopsis</i> LIMs interact with actin filaments in a direct manner	42
III. Characterisation of <i>Arabidopsis</i> LIM actin-regulatory activities	43
1. <i>Arabidopsis</i> LIMs stabilise the actin cytoskeleton	43
1.1. <i>Arabidopsis</i> LIMs stabilise the actin filaments <i>in vitro</i>	43
1.2. <i>Arabidopsis</i> LIMs protect the actin cytoskeleton against latrunculin-B induced depolymerisation	44
2. <i>Arabidopsis</i> LIMs are actin-bundling proteins	45
2.1. <i>Arabidopsis</i> LIMs crosslink actin filaments into higher-order structures <i>in vitro</i>	45
2.2. <i>Arabidopsis</i> LIMs crosslink actin filaments into bundles <i>in vitro</i>	46
2.3. <i>Arabidopsis</i> LIMs increase the cellular level of actin bundling	46
IV. Discussion	47

Chapter 3: Regulation of *Arabidopsis* WLIM1 and PLIM2c activities by pH and Ca²⁺

by pH and Ca²⁺	52
I. Introduction	52
II. Differential regulation of WLIM1 and PLIM2c activities by pH and Ca ²⁺	53
1. Actin filament stabilisation by WLIM1 and PLIM2c at different pH and [Ca ²⁺]	53
2. Actin filament bundling by WLIM1 and PLIM2c at different pH and [Ca ²⁺]	54
III. <i>In vivo</i> pH- and Ca ²⁺ -dependent regulation of WLIM1 and PLIM2c activities	55
1. Subcellular localisation of WLIM1 and PLIM2c in <i>Arabidopsis</i> cells submitted to artificially induced modification of pH _{cyt}	55
1.1. Design and validation of the experimental procedure to modify the cytoplasmic pH in <i>Arabidopsis</i> cells	56
1.2. An increase in pH _{cyt} specifically inhibits the binding of GFP-PLIM2c to actin filaments	57
2. Subcellular localisation of WLIM1 and PLIM2c in <i>Arabidopsis</i> cells submitted to artificially induced modification of [Ca ²⁺] _{cyt}	59
2.1. Design and validation of the experimental procedure to modify the cytoplasmic calcium concentration of <i>Arabidopsis</i> cell	59
2.2. An increase in [Ca ²⁺] _{cyt} inhibits the binding of both	

GFP-PLIM2c and GFP-WLIM1 to actin filaments	60
3. Subcellular localisation of GFP-PLIM2c and GFP-WLIM1 in lily growing pollen tubes	61
IV. <i>Arabidopsis</i> LIM C-terminal domain is involved in the direct responsiveness of PLIM activities to pH and Ca ²⁺	63
V. Discussion	65
Chapter 4: Conclusions and Perspectives	70
Chapter 5: Materials and Methods	72
Chapter 6: References	86
Chapter 7: Appendix	
I. Publications	
1. Publication 1	103
2. Publication 2	121
II. Detailed summary (in french)	123

Abbreviations

ABD2: fimbrin-derived actin-binding domain 2

ABP: actin-binding protein

ADF: actin depolymerising factor

ADP: adenosine diphosphate

AM: acetoxymethyl ester

Arabidopsis: *Arabidopsis thaliana*

AtCP: *Arabidopsis thaliana* capping protein

AtFH: *Arabidopsis thaliana* formin

AtFIM: *Arabidopsis thaliana* fimbrin

ATP: adenosine triphosphate

AtVLN: *Arabidopsis thaliana* villin

BAPTA: O,O'-bis(2-aminophenyl) ethyleneglycol-N,N,N',N'-tetraacetic acid tetraacetoxymethyl ester

BY-2: bright yellow-2

Ca²⁺: calcium

[Ca²⁺]: calcium concentration

[Ca²⁺]_{cyt}: cytoplasmic calcium concentration

CaMV: cauliflower mosaic virus

CAP1: adenylate cyclase-associated protein

CPA: cyclopiazonic acid

CPDK: calmodulin-like domain protein kinase

CRP: cysteine-rich protein

DNA: deoxyribonucleic acid

EST: expressed sequence tag

F-actin: filamentous actin

FCFAC: fraction of cytoplasmic fluorescence associated with the cytoskeleton

FH1: formin homology domain 1

FRAP: fluorescence recovery after photobleaching

G-actin: globular actin

GFP: green fluorescent protein

IBMP: institute of plant molecular biology (institut de biologie moléculaire des plantes)

Kd: dissociation constant

kDa: kilodalton

μ M: micromolar

μ m: micrometre

MLP: muscle LIM protein

mM: millimolar

mRNA: messenger RNA

nm: nanometre

nM: nanomolar

NMR: nuclear magnetic resonance

NtWLIM1: *Nicotiana tabacum* WLIM1

lily: *Lilium longiflorum*

LIM: LIN-11, ISL-1, MEC-3

pH_{cyt}: cytoplasmic pH

Plant LIMs: plant two LIM domain-containing proteins

PLIM: pollen LIM

PMB: pH-modifying buffer

PRF: profilin

pZM13: *Zea mays* pollen specific promoter

R_{FCFAC}: ratios of FCFACs

RNA: ribonucleic acid

RING: really interesting new gene

SDS-PAGE: sodium dodecyl sulfate polyacrylamide gel electrophoresis

SNARF5F: SNARF®-5F 5-(and-6)-carboxylic acid, acetoxymethyl ester

TIRF: total internal reflection fluorescence

WLIM: widely expressed LIM

Chapter 1

From the Actin Cytoskeleton
to the Plant LIM Proteins

Introduction

The Plant Molecular Biology laboratory focuses on evolutionary conserved proteins involved in the regulation of actin cytoskeleton organisation and dynamics. It has recently reported the existence of a novel tobacco actin-binding protein, namely NtWLIM1, which promotes the crosslinking of actin filaments into bundles, a major higher-order cytoskeletal structure (Thomas et al., 2006, 2007, 2008). NtWLIM1 belongs to a multi-member family of 200 amino acid-long LIM domain-containing proteins (LIMs) characterised by two LIM domains separated by a long interLIM spacer. Using a domain analysis, the plant molecular biology laboratory has established that both LIM domains of NtWLIM1 function as autonomous actin-binding and actin-bundling modules (Thomas et al., 2007, 2008). Since the LIM domain sequence is relatively well conserved among LIM family members, it is possible that some, possibly all LIMs, other than NtWLIM1 display actin-binding and -bundling activities and contribute to control the actin cytoskeleton organisation and dynamics. During my PhD thesis, I have addressed this possibility by investigating the actin-regulatory activities as well as the modes of regulation of the LIM family members of the model plant *Arabidopsis*. By combining *in vitro* biochemical and *in vivo* analyses, I provide strong evidence that plant LIMs define a ubiquitous family of actin-bundling proteins, with however varying activity levels and responsiveness to important cellular factors such as pH and calcium.

By surveying information regarding the functions and the regulation of the actin cytoskeleton in plants, **chapter 1** provides a comprehensible introduction of my PhD work. Particular attention is given to actin bundling and to the previous functional studies conducted on plant LIMs. This chapter includes a review article which has been published in 2009.

Chapter 2 focuses on the analysis of the actin-regulatory activities of *Arabidopsis* LIM proteins. Both ectopic/overexpression studies in transgenic plants and a series of biochemical assays provide evidence that all the six *Arabidopsis* LIM protein family members bind to, stabilise and bundle actin filaments with however different efficiencies.

Chapter 3 is dedicated to the study of the regulation of *Arabidopsis* LIM protein activities by pH and calcium. It particularly focuses on one member of the two differentially-expressed subfamilies of LIM proteins, i.e. the widely-expressed WLIM1 protein and the pollen-specific PLIM2c protein. It also includes a domain analysis aimed at characterising the regulatory domain of LIM proteins.

Both chapters 2 and 3 include a specific discussion section, **Chapter 4** presents a conclusion as well as a number of perspectives opened by this work.

A significant part of the data described in chapters 2 and 3 has been published “*Arabidopsis* LIM proteins: a family of actin bundlers with distinct expression patterns and modes of regulation.” *Plant Cell* **22**, 3034-3052. The article has been included in the **Appendix** section.

From the Actin Cytoskeleton to the Plant LIM Proteins

I. Generalities

Contrary to the historical view which first considered the cytoskeleton as a rigid structure, decades of research have revealed that it is actually a very dynamic structure that is subjected to continuous remodelling. The actin cytoskeleton basically comprises three types of polymers: the thin actin filaments, the intermediate filaments which can assemble from various types of proteins, e.g. keratins, vimentins, lamins, and the thick microtubules. According to their name, the average diameter of these polymers is 7-9 nm, 10 nm and 24 nm. Actin filaments and microtubules are both critical for a variety of cellular processes, including cell division, intracellular transport, motility, contractility, maintenance of cell architecture, cell expansion, response to environmental stimuli and pathogen attack. Although the roles of intermediate filaments remain relatively poorly understood in plants, they are generally assumed to predominantly display structural roles. (e.g. Dawson et al., 1985; Parke et al., 1987; Hargreaves et al., 1989; Blumenthal et al., 2004).

In animal cells, actin filament-myosin interactions power cell division, cell contraction, and cell migration. Actin filament polymerisation itself is used as a

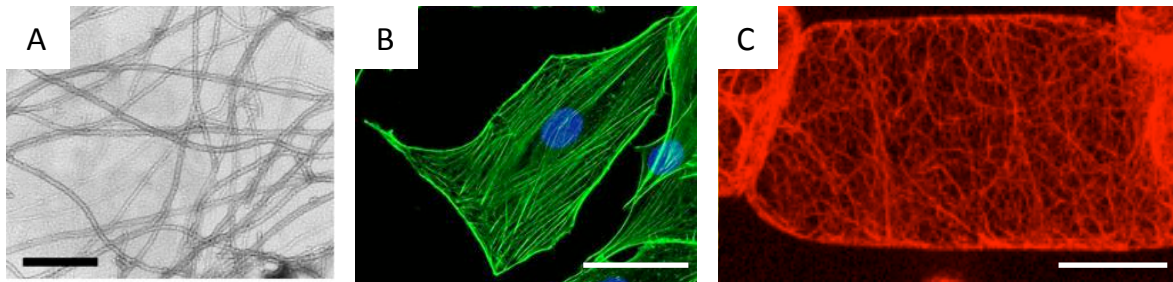


Figure 1: Actin filaments and the actin cytoskeleton in a vertebrate and a plant cells.

(A) Electron micrograph of *in vitro* polymerised actin filaments (4 μM , from Thomas et al., 2007). Bar = 70 nm.

(B) Actin cytoskeleton of human glioblastoma cells (U87) labelled with AlexaFluor 488-phalloidin . The nucleus is stained in blue with DAPI. Bar = 50 μm

(C) Actin cytoskeleton of tobacco BY-2 cells with labelled rhodamine-phalloidin.
Bar = 20 μm .

driving force that directs the growth of membrane protrusions and enables cells to alter their shape and to move. In plant cells, actin filaments are essential for the establishment and maintenance of cell polarity (Vidali and Hepler, 2001) as well as for the formation of plant-specific cytoskeletal structures, such as the phragmoplast and the preprophase band (e.g. Schmit, 2000). In addition to its direct functions, the actin cytoskeleton is a key target of many signalling events and acts itself as a transducer of signals in both animal and plant cells (Drobak et al., 2004). Actin filaments cooperate with microtubules via microtubule-associated proteins during the transport of vesicles and organelles as recently reviewed by Petrasek and Schwarzerova (2009) and Deeks et al. (2010). The following sections focus on the plant actin cytoskeleton (Figure 1) and its regulation by actin-binding proteins (ABPs), with particular regard to actin-bundling and plant LIM proteins.

II. Actin cytoskeleton organisation and dynamics in plant cells

1. Structure and assembly of the actin filaments

1.1. Actin monomers

Actin is one of the most conserved and abundant proteins in eukaryotes. Plant actins comprise 376 to 377 amino acid residues and exhibit a high degree of identity with actins of other kingdoms. For instance, plant actin isoforms are 83-88% identical to actins from green algae, other types of protists, fungi, and animals. In *Arabidopsis*, 10 actin gene sequences have been characterised (McDowell et al., 1996). At least eight of these *actin* genes are functional and are strongly expressed at specific time and place during plant development (An et al., 1996a, 1996b; Huang et al., 1996a, 1997; McDowell et al., 1996). Based on their distinct temporal and spatial expression patterns, the *Arabidopsis* actin genes can be basically divided into vegetative and reproductive classes (McDowell et al., 1996b; Meagher et al., 1999).

Monomeric actin is an asymmetric globular polypeptide of 42 kDa composed of four sub-domains, historically named Ia, IIa, Ib and IIb, each displaying a repeating motif comprising a multi-stranded β -sheet, a β -meander and a right-handed $\beta\alpha\beta$ unit

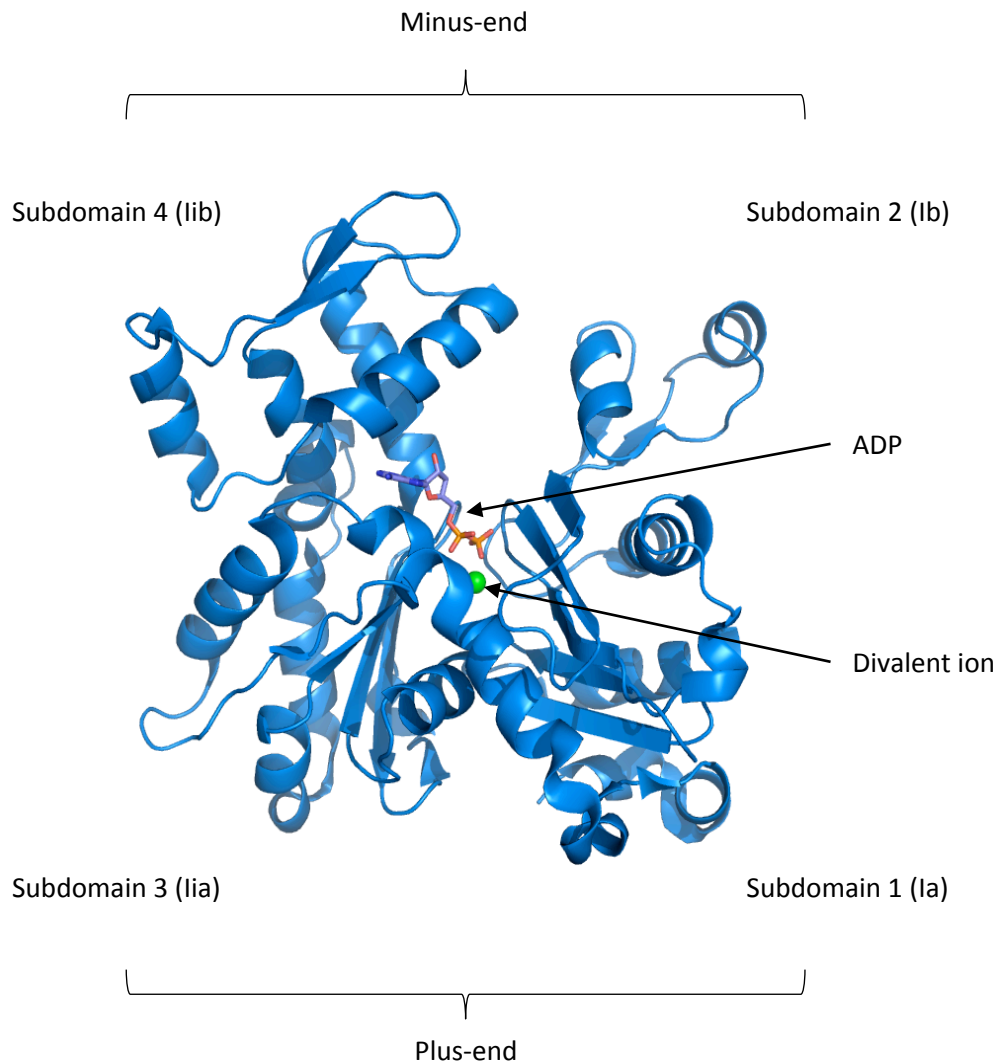


Figure 2: Structure of the actin monomer.

Subdomains 2 and 4 form the slow growing minus-end (pointed-end) and subdomains 1 and 3 form the fast growing plus-end (barbed-end). ADP and divalent cation are shown in the centre of the structure. The view has been processed using PyMol (DeLano, W.L. The PyMOL Molecular Graphics System (2002) DeLano Scientific, San Carlos, USA).

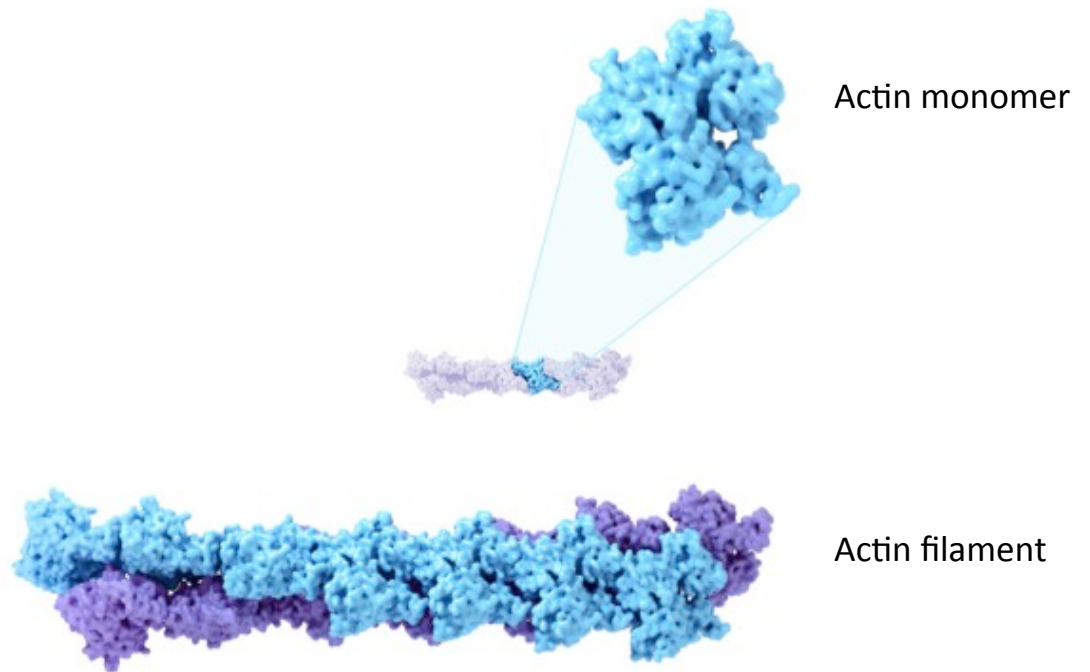


Figure 3: The double actin filament helix.

Representation of an actin filament (bottom panel) organised into a double helix by the association of actin monomers (top panel). Adapted from U.S. National Library of Medicine.

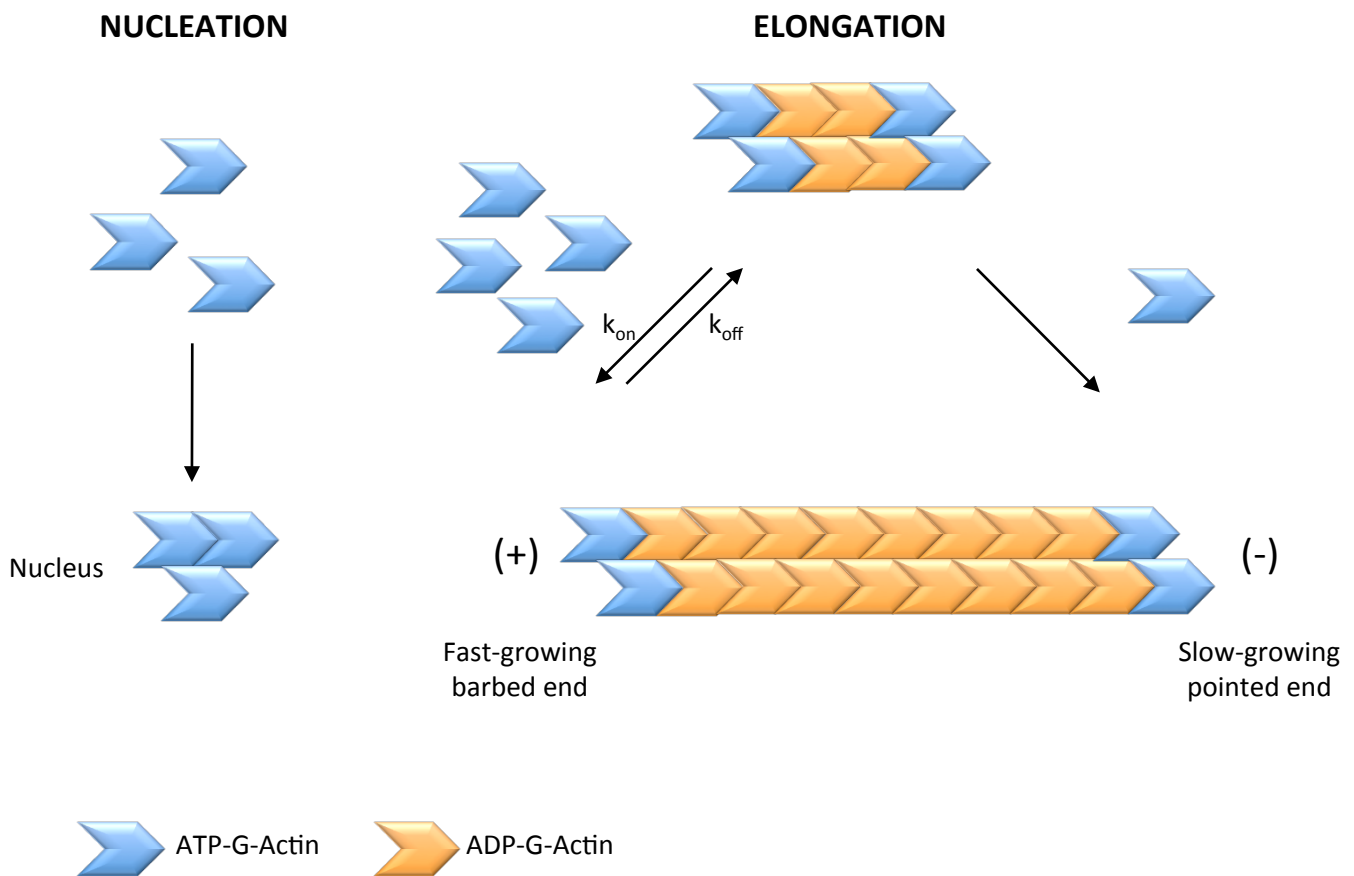


Figure 4: Basic principles of actin polymerisation.

Nucleation is the rate-limiting step of actin filament polymerisation. Fast growing plus-end (barbed-end) and a slow growing minus-end (pointed-end) are indicated. Association and dissociation of ATP-G-actin at each filament end depend on the respective association (k_{on}) and dissociation (k_{off}) constants.

(Figure 2; Sheterline et al., 1998). Sub-domains are organised around a deep cleft that contains the nucleotide- (ATP or ADP) and divalent cation- (Mg^{2+} or Ca^{2+}) binding sites (Kabsch et al., 1990). The nucleotide-binding site is usually occupied by ATP or ADP-Pi rather than ADP, which binds with lower affinity to both Mg^{2+} - and Ca^{2+} -G-actin (Kinosian et al., 1993; dos Remedios et al., 2003). *In vitro* ATP-G-actin subunits can spontaneously polymerise to generate actin filaments or F-actin.

Actin filaments are organised into a double helix with a right-handed helical twist (Figure 3; Holmes et al., 1990). Each twist is composed of 13 subunits (Oda et al., 2009, Holmes et al., 2009). Actin filaments exhibit polarity with a fast growing plus- (+) end also termed barbed-end, and a slow growing minus- (-) end, also termed pointed-end (Figure 4; Casella et al., 1981; Fox and Phillips, 1981; Tellam and Frieden, 1982; Yahara et al., 1982; Symons and Mitchison, 1991; Redmond et al., 1994).

1.2. Assembly of actin filaments

Assembly of actin filaments or polymerisation is a two-step process including actin nucleation and actin filament elongation. Nucleation, which is the rate-limiting step of actin polymerisation, itself can be subdivided into two stages: 1) the slow formation of actin dimers, which is a unfavourable reaction, i.e. actin dimers tend to rapidly dissociate into monomers rather than to further polymerise and, 2) the formation of stable actin trimers or nuclei which more readily continue to assemble into filaments. Within the cell, actin nucleation is facilitated by the so-called actin nucleators (see below). Basically, nucleation is the mechanism by which the cell can control the spatial and temporal assembly of actin filaments. The subsequent actin filament elongation step consists in the rapid assembly of actin monomers (Figure 4). *In vitro*, spontaneous polymerisation highly depends on ionic strength, pH, concentration of Mg^{2+} and Ca^{2+} , and temperature. When the ionic strength reaches a value close to the physiological one (100-150 mM KCl), Ca^{2+} substitutes Mg^{2+} within the actin monomer, giving rise to the so-called activated actin monomer. Elongation consists itself in the addition of ATP-bound G-actin subunits to both ends of the nucleus. As previously stated, the addition of actin monomers occurs more rapidly at the plus-ends than at the minus-ends. Once incorporated into a growing actin filament,

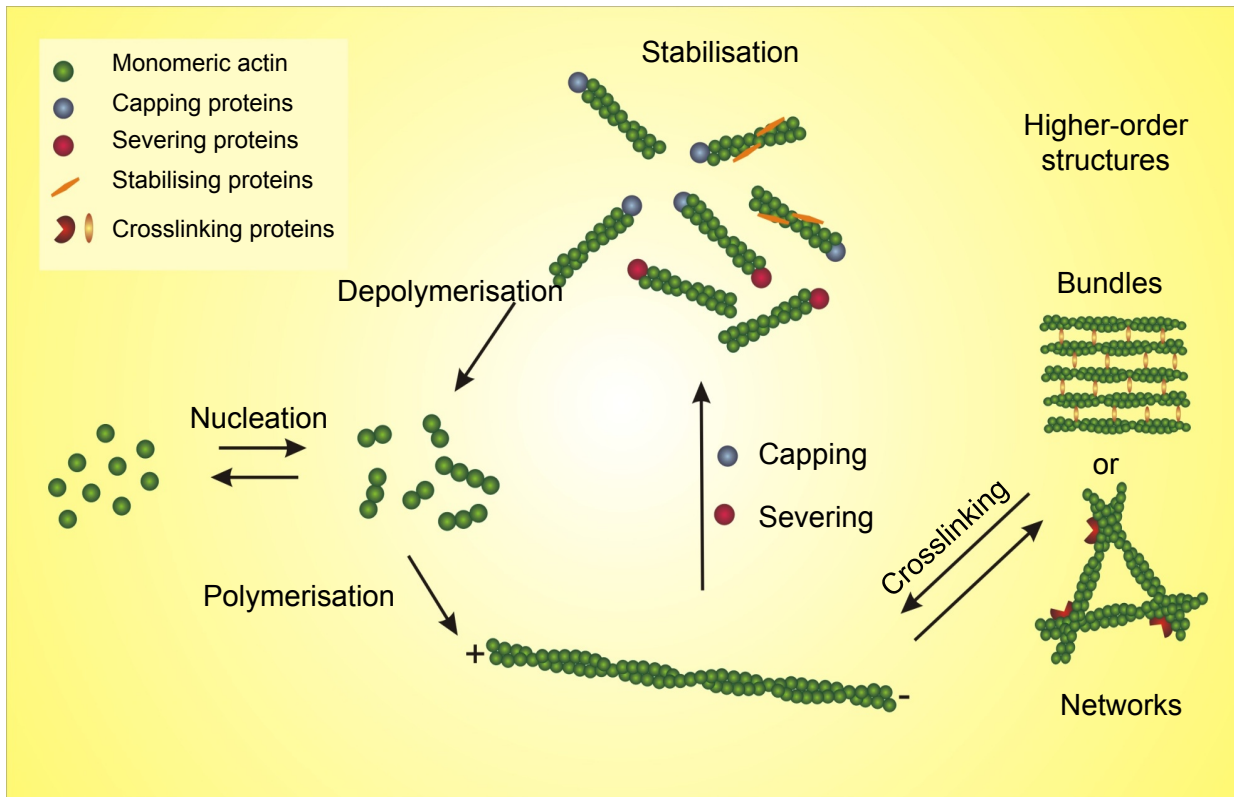


Figure 5: Regulation of the actin cytoskeleton organisation and dynamics by actin-binding proteins.

Schematic representation of the different types of processes regulated by actin-binding proteins (adapted from Winder and Ayscough, 2005).

ATP is hydrolysed into ADP generating ADP-actin subunits (Carlier and Pantaloni, 1997; Pollard and Cooper, 1986). Importantly, ATP hydrolysis is not temporally coupled with monomer incorporation and a lag phase has been clearly characterised (Korn, 1987). The incorporation and dissociation of monomers are respectively governed by the association and dissociation constants: k_{on} and k_{off} . These constants are not equivalent at both filament ends, the latter exhibiting different critical concentrations (Pollard et al., 1986). The critical concentration of one actin filament end is defined as the concentration of G-actin at which polymerisation occurs. When the addition of monomers at the plus-end is exactly balanced by the dissociation of monomers at the minus-end actin filaments seem not to grow and a dynamic steady-state equilibrium named “treadmilling” is established (Wegner, 1982; Korn, 1987; Pantaloni et al., 2001; Bugyi and Carlier, 2010; Guo et al., 2010, Staiger et al., 2010).

2. Regulation of actin cytoskeleton organisation and dynamics by actin-binding proteins (ABPs)

In vivo, the regulation of actin cytoskeleton organisation and dynamics is orchestrated by a plethora of actin-binding proteins (Figure 5). Monomer-binding proteins, e.g. profilin, primarily regulate both the size and activity of the actin subunit pool by sequestering and preventing actin polymerisation or, on the contrary, by activating actin monomers. As previously stated, nucleation is the rate limiting step of actin polymerisation. Proteins able to promote or enhance actin nucleation are termed nucleators, e.g. formins and the Arp2/3 complex. Capping proteins, such as the capping protein CP, bind to one filament end and prevent the addition or the release of subunits. Actin filament depolymerising proteins, such as ADF, promote the conversion of filamentous actin into actin monomers. Actin filament severing proteins, such as certain villins or ADFs, sever actin filaments to increase the depolymerisation rate or, inversely, to increase the number of filament ends that are competent for depolymerisation. Finally, crosslinking proteins, e.g. villins or LIM proteins, promote the assembly of higher-order structures such as orthogonal networks of filaments or actin bundles. Several examples of central plant ABP families are presented in details below.

Profilins are small, approximately 12-15 kDa, proteins exhibiting a high affinity for ATP-G-actin resulting in the formation of profilin-actin complexes (Valenta et al., 1993; Gibbon et al., 1998). Plant genomes encode several, relatively divergent profilin isoforms (Staiger et al., 1993; Vrtala et al., 1996; Kovar et al., 2000; Kandasamy et al., 2002, 2007). For instance, *Arabidopsis* possesses five profilin isoforms which are differentially expressed in plant organs and tissues. Two isoforms are abundantly expressed in floral tissues and pollen (class I) whereas the three remaining isoforms are expressed in vegetative tissues (class II; Gibbon et al., 1997; Kovar et al., 2000; Kandasamy et al., 2002). Levels of profilin expression in pollen have been estimated to be equal to those of total actin (Vidali and Heple, 1997; Gibbon et al., 1999; Snowman et al., 2002). Therefore, it has been proposed that most of pollen actin is bound to profilin (Gibbon et al., 1999; Snowman et al., 2002; Staiger and Blanchoin, 2006). Profilins sequester G-actin to prevent the spontaneous nucleation and suppress the addition of actin monomers at the minus-end of actin filaments. Additional roles have been suggested for animal profilins such as recharging ADP-G-actin with ATP but no similar activity has been reported for plant profilins so far. Wang et al. (2009) recently characterised and compared the *in vitro* and *in vivo* activities of *Arabidopsis* PRF1 and PRF2. Biochemical analyses revealed that PRF1 has higher affinity for both poly-L-proline and G-actin compared to PRF2. In addition, observations of living cells in stable transgenic *Arabidopsis* lines revealed that 35S::GFP-PRF1 formed a filamentous network, while 35S::GFP-PRF2 formed polygonal meshes which likely correspond to endoplasmic reticulum. Together these data suggest that all plant profilins are functionally equivalent.

The **adenylate cyclase-associated protein (CAP1)** is another abundant plant actin monomer-binding protein. Contrary to profilins, CAP1 only exhibits a moderate G-actin-binding activity (Chaundry et al., 2007; Deeks et al., 2007) and binds equally to ATP-G-actin and ADP-G-actin. Chaundry et al. (2007) identified AtCAP1 as the first nucleotide exchange factor for plant actin. CAP1 has been suggested to play an important role in the regulation of actin organisation and dynamics in tip-growing cells (Deeks et al., 2007). Indeed, knockout *Arabidopsis* mutants lack normal actin bundles in root hairs and displays defects in pollen germination and tube growth. The

underlying molecular mechanisms remain unclear.

The seven-subunit **Arp2/3 complex** is an evolutionary highly conserved actin nucleator that has been found in all eukaryotes including plants (Machesky and Gould, 1999; Deeks and Hussey, 2005). The complex is composed of two actin-related proteins (Arp2 and Arp3) and five other subunits (Pollard and Beltzner, 2002). The Arp2/3 complex attaches to the flanks of existing filaments and initiates a new F-actin branch at an angle of 70° relative to the parent filament (Mullins et al., 1998; Blanchoin et al., 2000; Amann and Pollard, 2001; Volkmann et al., 2001). *Arabidopsis* has been found to possess all the seven Arp2/3 complex genes (Klahre and Chua, 1999; McKinney et al., 2002). *Arabidopsis arp2/3* mutants have been associated with the distorted group of trichome mutants of *Arabidopsis* (Hulskamp et al., 1994; Le et al., 2003; Mathur et al., 2003a,b; El-Din El-Assal et al., 2004; Saedler et al., 2004a; Mathur, 2005). The Arp2/3 complex itself is inactive and needs to be activated to nucleate actin filaments. Recently, the mechanism underlying plant Arp2/3 complex activation has been characterised to some extent and shown to involve the SCAR/WAVE complex (Szymanski, 2005; Djakovic et al., 2006). Interestingly no data regarding the location or functions of Arp2/3 complex in pollen has been reported to date. In contrast, a bulk of data points out central roles for formins in the nucleation of actin filaments during the pollen tube growth (Ye et al., 2009; Blanchoin and Staiger, 2010; Cheung et al., 2010).

The *Arabidopsis* genome encodes 21 **formins** which subdivide into two main classes: class I comprises 10 isoforms and class II comprises 11 isoforms. Class I formins are characterised by a N-terminal transmembrane and an extracellular domain (Grunt et al., 2008). Numerous formins are expressed in pollen, although their expression level is usually much lower than profilin. One of the best-characterised plant formins is the *Arabidopsis* FORMIN1 (AtFH1). AtFH1 is able to nucleate actin filaments from both free and profilin-bound actin monomers (Michelot et al., 2005). Besides their central role in *de novo* actin nucleation, many formins exhibit accessory activities, including capping, bundling and severing (Staiger and Blanchoin, 2006; Vidali et al., 2009; Ye et al., 2009; Blanchoin and Staiger, 2010; Cheung et al., 2010; Martinière et al., 2011).

In plants, the **heterodimeric actin filament capping protein** from *Arabidopsis* (AtCP) has been extensively characterised (Huang et al., 2003, 2006). AtCP is known as CapZ from vertebrate muscle (Casella et al., 1987; Caldwell et al., 1989; Maruyama et al., 1990; Yamashita et al., 2003; Narita et al., 2006) and cap32/34 from *Dictyostelium* (Haus et al., 1991, 1993; Eddy et al., 1996). Huang et al. (2003) showed that AtCP binds to the plus-end of actin filaments with nanomolar affinity preventing the incorporation or release of actin subunits. In addition, it inhibits end-to-end annealing of filaments. AtCP was also shown to reduce the initial lag period for actin polymerisation and to increase the maximum rate of polymerisation. Michelot et al. (2005) reported that AtCP and formins compete for binding to actin filament ends.

ADFs and closely related cofilins in vertebrates and yeast define one of the most highly and widely expressed family of ABPs which play central roles in the control of actin cytoskeleton dynamics. A substantial body of work has revealed the various activities displayed by ADF/cofilins as well as the numerous signaling pathways controlling these activities (Van Troyes et al., 2008; Bernstein and Bambourg, 2010). *In vitro*, ADF/cofilins enhance the rate of actin filament turnover by promoting actin filament severing and/or facilitating pointed end depolymerisation (e.g. Carlier et al., 1997; Maciver, 1998; Ressad et al., 1998; Blanchoin and Pollard, 1999; Pope et al., 2000; Andrianantoandro and Pollard, 2006). In the presence of high concentrations of ATP-loaded actin monomers, uncapped ends of ADF/cofilin severed filaments can alternatively be used to increase polymerisation. In addition, at high ADF/cofilin:actin ratios, ADF/cofilins promote actin nucleation by a yet unclear mechanism (e.g. Carlier et al., 1997; Yeoh et al., 2002; Chen et al., 2004; Andrianantoandro and Pollard, 2006). Beside their function at the single filament level, ADF/cofilins also likely play central roles in the remodelling of higher-order cytoskeletal structures, e.g. dissociating actin filament branches mediated by the Arp2/3 complex (Blanchoin et al., 2000; Chan et al., 2009). Animal and plant ADFs are encoded by an ancient gene family. Plants exhibit particularly large families of ADFs. *Arabidopsis* possesses 11 functional ADF isoforms which can be classified into four subclasses according to their expression and phylogeny (Maciver and

Hussey, 2002; Ruzicka et al., 2007). Expression analyses have suggested a model for ADF co-evolving with the ancient and divergent actin isoforms (Ruzicka et al., 2007). Such a model is supported by elegant work showing that the phenotypic changes induced by the ectopic expression of a reproductive class actin in vegetative tissues can be specifically suppressed by co-expression of reproductive profilin and ADF isoforms (Kandasamy et al., 2007). Functional specificities among plant ADFs are further suggested by a relatively high degree of protein sequence variation (Ruzicka et al., 2007). For instance, *Arabidopsis* ADF1 (subclass I) and ADF9 (subclass III) only share 53 % of identity (and 78 % of similarity), although they are co-expressed in a wide range of tissues (Ruzicka et al., 2007) and therefore potentially interact with the same actin isoforms. The biochemical properties of ADF1 have been previously examined in great details (Carlier et al., 1997; Ressayat et al., 1998; Bowman et al., 2000). Noticeably, ADF1 was demonstrated to enhance actin filament turnover by increasing the depolymerisation rate at the pointed-end (Carlier et al., 1997). Accordingly, the over- and down-expression of ADF1 in transgenic *Arabidopsis* plants were found to reduce and to increase the number of cellular actin bundles respectively (Dong et al., 2001). Overexpression of NtADF1 resulted in the reduction of axially oriented actin cables in transformed pollen tubes and in the inhibition of pollen tube growth in a dose-dependent manner (Chen et al., 2002). Augustine et al. (2008) demonstrated that in tip-growing protonema cells lacking ADF function, the cortical fringe was unable to form.

How plant cells organise actin filaments into higher-order structures and the roles of the latter will be discussed in details in the following section.

III. Actin bundling in plants

This section aims at summarising what is known about the formation and the functions of actin bundles in plants. First, a review article that we published in 2009 in the journal *Cell Motility and the Cytoskeleton* is presented. In this article, we briefly discuss the different approaches to image the plant actin cytoskeleton, describe the subcellular distribution of actin bundles in diverse plant cell types, address the

functions of bundles during important cellular processes, and finally analyse the consequences of a perturbed actin bundle homeostasis. The four main families of plant actin bundling proteins, namely the villin, fimbrin, formin and LIM families, are also described. Second, the most recent bibliographic data on actin-bundling that could not be included in our review article is summarised.

1. Review article “Actin-Bundling in Plants”

Review Article

Actin Bundling in Plants

Clément Thomas,* Stéphane Tholl, Danièle Moes, Monika Dieterle,
Jessica Papuga, Flora Moreau, and André Steinmetz

*Plant Molecular Biology Laboratory, Centre de Recherche Public-Santé,
L-1526 Luxembourg*

Tight regulation of plant actin cytoskeleton organization and dynamics is crucial for numerous cellular processes including cell division, expansion and intracellular trafficking. Among the various actin regulatory proteins, actin-bundling proteins trigger the formation of bundles composed of several parallel actin filaments closely packed together. Actin bundles are present in virtually all plant cells, but their biological roles have rarely been addressed directly. However, decades of research in the plant cytoskeleton field yielded a bulk of data from which an overall picture of the functions supplied by actin bundles in plant cells emerges. Although plants lack several equivalents of animal actin-bundling proteins, they do possess major bundler classes including fimbrins, villins and formins. The existence of additional players is not excluded as exemplified by the recent characterization of plant LIM proteins, which trigger the formation of actin bundles both in vitro and in vivo. This apparent functional redundancy likely reflects the need for plant cells to engineer different types of bundles that act at different sub-cellular locations and exhibit specific function-related properties. By surveying information regarding the properties of plant actin bundles and their associated bundling proteins, the present review aims at clarifying why and how plants make actin bundles. *Cell Motil. Cytoskeleton* 66: 940–957, 2009. © 2009 Wiley-Liss, Inc.

Key words: actin-bundling; actin cytoskeleton; actin marker; fimbrin; forming; LIM proteins; myosin; pollen tube; root hair; villin

INTRODUCTION

The actin cytoskeleton is a complex and dynamic filamentous structure present in all eukaryotic cells. In addition to its elementary scaffolding function, the actin cytoskeleton plays central roles in numerous physiological processes including cell division, expansion, motility, organelle trafficking, endo- and exocytosis as well as signal transduction. Basically, filamentous (F-) actin is generated by the linear assembly of globular (G-) actin monomers into polymeric structures. Within the cells, actin filament (AF) assembly and disassembly are facilitated at spatial and temporal levels by a plethora of actin-binding proteins (ABPs), including nucleating, depolymerizing, severing, capping, F-actin stabilizing and G-actin sequestering proteins [Dos Remedios et al.,

2003]. Among the repertoire of actin-binding proteins (ABPs) that regulate AF dynamics, one may cite key players such as the Arp2/3 complex and formins, which direct the initiation of new branched and unbranched filaments respectively [Pollard, 2007], as well as the actin-depolymerizing factor (ADF)/cofilin family members,

*Correspondence to: Clément Thomas, Centre de Recherche Public-Santé, 84 Val Fleuri, L-1526 Luxembourg.
E-mail: clement.thomas@crp-sante.lu

Received 17 January 2009; Accepted 29 April 2009

Published online 5 June 2009 in Wiley InterScience (www.interscience.wiley.com).
DOI: 10.1002/cm.20389

which increase filament turnover [Bamburg et al., 1999; Van Troys et al., 2008]. An additional level of regulation is the assembly of AFs into higher-order structures such as orthogonal networks and parallel bundles by a specialized subset of ABPs, which are able to crosslink adjacent filaments through bivalent actin-binding [Puius et al., 1998].

In animal cells, actin bundles are central components of a variety of specialized cellular structures including microvilli, stress fibers, filopodia and growth cones. Recent data on the mechanisms underlying bundle formation indicate that animal cells use different combinations and sequences of actin-crosslinking proteins to assemble bundles with unique properties specific to their cellular functions [Bartles, 2000]. Indeed, at least two or three distinct actin-crosslinking proteins participate in the generation of highly specialized bundles found in neurosensory bristles of *Drosophila* [Tilney et al., 1995, 1996], as well as in brush border microvilli [Shibayama et al., 1987; Heintzelman and Mooseker, 1992], *Drosophila* nurse cells [Cant et al., 1994; Guild et al., 1997], hair cell stereocilia [Tilney et al., 1992], and sertoli cell ectoplasmic specializations [Russell and Peterson, 1985; Vogl et al., 1991]. Cooperative action of actin crosslinkers such as α -actinin and fascin has shown to significantly enhance the mechanical strength of cells [Tseng et al., 2005]. In contrast to the situation in animal cells outlined above, considerably less is known about plant cell actin bundles and their associated bundling proteins. Noticeably, actin bundles are present in virtually all plant cells. On the one hand, these bundles may appear less diverse in size and shape, compared to their analogs in animal cells. For example, there exists no plant equivalent to the long and highly organized bundles made of end-to-end joined preformed modules in the neurosensory bristles of *Drosophila* [Tilney et al., 1996]. Accordingly, plants also lack a number of actin-bundling proteins including forked, fascin, espin and quail [Hussey et al., 2002]. On the other hand, four distinct plant actin-bundling protein families have been identified and characterized over the last decade, suggesting that plants elaborate actin bundles of diverse properties and functions as well.

After briefly discussing the different approaches used to image the plant actin cytoskeleton, we review the subcellular distribution of actin bundles in diverse cell types. We more deeply address actin bundle functions by focusing on important processes including the cell cycle, tip-growth and cytoplasmic streaming, and by pinpointing the consequences of a perturbed actin bundle homeostasis. Finally, we survey what is known about the main plant actin-bundling proteins and try to shed light on how these proteins may be regulated in harmony with other ABPs to generate the appropriate actin structures within plant cells.

IMAGING THE PLANT ACTIN CYTOSKELETON

A crucial step towards a comprehensive understanding of plant actin cytoskeleton functions is the achievement of an accurate and complete view of how AFs are organized in cells. Imaging the plant actin cytoskeleton has not been an easy task since conventional fixation and embedding techniques result in poor F-actin preservation [Vitha et al., 2000]. In addition, the slowness of chemical fixation, which is accentuated in higher plant cells by the presence of a rigid cellulosic cell wall, was suspected to give rise to artifactual cytoskeletal rearrangements [He and Wetzstein, 1995; Doris and Steer, 1996]. Therefore, continuous effort has been devoted to improve chemical fixation procedures and to develop alternative methods such as cryofixation [Vitha et al., 2000; Collings and Wasteneys, 2005; Wilsen et al., 2006; Smertenko and Hussey, 2008]. Despite the wide use of live cell imaging (see below), classical actin immunolocalization or labeling using appropriately fixed material yielded important results, especially in root and pollen tissues [Collings and Wasteneys, 2005; Wilsen et al., 2006].

One major limitation inherent to the use of fixed material is that those samples only provide a static picture of the actin cytoskeleton whose nature is, on the contrary, extremely dynamic. Therefore, live imaging appears necessary to further depict actin cytoskeleton functions. Despite several successful examples, microinjection experiments remain challenging and are not applicable to all plant cell types [Schmit and Lambert, 1990; Cleary et al., 1992; Zhang et al., 1993; Cleary, 1995; Kovar et al., 2001]. The expression of live actin reporters, consisting of a fluorescent protein fused to an actin-binding domain (ABD), emerged as the most useful strategy. The possibility to produce stably transformed cell lines and plants exhibiting a fluorescent actin cytoskeleton significantly boosted the cytoskeleton research over the past decade. The actin-binding domain (ABD) of mouse talin fused to GFP [GFP-mTn, Kost et al., 1998] yielded substantial results in various cell types and plant species including *Arabidopsis* [Kost et al., 1998; Mathur et al., 1999], tobacco [Kost et al., 1998; Fu et al., 2001; Hoffmann and Nebenführ 2004; Yu et al., 2006] and rice [Holweg et al., 2004]. However, *Arabidopsis* fimbrin-derived reporters, such as the fusion of the second ABD of fimbrin to GFP [GFP-fABD2, Ketelaar et al., 2004; Sheahan et al., 2004; Voigt et al., 2005] turned out to be superior. First, GFP-fABD2 reveals AFs in a broader range of tissues than GFP-mTn, e.g. the root apex [Voigt et al., 2005] and resolution has recently been improved by adding a second GFP molecule at its C-terminus [GFP-fABD2-GFP; Wang et al., 2008b]. Secondly, GFP-mTn triggers more abundant and

severe side effects on actin cytoskeleton organization and cell growth than GFP-fABD2 [Ketelaar et al., 2004; Sheahan et al., 2004]. Holweg [2007] reported that, although a slight reduction in cellular motility occurred in both *Arabidopsis* GFP-FABD2 and GFP-mTn expressing lines, only the latter displayed actin cytoskeleton over-stabilization and a significantly reduced basipetal auxin transport. Although GFP-FABD2 and GFP-mTn are the most commonly used actin markers, other ABP-derived markers yielded substantial results. As an example, a recent study reaffirmed the suitability of GFP-fused tobacco and lily ADFs (GFP-NtADF1 and GFP-LIADF1) to investigate the actin cytoskeleton dynamics in elongating pollen tubes [Cheung et al., 2008]. In addition, it reported a tobacco LIM protein-derived fluorescent protein (NtPLIM2b-GFP) being a versatile marker in the functional study of pollen actin cytoskeleton regulators. A novel and promising marker is the yeast-derived “lifeact” [Riedl et al., 2008]. This only 17-amino-acid long peptide has moderate affinity for actin filaments and does not affect in vitro actin polymerization and depolymerization processes. In addition, as it has no homologous sequences in higher eukaryotes, it is expected to have reduced side effects. However, its use has not been reported in plants so far.

Generally, high expression levels of live actin reporters have been found to worsen side effects [Wilsen et al., 2006; Finka et al., 2007; Cheung et al., 2008]. Nevertheless, as they are practical and reliable when cautiously used, noninvasive fluorescent actin probes are remarkable tools to investigate the actin cytoskeleton organization and dynamics in plants. Warnings concerning possible side effects exhort to conduct all necessary controls and authenticate observations by the use of different live markers or classical labeling strategies.

F-ACTIN AND BUNDLE DISTRIBUTION IN PLANT CELLS

The availability of transgenic plants and cell lines expressing fluorescent actin reporters prompted an enthusiastic reexamination of the actin cytoskeleton organization in different cell types. Talin- and fimbrin-derived reporters reveal the presence of actin bundles in nearly all *Arabidopsis* cell types [Kost et al., 1998; Ketelaar et al., 2004; Sheahan et al., 2004; Wang et al., 2004, 2008; Voigt et al., 2005]. Indeed, in rosette leaves, epidermal pavement cells exhibit a dense network of randomly oriented fine and thick actin bundles, whereas mesophyll cells contain fine actin bundles that form cages around chloroplasts. The trichome nucleus is surrounded by a prominent F-actin cage from which elaborate arrays of longitudinal bundles extend through the branches. Open stomata of light-grown plants have actin

bundles partially arranged in radial arrays, whereas closed stomata of dark-grown plants possess more random or longitudinal bundles. Elongated hypocotyl and leaf petiole cells mainly contain thick longitudinal actin bundles, although a few obliquely oriented F-actin arrays also exist. The organization of AFs in inflorescence stems and flowers has been described in detail using the bright GFP-fABD2-GFP reporter [Wang et al., 2008b]. As a general feature, the most elongated cells predominantly exhibit longitudinal actin bundles, whereas more irregularly shaped cells contain more random AF networks. The same reporter enables the imaging of AFs in roots, including regions, such as the root meristem, that are not well resolved by former single GFP-fused markers. Importantly, results largely resemble those obtained by immunofluorescence labeling using optimally fixed root tissue [Collings and Wasteneys, 2005]. Cells from the distal elongation zone contain randomly organized cytoplasmic AFs surrounding the developing vacuole and rather transverse bundles at their cortex. In interphase cells of the division zone, cytoplasmic AFs enclose the nucleus, and cortical AFs lack any dominant orientation. Actin filaments are abundant in phragmoplasts and dividing cells exhibit an increased filament density at the basal and apical walls. Although the overall subcellular distribution of F-actin is reliably achieved at different mitotic stages, the detailed AF arrangement is difficult to resolve, suggesting a low level of actin-bundling in dividing cells. Interestingly, the gravity-sensing columella cells exhibit only diffuse signals i.e. no actin bundles, whereas distinct bundles are observed in the peripheral root cap cells. Elongating root hairs contain extensive longitudinal arrays of fine and thick bundles but their extreme tip is devoid of AFs.

Fluorescent live reporters have also been used in tobacco BY2 cells, providing a dynamic view of the typical actin arrays that occur during the cell cycle [Sano et al., 2005; Yu et al., 2006]. Interphase cells exhibit cortical AFs arranged in a dense meshwork of rather fine actin bundles. This cortical meshwork is believed to support peripheral structures including the cell wall and microtubules. In transvacuolar cytoplasmic strands, AFs organize into thick and long bundles connecting the cell periphery to the nucleus. The latter is surrounded by another actin meshwork often referred as the F-actin “basket”. This overall actin cytoskeletal organization, including an extensive bundling state, persists over G1, S and early G2 phases. Importantly, during its translocation to the center of the cell (at S phase), the nucleus remains connected to the cell periphery through endoplasmic actin bundles, suggesting that these bundles are involved in nuclear positioning [Kennard and Cleary, 1997; Grolig, 1998]. From late G2 phase to cytokinesis, the actin cytoskeleton is subjected to successive impor-

tant rearrangements. Typical actin structures including a pre-prophase AF band, a mitotic spindle AF cage and an AF phragmoplast are reported by both GFP-fABD2 [Sano et al., 2005] and GFP-mTn [Yu et al., 2006] markers. Strikingly, the overall actin-bundling level appears weak during the progression of cell division. Indeed, the size and number of cortical and transcytoplasmic actin bundles are obviously reduced compared to interphase cells. Dynamic mitotic actin structures rather contain unbundled and short filaments. However, due to the high AF density and thus to the high fluorescence level found in these structures, the presence of bundled AFs cannot be excluded.

In summary, extensive actin-bundling is taking place in most mature plant cells. The actin-bundling level appears to be temporally and locally down-regulated when the actin cytoskeleton is needed in a very dynamic state, e.g. during mitosis and at the very tip of the growing root hair. This is also consistent with observations in diffusely expanding cells, indicating that sub-cortical AF bundles condense when growth is inhibited, whereas networks of finer AFs correlate with rapid cell growth phases [Thimann et al., 1992; Waller et al., 2002]. The absence of actin bundles in gravity-sensing columella cells may be an exception directly related to the particular functions of these cells.

ACTINS BUNDLES IN TIP-GROWING CELLS

Pollen tubes resemble root hairs in that they both exhibit a tip mode of growth, allowing these cells to expand polarly at the apex [Hepler et al., 2001]. Inhibitory experiments have clearly established that polar cell growth largely depends on the actin cytoskeleton (e.g. Gibbon et al., 1999; Baluska et al., 2000, 2001). As they are amenable to *in vitro* assays and microscopic analysis, pollen tubes and root hairs emerged as attractive working models to investigate the role of the cytoskeleton during cell growth.

The population of long and rather thick actin bundles running along the pollen tube and the root hair length has been unambiguously revealed using both fixed and live material [e.g. Miller et al., 1999; Sheahan et al., 2004; Lovy-Wheeler et al., 2005; Cheung et al., 2008]. Unequivocally these bundles are the main tracks used by myosins to drive Golgi-derived vesicles towards the growing apical region. Their unipolar arrangement and organized alignment support the reverse fountain streaming observed in pollen tubes and root hairs [Kohno et al., 1990; Tominaga et al., 2000; Lenartowska and Michalska, 2008]. As the vesicles reach the subapical region, they are further transported to precise sites of growth [Geitmann and Emons, 2000; Hepler et al., 2001; Vidali and Hepler, 2001]. In the subapical region of both pollen

tubes and root hairs, the long actin bundles are replaced by other AF structures whose organization has been more challenging to resolve. Recent progress has shed light on the apparent difficulty to achieve a consensus view of the actin cytoskeleton organization in this region.

Using optimized tissue fixation procedures, Lovy-Wheeler et al. [2005] described a persuasive picture of the actin cytoskeleton organization in the subapical domain of lily and tobacco pollen tubes. In both cases, they observed a “cortical fringe of actin”, which consists of closely packed parallel actin bundles beginning at 1-5 and 1-3 μm from the extreme apex and basally extending for another 5-10 and 3-5 μm , respectively. Similar structures of actin bundles, though with structural dissimilarities, have been reported by other investigators. As a result, the terminology to describe AF organization in the subapical zone differs from one study to another and includes the idioms ring, collar, mesh, funnel-like structure and fringe. On the one hand, these dissimilarities may result from the use of different actin imaging methods or reporters, which do not all label the cytoskeleton equally. On the other hand, they have been strongly suggested to reflect the dynamic and fragile nature of the subapical actin structure [Cheung and Wu, 2008]. Notably, the cortical fringe remains at a finite distance from the elongating tube tip, suggesting that it is permanently un/rebuilt. The apex of the pollen tube is submitted to constant changes in ionic conditions, including a fluctuating apical Ca^{2+} gradient and a subapical alkaline region [Holdaway-Clarke and Hepler, 2003; Cheung and Wu, 2008], which regulate actin cytoskeleton dynamics and organization by the activation/inactivation of ABPs [Ren and Xiang, 2007]. As an example, ADF predominantly localizes to the subapical region, where its fragmenting activity is stimulated by alkaline pH conditions [Chen et al., 2002; Lovy-Wheeler et al., 2006]. Given the high degree of actin cytoskeleton remodeling in the subapical region, the series of subapical actin structures reported so far has been suggested to belong to a continuum of structural configurations that interconvert from one to another during pollen tube growth. This concept is convincingly supported by recent live cell studies [Cheung et al., 2008].

Similarly to the situation in pollen tubes, the actin cytoskeleton is subjected to significant rearrangements in the subapical region and the tip of root hairs. The longitudinal arrays of thick bundles emerging from the root hair base extend along the tube length up to the subapical region where they were observed to branch into finer net-axial bundles [Miller et al., 1999; Ketelaar et al., 2002]. However, the precise conformation of these bundles is not clearly defined yet, suggesting that, like in the pollen tube, the cytoskeleton is submitted to intensive remodeling in the subapical region. Importantly, the

extreme tip of actively growing root hairs appears devoid of actin bundles [e.g. Sheahan et al., 2004; Wang and Pesacreta, 2004; Voigt et al., 2005]. As the hair's growth slows down, the thick actin bundles cross the subapical region and extend to the tip [Miller et al., 1999; Ketelaar et al., 2002; Wang et al., 2004]. This event was suggested to impede the targeting of vesicles to active growth sites, which is believed to rely on the finer and shorter bundles [Miller et al., 1999].

From the above observations, developing pollen tubes and root hairs appear to possess at least two distinct actin bundle populations, i.e. the long and thick actin bundles in the pollen tube shank and root hair tube and the subapical short and rather fine bundles. In addition, a population of non-bundled actin filaments is sometimes predicted at the very tip, although it could not have been clearly defined so far. In addition to their dissimilar subcellular locations and morphologies, the two bundle populations are further characterized by their respective stabilities. Indeed, low concentrations of actin depolymerizing drugs induce the disruption of the subapical AF structure, whereas they do not severely affect the long actin bundles [Gibbon et al., 1999; Vidali et al., 2001; Ketelaar et al., 2003]. As only tip growth, but not cytoplasmic streaming, is affected by such treatment, the subapical actin structure is likely to be closely related with growth. Recently, the effects of low dosages of Latrunculin B on pollen tube growth have been carefully revisited [Cardenas et al., 2008]. Growth inhibition was shown to be associated with a degradation of the subapical cortical fringe, as well as with a loss of cytoplasmic zonation, a diminution of the Ca^{2+} gradient, and a forward motion of the alkaline band. These observations are consistent with a role of the subapical actin structure in the targeting of vesicles to the apex for exocytosis.

The mechanism underlying the targeting of vesicles to the apex remains a matter of debate. A current hypothesis is that the subapical actin structure would trap vesicles and thereby prevent them from leaving the tip region via the reverse fountain stream [Smith and Oppenheimer, 2005]. Then vesicles would further be conveyed to the tip through myosin-dependent transport and/or via actin polymerization-driven propulsion [Voigt et al., 2005]. The significance of the (relatively weak) bundling of AFs in the subapical region of pollen tubes and root hair remains ambiguous. As a hypothesis it may help to properly organize AFs in the apical region. It may also be required to temporarily stabilize AFs against depolymerization forces, which are expected to be considerable in the subapical region.

An additional role for actin-bundling emerges from studies aimed at understanding how the nucleus is maintained at a fixed distance from the growing root hair tip. Injection of an antibody directed against the bundling

protein villin into growing root hairs of *Arabidopsis* induces bundle dissociation and movement of the nucleus closer to the tip [Ketelaar et al., 2002]. Data point out a prominent role of the subapical actin structure in preventing the nucleus approaching the apex. In addition, the nuclear backward movement (toward the hair base) occurring during growth arrest is related to the disappearance of the subapical actin structures and involves the thick actin bundles within the root hair tube. Involvement of myosins in actin-based nuclear movement has been suggested but requires further examination [Chytlova et al., 2000].

ACTIN BUNDLES IN CYTOPLASMIC STREAMING AND TRANSVACUOLAR STRAND INTEGRITY

As the central vacuole generally occupies most of the plant cell's volume, a large fraction of the cytoplasm is confined to the subcortical and perinuclear regions [Marty, 1999]. In addition, cytoplasmic transvacuolar strands (TVSs) provide direct connections between distant cytoplasmic regions, thereby allowing the redistribution of molecules, vesicles and organelles [Grolig and Pierson, 2000]. This process, also referred to as cytoplasmic streaming, occurs with high velocities in various plant cells from algae to angiosperms and largely relies on the acto-myosin system [Kamiya, 1981; Shimmen and Yokota, 2004]. Shimmen [2007] has recently reviewed the 50 years of research establishing that the main motive force of cytoplasmic streaming is generated by the sliding of organelle-associated myosin XI along actin filaments. Although microtubules and their associated motors also contribute to intracellular movements in higher plant cells, they appear to be involved in short-distance movement and positioning of organelles at the cell cortex, rather than in long-distance or fast streaming [Van Gestel et al., 2002; Romagnoli et al., 2003, 2007; Lu et al., 2005].

Plant myosin XI directs the targeting of a broad variety of organelles including the ER [Liebe and Menzel, 1995; Samaj et al., 2000; Yokota et al., 2009], the Golgi apparatus [Nebenführ et al., 1999], the mitochondria [Romagnoli et al., 2007; Van Gestel et al., 2002], the plastids [Wang and Pesacreta, 2004; Paves and Truve, 2007], the peroxisomes [Hashimoto et al., 2005; Reisen and Hanson, 2007] and the nucleus [Heslop-Harrison and Heslop-Harrison, 1989]. Recently, an exhaustive study, in which each of the 13 *Arabidopsis* class XI myosin genes has been inactivated, suggested a high degree of redundancy in myosin XI functions [Peremyslov et al., 2008]. However, this study also pointed out the major roles played by myosin XI-K and XI-2 in the rapid movement of Golgi stacks, peroxisomes and mitochondria. Similar results have been obtained in tobacco for myosin XI-K but not for myosin XI-2, which, in tobacco, only

participated in peroxisome translocation [Avisar et al., 2008]. To transport the cellular cargoes attached to its C-terminal globular tail [Li and Nebenführ, 2007, 2008], myosin XI moves along actin tracks using its N-terminal catalytic motor domain which binds to actin filaments and hydrolyzes ATP [Tominaga et al., 2003; Hachikubo et al., 2007]. Although the sliding mechanism of myosin XI on AFs does not require a particular bundling state per se, several observations strongly suggest that actin bundles play major roles in cytoplasmic streaming.

Presumably, actin-bundling is the process used by plant cells to build, position and stabilize the main routes for organelle transport over long distances. As already stated, poorly and extensively bundled AF populations display different sensitivities to depolymerizing drugs, the first being disrupted by lower concentrations than the latter [Gibbon et al., 1999; Miller et al., 1999; Ketelaar et al., 2003]. Importantly, the specific depolymerization of the fine AF arrays does not significantly impair the streaming of organelles, indicating that prominent bundles are the preferred routes for organelle movements. This selectivity of F-actin-based motility has been recently suggested to mirror myosin selectivity [Walter and Holweg, 2008]. Indeed, the head-neck domain of the *Arabidopsis* myosin MYA2 (XI-2) fused to GFP has been shown to extensively colocalize with cytoplasmic actin bundles, whereas it only poorly labeled the finer AF arrays at the cell cortex. So far, no mechanism supporting the assumed preference of MYA2 for thick actin bundles has been characterized. One may hypothesize that the high stability of actin bundles and/or the presence of other bundle-associated ABPs, e.g. actin-bundling proteins, may potentiate myosin attachment. In turn, it is conceivable that myosins participate in actin bundle formation and/or maintenance.

More than just being highways that cluster actin motor transporters on desired cellular axes, prominent actin tracks also support higher velocities. Indeed, fastest organelle movements were recorded along robust actin bundles located in the transvacuolar strands [e.g. Holweg, 2007]. In contrast, organelle velocity is much slower in cortical regions where finer bundles and single AFs predominate. Although there is no explanation for these differences in velocities, it is tempting to relate them to the selectivity of myosins XI for actin bundles.

Cytoplasmic streaming has often been described as a polar process. A famous example is the simple circulatory streaming occurring in the giant *Chara* internodal cells. In these cells, the cytoplasm flows in a nearly parallel direction to the long cell axis. It goes up along one hemicylinder to the node and comes down along the other. More than 30 years ago, it has been discovered that such a course was related to the orientation of actin bundles and their AF subunits [Kersey, 1974; Palevitz

et al., 1974; Palevitz and Hepler, 1975; Kersey et al., 1976]. Indeed, actin bundles align with the cytoplasmic flow and contain AFs arranged with the same polarity, i.e. with barbed (+) ends pointing in the direction of the cytoplasmic stream. Similarly, the polarity of AFs is consistent with the direction of cytoplasmic streaming in other cell types, e.g. *Hydrocharis* root hairs [Tominaga et al., 2000] and *Haemanthus* pollen tubes [Lenartowska and Michalska, 2008]. Assuming that the myosins involved in cytoplasmic streaming and organelle transport move along actin tracks with processivity and directionality, i.e. towards the barbed (+) end of AFs [Tominaga et al., 2003; Hachikubo et al., 2007], the assembly of unipolar actin bundles can be regarded as the cellular mechanism determining the direction of cytoplasmic streaming. However, in *Nicotiana benthamiana* leaf epidermal cells, there is neither a preferential direction in organelle movement, nor a continuous movement of these organelles [Avisar et al., 2008]. Moreover, significantly different organelle velocities occur within the same cells. These recent observations claim the reconsideration of the generalized concept which defines cytoplasmic streaming as the coordinated flow of the cytosol components. Indeed, the elaboration of unipolar bundles dedicated to promote polar and synchronized streaming of organelles may be restricted to specific cell types, such as *Chara* internodal cells and elongating root hairs and pollen tubes [Peremyslov et al., 2008].

In addition to their direct roles in intracellular transport, actin bundles also play a central role in the maintenance of TVSSs. Noticeably, the structural integrity of TVSSs highly depends on a functional actin cytoskeleton as demonstrated by their rapid disappearance upon AF destabilization by various agents [Staiger et al., 1994; Shimmen et al., 1995; Hussey et al., 1998; Van Gestel et al., 2002; Sheahan et al., 2007]. Importantly, unbundling of AFs in root hairs, following the injection of antibodies against the lily bundling protein 135-kDa villin, induces broadening and eventual loss of TVSSs, indicating that actin bundles are essential for the integrity and continued existence of TVSSs [Tominaga et al., 2000]. In agreement with a mechanical support function, actin bundles localize at the periphery of the cytoplasmic strands, rather than at the center [Higaki et al., 2006].

TVSSs are remarkably dynamic elements that continuously change in shape and location [Hoffmann and Nebenführ, 2004; Ruthardt et al., 2005]. Given that TVSS integrity relies on actin filaments/bundles, TVSS rearrangements are likely caused by modification of the actin cytoskeleton organization. The latter could be achieved either by the synthesis of new AFs/bundles or by the displacement of existing AFs/bundles, the two mechanisms not being mutually exclusive [Hoffmann and Nebenführ, 2004]. The significant and reversible inhibition of TVSS

dynamics induced by myosin inhibitors strongly suggests that myosin-triggered movement of AFs/bundles is involved in TVS remodeling [Hoffmann and Nebenführ, 2004; Sheahan et al., 2007]. As discussed in van der Honing et al. [2007], a role of actin polymerization in the establishment of new TVVs is suggested by the presence, in plants, of homologs of many mammalian proteins involved in force generation. However, this conception has not been tested yet.

ACTIN BUNDLING VERSUS DEPOLYMERIZATION FORCES

Taken together, the above discussions suggest that a high actin-bundling state is inconsistent with a very dynamic actin cytoskeleton turnover and *vice versa*. However, the relationships between actin-bundling and cellular AF turnover forces need to be further examined. In addition to the already mentioned pharmacological studies, a number of reports indicate that the alteration of actin cytoskeleton dynamics by genetic tools significantly influences the cellular actin-bundling state. An example is the modification of the expression level of actin-depolymerization factor (ADF)/cofilin encoding genes. The ADF/cofilin family has emerged as a central regulator of actin turnover in eukaryotes including plants [Bamburg, 1999; Maciver and Hussey, 2002; Van Troys et al., 2008]. Through its AF severing and pointed end-depolymerizing activities, ADF/cofilin enhances actin cytoskeleton dynamics [Carrier et al., 1997; Blanchoin and Pollard, 1999; Pavlov et al., 2007]. Dong et al. [2001] reported that both an increase and a decrease of the *Arabidopsis ADF1* (*AtADF1*) expression level induce a significant effect on the overall cellular actin-bundling state. Indeed, the thick actin bundles disappear when *AtADF1* is over-expressed, whereas their population increases upon *AtADF1* down-regulation. These actin phenotypes are accompanied by either a reduction or stimulation of cell growth, respectively. In another study, over-expression of a pollen-specific ADF from tobacco, NtADF1, noticeably reduces the number of long axially oriented actin bundles in the pollen tube shank [Chen et al., 2002]. Regarding tip-growth, the subapical cortical fringe composed of parallel short bundles is unable to form in tip-growing moss protonema cells lacking ADF function [Augustine et al., 2008]. Instead, bundles assemble in prominent star-like structures attached to the cell cortex, indicating that the loss of ADF results in an excessive production of actin bundles as well as in their mislocalization. Recently, the down-regulation of one cotton ADF family member has been reported to improve the length and the strength of cotton fibers. These fibers also contain more abundant F-actin filaments in the cortical region of the cells [Wang et al.,

2009]. ADF proteins are therefore considered as candidates for the improvement of fiber traits via genetic engineering. It may be of interest to consider actin-bundling proteins as additional candidates.

Another example of indirectly manipulated actin-bundling level comes from functional studies on the actin interacting protein 1 (AIP1). AIP1 is an actin regulatory protein found in a wide range of eukaryotic species which enhances ADF/cofilin-induced actin disassembly by capping ends of severed filaments, thus preventing elongation from the barbed ends [Ono, 2003]. Accordingly, the *in vitro* actin-depolymerizing activity of lily pollen LIADF1 is massively increased in the presence of AIP1 [Allwood et al., 2002]. The biological relevance of the synergy between LIADF1 and AIP1 for actin reorganization in pollen is supported by their similar localization patterns: both proteins localize to F-actin bundles in dormant pollen grains, but are mainly cytosolic in growing pollen tubes. By facilitating ADF/cofilin activity in the subapical region of pollen tubes, AIP1 is suggested to maintain the actin cytoskeleton highly dynamic and therefore to prevent excessive bundling. In agreement with this hypothesis, a RNA interference-derived reduction of the AIP1 expression level in *Arabidopsis* plants induces developmental abnormalities that are correlated with an increase of actin-bundling [Ketelaar et al., 2004]. Leaves, shoots and roots, in which expansion is dramatically reduced, exhibit aberrant thick actin bundles. In addition, the incursion of actin bundles into the apex of growing root hairs correlates with a dramatic reduction of hair growth rate. Recently, the effects of AIP1 over-expression on plant growth and actin cytoskeleton organization have also been reported [Ketelaar et al., 2007]. Stem epidermal cells of AIP1 over-expressing lines exhibit thinner and shorter actin bundles than those of control plants. Interestingly, the overall orientation of bundles in epidermal cells, which is normally rather longitudinal, turned out to be rather transversal. Such a modification may be explained by the fact that the reduced length of bundles coerces them to contact proximal cortical sites in order to be stabilized.

Together, these examples illustrate the key roles of ADF/cofilin and AIP1 in maintaining a dynamic actin cytoskeleton and demonstrate that the cellular actin-bundling state is not only positively regulated by bundling proteins (see next section), but also actively down-regulated by the cellular depolymerizing forces.

PLANT ACTIN-BUNDLING PROTEINS AND THEIR BIOLOGICAL ROLES

Generalities

To date, four distinct types of actin-bundling proteins have been identified in plants, including the villins,

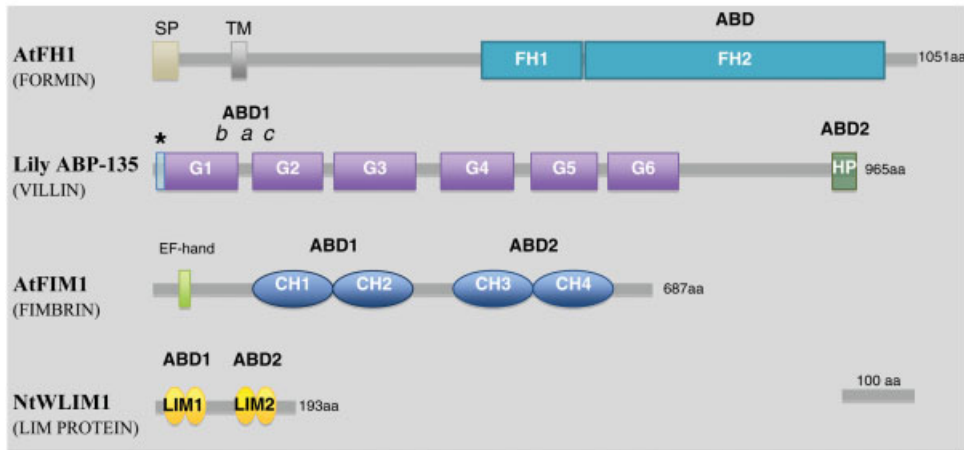
fimbrins, LIM domain-containing (LIM) proteins and formins. In *Arabidopsis*, these proteins are encoded by multigene families of five, five, six and more than 20 genes, respectively. Published work generally focuses on the same or on only a few members of one given family, so that only predictions can be made for the others. In the case of the wide *Arabidopsis* formin family, several proteins have been functionally analyzed but among those only one, namely the *Arabidopsis* AtFH1 [Banno and Chua, 2000], has been biochemically demonstrated to organize filaments into tight bundles [Michelot et al., 2005]. As it has been already established for mammalian and yeast formins [Moseley and Goode, 2005; Harris et al., 2006], actin-bundling activity may not be retained by all *Arabidopsis* formins. Based on the current data, one can distinguish between bundling proteins that do possess multiple actin regulatory activities, i.e. villins and formins, and those that are exclusively involved in the formation of actin bundles, i.e. fimbrins and LIM proteins. Indeed, nucleating, capping and/or severing activities have been attributed to members of the villin [Yokota et al., 2005] and formin families [Deeks et al., 2005; Ingouff et al., 2005; Michelot et al., 2005; Yi et al., 2005] but not yet to a plant fimbrin or LIM protein. Also, additional rigorous biochemical work is needed to assert that fimbrin and LIM proteins are specifically dedicated to the bundling of AFs. Importantly, not all the members of the villin and formin family do exhibit the same range of actin-regulatory activities. As an example, AtVLIN1 is able to generate actin bundles (in an unusual Ca^{2+} /CaM dependent manner) but lacks nucleating, severing or capping activities, which are predicted for most of the other *Arabidopsis* villins [Huang et al., 2005]. In addition, the comparative analysis of the different members of the plant formin family reveals a variability in the biochemically characterized activities and/or cellular functions displayed [Blanchoin and Staiger, 2009]. Homology-based predictions, including those concerning actin-bundling, are particularly difficult to make because of the highly variable domain organization among formins [Grunt et al., 2008]. This emphasizes the need for detailed *in vitro* and *in vivo* analyses for each member of any actin-bundling protein family to define their exact biological role(s). So far, the classical reverse genetics approach by insertional mutagenesis did not yield conclusive results. Indeed, no obvious actin phenotype following knockout or down-regulation of a single actin-bundling protein gene has been reported so far. This may result from overlapping expression patterns, as well as from functional redundancies among the members of a given actin-bundling protein family. Therefore, most of the data regarding functions of actin-bundling proteins in plants come from biochemical, cell microinjection, and ectopic (over-expression) studies.

Villins

As many other protein classes, ABPs have evolved using “modular strategies” [Puius et al., 1998; Van Troys et al., 1999; Grunt et al., 2008]. Functional diversity is achieved by modification, shuffling and combination of a limited number of fundamental modules as well as by the introduction of regulatory features. Therefore it is not surprising that every here-discussed bundling protein family belongs to larger ABP families, the latter being defined by one or several structural signatures. Plant villins belong to the villin/gelsolin/fragmin superfamily, which has been recently reviewed in Su et al. [2007]. Villin/gelsolin/fragmin members share three or six tandem 125-150 amino acid-long gelsolin homology domains (G1-G6), which potentially retain F-actin severing, capping and nucleating activities (Fig. 1A). Villins are the only family members to contain an additional C-terminal ABD termed the headpiece (HP). Therefore, villins have been speculated to use two ABDs, the first located in the core (in G1 and G2 domain) and the second in the HP, to bundle AFs [Glennay and Werber, 1981; Friederich et al., 1999; Fig. 1B, model a). However, recent structure analyses suggest the existence of three ABDs [Hampton et al., 2008; Fig. 1A). The corresponding bundling model proposes that the headpiece holds villin on F-actin, whereas the two other and proximal ABDs mapped in G1 and G2 are more directly responsible for AF crosslinking (Fig. 1B, model b). In contradiction with these data George et al. [2007] demonstrated that villin can form dimers both *in vitro* and *in vivo* [George et al., 2007]. In their model, bundling activity implicates the parallel arrangement of villin dimers mediated by an N-terminal domain, and involves exclusively one ABD in the HP (Fig. 1B, model c).

The two first plant villins identified, i.e. P-135-ABP and P-115-ABP, were isolated from lily (*Lilium longiflorum*) by biochemical fractionation [Nakayasu et al., 1998; Yokota et al., 1998] and subsequently recognized as being homologues of animal villins [Vidali et al., 1999; Yokota et al., 2003]. The two proteins were found to organize actin filaments into bundles with uniform polarity [Yokota and Shimmen, 1999; Yokota et al., 2003], and in both cases, this bundling activity was suppressed by Ca^{2+} /CaM [Yokota et al., 2000, 2003]. Microinjection of antisera directed against the two lily proteins into living root hair cells causes the disappearance of transvacuolar strands and the alteration of the cytoplasmic streaming [Tominaga et al., 2000; Yokota et al., 2003]. Based on these observations it was proposed that P-115-ABP and P-135-ABP villins contribute to the AF arrangement in root hairs and pollen tubes [Yokota et al., 1998; Vidali et al., 1999]. In addition to its role in the formation of actin bundles in the

A



B

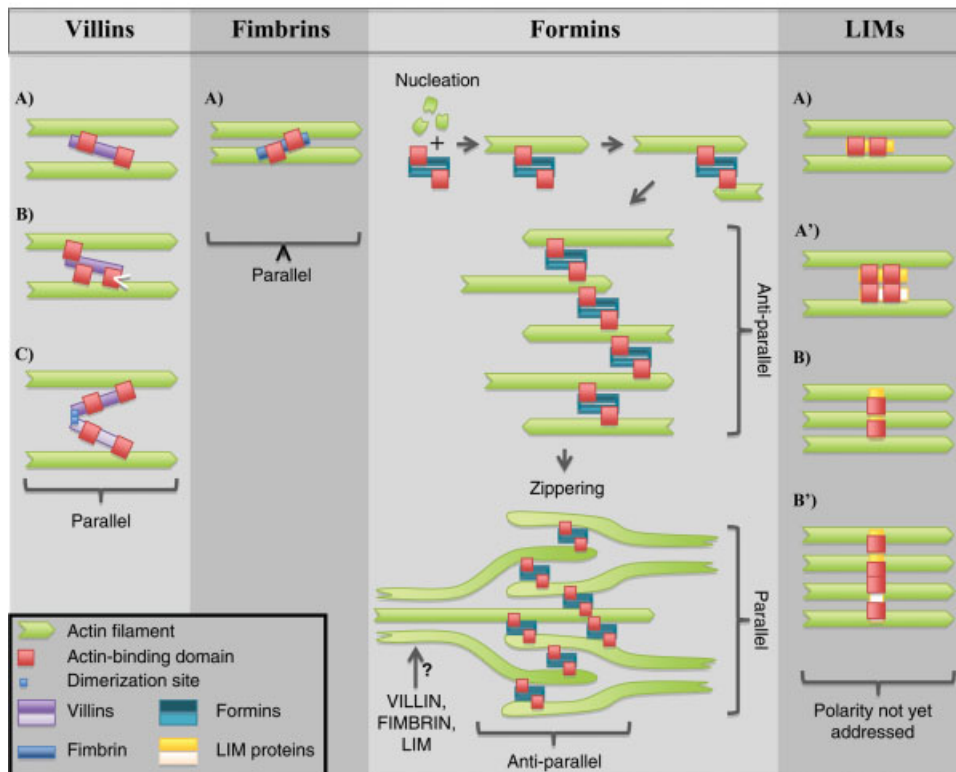


Fig. 1. Domain organization of plant actin-bundling proteins (A) and current models of AF bundling by these proteins (B). A: Domain organization and actin-binding domains (ABDs) of the best-studied member of each plant actin-bundling family. *Arabidopsis* AtFH1 contains two formin homology domains (FH1 and FH2), a signal peptide (SP) and a transmembrane domain (TM). *Lily ABP-135* contains six gelsoolin-like domains (G1-G6) and a C-terminal headpiece (HP). The asterisk indicates the position of a potential dimerization site [George et al., 2007]. An alternative to a single ABD located between G1 and G2 (ABD1a), is two ABDs located in G1 (ABD1b) and G2 (ABD1c), respectively [Hampton et al., 2008]. *Arabidopsis* AtFIM1 contains two tandem repeat of calponin-homology domains (CH1, CH2 and CH3, CH4) as well as a potential N-terminal calcium-binding site (EF-hand). *Tobacco NtWLIM1* contains two LIM domains, each composed of a tandem zinc finger motif. B: Models of AF bundling for each bundling protein family. Polarity of AFs in the bundles is indicated. *Villins*. (1) AF bundling by ABD1a (villin core) and ABD2 (villin headpiece). (2) AF bundling by ABD1b and ABD1c [Hampton et al., 2008]. In this case, ABD2 only holds villin on the first AF. (3) AF bundling by ABD2 following villin dimerization [George et al., 2007]. *Fimbrins*. Tight crosslink of AFs is triggered by the two proximal ABDs and fimbrin dimerization is not required [Volkman et al., 2001; Klein et al., 2004]. *Formins*. This model was proposed for AtFH1, which is a nonprocessive formin [Michelot et al., 2006] and therefore is not applicable to other type of formins [see Blanchoin and Staiger, 2009]. After nucleation, AtFH1 moves from the end to the side of an AF and nucleates a new AF, thereby initiating the formation of an antiparallel bundle. Proximal elongating filaments tend to interact with each other because the thermal fluctuation and therefore assemble into parallel bundles, which may be further stabilized by other bundling proteins. *LIM proteins*. (1) Both LIM domains crosslink the same AF pair. (1') The same model upon LIM protein dimerization. (2) Both LIM domains crosslink distinct pairs of AFs. (2') The same model upon LIM protein dimerization.

piece). (2) AF bundling by ABD1b and ABD1c [Hampton et al., 2008]. In this case, ABD2 only holds villin on the first AF. (3) AF bundling by ABD2 following villin dimerization [George et al., 2007]. *Fimbrins*. Tight crosslink of AFs is triggered by the two proximal ABDs and fimbrin dimerization is not required [Volkman et al., 2001; Klein et al., 2004]. *Formins*. This model was proposed for AtFH1, which is a nonprocessive formin [Michelot et al., 2006] and therefore is not applicable to other type of formins [see Blanchoin and Staiger, 2009]. After nucleation, AtFH1 moves from the end to the side of an AF and nucleates a new AF, thereby initiating the formation of an antiparallel bundle. Proximal elongating filaments tend to interact with each other because the thermal fluctuation and therefore assemble into parallel bundles, which may be further stabilized by other bundling proteins. *LIM proteins*. (1) Both LIM domains crosslink the same AF pair. (1') The same model upon LIM protein dimerization. (2) Both LIM domains crosslink distinct pairs of AFs. (2') The same model upon LIM protein dimerization.

basal and shank regions of the pollen tube, lily P-135-ABP has been suggested to increase actin dynamics in the calcium-rich apical region through its calcium-activated G-actin binding, capping and depolymerizing activities [Yokota et al., 2005]. Therefore, villin activities and their mode of regulation could explain (at least partially) the fragmentation of actin filaments in pollen tubes upon increase of Ca^{2+} concentration [Kohno and Shimmen, 1988a,b]. However, as already stated, not all plant villins retain the full range of the possible actin-regulatory activities. Indeed, recombinant *Arabidopsis* AtVLN1 has been shown to be a simple actin-bundling protein that is not regulated by $\text{Ca}^{2+}/\text{CaM}$ [Huang et al., 2005]. It may thus be specialized in protection of actin bundles against the cytoplasmic Ca^{2+} oscillations. Accordingly, it inhibits the ability of ADF/cofilin to disassemble actin filaments [Huang et al., 2005]. Since each of the five villin genes present in the *Arabidopsis* genome (AtVLN1-5) is abundantly expressed in a wide range of tissues [Klahre et al., 2000; Staiger and Hussey, 2004], plant villins are anticipated to fulfill more general functions than the animal villin, whose expression is restricted to epithelial cells [Khurana and George, 2008].

Fimbrins

Fimbrins are composed of two ABDs (ABD1 and ABD2), each containing tandem calponin-homology (CH) domains [Klein et al., 2004; Fig. 1A]. In animals, the presence of a CH domain defines a superfamily of actin crosslinkers including α -actinin, spectrin and dystrophin, which, however, do not exist in plants. Although the ABDs of plant fimbrins show a relatively high degree of conservation with those of non-plant fimbrins, the calcium-binding domain consisting of two EF-hand-like motifs present in mammalian fimbrins is only poorly conserved [Kovar et al., 2000; McCurdy and Staiger, 2000]. Two types of 2D arrays are formed when fimbrin crosslinks AFs on a lipid monolayer, suggesting polymorphism among fimbrin crosslinks [Volkman et al., 2001]. In one type, adjacent AFs are in axial register, whereas in the second, adjacent AFs are axially displaced. In both cases, the close proximity of the two ABDs allows fimbrin to function as a monomer and direct the formation of tightly bundled AF assemblies [Volkman et al., 2001; Klein et al., 2004; Fig. 1B]. A recent model proposes that ABD1 becomes activated for the binding of a second AF after ABD2 is bound to a first filament [Galkin et al., 2008]. Accordingly, a former study using GFP-fused truncated versions of *Arabidopsis* AtFIM1 established the crucial role played by ABD2 in the in vivo F-actin-binding activity [Wang et al., 2004].

To the best of our knowledge, all functional studies on plant fimbrins up to now focused on the same protein,

namely the *Arabidopsis* Fimbrin1 (AtFIM1). In addition, although its actin-binding domains have been largely assessed as actin cytoskeleton markers (see previous section), AtFIM1 itself has drawn less attention than its animal counterparts (called plastins in humans), which are implicated in cell motility and human cancer development [Samstag and Klemke, 2007]. *AtFIM1* is widely expressed throughout the plant body [McCurdy and Kim, 1998]. Kovar et al. [2000] provided biochemical evidence that recombinant AtFIM1 crosslinks AFs into higher-order structures which, however, resemble irregular masses of AFs rather than well-defined longitudinal actin bundles. Consistent with the non-conservative substitutions in the presumptive calcium-binding site [McCurdy and Staiger, 2000], the actin-crosslinking activity of AtFIM1 is independent of the Ca^{2+} concentration [Kovar et al., 2000]. Microinjection of recombinant AtFIM1 in *Tradescantia* stamen cells induces a rapid arrest of both cytoplasmic streaming and strand dynamics, which in turn inhibits the movement of the nucleus [Kovar et al., 2000]. In a co-injection experiment, AtFIM1 antagonizes profilin activity, which normally causes destruction of the cytoplasmic strands and subsequent rejection of the nucleus to the cell wall [Gibbon and Staiger, 2000]. Direct protection of AFs by AtFIM1 against profilin-induced depolymerization is further demonstrated by in vitro analyses. Although AtFIM1 associates with the actin cytoskeleton in diverse cell types, including *Tradescantia* stamen hair cells [Kovar et al., 2001], *Arabidopsis* root cells, tobacco epidermal cells and onion inner epidermal cells [Wang et al., 2004], an increase of the cellular actin-bundling state upon AtFIM1 over-expression is not clearly demonstrated.

Formins

The multifunctional formin family members are characterized by the presence of a formin homology-2 (FH2) domain, which is sufficient to trigger many formin activities, including actin nucleating and barbed-end binding/capping [Wallar and Alberts, 2003, Fig. 1A]. Upstream of their FH2 domain, plant formins contain a relatively variable proline-rich FH1 domain, which functions in binding to profilin and the profilin/actin complex [Blanchoin and Staiger, 2009]. Based on phylogenetic analyses of the conserved FH2 sequences and the organization of their N-terminal domains, *Arabidopsis* formins have been divided into two distinct classes, namely class I and II, although a novel formin class III has been recently identified in non-seed green plants [Cvrckova et al., 2004; Grunt et al., 2008]. Noticeably, class I formins possess a predicted N-terminal membrane insertion signal and a transmembrane region, suggesting an in vivo membrane association [Cvrckova, 2000].

Arabidopsis AtFH1 belongs to the group I of plant formins and is accordingly targeted to the cell membrane by its N-terminal region [Cheung and Wu, 2004]. Over-expression of AtFH1 in pollen tubes stimulates the formation of actin bundles, with an estimated 10-fold increase of the bundle population. As could be expected, most of these bundles project from the cell membrane into the cytoplasm. Together, these data strongly suggest that AtFH1 induces bundle assembly from the cell membrane. The mechanism underlying AtFH1 bundling activity is suggested to be related to the unusual non-processive behavior of this formin observed at filament ends [Michelot et al., 2006]. Indeed, AtFH1 not only has a high affinity for actin-filament barbed ends but it is also able to bind to the side of actin filaments. The mechanism of bundle formation proposed by the authors is similar to the one described for the formation of filopodia-like bundles which implicates a tight coordination between an activated nucleator (the Arp2/3 complex) and a bundler like fascin [Haviv et al., 2006; Vignjevic et al., 2003]. The originality of this model resides in the fact that formin would accomplish both functions [Michelot et al., 2006; Blanchoin and Staiger, 2009; Fig. 1B]. After having nucleated an actin filament, AtFH1 would move from the end to the side of the filament from where it could subsequently nucleate a new filament, and therefore produce (short) actin bundles in anti-parallel orientation. As the filaments elongate, thermal fluctuations would favor filament-filament interactions by a so-called zipper process, inducing the formation of (longer) bundles in parallel orientation. The latter may be further stabilized by other bundling proteins. Such a model accounts for the existence of in vitro bundles in antiparallel orientation near the origin of nucleation, whereas they are in parallel orientation aside from the origin of nucleation [Michelot et al., 2006]. Indeed FH1, and possibly other membrane-associated group I formins (see hereafter), may play crucial roles in the initiation of actin bundles at the plasma membrane, rather than being simple bundle stabilizers. The hypothesized cooperation between different types of plant actin-bundling proteins requires further experimental support, e.g. by analyzing the effects of different combinations of plant actin-bundling proteins on bundle assembly. Although this remains speculative, (some of the) group II formins may promote the assembly of actin bundles from locations other than the plasma membrane [Baluska and Hlavacka, 2005].

A function similar to that of AtFH1 has been suggested for AtFH6, although its actin-bundling activity has not been biochemically characterized [Favery et al., 2004]. The AtFH6 gene has been isolated, together with two other formin genes, from a biological screen aimed at identifying plant cytoskeleton genes involved in the

formation of nematode-induced giant cells. These cells contain abnormally thick actin bundles with longitudinal and transversal orientation, which are mainly localized at the cell cortex. In contrast, cells of uninfected root tissue predominantly exhibit longitudinal AF arrays [de Almeida-Engler et al., 2004]. The potential ability of AtFH6 to trigger a cytoskeletal reorganization was assessed by functional complementation of a yeast mutant deficient for the BNI1p and BNR1p formins, which both control the assembly of yeast actin bundles [Evangelista et al., 2002; Sagot et al., 2002]. Based on its ability to rescue the *bin1Δbnr1Δ* yeast mutant phenotype and on its localization at the plasma membrane, AtFH6 was proposed to be, at least partially, responsible for the assembly of the cortical actin bundles required for vesicle trafficking during the extensive plasma membrane and cell wall biogenesis [Favery et al., 2004].

The over-expression of *Arabidopsis* formin AtFH8 was observed to cause an increase in the overall amount of filamentous actin within root hairs, as well as the precocious extension of actin bundles to the extreme tip [Yi et al., 2005]. In addition, the morphological effects on root hairs resemble those induced on pollen tubes by the over-expression of AtFH1 [Cheung and Wu, 2004], including swelling, defects in polarization and growth arrest. However, direct biochemical evidence of the bundling activity is also missing for AtFH8. Together, these observations emphasize once more the importance of a tight regulation of actin-bundling in tip growth processes and suggest that formins trigger actin bundle initiation at least in tip-growing cells.

LIM Proteins

The LIM domain is a tandem zinc finger motif of (55 amino acids that basically function in protein-protein interactions) [Schmeichel and Beckerle, 1997; Kadmas and Beckerle, 2004]. Whereas animals possess numerous LIM proteins of diverse structures and functions, plants only contain a limited number of LIM proteins [Arnaud et al., 2007]. One family of these proteins is related to the vertebrate cysteine-rich proteins (CRPs), which function as actin-binding and possibly -bundling proteins [Grubinger and Gimona, 2004; Tran et al., 2005]. They are small (200 amino acid long proteins that comprise two well-conserved LIM domains separated by a 40- to 50-residue-long spacer, and a variable C-terminal domain) (Fig. 1A).

Recently, two LIM-containing (LIM) proteins have been proposed to define an additional type of bundling proteins in plants. Biochemical analyses revealed that both tobacco NtWLIM1 and lily LILIM11 bind to, stabilize and bundle AFs in vitro [Thomas et al., 2006; Wang et al., 2008a]. Comparative studies with fimbrin- and talin-derived actin markers indicate that the over-express-

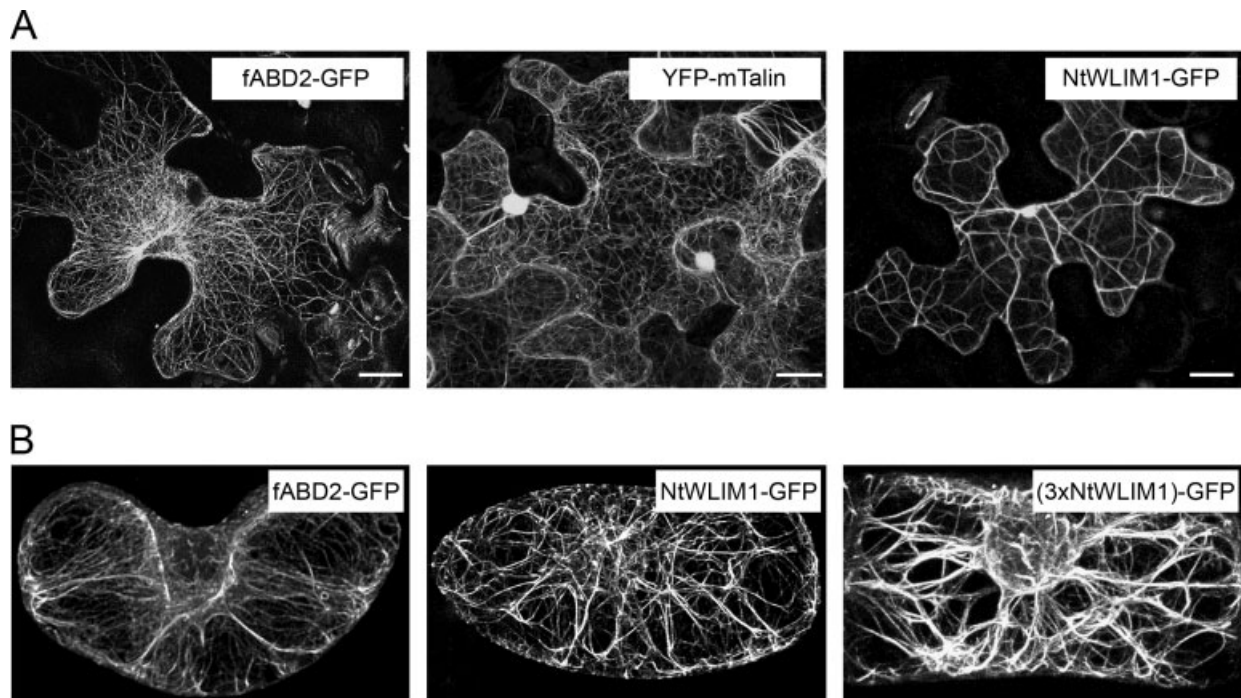


Fig. 2. Tobacco NtWLM1 enhances the cellular actin-bundling state. **A:** Typical fluorescent patterns in *Nicotiana benthamiana* leaf cells expressing fABD2-GFP (control 1), YFP-mTalin (control 2) and NtWLM1-GFP. NtWLM1-GFP induces a reduction of the actin filament/bundle number and a thickening of actin bundles. Figure modified from Thomas C, Hoffmann C, Dieterle M, Van Troys M, Ampe C, Steinmetz A. Tobacco WLM1 is a novel F-actin binding protein involved in actin cytoskeleton remodeling. *Plant Cell* 2006;18:2194–

2206, copyright ASPB. **B:** Typical fluorescent patterns in tobacco BY2 cells expressing fABD2-GFP (control), NtWLM1-GFP and a chimeric protein containing three NtWLM1 copies in tandem (3xNtWLM1-GFP). Notice the very high level of bundling induced by the multi NtWLM1 copy protein. Figure modified from Thomas C, Dieterle M, Gatti S, Hoffmann C, Moreau F, Papuga J, Steinmetz A. Actin bundling via LIM domains. *Plant Signaling Behavior* 2008; 3:320–321.

sion of NtWLM1 increases the actin-bundling state in both tobacco leaf epidermis and BY2 cells [Thomas et al., 2006, 2008, Figs. 2A and 2B, respectively]. Similar effects are reported for transient over-expression of LILIM1 in lily pollen tubes [Wang et al., 2008a]. Interestingly, in the latter, unusual asterisk-shaped actin bundle aggregates appear occasionally in the subapical region. The appearance of these hyper-bundled structures is correlated with defects in targeting of signaling molecules and in endomembrane trafficking, which impairs pollen tube elongation. In addition, pleiotropic tip morphologies are reported upon high expression levels of LILIM1, including abnormal tip, swollen tip and multiple tubes emerging out of a single pollen grain. Importantly, *in vitro* cosedimentation assays indicate that LILIM1 exhibits higher affinity for AFs under low pH and calcium concentration. *In vivo* regulation by pH and calcium is supported since the formation of LILIM1-induced asterisk-shaped actin aggregates exhibits oscillatory changes correlating with pollen tube growth. As LILIM1 is preferentially expressed in pollen and pollen tubes, it is likely contributing to actin bundle formation and/or maintenance in the elongating pollen tube. Sup-

porting a significant role of LIM proteins in pollen tube growth, three out of the six *Arabidopsis* LIM genes are abundantly and almost exclusively expressed in pollen [Eliasson et al., 2000; Arnaud et al., 2007]. In contrast to LILIM1, NtWLM1, which is a non-pollen LIM protein, does not display any obvious regulation by pH and calcium, indicating a different mode of regulation for pollen and non-pollen LIM proteins (our unpublished results). As for the other bundlers, no clear phenotype associated with single and double LIM gene knockouts could be identified (Dieterle et al., unpublished). Also in this case, only simultaneous knock down/out of all the pollen-specific LIM members is expected to yield detectable phenotypes.

Regarding the mechanism underlying LIM protein-mediated actin bundling, each single LIM domain of NtWLM1 is able to autonomously bundle AFs *in vitro*, although with a reduced efficiency compared to the full-length, two-LIM domain containing, protein [Thomas et al., 2007]. From those data, two main models of bundling can be proposed (Fig. 1B). In the first, the two LIM domains of NtWLM1 bind to and bundle the same AF pair, so that the WLM1 body is parallel to the long bun-

dle axis (Fig. 1B, model a). In the second model, each LIM domain crosslinks distinct pairs of AFs so that the WLIM1 body is orthogonal to the long bundle axis (Fig. 1B, model b). As several animal LIM proteins, including CRPs, have been reported to dimerize through their LIM domains [Feuerstein et al., 1994; Arber and Caroni, 1996], WLIM1 dimerization should be considered possible (Fig. 1B, models a' and b'). Interestingly, the expression of a chimeric protein made of three WLIM1 copies in tandem, obviously increases the thickness of actin bundles in tobacco BY2 cells [Thomas et al., 2008; Fig. 2B]. This observation supports the second LIM bundling model (Fig. 1B, model b and b') that predicts that an increase of the LIM domain number within a protein will increase the number of AFs bundled by this protein and consequently amplify bundle thickness.

CONCLUSION

Whereas some of the important roles for actin bundles in plant cells are clearly established, others still require further examination. Here we summarize and briefly discuss the different (potential) functions of plant actin bundles addressed in the above sections:

- Actin-bundling is the process used by cells to build the main long-distance tracks required for vesicle and organelle transport. This function is particularly obvious in tip-growing cells that can reach several centimeters in length. Group I formins are likely to play key roles in the initiation of bundles near/at the plasma membrane, whereas other bundling proteins may rather contribute to stabilize these bundles within the cytoplasm. However, the ability of other formins than AtFH1 to bind to the side of AFs and crosslink those in tight actin bundle should be biochemically addressed.

- Several observations suggest that actin-bundling optimizes the binding of myosin XI and facilitates the movement of the latter, and therefore potentiates intracellular transport. Comparative motility assays using single AFs and AF bundles generated with different actin-bundling proteins are clearly not an easy task to accomplish, given the difficulty to produce recombinant myosins or to purify native ones. Nonetheless, this approach should provide valuable data that would help to resolve the apparent *in vivo* preference of (some) myosins XI for actin bundles.

- The assembly of unipolar actin bundles from newly formed or existing AFs is an important mechanism used to create and/or maintain cell polarity. As an example, it can determine the direction of the cytoplasmic streaming and is responsible for the typical reverse fountain pattern observed in tip-growing cells. However, the mechanism underlying the spatial rearrangement of

AFs/bundles that is required for the stream to change its direction at the subapical zone remains obscure.

- Nuclear positioning and movement in root hairs clearly involve actin bundles from the tube and from the subapical region [Ketelaar et al., 2002]. As these bundle populations are specific to tip-growing cells, further experimentation is required to make sure that actin bundles play similar roles in other cell types. Importantly, the molecular mechanism behind actin-dependent nuclear movement remains unexplored although the participation of myosins has been suggested.

In partial agreement with the former simplistic view considering the cytoskeleton as a rather static structure exclusively devoted to cell architecture maintenance, actin bundles do well serve as backbones in cytoplasmic strands. However, the latter are very dynamic and their remodeling relies on the extraordinary actin cytoskeleton plasticity. In the near future, it will be of interest to determine whether and how AF bundling contributes, together with AF nucleation and polymerization, to generate the force required to initiate and elongate transcytoplasmic strands [van der Honing et al., 2007].

The role of plant actin bundles in various important cell functions becomes evident. In contrast, data regarding plant actin-bundling proteins remains sparse. A rigorous biochemical characterization of not yet studied bundling proteins is required since important differences in the range of activities and regulations within a given family are expected from the already available examples. Calcium ion concentration and pH appear as two important factors that regulate the activity of some pollen actin-bundling proteins. However, the upstream signaling pathways regulating the cellular actin-bundling activity remain unknown. Interestingly, the over-expression of Rac/Rop GTPases (plant Rho GTPases, recently reviewed in Kost [2008]) induces excessive and isotropic growth of pollen tube as well as the formation of extensive actin bundles, whereas a reduction in Rac activity has the opposite effects [Kost et al., 1999; Fu et al., 2001; Chen et al., 2003]. Although these effects are partially mediated by the regulation of ADF activity [Chen et al. 2003], it is conceivable that the Rac/Rop-signaling also target actin-bundling proteins.

How the different plant actin-bundling proteins cooperate to generate bundles of different shapes and properties remain poorly understood. Tip-growing cells appear as excellent working models as they contain spatially distinct populations of highly organized AF bundles and express a wide range of actin-bundling proteins. The simultaneous knock out/down of bundling protein genes belonging to the same or even different families (in the case of similarly expression patterns), as well as the careful analysis of the resulting effects on AF organi-

zation, should reveal possible synergies and provide a clearer view of the *in vivo* functions of each bundling protein family. An ultimate goal would be to correlate such *in vivo* data with the structural features of actin-bundling proteins, e.g. the distance between the ABDs responsible for the bundling activity.

REFERENCES

- Allwood EG, Anthony RG, Smertenko AP, Reichelt S, Drobak BK, Doonan JH, Weeds AG, Hussey PJ. 2002. Regulation of the pollen-specific actin-depolymerizing factor LIADF1. *Plant Cell* 14(11):2915–2927.
- Arber S, Caroni P. 1996. Specificity of single LIM motifs in targeting and LIM/LIM interactions *in situ*. *Genes Dev* 10(3):289–300.
- Arnaud D, Dejardin A, Leple JC, Lesage-Descauses MC, Pilate G. 2007. Genome-wide analysis of LIM gene family in *Populus trichocarpa*, *Arabidopsis thaliana*, and *Oryza sativa*. *DNA Res* 14(3):103–116.
- Augustine RC, Vidali L, Kleinman KP, Bezanilla M. 2008. Actin depolymerizing factor is essential for viability in plants, and its phosphoregulation is important for tip growth. *Plant J* 54(5):863–875.
- Avisar D, Prokhnovsky AI, Makarova KS, Koonin EV, Dolja VV. 2008. Myosin XI-K is required for rapid trafficking of Golgi stacks, peroxisomes, and mitochondria in leaf cells of *Nicotiana benthamiana*. *Plant Physiol* 146(3):1098–1108.
- Baluska F, Hlavacka A. 2005. Plant formins come of age: Something special about cross-walls. *New Phytol* 168(3):499–503.
- Baluska F, Salaj J, Mathur J, Braun M, Jasper F, Samaj J, Chua NH, Barlow PW, Volkmann D. 2000. Root hair formation: F-actin-dependent tip growth is initiated by local assembly of profilin-supported F-actin meshworks accumulated within expansin-enriched bulges. *Dev Biol* 227(2):618–632.
- Baluska F, Jasik J, Edelmann HG, Salajova T, Volkmann D. 2001. Latrunculin B-induced plant dwarfism: Plant cell elongation is F-actin-dependent. *Dev Biol* 231(1):113–124.
- Bamburg JR, McGough A, Ono S. 1999. Putting a new twist on actin: ADF/cofilins modulate actin dynamics. *Trends Cell Biol* 9(9):364–370.
- Banno H, Chua NH. 2000. Characterization of the arabidopsis formin-like protein AFH1 and its interacting protein. *Plant Cell Physiol* 41(5):617–626.
- Bartles JR. 2000. Parallel actin bundles and their multiple actin-bundling proteins. *Curr Opin Cell Biol* 12(1):72–78.
- Blanchoin L, Pollard TD. 1999. Mechanism of interaction of Acanthamoeba actophorin (ADF/Cofilin) with actin filaments. *J Biol Chem* 274(22):15538–15546.
- Blanchoin L, Staiger CJ. 2009. Plant formins: Diverse isoforms and unique molecular mechanism. *Biochim Biophys Acta* (in press).
- Cant K, Knowles BA, Mooseker MS, Cooley L. 1994. Drosophila singed, a fascin homolog, is required for actin bundle formation during oogenesis and bristle extension. *J Cell Biol* 125(2):369–380.
- Cardenas L, Lovy-Wheeler A, Kunkel JG, Hepler PK. 2008. Pollen tube growth oscillations and intracellular calcium levels are reversibly modulated by actin polymerization. *Plant Physiol* 146(4):1611–1621.
- Carlier MF, Laurent V, Santolini J, Melki R, Didry D, Xia GX, Hong Y, Chua NH, Pantaloni D. 1997. Actin depolymerizing factor (ADF/cofilin) enhances the rate of filament turnover: Implication in actin-based motility. *J Cell Biol* 136(6):1307–1322.
- Chen CY, Wong EI, Vidali L, Estavillo A, Hepler PK, Wu HM, Cheung AY. 2002. The regulation of actin organization by actin-depolymerizing factor in elongating pollen tubes. *Plant Cell* 14(9):2175–2190.
- Chen CY, Cheung AY, Wu HM. 2003. Actin-depolymerizing factor mediates Rac/Rop GTPase-regulated pollen tube growth. *Plant Cell* 15(1):237–249.
- Cheung AY, Duan QH, Costa SS, de Graaf BHJ, Di Stilio VS, Feijo J, Wu HM. 2008. The dynamic pollen tube cytoskeleton: Live cell studies using actin-binding and microtubule-binding reporter proteins. *Mol Plant* 1(4):686–702.
- Cheung AY, Wu HM. 2004. Overexpression of an Arabidopsis formin stimulates supernumerary actin cable formation from pollen tube cell membrane. *Plant Cell* 16(1):257–269.
- Cheung AY, Wu HM. 2008. Structural and signaling networks for the polar cell growth machinery in pollen tubes. *Annu Rev Plant Biol* 59:547–572.
- Chytilova E, Macas J, Sliwinska E, Rafelski SM, Lambert GM, Galbraith DW. 2000. Nuclear dynamics in *Arabidopsis thaliana*. *Mol Biol Cell* 11(8):2733–2741.
- Cleary AL. 1995. F-actin redistributions at the division site in living *Tradescantia* stomatal complexes as revealed by microinjection of rhodamine-phalloidin. *Protoplasma* 185(3):152–165.
- Cleary AL, Brian ESG, Wasteneys GO, Hepler PK. 1992. Microtubule and F-actin dynamics at the division site in living *Tradescantia* stamen hair cells. *J Cell Sci* 103:977–988.
- Collings DA, Wasteneys GO. 2005. Actin microfilament and microtubule distribution patterns in the expanding root of *Arabidopsis thaliana*. *Can J Bot* 83:579–590.
- Cvrckova F. 2000. Are plant formins integral membrane proteins? *Genome Biol* 1(1):RESEARCH001.
- Cvrckova F, Novotny M, Pickova D, Zarsky V. 2004. Formin homology 2 domains occur in multiple contexts in angiosperms. *BMC Genomics* 5(1):44.
- de Almeida Engler J, Van Poucke K, Karimi M, De Groot R, Gheysen G, Engler G. 2004. Dynamic cytoskeleton rearrangements in giant cells and syncytia of nematode-infected roots. *Plant J* 38(1):12–26.
- Deeks MJ, Cvrckova F, Machesky LM, Mikitova V, Ketelaar T, Zarsky V, Davies B, Hussey PJ. 2005. Arabidopsis group Ie formins localize to specific cell membrane domains, interact with actin-binding proteins and cause defects in cell expansion upon aberrant expression. *New Phytol* 168(3):529–540.
- Dong CH, Kost B, Xia G, Chua NH. 2001. Molecular identification and characterization of the Arabidopsis AtADF1. AtADFS and AtADF6 genes. *Plant Mol Biol* 45(5):517–527.
- Doris FP, Steer MW. 1996. Effects of fixatives and permeabilisation buffers on pollen tubes: Implications for localization of actin microfilaments using phalloidin staining. *Protoplasma* 195:25–36.
- Dos Remedios CG, Chhabra D, Kekic M, Dedova IV, Tsubakihara M, Berry DA, Nosworthy NJ. 2003. Actin binding proteins: Regulation of cytoskeletal microfilaments. *Physiol Rev* 83(2):443–473.
- Eliasson A, Gass N, Mundel C, Baltz R, Krauter R, Evrard JL, Steinmetz A. 2000. Molecular and expression analysis of a LIM protein gene family from flowering plants. *Mol Gen Genet* 264(3):257–267.
- Evangelista M, Pruyne D, Amberg DC, Boone C, Bretscher A. 2002. Formins direct Arp2/3-independent actin filament assembly to polarize cell growth in yeast. *Nat Cell Biol* 4(1):32–41.
- Favery B, Chelysheva LA, Lebris M, Jammes F, Marmagne A, De Almeida-Engler J, Lecomte P, Vaury C, Arkowitz RA, Abad P. 2004. Arabidopsis formin AtFH6 is a plasma membrane-associated protein upregulated in giant cells induced by parasitic nematodes. *Plant Cell* 16(9):2529–2540.

- Feuerstein R, Wang X, Song D, Cooke NE, Liebhaber SA. 1994. Proc Natl Acad Sci USA 91(22):10655–10659.
- Finka A, Schaefer DG, Saidi Y, Goloubinoff P, Zryd JP. 2007. In vivo visualization of F-actin structures during the development of the moss *Physcomitrella patens*. New Phytol 174(1):63–76.
- Friederich E, Vancompernelle K, Louvard D, Vandekerckhove J. 1999. Villin function in the organization of the actin cytoskeleton. Correlation of in vivo effects to its biochemical activities in vitro. J Biol Chem 274(38):26751–26760.
- Fu Y, Wu G, Yang Z. 2001. Rop GTPase-dependent dynamics of tip-localized F-actin controls tip growth in pollen tubes. J Cell Biol 152(5):1019–1032.
- Galkin VE, Orlova A, Cherepanova O, Lebart MC, Egelman EH. 2008. High-resolution cryo-EM structure of the F-actin-fimbrin/plastin ABD2 complex. Proc Natl Acad Sci USA 105(5):1494–1498.
- Geitmann A, Emons AM. 2000. The cytoskeleton in plant and fungal cell tip growth. J Microsc 198(Part 3):218–245.
- George SP, Wang Y, Mathew S, Srinivasan K, Khurana S. 2007. Dimerization and actin-bundling properties of villin and its role in the assembly of epithelial cell brush borders. J Biol Chem 282(36):26528–26541.
- Gibbon BC, Kovar DR, Staiger CJ. 1999. Latrunculin B has different effects on pollen germination and tube growth. Plant Cell 11(12):2349–2363.
- Gibbon BC, Staiger CJ. 2000. Profilin. In: Staiger CJ, Baluska F, Volkmann D, Barlow P, editors. Actin: A Dynamic Framework for Multiple Plant Cell Functions. First ed; p 676.
- Glenney JR, Jr, Weber K. 1981. Calcium control of microfilaments: Uncoupling of the F-actin-severing and -bundling activity of villin by limited proteolysis in vitro. Proc Natl Acad Sci USA 78(5):2810–2814.
- Grolig F. 1998. Nuclear centering in *Spirogyra*: Force integration by microfilaments along microtubules. Planta 204(1):54–63.
- Grolig F, Pierson ES. 2000. Actin: A dynamic framework for multiple plant cell functions. In: Staiger CJ, Baluska F, Volkmann D, Barlow P, editors. Actin: A Dynamic Framework for Multiple Plant Cell Functions (Developments in Plant and Soil Sciences, 89). Dordrecht, The Netherlands: Kluwer Academic Publishers. pp 165–190.
- Grubinger M, Gimona M. 2004. CRP2 is an autonomous actin-binding protein. FEBS Lett 557(1–3):88–92.
- Grunt M, Zarsky V, Cvrckova F. 2008. Roots of angiosperm formins: The evolutionary history of plant FH2 domain-containing proteins. BMC Evol Biol 8:115.
- Guild GM, Connelly PS, Shaw MK, Tilney LG. 1997. Actin filament cables in *Drosophila* nurse cells are composed of modules that slide passively past one another during dumping. J Cell Biol 138(4):783–797.
- Hachikubo Y, Ito K, Schiefelbein J, Manstein DJ, Yamamoto K. 2007. Enzymatic activity and motility of recombinant Arabidopsis myosin XI. MYA1. Plant Cell Physiol 48(6):886–891.
- Hampton CM, Liu J, Taylor DW, DeRosier DJ, Taylor KA. 2008. The 3D structure of villin as an unusual F-Actin crosslinker. Structure 16(12):1882–1891.
- Harris ES, Rouiller I, Hanein D, Higgs HN. 2006. Mechanistic differences in actin bundling activity of two mammalian formins. FRL1 and mDia2. J Biol Chem 281(20):14383–14392.
- Hashimoto K, Igarashi H, Mano S, Nishimura M, Shimmen T, Yokota E. 2005. Peroxisomal localization of a myosin XI isoform in Arabidopsis thaliana. Plant Cell Physiol 46(5):782–789.
- Haviv L, Brill-Kamiely Y, Mahaffy R, Backouche F, Ben-Shaul A, Pollard TD, Bernheim-Groswasser A. 2006. Reconstitution of the transition from lamellipodium to filopodium in a membrane-free system. Proc Natl Acad Sci USA 103(13):4906–4911.
- He Y, Wetzstein HY. 1995. Fixation induces differential tip morphology and immunolocalization of the cytoskeleton in pollen tubes. Physiol Plant 93:757–763.
- Heintzelman MB, Mooseker MS. 1992. Assembly of the intestinal brush border cytoskeleton. Curr Top Dev Biol 26:93–122.
- Hepler PK, Vidali L, Cheung AY. 2001. Polarized cell growth in higher plants. Annu Rev Cell Dev Biol 17:159–187.
- Heslop-Harrison J, Heslop-Harrison Y. 1989. Actomyosin and movement in the angiosperm pollen tube: An interpretation of some recent results. Sexual Plant Reproduction 2(4):199–207.
- Higaki T, Kutsuna N, Okubo E, Sano T, Hasezawa S. 2006. Actin microfilaments regulate vacuolar structures and dynamics: Dual observation of actin microfilaments and vacuolar membrane in living tobacco BY-2 Cells. Plant Cell Physiol 47(7):839–852.
- Hoffmann A, Nebenfuhr A. 2004. Dynamic rearrangements of trans-vacuolar strands in BY-2 cells imply a role of myosin in remodeling the plant actin cytoskeleton. Protoplasma 224(3–4):201–210.
- Holdaway-Clarke TL, Hepler PK. 2003. Control of pollen tube growth: role of ion gradients and fluxes. New Phytol 159:539–563.
- Holweg C, Susslin C, Nick P. 2004. Capturing in vivo dynamics of the actin cytoskeleton stimulated by auxin or light. Plant Cell Physiol 45(7):855–863.
- Holweg CL. 2007. Living markers for actin block myosin-dependent motility of plant organelles and auxin. Cell Motil Cytoskeleton 64(2):69–81.
- Huang S, Robinson RC, Gao LY, Matsumoto T, Brunet A, Blanchoin L, Staiger CJ. 2005. Arabidopsis VILLIN1 generates actin filament cables that are resistant to depolymerization. Plant Cell 17(2):486–501.
- Hussey PJ, Allwood EG, Smertenko AP. 2002. Actin-binding proteins in the Arabidopsis genome database: Properties of functionally distinct plant actin-depolymerizing factors/cofilins. Philos Trans R Soc Lond B Biol Sci 357(1422):791–798.
- Hussey PJ, Yuan M, Calder G, Khan S, Lloyd CW. 1998. Microinjection of pollen-specific actin-depolymerizing factor, ZmADF1, reorients F-actin strands in *Tradescantia* stamen hair cells. Plant J 14:353–357.
- Ingouff M, Fitz Gerald JN, Guerin C, Robert H, Sorensen MB, Van Damme D, Geelen D, Blanchoin L, Berger F. 2005. Plant formin AtFH5 is an evolutionarily conserved actin nucleator involved in cytokinesis. Nat Cell Biol 7(4):374–380.
- Kadrmaz JL, Beckerle MC. 2004. The LIM domain: from the cytoskeleton to the nucleus. Nat Rev Mol Cell Biol 5(11):920–931.
- Kamiya N. 1981. Physical and Chemical Basis of Cytoplasmic Streaming. Annual Rev Plant Physiol 32(1):205.
- Kennard JL, Cleary AL. 1997. Pre-mitotic nuclear migration in subsidiary mother cells of *Tradescantia* occurs in G1 of the cell cycle and requires F-actin. Cell Motil Cytoskeleton 36(1):55–67.
- Kersey YM. 1974. Correlation of polarity of actin filaments with protoplasmic streaming in Characean algae. J Cell Biol 63(2, Pt. 2): 165 a (abstract).
- Kersey YM, Hepler PK, Palevitz BA, Wessells NK. 1976. Polarity of actin filaments in Characean algae. Proc Natl Acad Sci USA 73(1):165–167.
- Ketelaar T, Faivre-Moskalenko C, Esseling JJ, de Ruijter NC, Grierson CS, Dogterom M, Emons AM. 2002. Positioning of nuclei in Arabidopsis root hairs: An actin-regulated process of tip growth. Plant Cell 14(11):2941–2955.

- Ketelaar T, de Ruijter NC, Emons AM. 2003. Unstable F-actin specifies the area and microtubule direction of cell expansion in Arabidopsis root hairs. *Plant Cell* 15(1):285–292.
- Ketelaar T, Allwood EG, Anthony R, Voigt B, Menzel D, Hussey PJ. 2004. The actin-interacting protein AIP1 is essential for actin organization and plant development. *Curr Biol* 14(2):145–149.
- Ketelaar T, Allwood EG, Hussey PJ. 2007. Actin organization and root hair development are disrupted by ethanol-induced over-expression of Arabidopsis actin interacting protein 1 (AIP1). *New Phytol* 174(1):57–62.
- Khurana S, George SP. 2008. Regulation of cell structure and function by actin-binding proteins: Villin's perspective. *FEBS Lett* 582(14):2128–2139.
- Klahre U, Friederich E, Kost B, Louvard D, Chua NH. 2000. Villin-like actin-binding proteins are expressed ubiquitously in Arabidopsis. *Plant Physiol* 122(1):35–48.
- Klein MG, Shi W, Ramagopal U, Tseng Y, Wirtz D, Kovar DR, Staiger CJ, Almo SC. 2004. Structure of the actin crosslinking core of fimbrin. *Structure* 12(6):999–1013.
- Kohno T, Chaen S, Shimmen T. 1990. Characterization of the translocator associated with pollen tube organelles. *Protoplasma* 154:179–183.
- Kohno T, Shimmen T. 1988a. Accelerated sliding of pollen tube organelles along Characeae actin bundles regulated by Ca²⁺. *J Cell Biol* 106(5):1539–1543.
- Kohno T, Shimmen T. 1988b. Mechanism of Ca inhibition of cytoplasmic streaming in lily pollen tubes. *J Cell Sci* 91:501–509.
- Kost B. 2008. Spatial control of Rho (Rac-Rop) signaling in tip-growing plant cells. *Trends Cell Biol* 18(3):119–127.
- Kost B, Spielhofer P, Chua NH. 1998. A GFP-mouse talin fusion protein labels plant actin filaments in vivo and visualizes the actin cytoskeleton in growing pollen tubes. *Plant J* 16(3):393–401.
- Kost B, Mathur J, Chua NH. 1999. Cytoskeleton in plant development. *Curr Opin Plant Biol* 2(6):462–470.
- Kovar DR, Gibbon BC, McCurdy DW, Staiger CJ. 2001. Fluorescently-labeled fimbrin decorates a dynamic actin filament network in live plant cells. *Planta* 213(3):390–395.
- Kovar DR, Staiger CJ, Weaver EA, McCurdy DW. 2000. AtFim1 is an actin filament crosslinking protein from Arabidopsis thaliana. *Plant J* 24(5):625–636.
- Lenartowska M, Michalska A. 2008. Actin filament organization and polarity in pollen tubes revealed by myosin II subfragment I decoration. *Planta* 228(5):891–896.
- Li JF, Nebenfuhr A. 2007. Organelle targeting of myosin XI is mediated by two globular tail subdomains with separate cargo binding sites. *J Biol Chem* 282(28):20593–20602.
- Li JF, Nebenfuhr A. 2008. Inter-dependence of dimerization and organelle binding in myosin XI. *Plant J* 55(3):478–490.
- Liebe S, Menzel D. 1995. Actomyosin-based motility of endoplasmic reticulum and chloroplasts in Vallisneria mesophyll cells. *Biol Cell* 85(2–3):207–222.
- Lovy-Wheeler A, Wilsen KL, Baskin TI, Hepler PK. 2005. Enhanced fixation reveals the apical cortical fringe of actin filaments as a consistent feature of the pollen tube. *Planta* 221(1):95–104.
- Lovy-Wheeler A, Kunkel JG, Allwood EG, Hussey PJ, Hepler PK. 2006. Oscillatory increases in alkalinity anticipate growth and may regulate actin dynamics in pollen tubes of lily. *Plant Cell* 18(9):2182–2193.
- Lu L, Lee YR, Pan R, Maloof JN, Liu B. 2005. An internal motor kinesin is associated with the Golgi apparatus and plays a role in trichome morphogenesis in Arabidopsis. *Mol Biol Cell* 16(2):811–823.
- Maciver SK, Hussey PJ. 2002. The ADF/cofilin family: Actin-remodeling proteins. *Genome Biol* 3(5):reviews 3007.
- Marty F. 1999. Plant vacuoles. *Plant Cell* 11(4):587–600.
- Mathur J, Spielhofer P, Kost B, Chua N. 1999. The actin cytoskeleton is required to elaborate and maintain spatial patterning during trichome cell morphogenesis in Arabidopsis thaliana. *Development* 126(24):5559–5568.
- McCurdy DW, Kim M. 1998. Molecular cloning of a novel fimbrin-like cDNA from Arabidopsis thaliana. *Plant Mol Biol* 36(1):23–31.
- McCurdy DW, Staiger CJ. 2000. Fimbrin. In: Staiger CJ, Baluska F, Volkmann D, Barlow P, editors. *Actin: A Dynamic Framework for Multiple Plant Cell Functions*. Dordrecht, The Netherlands: Kluwer Academic Publishers, pp 87–102.
- Michelot A, Guerin C, Huang S, Ingouff M, Richard S, Rodiuc N, Staiger CJ, Blanchoin L. 2005. The formin homology 1 domain modulates the actin nucleation and bundling activity of Arabidopsis FORMIN1. *Plant Cell* 17(8):2296–2313.
- Michelot A, Derivery E, Paterski-Boujemaa R, Guerin C, Huang S, Parcy F, Staiger CJ, Blanchoin L. 2006. A novel mechanism for the formation of actin-filament bundles by a nonprocessive formin. *Curr Biol* 16(19):1924–1930.
- Miller DD, De Ruijter NC, Bisseling T, Emons AM. 1999. The role of actin in root hair morphogenesis: Studies with lipochito-oligosaccharide as a growth stimulator and cytochalasin as an actin perturbing drug. *Plant J* 17(2):141–154.
- Moseley JB, Goode BL. 2005. Differential activities and regulation of Saccharomyces cerevisiae formin proteins Bni1 and Bnr1 by Bud6. *J Biol Chem* 280(30):28023–28033.
- Nakayasu T, Yokota E, Shimmen T. 1998. Purification of an actin-binding protein composed of 115-kDa polypeptide from pollen tubes of lily. *Biochem Biophys Res Commun* 249(1):61–65.
- Nebenfuhr A, Gallagher LA, Dunahay TG, Frohlick JA, Mazurkiewicz AM, Meehl JB, Staehelin LA. 1999. Stop-and-go movements of plant Golgi stacks are mediated by the acto-myosin system. *Plant Physiol* 121(4):1127–1142.
- Ono S. 2003. Regulation of actin filament dynamics by actin depolymerizing factor/cofilin and actin-interacting protein 1: New blades for twisted filaments. *Biochemistry* 42(46):13363–13370.
- Palevitz BA. 1987. Actin in the preprophase band of Allium cepa. *J Cell Biol* 104(6):1515–1519.
- Palevitz BA, Hepler PK. 1975. Identification of actin in situ at the ectoplasm-endoplasm interface of Nitella. Microfilament-chloroplast association. *J Cell Biol* 65(1):29–38.
- Palevitz BA, Ash JF, Hepler PK. 1974. Actin in the green alga Nitella. *Proc Natl Acad Sci USA* 71(2):363–366.
- Paves H, Truve E. 2007. Myosin inhibitors block accumulation movement of chloroplasts in Arabidopsis thaliana leaf cells. *Protoplasma* 230(3–4):165–169.
- Pavlov D, Muhrad A, Cooper J, Wear M, Reisler E. 2007. Actin filament severing by cofilin. *J Mol Biol* 365(5):1350–1358.
- Peremyslov VV, Prokhnevsky AI, Avisar D, Dolja VV. 2008. Two class XI myosins function in organelle trafficking and root hair development in Arabidopsis. *Plant Physiol* 146(3):1109–1116.
- Pollard TD. 2007. Regulation of actin filament assembly by Arp2/3 complex and formins. *Annu Rev Biophys Biomol Struct* 36:451–477.
- Puius YA, Mahoney NM, Almo SC. 1998. The modular structure of actin-regulatory proteins. *Curr Opin Cell Biol* 10(1):23–34.
- Reisen D, Hanson MR. 2007. Association of six YFP-myosin XI-tail fusions with mobile plant cell organelles. *BMC Plant Biol* 7:6.
- Ren H, Xiang Y. 2007. The function of actin-binding proteins in pollen tube growth. *Protoplasma* 230(3–4):171–182.

- Riedl J, Crevenna AH, Kessenbrock K, Yu JH, Neukirchen D, Bista M, Bradke F, Jenne D, Holak TA, Werb Z, et al. 2008. Lifeact: A versatile marker to visualize F-actin. *Nat Methods* 5(7):605–607.
- Romagnoli S, Cai G, Cresti M. 2003. In vitro assays demonstrate that pollen tube organelles use kinesin-related motor proteins to move along microtubules. *Plant Cell* 15(1):251–269.
- Romagnoli S, Cai G, Faleri C, Yokota E, Shimmen T, Cresti M. 2007. Microtubule- and actin filament-dependent motors are distributed on pollen tube mitochondria and contribute differently to their movement. *Plant Cell Physiol* 48(2):345–361.
- Russell LD, Peterson RN. 1985. Sertoli cell junctions: Morphological and functional correlates. *Int Rev Cytol* 94:177–211.
- Ruthardt N, Gulde N, Spiegel H, Fischer R, Emans N. 2005. Four-dimensional imaging of transvacuolar strand dynamics in tobacco BY-2 cells. *Protoplasma* 225(3–4):205–215.
- Sagot I, Klee SK, Pellman D. 2002. Yeast formins regulate cell polarity by controlling the assembly of actin cables. *Nat Cell Biol* 4(1):42–50.
- Samaj J, Peters M, Volkmann D, Baluska F. 2000. Effects of myosin ATPase inhibitor 2, 3-butanedione 2-monoxime on distributions of myosins, F-actin, microtubules, and cortical endoplasmic reticulum in maize root apices. *Plant Cell Physiol* 41(5):571–582.
- Samstag Y, Klemke M. 2007. Ectopic expression of L-plastin in human tumor cells: diagnostic and therapeutic implications. *Adv Enzyme Regul* 47:118–126.
- Sano T, Higaki T, Oda Y, Hayashi T, Hasezawa S. 2005. Appearance of actin microfilament ‘twin peaks’ in mitosis and their function in cell plate formation, as visualized in tobacco BY-2 cells expressing GFP-fimbrin. *Plant J* 44(4):595–605.
- Schmeichel KL, Beckerle MC. 1997. Molecular dissection of a LIM domain. *Mol Biol Cell* 8(2):219–230.
- Schmit AC, Lambert AM. 1990. Microinjected fluorescent phalloidin in vivo reveals the F-actin dynamics and assembly in higher plant mitotic cells. *Plant Cell* 2(2):129–138.
- Sheahan MB, Staiger CJ, Rose RJ, McCurdy DW. 2004. A green fluorescent protein fusion to actin-binding domain 2 of Arabidopsis fimbrin highlights new features of a dynamic actin cytoskeleton in live plant cells. *Plant Physiol* 136(4):3968–3978.
- Sheahan MB, Rose RJ, McCurdy DW. 2007. Actin-filament-dependent remodeling of the vacuole in cultured mesophyll protoplasts. *Protoplasma* 230(3–4):141–152.
- Shibayama T, Carboni JM, Mooseker MS. 1987. Assembly of the intestinal brush border: Appearance and redistribution of microvillar core proteins in developing chick enterocytes. *J Cell Biol* 105(1):335–344.
- Shimmen T. 2007. The sliding theory of cytoplasmic streaming: Fifty years of progress. *J Plant Res* 120(1):31–43.
- Shimmen T, Yokota E. 2004. Cytoplasmic streaming in plants. *Curr Opin Cell Biol* 16(1):68–72.
- Shimmen T, Hamatani M, Saito S, Yokota E, Mimura T, Fusetani N, Karaki H. 1995. Roles of actin filaments in cytoplasmic streaming and organization of transvacuolar strands in root hair cells of *Hydrocharis*. *Protoplasma* 185:188–193.
- Smertenko AP, Hussey PJ. 2008. Immunolocalization of proteins in somatic embryos: Applications for studies on the cytoskeleton. *Methods Mol Biol* 427:157–171.
- Smith LG, Oppenheimer DG. 2005. Spatial Control of Cell Expansion by the Plant Cytoskeleton. *Annu Rev Cell Dev Biol* 21:271–295.
- Staiger CJ, Hussey PJ. 2004. Actin and actin-modulating proteins. In: Hussey PJ, editor. *The Plant Cytoskeleton in Cell Differentiation and Development*. Oxford: Blackwell Publishers, pp 32–80.
- Staiger CJ, Yuan M, Valenta R, Shaw PJ, Warn RM, Lloyd CW. 1994. Microinjected profilin affects cytoplasmic streaming in plant cells by rapidly depolymerizing actin microfilaments. *Curr Biol* 4(3):215–219.
- Su H, Wang T, Dong H, Ren H. 2007. The Villin/Gelsolin/Fragmin Superfamily Proteins in Plants. *J Integr Plant Biol* 49(8):1183–1191.
- Thimann KV, Reese K, Nachmias VT. 1992. Actin and the elongation of plant cells. *Protoplasma* 171(3):153–166.
- Thomas C, Hoffmann C, Dieterle M, Van Troys M, Ampe C, Steinmetz A. 2006. Tobacco WLIM1 is a novel F-actin binding protein involved in actin cytoskeleton remodeling. *Plant Cell* 18(9):2194–2206.
- Thomas C, Moreau F, Dieterle M, Hoffmann C, Gatti S, Hofmann C, Van Troys M, Ampe C, Steinmetz A. 2007. The LIM domains of WLIM1 define a new class of actin bundling modules. *J Biol Chem* 282(46):33599–33608.
- Thomas C, Dieterle M, Gatti S, Hoffmann C, Moreau F, Papuga J, Steinmetz A. 2008. Actin bundling via LIM domains. *Plant Signal Behav* 3(5):320–321.
- Tilney LG, Tilney MS, DeRosier DJ. 1992. Actin filaments, stereocilia, and hair cells: How cells count and measure. *Annu Rev Cell Biol* 8:257–274.
- Tilney LG, Tilney MS, Guild GM. 1995. F actin bundles in *Drosophila* bristles. I. Two filament cross-links are involved in bundling. *J Cell Biol* 130(3):629–638.
- Tilney LG, Connelly P, Smith S, Guild GM. 1996. F-actin bundles in *Drosophila* bristles are assembled from modules composed of short filaments. *J Cell Biol* 135(5):1291–1308.
- Tominaga M, Yokota E, Vidali L, Sonobe S, Hepler PK, Shimmen T. 2000. The role of plant villin in the organization of the actin cytoskeleton, cytoplasmic streaming and the architecture of the transvacuolar strand in root hair cells of *Hydrocharis*. *Planta* 210(5):836–843.
- Tominaga M, Kojima H, Yokota E, Orii H, Nakamori R, Katayama E, Anson M, Shimmen T, Oiwa K. 2003. Higher plant myosin XI moves processively on actin with 35 nm steps at high velocity. *EMBO J* 22(6):1263–1272.
- Tran TC, Singleton C, Fraley TS, Greenwood JA. 2005. Cysteine-rich protein 1 (CRP1) regulates actin filament bundling. *BMC Cell Biol* 6(1):45.
- Tseng Y, Kole TP, Lee JS, Fedorov E, Almo SC, Schafer BW, Wirtz D. 2005. How actin crosslinking and bundling proteins cooperate to generate an enhanced cell mechanical response. *Biochem Biophys Res Commun* 334(1):183–192.
- van der Honing HS, Emons AM, Ketelaar T. 2007. Actin based processes that could determine the cytoplasmic architecture of plant cells. *Biochim Biophys Acta* 1773(5):604–614.
- Van Gestel K, Kohler RH, Verbelen JP. 2002. Plant mitochondria move on F-actin, but their positioning in the cortical cytoplasm depends on both F-actin and microtubules. *J Exp Bot* 53(369):659–667.
- Van Troys M, Vandekerckhove J, Ampe C. 1999. Structural modules in actin-binding proteins: towards a new classification. *Biochim Biophys Acta* 1448(3):323–348.
- Van Troys M, Huyck L, Leyman S, Dhaese S, Vandekerckhove J, Ampe C. 2008. Ins and outs of ADF/cofilin activity and regulation. *Eur J Cell Biol* 87(8–9):649–667.
- Vidali L, Hepler PK. 2001. Actin and pollen tube growth. *Protoplasma* 215(1–4):64–76.
- Vidali L, McKenna ST, Hepler PK. 2001. Actin polymerization is essential for pollen tube growth. *Mol Biol Cell* 12(8):2534–2545.

- Vidali L, Yokota E, Cheung AY, Shimmen T, Hepler PK. 1999. The 135-kDa actin-bundling protein from *Lilium longiflorum* pollen is the plant homolog of villin. *Protoplasma* 209:283–291.
- Vignjevic D, Yazar D, Welch MD, Peloquin J, Svitkina T, Borisy GG. 2003. Formation of filopodia-like bundles in vitro from a dendritic network. *J Cell Biol* 160(6):951–962.
- Vitha S, Baluska F, Braun M, Samaj J, Volkmann D, Barlow PW. 2000. Comparison of cryofixation and aldehyde fixation for plant actin immunocytochemistry: Aldehydes do not destroy F-actin. *Histochem J* 32(8):457–466.
- Vogl AW, Pfeiffer DC, Redenbach DM. 1991. Ectoplasmic (“junctional”) specializations in mammalian Sertoli cells: Influence on spermatogenic cells. *Ann N Y Acad Sci* 637:175–202.
- Voigt B, Timmers AC, Samaj J, Muller J, Baluska F, Menzel D. 2005. GFP-FABD2 fusion construct allows in vivo visualization of the dynamic actin cytoskeleton in all cells of *Arabidopsis* seedlings. *Eur J Cell Biol* 84(6):595–608.
- Volkmann N, DeRosier D, Matsudaira P, Hanein D. 2001. An atomic model of actin filaments cross-linked by fimbrin and its implications for bundle assembly and function. *J Cell Biol* 153(5):947–956.
- Waller BJ, Alberts AS. 2003. The formins: Active scaffolds that remodel the cytoskeleton. *Trends Cell Biol* 13(8):435–446.
- Waller F, Riemann M, Nick P. 2002. A role for actin-driven secretion in auxin-induced growth. *Protoplasma* 219(1–2):72–81.
- Walter N, Holweg CL. 2008. Head-neck domain of *Arabidopsis* myosin XI. MYA2, fused with GFP produces F-actin patterns that coincide with fast organelle streaming in different plant cells. *BMC Plant Biol* 8:74.
- Wang HJ, Wan AR, Jauh GY. 2008a. An actin binding protein, LILIM1, mediates Ca and H regulation of actin dynamics in pollen tubes. *Plant Physiol* 147(4):1619–1636.
- Wang YS, Yoo CM, Blancaflor EB. 2008b. Improved imaging of actin filaments in transgenic *Arabidopsis* plants expressing a green fluorescent protein fusion to the C- and N-termini of the fimbrin actin-binding domain 2. *New Phytol* 177(2):525–536.
- Wang HY, Wang J, Gao P, Jiao GL, Zhao PM, Li Y, Wang GL, Xia GX. 2009. Down-regulation of GhADF1 gene expression affects cotton fibre properties. *Plant Biotechnol J* 7(1):13–23.
- Wang YS, Motes CM, Mohamalawari DR, Blancaflor EB. 2004. Green fluorescent protein fusions to *Arabidopsis* fimbrin 1 for spatio-temporal imaging of F-actin dynamics in roots. *Cell Motil Cytoskeleton* 59(2):79–93.
- Wang YS, Yoo CM, Blancaflor EB. 2008b. Improved imaging of actin filaments in transgenic *Arabidopsis* plants expressing a green fluorescent protein fusion to the C- and N-termini of the fimbrin actin-binding domain 2. *New Phytol*.
- Wang Z, Pesacreta TC. 2004. A subclass of myosin XI is associated with mitochondria, plastids, and the molecular chaperone subunit TCP-1alpha in maize. *Cell Motil Cytoskeleton* 57(4):218–232.
- Wilson LK, Lovy-Wheeler A, Voigt B, Menzel D, Kunkel JG, Hepler PK. 2006. Imaging the actin cytoskeleton in growing pollen tubes. *Sex Plant Reprod* 19(2):51–62.
- Yi K, Guo C, Chen D, Zhao B, Yang B, Ren H. 2005. Cloning and functional characterization of a formin-like protein (AtFH8) from *Arabidopsis*. *Plant Physiol* 138(2):1071–1082.
- Yokota E, Shimmen T. 1999. The 135-kDa actin-bundling protein from lily pollen tubes arranges F-actin into bundles with uniform polarity. *Planta* 209:264–266.
- Yokota E, Muto S, Shimmen T. 2000. Calcium-calmodulin suppresses the filamentous actin-binding activity of a 135-kilodalton actin-bundling protein isolated from lily pollen tubes. *Plant Physiol* 123(2):645–654.
- Yokota E, Takahara K, Shimmen Ki TT. 1998. Actin-bundling protein isolated from pollen tubes of lily. Biochemical and immunocytochemical characterization. *Plant Physiol* 116(4):1421–1429.
- Yokota E, Vidali L, Tominaga M, Tahara H, Orii H, Morizane Y, Hepler PK, Shimmen T. 2003. Plant 115-kDa actin-filament bundling protein, P-115-ABP, is a homologue of plant villin and is widely distributed in cells. *Plant Cell Physiol* 44(10):1088–1099.
- Yokota E, Tominaga M, Mabuchi I, Tsuji Y, Staiger CJ, Oiwa K, Shimmen T. 2005. Plant Villin, Lily P-135-ABP, possesses g-actin binding activity and accelerates the polymerization and depolymerization of actin in a Ca^{2+} -sensitive manner. *Plant Cell Physiol* 46(10):1690–1703.
- Yokota E, Ueda S, Tamura K, Orii H, Uchi S, Sonobe S, Hara-Nishimura I, Shimmen T. 2009. An isoform of myosin XI is responsible for the translocation of endoplasmic reticulum in tobacco cultured BY-2 cells. *J Exp Bot* 60(1):197–212.
- Yu M, Yuan M, Ren H. 2006. Visualization of actin cytoskeletal dynamics during the cell cycle in tobacco (*Nicotiana tabacum* L. cv Bright Yellow) cells. *Biol Cell* 98(5):295–306.
- Zhang D, Wadsworth P, Hepler PK. 1993. Dynamics of microfilaments are similar, but distinct from microtubules during cytokinesis in living, dividing plant cells. *Cell Motility and the Cytoskeleton* 24(3):151–155.

2. Last developments in plant actin-bundling

The following section updates the above review article by summarizing the most significant information that has been published on plant actin-bundling proteins since 2009. It is noteworthy that these two last years were particularly productive and that the data produced strongly support a significant role in actin-bundling for each of the four families described in our review article.

Villins. Khurana et al. (2010) provide evidence that AtVLN1 and AtVLN3 exhibit overlapping and distinct activities. Noticeably, *in vitro* activities of both villins were examined in a direct manner by total internal reflection fluorescence (TIRF) microscopy. AtVLN1 was found to function as a simple Ca²⁺-insensitive actin-bundling protein, whereas AtVLN3 was shown to sever actin filaments and bundles in a Ca²⁺-dependent manner.

Zhang et al. (2010) functionally characterised the pollen-enriched AtVLN5 protein. The latter was reported to combine barbed-end capping, actin-bundling and Ca²⁺-dependent severing activities. VLN5 loss-of-function retarded pollen tube growth and sensitized actin filaments in pollen grains and tubes to the actin-depolymerising drug latrunculin B.

The above data confirm the central roles played by plant villins and further illustrate that members of one actin-binding family can have distinct activities and respond differently to regulatory factors.

Fimbrins. Wu et al. (2010) characterised an additional *Arabidopsis* fimbrin isoform, namely AtFIM5. The latter was shown to be preferentially expressed in pollen and to exhibit actin-binding, -stabilising and -bundling activities. Noticeably AtFIM5-GFP decorates actin filaments throughout mature pollen grains and growing pollen tubes. Actin bundles are disorganised in pollen grains and, surprisingly, protruded into the tip of pollen tube in *fim5* mutants resulting in a delay in pollen germination and inhibition of pollen tube growth. In addition, both the direction and the velocity of cytoplasmic streaming were significantly modified in *fim5* pollen tubes. Together these data strongly support the previous assumptions that plant fimbrins define a major family of actin bundlers (Kovar et al., 2000).

Formins. Ye et al. (2009) combined *in vitro* biochemical and genetic approaches to investigate the function of the pollen-specific AtFH3, a class I formin. They showed that the FH1FH2 domain of AtFH3 nucleates actin filaments and binds to their barbed-end, thereby preventing actin polymerisation and depolymerisation from this end *in vitro*. They also demonstrated that AtFH3 is required for the assembly of actin bundles in pollen tubes and that the disruption of these bundles caused by RNAi-induced down-regulation of AtFH3 is associated with an inhibition of cytoplasmic streaming as well as with growth depolarisation. This provides direct evidence that AtFH3-induced bundles are involved in the regulation of cytoplasmic streaming and polarized pollen tube growth.

Cheung et al. (2010) showed that the pollen tube tip-located *Arabidopsis* formin AtFH5 is responsible for actin assembly in the subapical region of pollen tubes. They proposed that AtFH5 plays a pivotal role in establishing the subapical actin and apical vesicular organisation, which is critical for tip-focused growth in pollen tubes.

Very recently, Martinière et al. (2011) have established the role of the extracellular domain of AtFH1. They demonstrate that AtFH1 forms a bridge from the actin cytoskeleton, across the plasma membrane and is anchored within the cell wall. Anchoring of AtFH1 in the cell wall is correlated with increased actin-bundling and the overexpression of AtFH1 has an inhibitory effect on actin-dependent organelle dynamics. The AtFH1 bridge provides stable anchor points for the actin cytoskeleton and is probably a crucial component of the signalling response and actin-remodelling mechanisms.

Finally, two recent studies on the class I AtFH4 (Deeks et al., 2010) and the class II AtFH14 (Li et al., 2010) revealed that these formins also interact with microtubules suggesting that they are involved in the coordination of the actin and microtubule cytoskeleton.

In conclusion, formins emerge as central actin nucleators in plants, especially in pollen which has received much attention because of its tip-localised mode of growth. Noticeably, formins promote the assembly of actin filaments which subsequently assemble into bundles. However, it remains unclear to what extent formins contribute to the crosslinking of actin filaments itself.

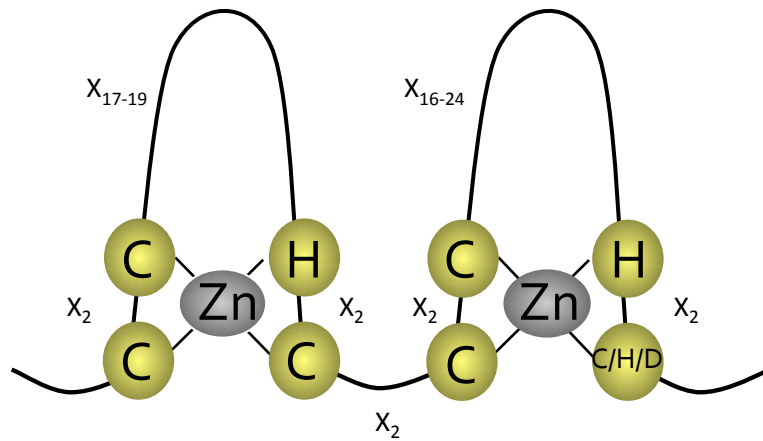


Figure 6: The LIM domain is a tandem zinc finger motif.

The LIM domain is a two-zinc finger motif composed of about 55 amino acids. Zinc is indicated in grey and zinc ligands in yellow. Zn: zinc ion, C: cysteine, H: histidine, D: aspartic acid, X: amino acid.

A novel actin-bundling protein in plants

Whippo et al. (2011) have recently identified THRUMIN1 as a novel class of plant actin-bundling protein involved in chloroplast motility. THRUMIN1 belongs to a family of proteins found in plants and animals that contain conserved C-terminal glutaredoxin-like, putative zinc-binding cysteine-rich domains and proline-rich region in the N-terminal domain (Navrot et al. 2006). *In vitro* biochemical analyses as well as fluorescence light microscopy established that THRUMIN1 exhibits actin-binding and -bundling activities. THRUMIN1 localises at the plasma membrane and displays light- and phototropin-dependent actin filament binding activity. These results suggest that THRUMIN1 is involved in the bundling of actin filaments at the plasma membrane in response to blue light perceived by the phototropin photoreceptors (Whippo et al., 2011).

IV. Plant LIM proteins

1. Generalities

The name LIM derived from the first letter of the proteins in which the LIM domain was historically identified: *Caenorhabditis elegans* LIN-11 (Freyd et al., 1990), rat ISL-1 (Karlsson et al., 1990) and *Caenorhabditis elegans* MEC-3 (Way and Chalfie, 1988). The LIM domain basically consists of a tandem zinc finger motif composed of approximately 55 amino acids that was rapidly recognised to function as a protein-protein interaction module (Schmeichel and Beckerle, 1997; Kadrmas and Beckerle, 2004). The consensus sequence of the LIM domain has been identified in plants as well as in animals as [C-X₂-C-X₁₇₋₁₉-H-X₂-C]-X₂-[C-X₂-C-X₁₆₋₂₄-C-X₂-(C,D,H)] (Figure 6; Eliasson et al., 2000). The LIM domain is present in a wide variety of eukaryotic proteins. For instance, the human genome comprises more than 135 LIM domain-encoding sequences corresponding to about 60 different proteins. LIM proteins contain 1 to 5 LIM domains that are associated or not with other domains including homeodomains, catalytic domains (e.g. a kinase domain), cytoskeleton-binding domains or other protein-binding domains (e.g. SH3 or LD domains; Kadrmas and Beckerle, 2004). In contrast to humans and vertebrates, plants

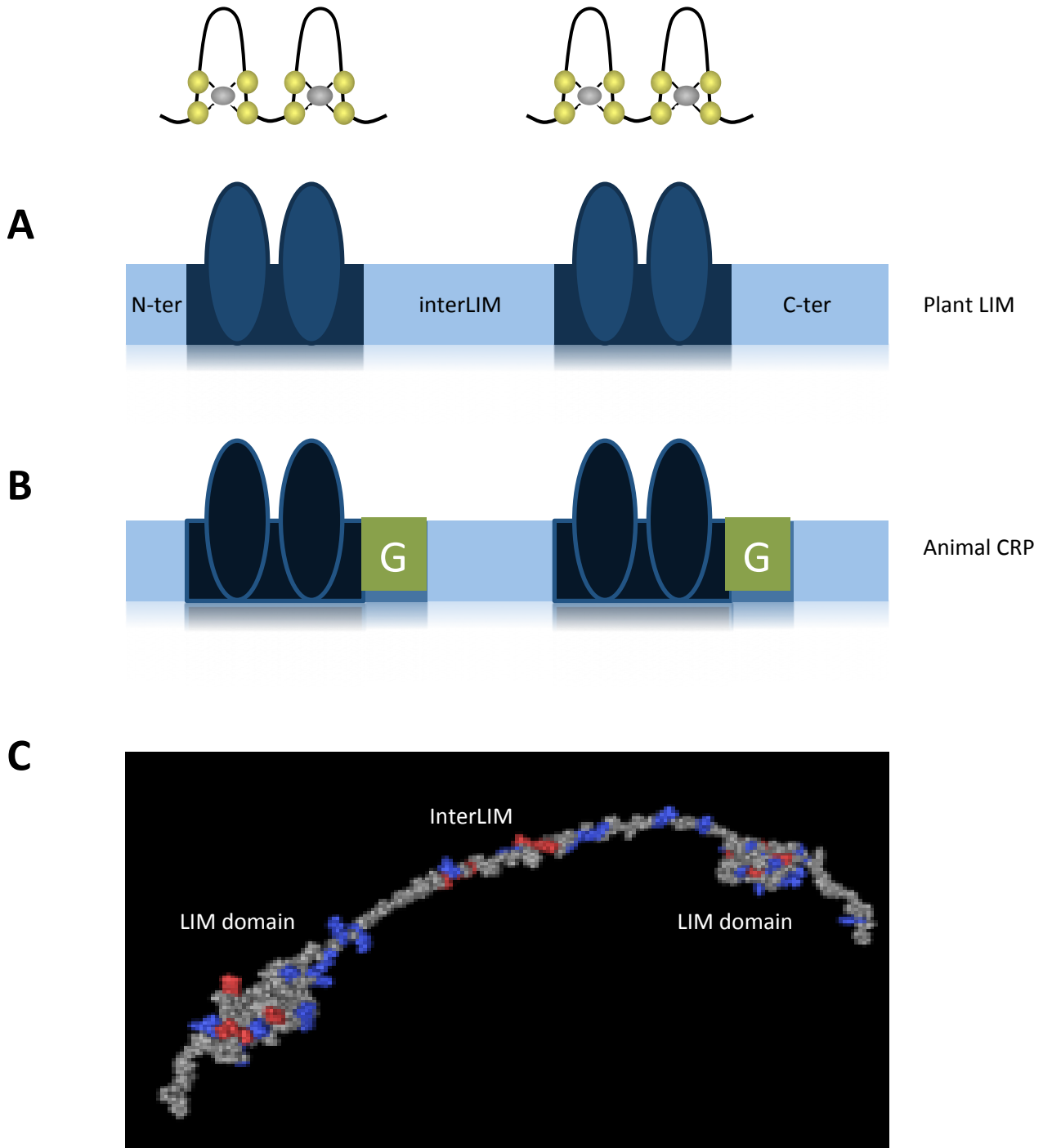


Figure 7: Domain organisation of plant and animal two LIM domain-containing proteins.

(A) Typical domain organisation of plant LIM proteins (LIMs).

(B) Typical domain organisation of animal cysteine-rich proteins (CRPs). The glycine-rich repeat (G) is only present in CRPs.

(C) Solution structure of the chicken CRP1 showing that the interLIM spacer is highly flexible. Adapted from Yao et al. (1999).

G: glycine-rich region.

contain only a limited number of LIM proteins (Arnaud et al., 2007). Two distinct families of plant LIM proteins have been identified: the plant-specific and yet poorly understood LIM-RING-like family whose members combine one LIM domain, one RING-like domain and frequently several ubiquitin interacting motifs (Li et al., 2008), and the two-LIM domain-containing proteins (hereafter referred to as plant LIMs) family. Plant LIMs are structurally related to the vertebrate cysteine-rich protein (CRP) LIM subfamily (Baltz et al., 1992; Eliasson et al., 2000). CRP-related proteins have also been identified in insects (Stronach et al., 1996) and protozoa (Khurana et al., 2002), indicating that these proteins participate in important processes conserved in eukaryotes. Plant LIMs and vertebrate CRPs are rather small proteins of about 200 amino acids that basically consist of two LIM domains with > 50% sequence identity, a 40- to 50-residue-long interLIM spacer and a relatively variable C-terminal domain (Figure 7A-B). Contrary to the animal CRPs, plant LIMs have a longer C-terminal domain and lack the glycine-rich region following each LIM domain. Nuclear Magnetic Resonance (NMR) solution structures of vertebrate CRPs and of their individual LIM domains have revealed that each LIM domain folds separately and that the interLIM spacer does not adopt any preferential conformation, providing a high degree of liberty to each LIM domain (Figure 7C; Perez-Alvadaro et al., 1994; Hammarstrom et al., 1996; Perez-Alvadaro et al., 1996; Konrat et al. 1998; Kontaxis et al., 1998; Yao et al., 1999; Velyvis et al. 2001; Schallus et al., 2003, 2007).

2. Two differentially expressed subfamilies of plant *LIM* genes

The first gene encoding a plant LIM protein was isolated from sunflower in Steinmetz's laboratory (Baltz et al, 1992a and b). It was first named SF3 and later renamed PLIM1 for pollen LIM protein1 as its expression was restricted to pollen. Subsequent work on plant LIMs has revealed that plants do possess several *LIM* genes that can be classified into two main subfamilies according to their expression pattern. The number of *LIM* genes ranges from six in *Arabidopsis* and rice to twelve in poplar (Arnaud et al., 2007). The so-called *WLIM* (for widely-expressed LIM) genes exhibit a wide expression pattern in vegetative and reproductive tissues but are not or only weakly expressed in pollen (Figure 8; Brière et al., 2003; Eliasson et al., 2000; Mundel et al., 2000; Arnaud et al., 2007). In contrast, the so-called *PLIM* (for pollen

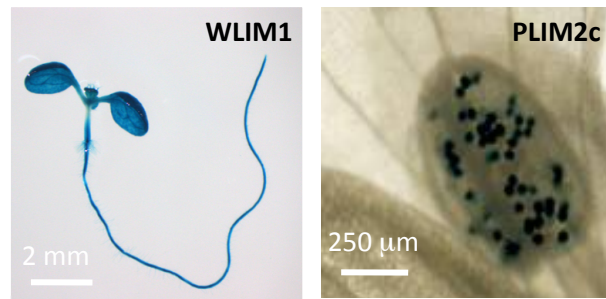


Figure 8: Typical expression patterns of the widely-expressed WLIM1 and pollen PLIM2c proteins.

WLIM1 and *PLIM2* gene expression patterns as visualised by GUS staining in a 7-day-old seedling (left panel) and adult plant flower (right panel) of *Arabidopsis* transgenic lines expressing a GUS reporter gene under the control of *WLIM1* and *PLIM2c* gene regulatory sequences respectively. Adapted from Papuga and Hoffmann et al., 2010.

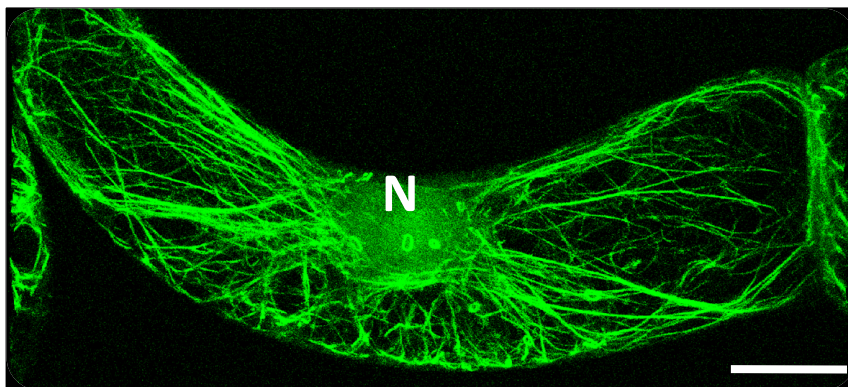


Figure 9: Subcellular localisation of the GFP-fused tobacco WLIM1 protein.

GFP-WLIM1 decorates the actin cytoskeleton in the cytoplasm and accumulates in the nucleoplasm.

Bar = 20 μm . N: nucleus. Adapted from Thomas et al., 2006.

LIM) genes are abundantly and preferentially expressed in pollen grains (Figure 8). Based on a genome-wide analysis of *LIM* genes of various plant species, Arnaud et al. (2007) recently proposed a refined classification of LIM proteins into four groups, which subdivide according to their specificity to a taxonomic class and/or their tissue-specific expression. Interestingly, in poplar, the distribution of ESTs corresponding to some *LIM* genes suggests the involvement of the LIM proteins in wood fibre formation and/or vascular development. Consistent with this hypothesis, a tobacco LIM protein has been suggested to be involved in the regulation of the expression of important lignin biosynthesis genes (Kawaoka et al., 2000; see also § V.4.).

3. Subcellular localisation of LIM proteins

Like their vertebrate counterparts (e.g. Arber and Caroni, 1996), plant LIMs have been found to localise to both the cytoplasm and the nucleus suggesting that they display cytoplasmic as well as nuclear functions (Figure 9; Baltz et al., 1999; Brière et al., 2003; Mundel et al., 2000; Thomas et al., 2006). It is noteworthy that particularly high expression levels of *PLIMs* genes in pollen were indicated by previous studies (Eliasson et al., 2000). It was estimated that mRNA encoding PLIMs make up 3 % of the total mRNA population in mature pollen grains of sunflower. Although immunocytological analyses have shown that sunflower PLIM1 concentrates in the germination cones of mature pollen grains, a region that also contains high amounts of F-actin (Baltz et al., 1999), direct evidence for an interaction between plant LIMs and the actin cytoskeleton was long missing. This was likely due to the poor preservation of the actin cytoskeleton by classical fixation procedures (Kost et al., 1999; Vitha et al., 2000). In addition, recent immunolocalisation experiments performed in our laboratory pointed out that (GFP-fused) LIMs tend to detach from the actin cytoskeleton when submitted to chemical treatments allowing a satisfactory preservation of actin filaments (Moes, personal communication). Our group was the first to report that one plant LIM, namely the tobacco WLIM1, prominently decorates the actin cytoskeleton of live cells when fused to GFP (Figure 9; Thomas et al., 2006). A promising alternative to preserve the structure of the actin cytoskeleton and simultaneously detect (GFP-fused) LIMs on actin filaments is the use of cryofixation (Vitha et al., 2000). It should however be kept in mind that direct immunolocalisation

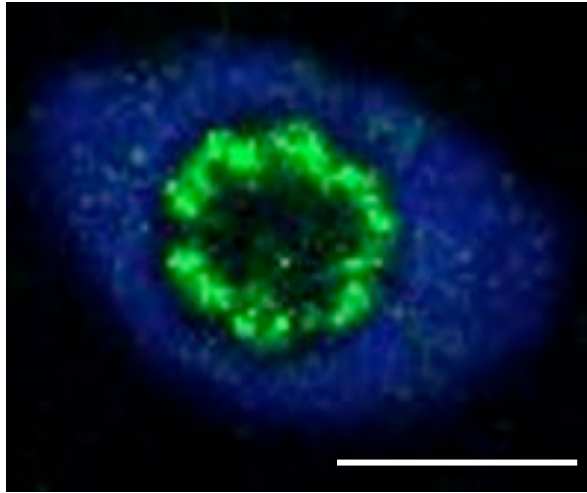


Figure 10: Immunolocalisation of the tobacco WLIM2 in the nucleus of tobacco BY-2.

WLIM2 was immunolocalised using a primary anti-WLIM2 mouse antibody and a secondary anti-mouse goat antibody (Invitrogen). WLIM2 is detected in nucleolar dot-like structures (green). The nucleoplasm is shown in blue (DAPI). The picture is a single confocal plane.

Bar = 10 μm .

of a native plant LIM on the actin cytoskeleton has not been reported yet.

4. Nuclear functions of plant LIMs

In contrast to vertebrate CRPs whose nuclear functions have been largely studied, very little is known about the role of plant LIMs in the nucleus. It has become clear that a common function of CRPs is to associate with DNA-binding transcription complexes and chromatin-modifying factors to modulate gene expression and reprogram cell fate. Most noticeably, CRPs promote the smooth (CRP1 and CRP2) and skeletal (CRP3/MLP) muscle phenotypic switch (e.g. Kong et al., 1997; Chang et al., 2003 and 2007). Until recently, tobacco WLIM1 was the only plant LIM whose nuclear functions were characterised to some extent. Tobacco WLIM1 has been suggested to bind to DNA through a specific PAL-box motif, which is highly conserved in gene promoter sequences of lignin biosynthesis genes (Kawaoka et al., 2000). Consistent with a role of WLIM1 in gene expression regulation, transgenic tobacco plants with a reduced *WLIM1* expression were found to have reduced lignin content and decreased expression of PAL, 4CL and CAD, three enzymes involved in the lignin biosynthesis. Using electrophoretic mobility shift assays, our laboratory recently demonstrated the ability of the tobacco WLIM2 to directly interact with specific sequence regions of the histone H4 promoter (S. Gatti, unpublished data). Importantly, tobacco WLIM2 was shown to be able to trans-activate a reporter gene placed under the control of the histone H4 promoter in *Arabidopsis* protoplasts (D. Moes, unpublished data). Together, these data support that, in the nucleus, plant LIMs regulate the expression of specific genes. Microarray experiments aiming at identifying LIM-regulated genetic pathways are currently conducted in our laboratory.

Additional nuclear functions have been recently pointed out by immunolocalisation (Figure 10) and high-resolution immunolocalisation (stimulated emission depletion microscopy) of tobacco WLIM2 in yet unidentified nucleolar dot-like structures (Moes, unpublished data).

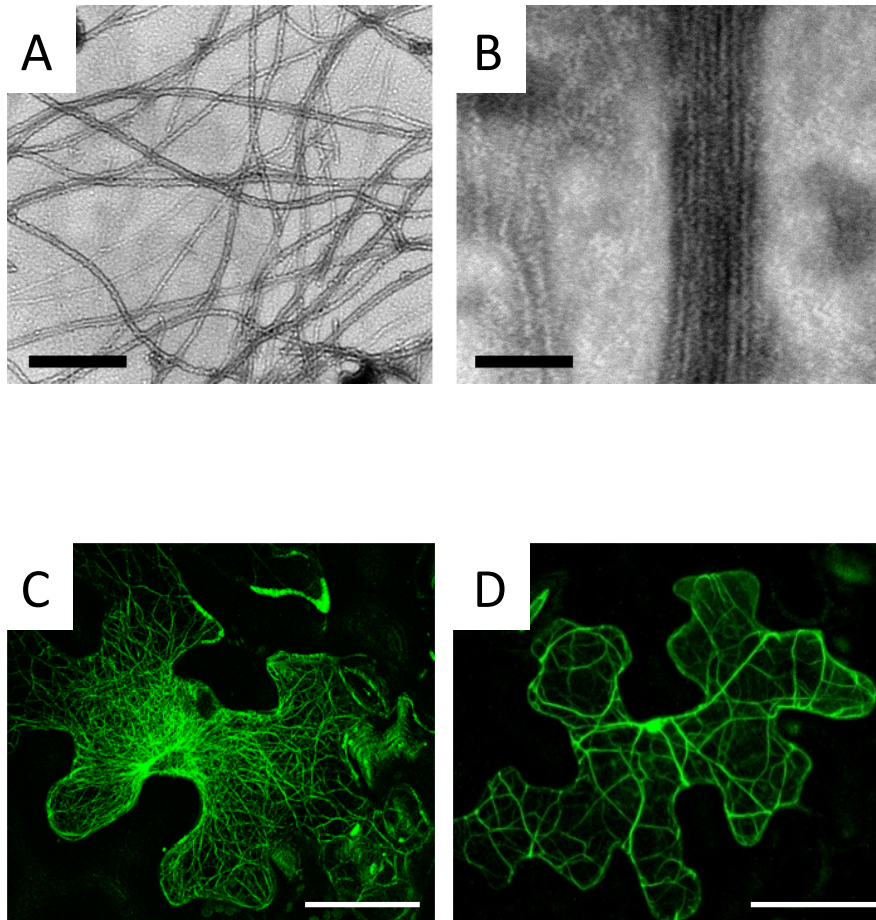


Figure 11: WLIM1-induced actin bundles.

Electron micrographs of negatively stained preparations containing 4 μM actin filaments polymerised in the absence (A) or in the presence of 2 μM purified recombinant NtWLIM1 (B). Bars = 70 nm. Adapted from Thomas et al., 2007.

Typical fluorescence patterns of leaf epidermal cells agro-infiltrated with the fimbrin derived actin marker ABD2-GFP (C) and GFP-WLIM1 (D). Note that WLIM1-GFP induced a reduction of the actin filament/bundle number and a thickening of actin bundles. Bars = 50 μm . Adapted from Thomas et al., 2006.

5. Cytoplasmic functions of plant LIMs

As previously stated, vertebrate CRPs and related plant LIM exhibit a dual nuclear and cytoplasmic localisation pattern. In contrast to their nuclear roles, the cytoplasmic functions have remained enigmatic. Cytoskeletal functions of CRPs have been initially suggested by their predominant localisation to actin filaments and interaction with α -actinin and zyxin, two central actin regulatory proteins (Arber and Caroni, 1996; Louis et al., 1997; Pomiès et al., 1997; Schmeichel and Beckerle, 1998). Although CRPs were reported to stabilise the actin cytoskeleton, this effect has generally been considered as an indirect consequence of the ability of CRPs to potentiate the activities of α -actinin and zyxin. Controversy emerged with increasing evidence that human CRP1 and CRP2 display direct actin-binding activity (Grubinger and Gimona, 2004; Tran et al., 2005; Jang et al., 2009). Supporting this view, our laboratory has demonstrated that the tobacco WLIM1 directly binds to actin filaments and crosslinks the latter into long parallel arrays or actin bundles (Figure 11; Thomas et al., 2006, 2007). More recently, the pollen-enriched lily LIM1 has been reported to display a similar actin regulatory activity (Wang et al., 2008b). It is worth noting that the plant genome does not encode for any α -actinin or zyxin equivalents. Therefore CRPs and plant LIMs emerge as a novel family of actin-binding proteins most likely involved in the crosslinking and stabilisation of actin filaments (Tran et al., 2005; Thomas et al., 2006; Wang et al., 2008b). By a domain analysis, our laboratory has provided evidence that tobacco WLIM1 actin regulatory activities rely on its two LIM domains (the most conserved regions between CRPs and plant LIMs), which function as autonomous actin-binding modules (Thomas et al., 2007).

Interestingly, lily LIM1 overexpression induced an oscillatory formation of asterisk-shaped actin filament aggregates in the subapical region of growing pollen tubes (Wang et al., 2008b). *In vitro* high-speed co-sedimentation assays have suggested that the interaction of LIM and actin filaments is regulated by pH and Ca^{2+} , two central regulators of pollen tube oscillatory growth that are assumed to function through activation/deactivation of several ABPs (Cheung and Wu, 2008; Staiger et al., 2010). Therefore, lily LIM1 has been proposed, along with pH and Ca^{2+} , to be part of the central oscillatory mechanism that regulates actin cytoskeleton remodelling during

pollen tube elongation (Wang et al., 2008b). However, evidence of pH and Ca^{2+} -dependent regulation of lily LIM1 in the context of live cells is lacking.

Chapter 2

Comparative study of the actin cytoskeleton regulatory activities of the *Arabidopsis* LIM protein family members

Chapter 2: Comparative study of the actin cytoskeleton regulatory activities of the *Arabidopsis* LIM protein family members

I. Introduction

These last years, a number of laboratories including ours, have suggested that the plant two LIM domain-containing proteins (LIMs) and related mammalian proteins, namely the cysteine-rich proteins (CRPs), participate in the regulation of the actin cytoskeleton organisation and dynamics (Sadler et al., 1992; Crawford et al., 1994; Arber and Caroni, 1996; Louis et al., 1997; Pomies et al., 1997; Henderson et al., 1999; Weiskirchen and Gunther, 2003; Grubinger and Gimona, 2004; Tran et al., 2005; Thomas et al., 2006; Thomas et al., 2007; Sagave et al., 2008; Wang et al., 2008b; Jang and Greenwood, 2009; Papalouka et al., 2009; Papuga et al., 2010). In plants, tobacco WLIM1 and lily LIM1 have been shown to bind directly to actin filaments and to promote the formation of actin bundles in vegetative tissues and pollen, respectively (Thomas et al., 2006; Thomas et al., 2007; Wang et al., 2008b). Remarkably, plant genomes encode small families of LIMs. A recent detailed phylogenetic analysis has revealed that the *LIM* gene family ranges from six members in *Arabidopsis* and rice to twelve members in poplar (Arnaud et al., 2007). One central question that remains to be answered is: do all plant LIM gene/protein family members play identical/similar actin-regulatory activities and functions?

Although the expression pattern of some *Arabidopsis* *LIM* genes was previously described to some extent (Eliasson et al., 2000) our laboratory has recently conducted a detailed and exhaustive expression analysis including all six members of the *Arabidopsis* *LIM* gene family (Papuga and Hoffmann et al., 2010). Histological examination of transgenic plants expressing a β -glucuronidase (GUS) reporter gene under the control of individual *LIM* gene promoters confirmed the existence of two differentially expressed subfamilies of *Arabidopsis* LIMs. The so-called WLIM, for **W**idely-expressed **LIM** protein gene subfamily, comprises three members, namely *WLIM1*, *WLIM2a* and *WLIM2b*, which exhibit a wide expression pattern in both

vegetative and reproductive tissues with the exception of pollen grains where no or only very weak expression level can be detected. The so-called PLIM, for Pollen LIM protein gene subfamily, comprises the three remaining genes, namely *PLIM2a*, *PLIM2b* and *PLIM2c*, which are abundantly and almost exclusively expressed in pollen grains. In order to establish whether the three *Arabidopsis* WLIMs and the three *Arabidopsis* PLIMs all trigger similar actin-regulatory activities, we have conducted an exhaustive comparative study.

In this chapter, we provide evidence that the six members of the *Arabidopsis* LIM family function as “true” actin-binding proteins that stabilise and crosslink actin filaments into bundles. Transgenic plants overexpressing individual *Arabidopsis* LIM fused to the Green Fluorescent Protein (GFP-LIM) have been produced and analysed. Confocal microscope analyses revealed that the six fusion proteins decorated a filamentous network whose nature was examined. Both co-localisation experiments and F-actin disrupting drug-based assays established that *Arabidopsis* LIMs interact with the actin cytoskeleton. The actin cytoskeleton of transgenic *Arabidopsis* plants overexpressing GFP-LIMs exhibited an increased level of actin bundling. High-speed co-sedimentation assays showed that recombinant WLIMs and PLIMs bind to actin filaments in a direct manner although with different affinities. Depolymerisation and low-speed co-sedimentation assays established that the six LIMs efficiently stabilise and crosslink actin filaments into higher-order structures. The latter were readily identified as being actin bundles by direct microscope visualisation. Together these data indicate that the six *Arabidopsis* LIMs promote the formation actin bundling *in vitro* as well as *in vivo*.

II. The six *Arabidopsis* LIMs are actin-binding proteins

1. Production and characterisation of GFP-fused LIM expressing *Arabidopsis* lines

To investigate the subcellular localisation of the six *Arabidopsis* LIMs, transgenic *Arabidopsis* lines expressing individual LIMs fused to the GFP under the control of the constitutive cauliflower mosaic virus (CaMV) 35S promoter were produced by floral dip (Clough and Bent, 1998). GFP expression in hygromycin

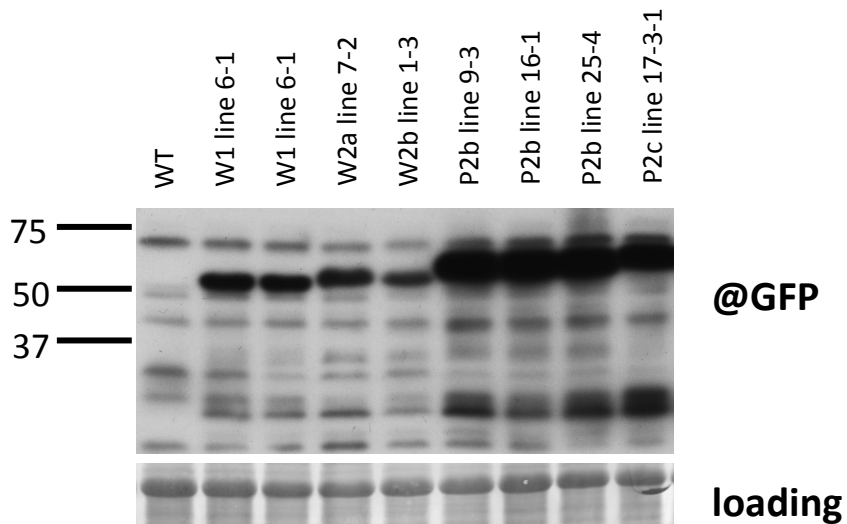


Figure 12: Detection of GFP-LIM fusion proteins in transgenic seedlings

Ten μg of total protein extracts (10 μg) from 7-day-old seedlings of wild type (WT), and several lines of homozygous GFP-LIM expressing plants were separated by SDS-PAGE and transferred onto a PVDF membrane. GFP-LIM fusion proteins were detected with a GFP antibody. The amidoblack stained membrane is shown as loading control.

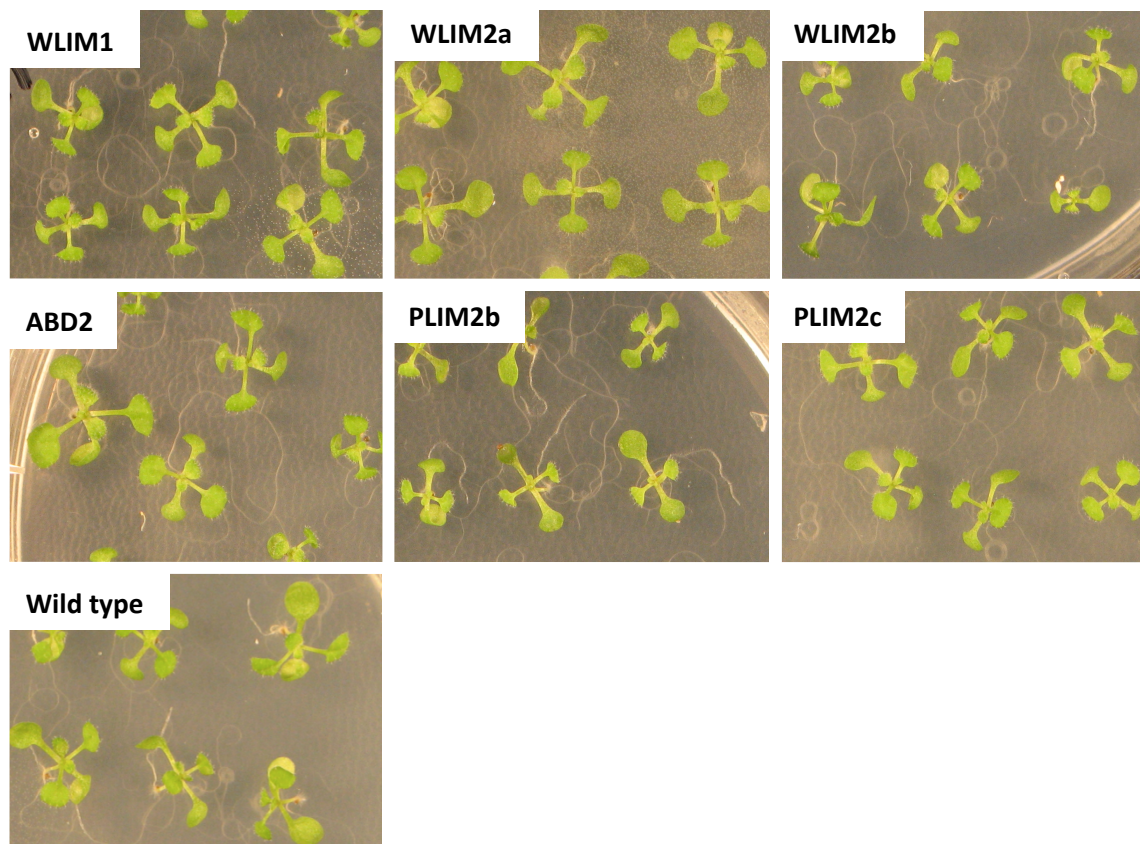


Figure 13: Morphology of *Arabidopsis* wild type, GFP-LIM and GFP-ABD2-GFP expressing plants.

Wild type, GFP-WLIM1, GFP-WLIM2a, GFP-WLIM2b, GFP-PLIM2b, GFP-PLIM2c and GFP-ABD2-GFP expressing plants were grown for 10 days on standard medium (1/2 MS) supplemented with 2% sucrose. Pictures were taken after 10 days.

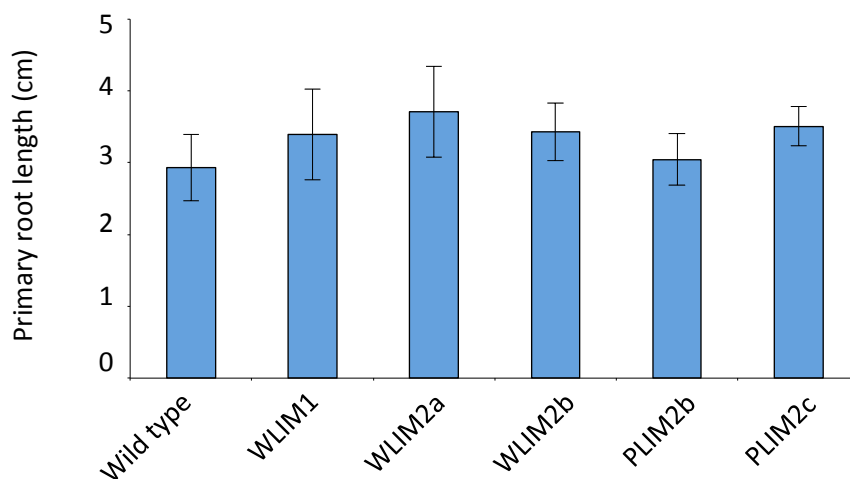


Figure 14: Primary root length average in 7-day-old wild type and GFP-LIM expressing plants.

Plants were grown for 7 days in thin vertical chambers on standard medium (1/ MS) supplemented with 2 % sucrose. Each individual experiment includes 10 plants of each background. Data indicate mean root length values calculated from three independent experiments. Error bars indicate standard deviation.

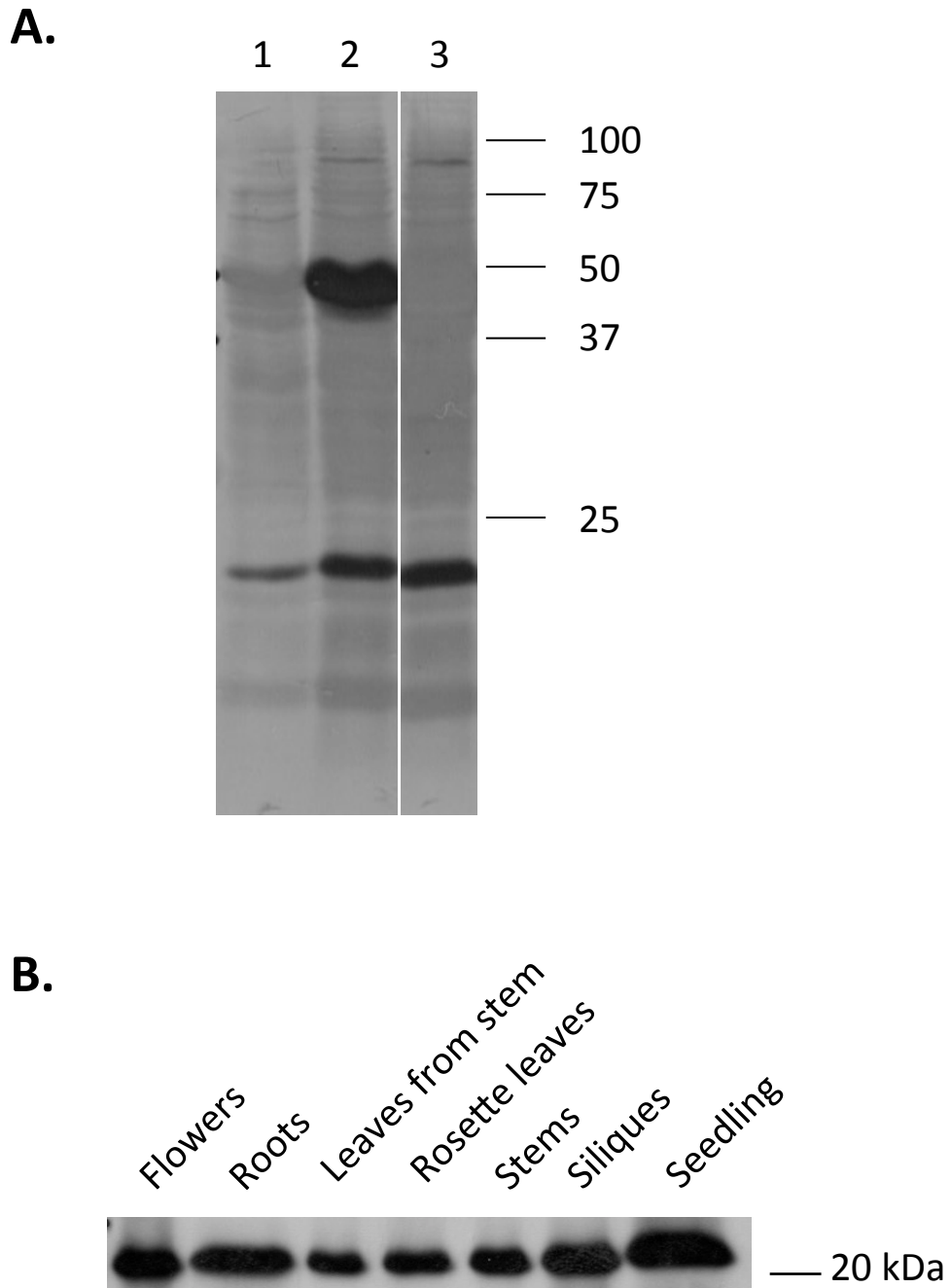


Figure 15: Immunoblot detection of GFP-fused and endogenous WLIM1.

A. Total proteins extracts (5 ug) were extracted from 10-day-old seedlings of wild type plants (lane 1), GFP-WLIM1 (lane 2) and GFP-PLIM2c (lane 3) expressing plants, separated by SDS-PAGE and transferred onto a PVDF membrane. GFP-WLIM1 was detected using a primary anti-WLIM1 antibody from mouse and a secondary HRP-coupled anti-mouse antibody from goat. GFP-WLIM1 was detected at the expected size of 50 kDa. An unspecific band was present in all samples including the wild type control.

B. Total proteins extracts (5 ug) were extracted from different organs and tissues of 2-month-old wild type *Arabidopsis* plants (Col-0), separated by SDS-PAGE and transferred onto a PVDF membrane. WLIM1 was detected at the expected size of 22 kDa in all organs and tissues using the high-sensitivity kit.

resistant T1 seedlings was verified by epifluorescence microscopy. Frequently, no expression or only a patchy expression pattern was observed. The transgenic lines exhibiting homogenous and sufficient fluorescence were selected for further analyses. Loss of hygromycin resistance and/or GFP fluorescence was often observed in following generations for all GFP-LIMs. Therefore, homozygous lines are not yet available for GFP-PLIM2a.

To verify the expression and the integrity of GFP-LIMs, total protein extracts of transgenic plants were analysed. Figure 12 shows immunoblot detection of GFP-LIMs in total protein extract of GFP-WLIM1 expressing plants using an anti-GFP antibody. The expected sizes of the GFP fusion proteins are 50.5 kDa for GFP-WLIM1, 51.5 kDa for GFP-WLIM2a, 51.2 kDa for GFP-WLIM2b, 52.5 kDa for GFP-PLIM2b and 53.3 kDa for GFP-PLIM2c. A typical ~50 kDa band was detected in all transgenic lines indicating that the GFP-LIM fusion proteins were not truncated (Figure 12). As expected, the size of the GFP-WLIMs is slightly reduced compared to GFP-PLIMs. Different expression levels between the individual lines can be detected with GFP-PLIM expression being clearly stronger than the expression of GFP-WLIM1 in the analysed lines. Similar intensities of GFP were observed by confocal microscopy.

Transgenic plants did not exhibit any obvious mutant phenotype. However, to check whether the overexpression of GFP-LIMs induced a mild phenotype that could be readily identified, the morphology of aerial green parts and the length of primary root of *Arabidopsis* wild type and transgenic plants grown for 10 days under standard conditions were compared. The F-actin marker line expressing the fimbrin-derived marker GFP-ABD2-GFP (Wang et al., 2008a) was also included in this study as a reference in the subsequent localisation experiments. Aerial green parts of transgenic plants exhibited very similar morphology and size compared to those of control plants (Figure 13). In addition, the length of the primary root did not significantly differ between transgenic and control plants with mean values ranging from 2.9 cm \pm 0.5 (wild type plants) to 3.5 cm \pm 0.6 (GFP-WLIM2a expressing plants; Figure 14). These results confirmed that there are no major morphological or developmental differences between transgenic and control plants (Figure 13).

As shown in Figure 15B, WLIM1 is readily detectable by protein immunoblot in seedlings and all analysed organs and tissues. Therefore, the lack of an obvious

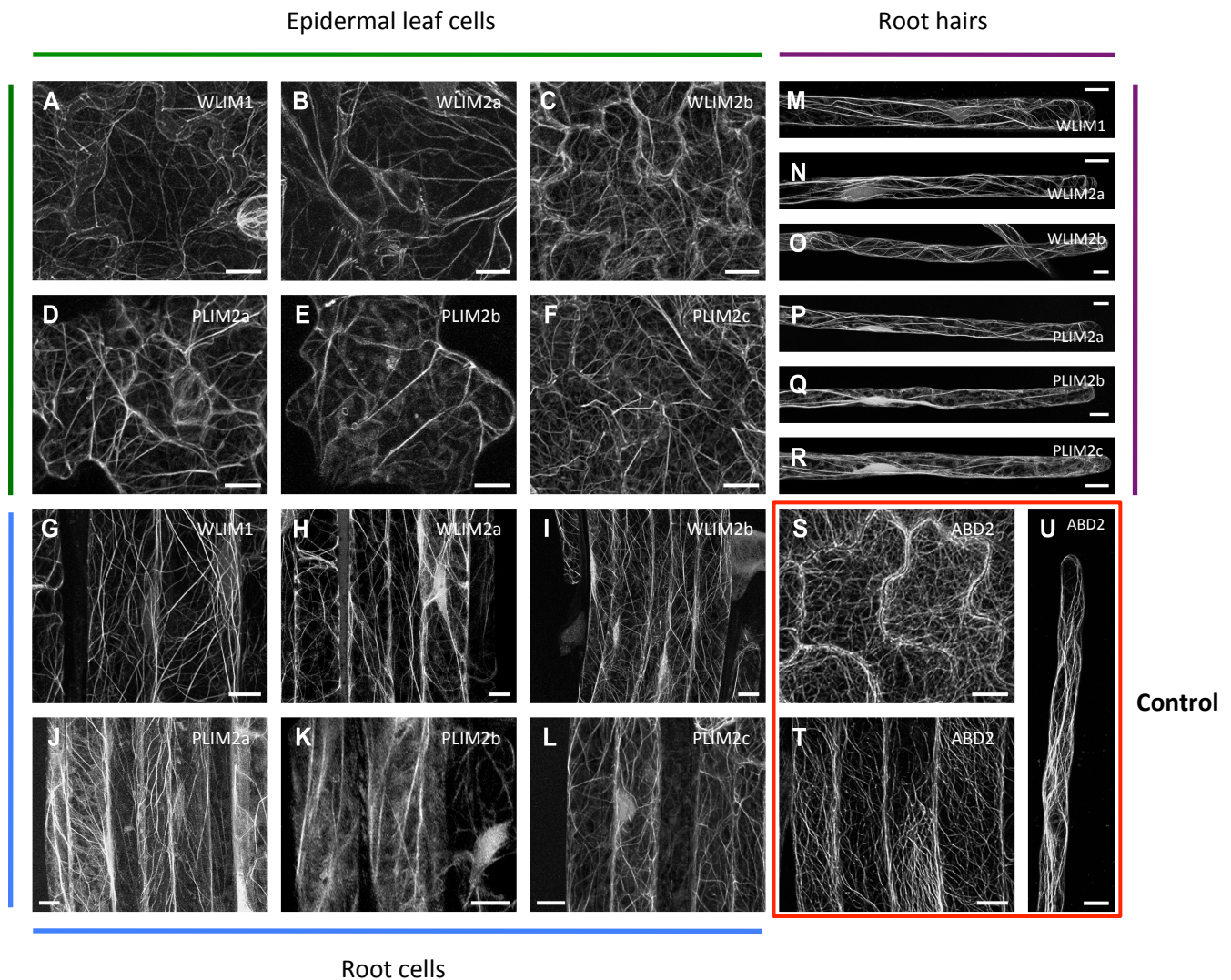


Figure 16: Localisation of GFP-LIMs in different tissues of transgenic *Arabidopsis* seedlings.

Typical fluorescent patterns observed for GFP-WLIM1 (A, G and M), GFP-WLIM2a (B, H and N), GFP-WLIM2b (C, I and O), GFP-PLIM2a (D, J and P), GFP-PLIM2b (E, K and Q), GFP-PLIM2c (F, L and R) and the actin cytoskeleton marker GFP-ABD2-GFP (S, T and U) in epidermal leaf cells (A to F and S), cortical root cells (G to L and T) and root hairs (M to R and U).

Bars = 10 μ m.

mutant phenotype of the transgenic plant might be due to a low expression level of the GFP-WLIM1 fusion protein in comparison to the endogenous WLIM1. To exclude the possibility, we compared the amount of GFP-WLIM1 to the endogenous WLIM1 signal. Figure 15A shows an immunoblot detection of WLIM1 in total protein extract of wild type and GFP-WLIM1 expressing seedlings using an anti-WLIM1 antibody. A typical 50 kDa band was detected for GFP-WLIM1 (Figure 15A, lane 2). The signal intensity of this band was higher than for the endogenous WLIM1 at 20 kDa indicating that the GFP-WLIM1 seedling indeed overexpress GFP-WLIM1.

2. Subcellular localisation of GFP-fused LIMs

Although several analyses have been conducted with all the six GFP-LIM expressing plants, some more specific and demanding analyses have been conducted using plants expressing one member of each sub-family, namely GFP-WLIM1 and GFP-PLIM2c.

2.1 GFP-fused LIMs interact with a filamentous network resembling the actin cytoskeleton

In order to determine the subcellular localisation of GFP-LIMs, the above-described transgenic plants were analysed by confocal microscopy. Figure 16 shows the typical localisation pattern for each GFP-LIM fusion protein in different tissues and organs including leaf epidermis (Figure 16A-F), primary root (Figure 16G-L) and root hairs (Figure 16M-R). All the six GFP-LIMs decorated a filamentous network in all the observed organs and tissues similar to the one revealed by the fimbrin-derived actin cytoskeleton marker GFP-ABD2-GFP (Figure 16S-U). Comparison of confocal images suggested that PLIMs interact less efficiently with the cytoskeleton than WLIMs. Indeed, most of cells overexpressing GFP-PLIMs exhibited a relatively high level of diffuse cytoplasmic fluorescence (Figure 16D-F, 16J-L, 16P-R), whereas GFP-WLIMs more sharply decorated the filamentous network (Figure 16A-C, 16G-I, 16M-O). The difference in the subcellular distribution of GFP-PLIMs and GFP-WLIMs was more precisely characterised in § II.3.

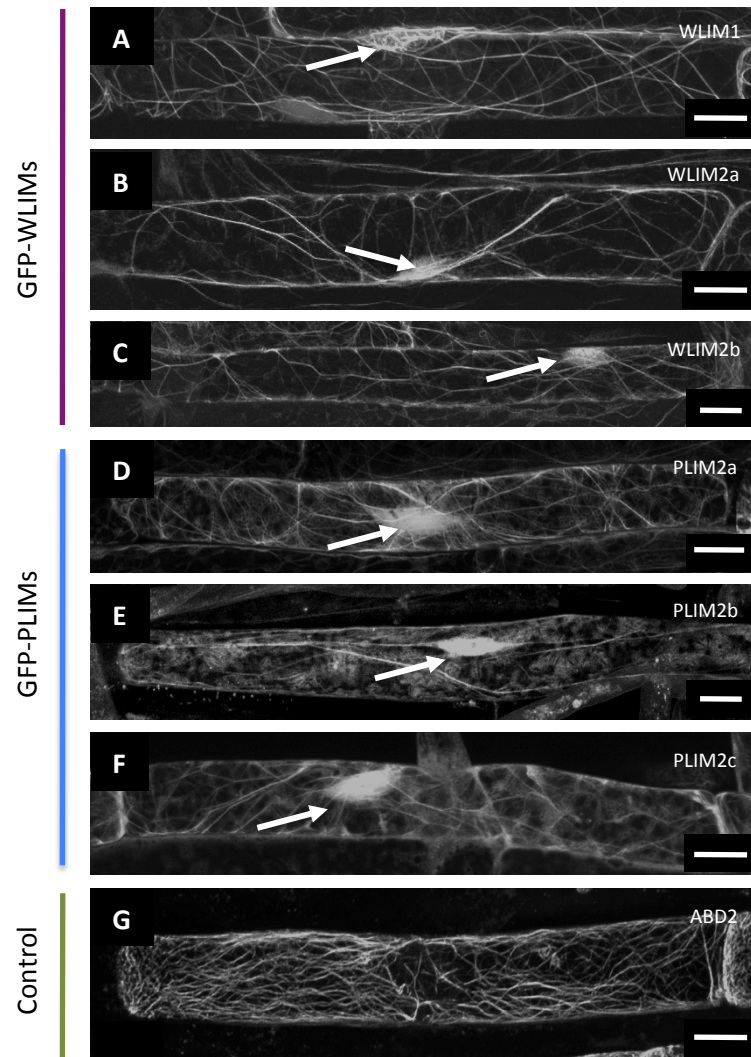


Figure 17: Localisation of GFP-LIMs in single cortical root cells of transgenic *Arabidopsis* seedlings.

Typical fluorescent patterns observed for GFP-WLIM1 (A), GFP-WLIM2a (B), GFP-WLIM2b (C), GFP-PLIM2a (D), GFP-PLIM2b (E), GFP-PLIM2c (F) and the actin cytoskeleton marker GFP-ABD2-GFP (G) in single root cells. Note that the six GFP-LIMs localise in both the cytoplasm and the nucleus.

Bars = 10 μ m. Arrows: nuclei.

In addition to their cytoplasmic localisation, all the six GFP-LIMs accumulate in the nucleus. Indeed, most of cells exhibit a relatively strong, although not always of identical intensity, fluorescent signal in their nucleoplasm. This is particularly well visible in the elongated cells of primary roots (Figure 17A-F, arrows). In contrast, no such nuclear signal is detected for GFP-ABD2-GFP (Figure 16S-U and Figure 17).

Together these observations suggest that all *Arabidopsis* LIMs display cytoskeletal-associated functions (in the cytoplasm) as well nuclear functions. The following studies only focus on the cytoskeleton-associated functions of *Arabidopsis* LIMs. However, LIM nuclear functions are also investigated in our laboratory.

2.2. GFP-fused LIMs interact with the actin cytoskeleton

In order to confirm that the cytoplasmic network labelled by GFP-LIMs corresponds to the actin cytoskeleton, co-labelling experiments with rhodamine-phalloidin as well as actin depolymerisation experiments using the F-actin disrupting drug latrunculin B have been conducted. These experiments have been conducted on cell cultures derived from the homozygous plant lines expressing GFP-WLIM1, GFP-PLIM2c and GFP-ABD2-GFP (control, Figure 18).

As expected, rhodamine-phalloidin labelled the same filamentous network as the actin marker GFP-ABD2-GFP (control, Figure 19G-I). It also extensively co-localised with GFP-WLIM1 and GFP-PLIM2c-decorated network (Figure 19A-C and D-F, respectively) indicating that both WLIM1 and PLIM2c well interact with actin filaments. Interestingly, some segments of cytoskeleton were recalcitrant to dual labelling, suggesting that LIMs (and the ABD2 domain of fimbrin) compete with phalloidin for actin binding.

In addition to co-localisation experiments, GFP-WLIM1, GFP-PLIM2c and GFP-ABD2-GFP (control) expressing cells were treated with latrunculin B (e.g. Gibbon et al., 1999). A 60 min-treatment of latrunculin B induced a complete disruption of the filamentous actin cytoskeleton as shown in Figure 19N-O. It also resulted in an extensive diffuse fluorescent signal in GFP-WLIM1 and GFP-PLIM2c expressing cells, supporting that GFP-WLIM1 and GFP-PLIM2c interact with the actin cytoskeleton (Figure 19J-K and L-M, respectively).

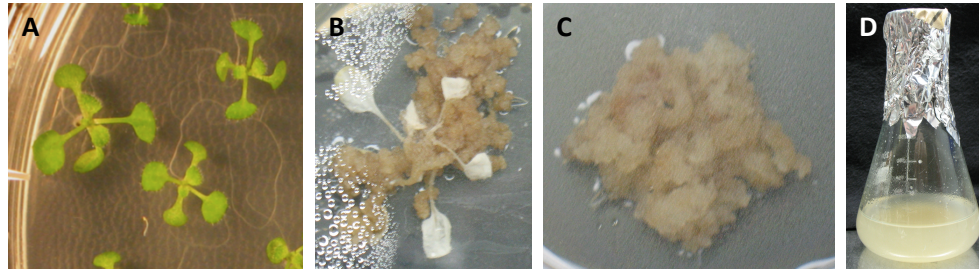


Figure 18: Production of cell suspension culture from transgenic *Arabidopsis* seedlings.

GFP-WLIM1, GFP-PLIM2c or GFP-ABD2-GFP expressing seedlings were grown on standard medium (1/2 MS) supplemented with 1 % sucrose (A). Three-week-old seedlings were transferred to a callus-inducing (CI) medium (B). The resulting calluses were transferred to fresh CI medium to allow then increasing in size (C). Well-dividing cells of each callus were transferred to liquid medium in order to obtain a cell suspension culture (D).

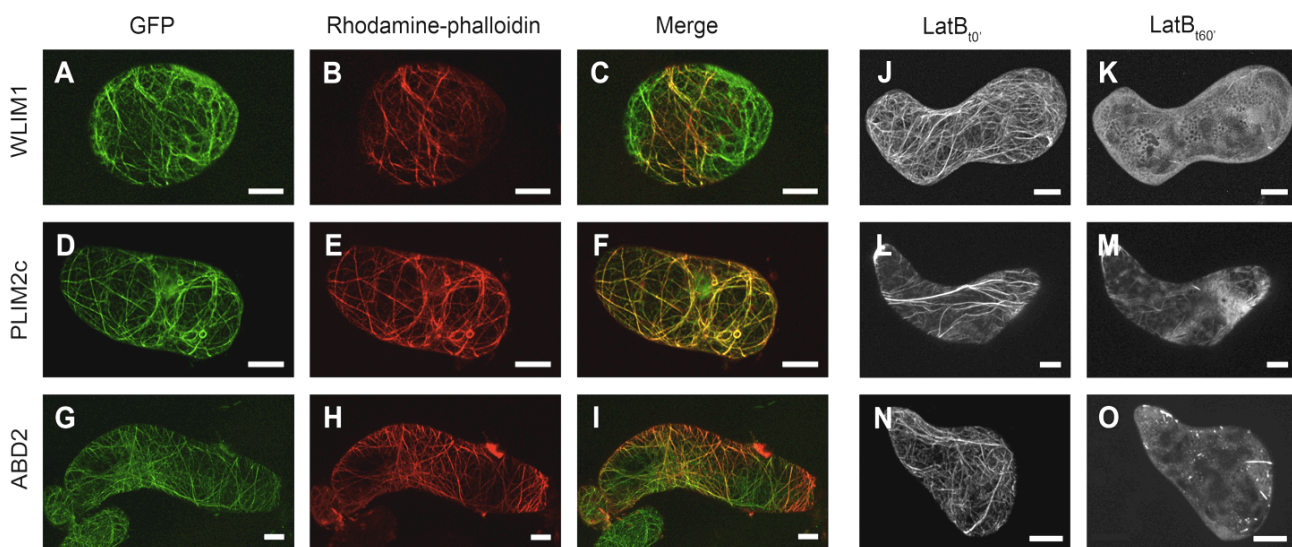


Figure 19: The LIM-decorated filamentous network is the actin cytoskeleton.

(A-I) Co-labelling experiments of GFP-WLIM1 (A), GFP-PLIM2c (D) and GFP-ABD2-GFP (G) with rhodamine-phalloidin (B, E and H). Merges images are shown in (C, F and I). Co-localisation is indicated by yellow colour.

(J-O) GFP-WLIM1 (J-K), GFP-PLIM2c (L-M) and GFP-ABD2-GFP (N-O) expressing cells were visualised before (J, L and N) and after 60 min latrunculin B treatment (100 mM; K, M and O)

Bars = 10 μ m.

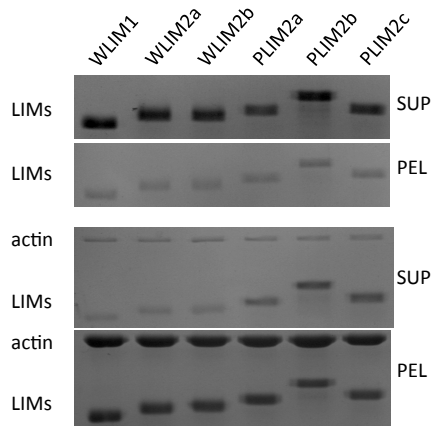


Figure 20: Recombinant *Arabidopsis* LIMs interact with actin filaments in a direct manner.

High-speed co-sedimentation assays were conducted at pH 6.2 and in low [Ca^{2+}] (± 5 nM free Ca^{2+}). After centrifugation at 100,000 g, whereas in the absence of actin LIMs ($4 \mu\text{M}$) remain in the supernatant fraction (top panel), in the presence of actin ($4 \mu\text{M}$) all the six LIMs accumulate in the pellet fraction (bottom gel panel).

SUP: supernatant fraction; PEL: pellet fraction.

Protein	K_D (μM)	B_{max}
WLIM1	0.4 ± 0.2	1.4 ± 0.2
WLIM2a	0.4 ± 0.2	1.1 ± 0.2
WLIM2b	0.5 ± 0.3	1.5 ± 0.2
PLIM2a	1.3 ± 0.2	1.5 ± 0.1
PLIM2b	1.7 ± 0.9	1.5 ± 0.1
PLIM2c	1.5 ± 1.1	1.8 ± 0.2

Table 1: Affinities of the six *Arabidopsis* LIM proteins for actin filaments.

Apparent equilibrium dissociation constants (K_D) and maximum binding capacities (B_{max}) values ($\pm\text{SD}$) were calculated from three independent high-speed co-sedimentation assay experiments after fitting the data (bound protein plotted against free protein) with a hyperbolic function.

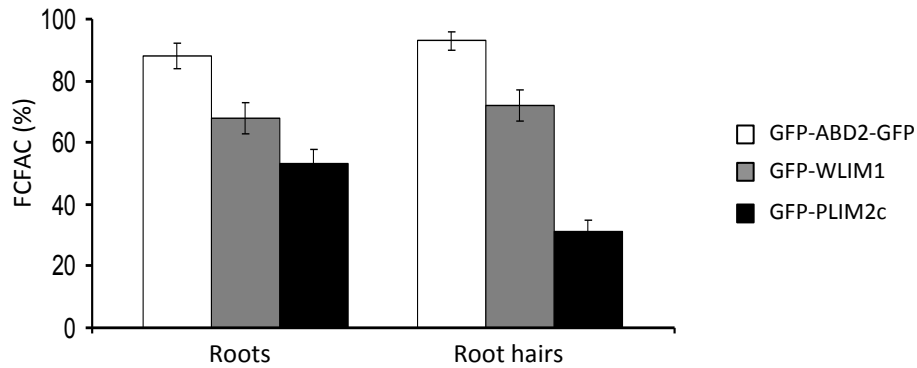


Figure 21: Fraction of cytoplasmic fluorescence associated with the cytoskeleton (FCFAC) in GFP-ABD2-GFP, GFP-WLIM1 and GFP-PLIM2c expressing root and root hair cells.

Total cytoplasmic fluorescence and fluorescence associated with the filamentous actin cytoskeleton in root and root hair cells of 5-day-old *Arabidopsis* seedlings were quantified on projections of confocal stacks using the Metamorph software (Molecular Devices, USA). The fraction of cytoplasmic fluorescence associated with the cytoskeleton (FCFAC) is expressed as a percentage of the total cytoplasmic fluorescence (n = 10; standard deviations are indicated by error bars). Note that GFP-ABD2-GFP and GFP-WLIM1 are more concentrated on actin filaments than GFP-PLIM2c.

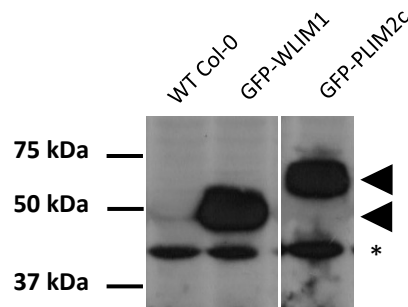


Figure 22: Immunoblot detection of GFP-WLIM1 and GFP-PLIM2c fusion proteins in the transgenic *Arabidopsis* lines used in the FCFAC quantification.

Total proteins (10 μ g) were extracted from 5-day-old seedlings, separated by SDS PAGE and transferred onto a PVDF membrane. Recombinant fusion proteins were detected using a primary monoclonal anti-GFP antibody from rabbit and a secondary HRP-coupled anti-rabbit antibody from goat. Both GFP-WLIM1 and GFP-PLIM2c were detected at the expected size (arrowheads). An unspecific band was detected in all samples including the wild type control (asterisk). It serves as an internal loading control.

Together our data demonstrate that *Arabidopsis* LIMs interact with the filamentous actin cytoskeleton.

3. *Arabidopsis* LIMs interact with actin filaments in a direct manner

In order to assess the ability of *Arabidopsis* LIMs to bind directly to actin filaments, high-speed co-sedimentation assays were performed. Recombinant LIMs were produced in *Escherichia coli* and purified by affinity chromatography. Actin was polymerised in the presence or in the absence of individual *Arabidopsis* LIMs and centrifuged at 100,000 g. The resulting pellet and supernatant fractions were analysed by SDS-PAGE (Figure 20). Control experiments showed that recombinant LIMs do not sediment significantly when centrifuged alone (Figure 20, top panel). In the presence of actin filaments, the six *Arabidopsis* LIMs accumulated in the pellet fraction, indicating that they interact directly with the actin filaments in an autonomous manner (Figure 20, bottom panel). Interestingly, the relative amounts of protein that sediment were slightly lower for the three PLIM proteins, suggesting differences between WLIMs and PLIMs in their affinity for the actin filaments.

Additional high-speed co-sedimentation assays were conducted using increasing concentrations of recombinant *Arabidopsis* LIMs and the apparent equilibrium dissociation constant (K_d) were calculated. In the experimental conditions used, i.e. pH 6.2 and 100 nM Ca²⁺, the three WLIMs displayed relatively high and similar affinities for actin filaments as indicated by apparent K_d values (Table 1) of 0.4 ± 0.2 μM (WLIM1), 0.4 ± 0.2 μM (WLIM2a) and 0.5 ± 0.3 μM (WLIM2b, n = 3). Noticeably, these values were significantly lower than those calculated for PLIMs, which ranged from 1.3 ± 0.2 μM (PLIM2a) to 1.7 ± 0.9 μM (PLIM2b). Therefore these data confirmed that WLIMs possess a higher affinity for actin filaments than PLIMs.

These data prompted us to refine our previous *in vivo* analyses suggesting that WLIMs bind more efficiently to the actin cytoskeleton than PLIMs. The fractions of cytoplasmic fluorescence associated with the cytoskeleton (FCFAC) were determined in GFP-WLIM1, GFP-PLIM2c and GFP-ABD2-GFP expressing plants. In primary root cells 53% ± 5% of the fluorescent signal due to GFP-PLIM2c concentrates on the actin cytoskeleton (Figure 21, left panel black column). In root hairs, the FCFAC

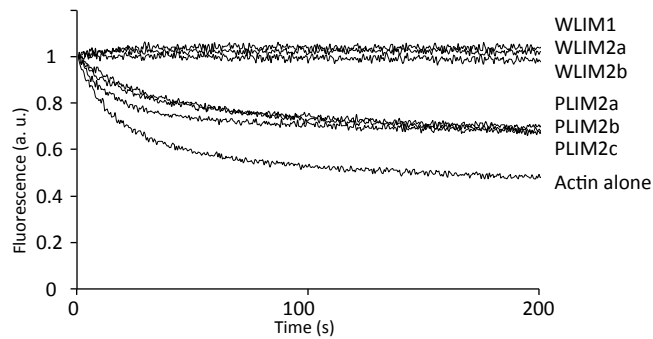


Figure 23: *Arabidopsis* LIMs efficiently stabilise actin filament *in vitro*.

Depolymerisation assay. Time course of pyrene-actin filaments (4 μM) depolymerisation in the absence and in the presence of individual LIMs (6 μM) was monitored by fluorimetric measurements. Initial fluorescence was set to 1. Note that WLIMs stabilise actin filaments more efficiently than PLIMs. Experiments were conducted at pH 6.2 and in low $[\text{Ca}^{2+}]$ ($\pm 5 \text{ nM}$ free Ca^{2+}).

dropped to $31\% \pm 5\%$, indicating that roughly 70% of the GFP-PLIM2c population was unbound and remained in the cytoplasm (Figure 21, right panel black column). In contrast, GFP-WLIM1 and GFP-ABD2-GFP (Figure 21, grey and white columns, respectively) predominantly associated with the actin cytoskeleton, as indicated by FCFAC values of roughly 70 and 90% in both types of cells, respectively. Importantly, immunoblot analysis confirmed that the above differences in FCFAC values were not due to unequal expression levels of the transgenes (Figure 22). The lower values of FCFAC measured for GFP-PLIM2c expressing plants are well consistent with *in vitro* data indicating that GFP-PLIM2c has a lower affinity for actin filaments than GFP-WLIM1.

In conclusion, the six members of the *Arabidopsis* LIM family interact with actin filaments in a direct manner. In addition, both *in vitro* and *in vivo* data support that, in the tested conditions, WLIMs display a higher affinity for actin filaments than PLIMs.

III. Characterisation of *Arabidopsis* LIM actin-regulatory activities

Tobacco WLIM1 and lily LIM1 have been previously demonstrated to stabilise and bundle actin filaments (Thomas et al., 2006; Thomas et al., 2007; Wang et al., 2008b). In order to assess whether all the *Arabidopsis* LIMs exhibit similar activities, a series of *in vitro* and *in vivo* experiments were conducted.

1. *Arabidopsis* LIMs stabilise the actin cytoskeleton

1.1. *Arabidopsis* LIMs stabilise actin filaments *in vitro*

The effect of *Arabidopsis* LIM binding on actin filament dynamics was examined in actin depolymerisation assays. Pyrene-labelled actin filaments ($4 \mu\text{M}$) were copolymerised with individual *Arabidopsis* LIMs ($6 \mu\text{M}$) and subsequently subjected to depolymerisation by diluting the samples to a final concentration of actin below the critical concentration, i.e. $0.2 \mu\text{M}$. Depolymerisation kinetics were recorded

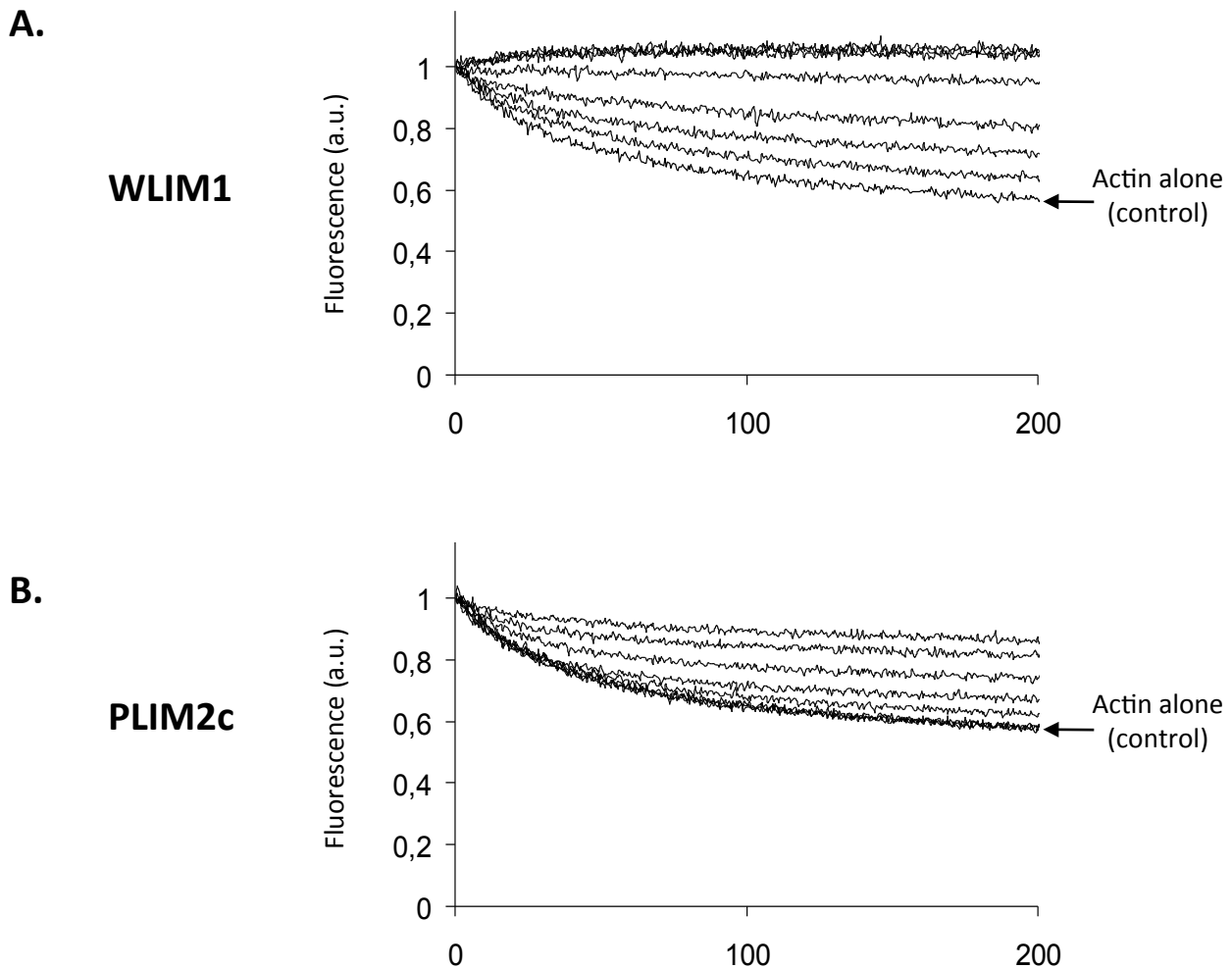


Figure 24: Actin filament stabilising activity of *Arabidopsis* LIMs is concentration-dependent

Depolymerisation assay. Time courses of pyrene-actin filaments ($4 \mu\text{M}$) depolymerisation in the absence and in the presence of individual increasing concentrations (1; 2; 4; 8; 16 and $20 \mu\text{M}$) of WLIM1 (a) and PLIM2c (B) were monitored by fluorimetric measurements. Initial fluorescence was set to 1. Experiments were conducted at pH 6.2 and in low $[\text{Ca}^{2+}]$ ($\pm 5 \text{ nM}$ free Ca^{2+}).

by monitoring fluorescence intensity over time as exemplified in Figure 23. In the absence of *Arabidopsis* LIMs (actin alone), the actin filaments promptly depolymerised, as shown by the rapid decline of fluorescence. In contrast, in the presence of individual *Arabidopsis* LIMs, the depolymerisation rate was markedly decreased. Noticeably, the two *Arabidopsis* LIM subfamilies exhibited similar but non-identical stabilisation capabilities. Whereas WLIMs fully stabilised the actin filaments, as shown by stable fluorescence curves, PLIMs only reduced the actin filament depolymerisation rate. Remarkably, the three members of each subfamily displayed roughly identical stabilising capabilities, indicating specific subfamily properties.

To evaluate whether LIMs stabilise actin filaments in a concentration-dependent manner, additional depolymerisation assays were performed using increasing concentrations of *Arabidopsis* LIMs. Here we only focused on WLIM1 and PLIM2c. As expected, the actin filament depolymerisation rate was reduced proportional to the relative amount of WLIM1 or PLIM2c used. Indeed, 2 μM WLIM1 only induced a partial stabilisation of actin filaments as shown by the slower depolymerisation curve than the control (Figure 24A). A four micromolar concentration of WLIM1 fully stabilised actin filaments as indicated by a stable depolymerisation curve (Figure 24A). Similar results were obtained with PLIM2c. However, full actin filament stabilisation required 20 μM PLIM2c (Figure 24B) indicating that, in the tested conditions, WLIM1 has a higher actin filament stabilisation capability than PLIM2c.

Together these data show that *Arabidopsis* LIMs stabilise actin filaments in a concentration-dependent manner. In agreement with the affinity constants and FCFAC values previously calculated, WLIM subfamily members exhibit a higher ability to stabilise actin filaments than PLIM subfamily members.

1.2. *Arabidopsis* LIMs protect the actin cytoskeleton against latrunculin B-induced depolymerisation

To confirm that *Arabidopsis* LIMs also stabilise the actin cytoskeleton in a cellular context, we evaluated their ability to delay latrunculin B-induced depolymerisation. This set of experiments has been conducted using the previously

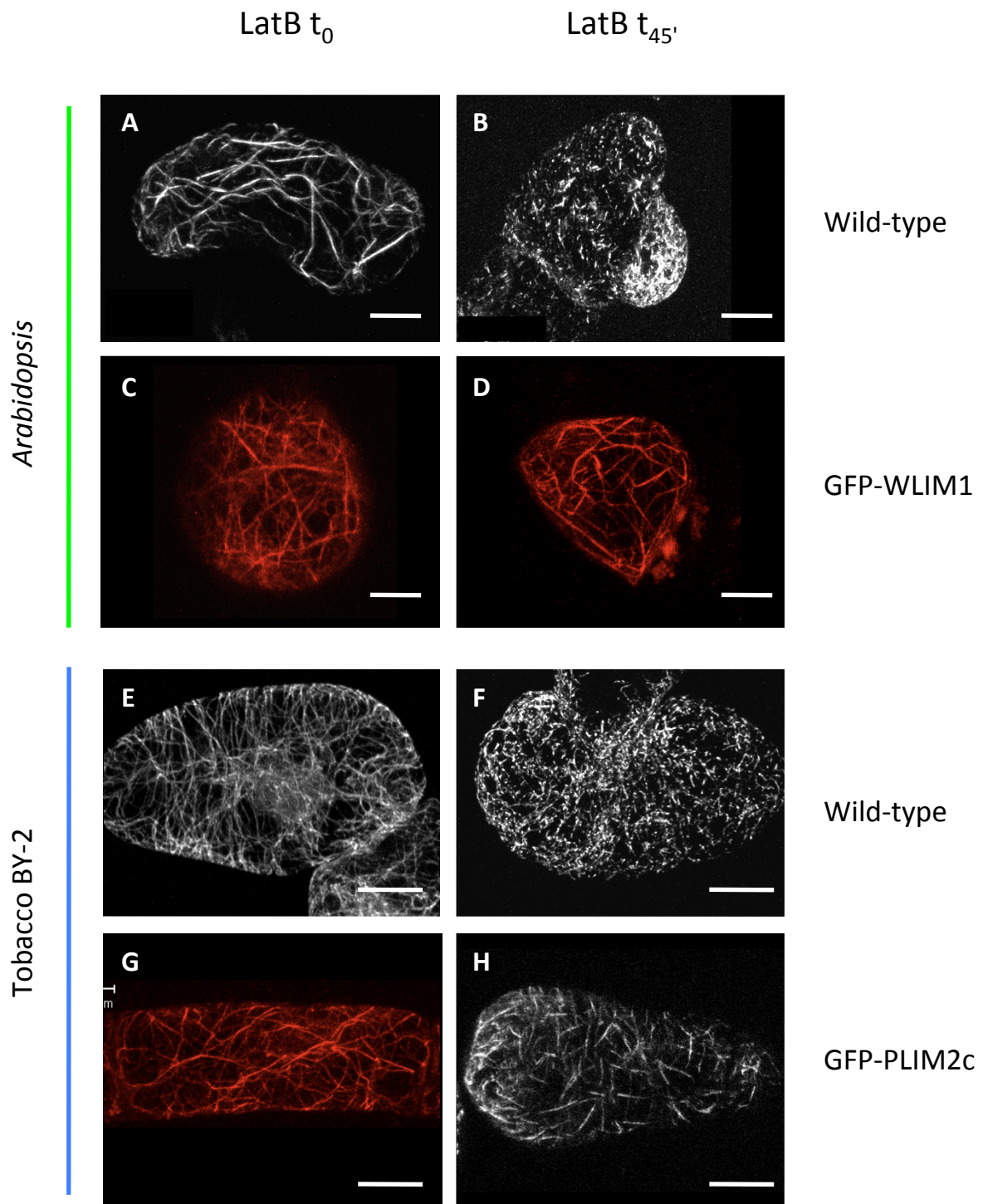


Figure 25: GFP-LIMs protect the actin cytoskeleton against latrunculin B-induced depolymerisation.

Actin cytoskeleton visualised by rhodamine-phalloidin staining in *Arabidopsis* wild type (A, B) and GFP-WLIM1 expressing (C, D) cells; and in tobacco BY-2 wild type (E, F) and GFP-PLIM2c expressing (G, H) cells. Confocal acquisitions before (A, C, E and F) and after 45 min latrunculin B (B, D, F and H) Bars = 10 mm.

described GFP-WLIM1 expressing cell lines as well as a newly generated GFP-PLIM2c expressing tobacco BY-2 cell line (unfortunately, the corresponding *Arabidopsis* cell line was lost).

Arabidopsis and tobacco BY-2 cells were treated with 200 nM and 500 nM latrunculin B, respectively. It is worth noting that these concentrations are much lower than those previously used to investigate GFP-LIM subcellular localisation (§ II.2.2.). The organisation of the actin cytoskeleton was monitored over time by confocal microscopy after a rhodamine-phalloidin labelling. The actin cytoskeleton of control wild type *Arabidopsis* and tobacco BY-2 cells was fully disrupted after a 45 min treatment as shown in Figure 25B and 25F, respectively. In contrast, after identical treatment, many actin filaments and bundles were still present in transgenic *Arabidopsis* and tobacco BY-2 cells expressing GFP-WLIM1 (Figure 25D) or GFP-PLIM2c (Figure 25H), supporting WLIM1 and PLIM2c effectively stabilise the actin cytoskeleton *in vivo* as well.

2. *Arabidopsis* LIMs are actin-bundling proteins

2.1. *Arabidopsis* LIMs crosslink actin filaments into higher-order structures *in vitro*

To determine whether the six *Arabidopsis* LIMs promote the formation of higher-order structures in a similar manner as tobacco WLIM1 (Thomas et al., 2006), low-speed co-sedimentation assays were conducted. Briefly, actin filaments (4 μ M) were co-polymerised with individual LIMs (6 μ M) and centrifuged at 12,500 g. The resulting pellet and supernatant fractions were analysed by SDS-PAGE (Figure 26). In the absence of LIM (actin alone), most of the actin was detected in the supernatant fraction. In contrast, in the presence of individual LIMs, actin massively sedimented, indicating the presence of higher-order actin structures.

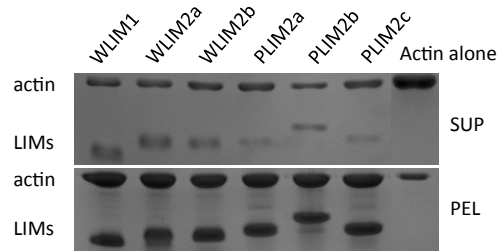


Figure 26: *Arabidopsis* LIMs crosslink actin filaments into higher-order structures.

Low-speed co-sedimentation assays were conducted at pH 6.2 and in low $[Ca^{2+}]$ (± 5 nM free Ca^{2+}). After centrifugation at 12,500 g, actin filaments (4 μ M) do not sediment and are predominantly detected in the supernatant fraction. In the presence of LIMs (6 μ M), actin filaments and LIMs co-sediment and are detected in the pellet fractions.

SUP: supernatant fraction; PEL: pellet fraction.

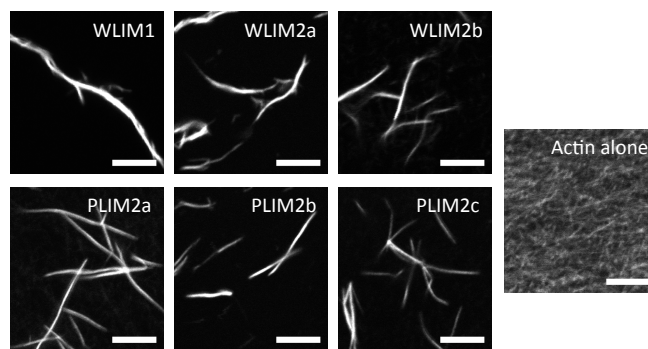


Figure 27: LIM crosslinked structures are actin bundles.

Actin (4 μ M) was polymerised in the absence or in the presence of individual LIMs (6 μ M). Afterwards, resulting actin structures were labelled with rhodamine-phalloidin and examined by confocal microscopy.

Bars = 5 μ m. Experiments were conducted at pH 6.2 and in low $[Ca^{2+}]$ (± 5 nM free Ca^{2+}).

2.2. *Arabidopsis* LIMs crosslink actin filaments into bundles *in vitro*

The type of higher-order actin structures induced by *Arabidopsis* LIMs was directly examined by confocal microscopy. In brief, actin (4 μM) was polymerised in the presence or in the absence of individual *Arabidopsis* LIM (6 μM) and subsequently labelled with rhodamine-phalloidin. Actin filaments polymerised alone do not assemble in any higher-order structures as observed in Figure 27 (right panel). In the presence of individual *Arabidopsis* LIMs, actin filaments assemble into thick and longitudinal actin bundles, which do not exhibit any branched aspect (Figure 27).

In the attempt to better characterise the LIM-induced actin bundles, electron microscopy experiments were conducted (with the technical support of the Science and Analysis of Material Department of the Public Research Centre-Gabriel Lippmann of Luxembourg). Unfortunately, the quality of electron micrographs obtained was too low to estimate the number of actin filaments per bundle or the relative orientation of filaments in myosin sub-fragment (S1)-decorated bundles. Data however confirmed that *Arabidopsis* LIMs promote the formation of long and predominantly straight actin bundles as exemplified for PLIM2c in Figure 28.

2.3. *Arabidopsis* LIMs increase the cellular level of actin bundling

Confocal images shown in Figure 16 support that GFP-LIM overexpression increase the level of actin bundling in *Arabidopsis* cells. However, further evidence was required. Indeed, the density of fluorescent filamentous structures, i.e. actin filaments and bundles was quantified in root and root hair cells of GFP-WLIM1, GFP-PLIM2c and GFP-ABD2-GFP (control) expressing plants using ImageJ software (in collaboration with J. Mutterer, IBMP, Strasbourg, Figure 29). The number of actin filaments/bundles was determined in 15 μm -width cross-sections corresponding to approximately the width of a cortical root cell and of a root hair. We estimated that cortical root cells and root hairs of control plants contain about 19 (± 2 , $n = 10$) and about 21 (± 3 , $n = 10$) actin filaments/bundles, respectively (Figure 29, white columns). In comparison, cortical root cells and root hairs of plants overexpressing GFP-WLIM1 and GFP-PLIM2c exhibited a dramatically reduced actin bundle density, i.e. 11 ± 1 and 8 ± 1 for cortical root cells and 11 ± 2 and 5 ± 1 for root hairs,

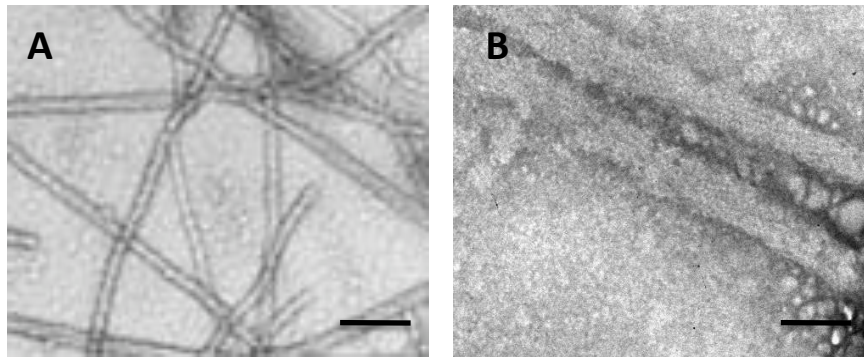


Figure 28: Electron micrograph of PLIM2c induced actin bundles.

Actin (4 μM) was polymerised in the absence (A) or in the presence of PLIM2c (8 μM , B). Afterward resulting actin structures were negatively stained with uranyl acetate (2 %) and examined by transmission electron microscopy.

Bars = 70 nm. Experiments were conducted at pH 6.2 and in low $[\text{Ca}^{2+}]$ (± 5 nM free Ca^{2+}).

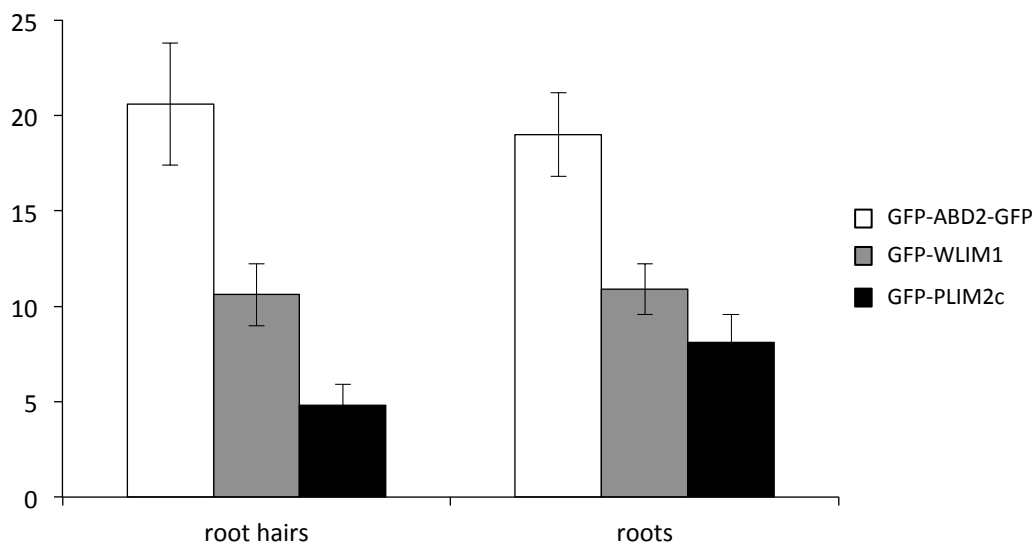


Figure 29: Quantitative analysis of the actin bundle density in GFP-WLIM1, GFP-PLIM2c and GFP-ADB2-GFP expressing cortical primary root cells and root hairs.

The average number of bundles was determined along a transversal section of 15 μm corresponding approximately to the width of a single primary root cell and of a single root hair in 4-day-old *Arabidopsis* seedlings. Quantification was performed using ImageJ. Note that GFP-WLIM1 (grey columns) and GFP-PLIM2c (black columns) expressing cells exhibit a reduced number of bundles compared to cells expressing the GFP-ABD2-GFP actin marker (white columns).

respectively (Figure 29, grey and black columns, respectively). The increase in actin bundle thickness previously reported in GFP-LIM-overexpressing plants (Figure 16) is concomitant with a decreased bundle density. Together, this strongly support that LIMs promote the formation of actin bundles *in vivo*. As previously reported, the filamentous structures in GFP-WLIM1 and GFP-PLIM2c expressing plants were significantly thicker than those observed in GFP-ABD2-GFP expressing plants (data not shown). Therefore, *Arabidopsis* LIMs induce both a thickening of actin bundles and a decrease in bundle density, supporting that they promote actin bundling *in vivo*.

IV. Discussion

Actin-binding, -stabilising and -bundling activities are common features to plant LIMs

In this chapter we demonstrate that all the six *Arabidopsis* LIMs function as true ABPs, i.e. they bind to actin filaments in a direct manner and promote the formation of thick and stable actin bundles. Importantly, *in vitro* biochemical data are well consistent with the effects of the ectopic/overexpression of GFP-LIMs on the actin cytoskeleton organisation and dynamics in transgenic plant cells. Noticeably, GFP-LIM expressing cells exhibit a reduced number of individualised actin filaments/bundles compared to GFP-ABD2-GFP control plants as well as an apparent increase in bundle thickness (Figure 16 and 29). We also provide evidence that the six *Arabidopsis* LIMs stabilise the actin filaments in a concentration-dependent manner both *in vitro* and in the cellular context. Similar data have been previously reported for tobacco WLIM1 and lily LIM1 (Thomas, Hoffmann et al., 2006; Wang et al., 2008b) suggesting that all plant LIM proteins display actin-binding, -stabilising and -bundling activities.

The vertebrate counterparts of plant LIMs, namely cysteine-rich proteins (CRPs), were initially suggested to interact only indirectly with actin filaments *via* ABPs, such as zyxin and α -actinin (Sadler et al., 1992; Louis et al., 1997; Pomies et al., 1997; Jang and Greenwood, 2009). However, recently, two out of the three mammalian CRPs have been reported to bind to actin filaments autonomously (Grubinger and Gimona, 2004; Tran et al., 2005; Jang and Greenwood, 2009). In

addition, autonomous actin-bundling activity has been biochemically demonstrated for rat CRP1 (Tran et al., 2005; Jang and Greenwood, 2009). Our laboratory recently confirmed and extended these data by demonstrating that all three CRPs exhibit autonomous actin-binding, -stabilising and -bundling activities (Moreau et al., unpublished data). This strongly supports that these actin-regulatory activities are common features to all CRPs and CRP-like proteins, including plant LIMs.

In addition to their actin-regulatory activities in the cytoplasm, *Arabidopsis* LIMs are likely to play a role in the nucleus. Indeed, beside their cytoplasmic localisation, GFP-LIMs accumulate in the nucleus of various cell types (Figure 17). A similar dual localisation was previously reported for the vertebrate CRPs (e.g. Arber et Caroni, 1996). Interestingly, in contrast to CRPs (Gehmlich et al., 2008; Boateng et al., 2009), plant LIMs sequences do not contain any known nuclear localisation signal. Importantly, fluorescence recovery after photobleaching (FRAP) experiments support that GFP-LIMs do not diffuse passively across the nuclear pores (C. Thomas, unpublished data). The nuclear localisation signal of plant LIMs remain to be identified. Alternatively, it is not excluded that plant LIMs are co-imported/exported with another protein, e.g. actin itself. As stated in the chapter 1 (IV.4.), nuclear functions of plant LIMs are currently investigated in our laboratory. Data support that plant LIMs participate in the regulation of gene expression (S. Gatti and D. Moes, unpublished data). In addition, additional nucleolar functions have been recently suggested by the localisation of tobacco WLIM2 to nucleolar dot-like structures (D. Moes, personal communication).

Are plant LIMs highly specialised in actin bundling?

As above stated, the six *Arabidopsis* LIMs crosslink actin filaments into bundles, suggesting that actin-bundling is a major actin regulatory function of plant LIMs rather than an accessory function. Interestingly, the cytoskeletal rearrangements induced by LIM ectopic/overexpression, i.e. an increase of actin bundle thickness and a concurrent decrease of the number of bundles (Figure 16; Thomas et al., 2006, 2008), differ from those resulting from the overexpression of *Arabidopsis* AtFH1, an *Arabidopsis* formin that has been reported to bundle actin filaments *in vitro* (Michelot et al., 2005, 2006). Indeed, AtFH1 overexpression increases the number of actin

bundles in pollen tubes (Cheung and Wu, 2004). Opposite effects on bundle population induced by the two classes of actin-bundling proteins may be explained by the fact that only AtFH1 displays an actin-nucleating activity. Mechanistic studies have suggested that AtFH1 functions as a non-processive nucleating factor that detaches from the barbed end after nucleation and moves to the side of the growing filament to promote the assembly of a novel filament, thereby facilitating the formation of actin bundles (Michelot et al., 2006; Blanchoin and Staiger, 2010). Therefore, AtFH1, in addition to its bundling activity, promotes *de novo* formation of actin bundles whereas LIMs only crosslink existing filaments, thereby reducing the number of individual filaments and small bundles. Recent genetic studies have provided evidence of the central role played by two other formins, namely, AtFH3 and AtFH5, in the nucleation of longitudinal actin bundles in *Arabidopsis* pollen tubes (Ye et al., 2009; Cheung et al., 2010). However, *in vitro* analyses failed to reveal autonomous crosslinking activity for AtFH3, suggesting that, *in vivo*, the bundling of formin-nucleated actin filaments requires the action of other ABPs (e.g., villins or LIMs). Noticeably, the supernumerary actin bundles induced by AtFH3 overexpression were abnormally thin (Ye et al., 2009). This possibly results from insufficient levels of actin-bundling proteins to assemble bundles of normal thickness. Together these data strongly suggest that plant LIMs do not promote actin nucleation. However, this remains to be carefully assessed in *in vitro* biochemical assays.

Fluorimetric data ruled out a cofilin-like severing activity, which could have been identified by faster actin depolymerisation rates in the presence of LIMs. In conclusion, *Arabidopsis* LIMs most likely lack actin-nucleating and -severing activities and are, therefore, highly specialised in actin-bundling.

Why does LIM ectopic/overexpression not induce morphological or developmental phenotypes?

GFP-LIMs expressing plants do not exhibit any obvious morphological or developmental phenotype. This is relatively surprising considering the high level of actin bundling in these plants and the previously reported damages that abnormal levels of actin bundling cause to plant growth and morphogenesis. Good examples are found in functional studies of plant actin depolymerisation factors (ADFs). For

instance, Dong et al. (2001) reported that both an increase and a decrease of the *Arabidopsis* ADF1 expression level significantly modify the cellular actin-bundling level. Indeed, thick actin bundles disappeared upon AtADF1 overexpression, whereas their population increases upon AtADF1 down-regulation. These actin phenotypes were accompanied by a reduction and a stimulation of cell growth, respectively. One hypothesis that could explain the absence of morphological or developmental phenotype in GFP-LIM expressing plants is that LIM actin-bundling activity is actually properly regulated by cellular regulatory factors or balanced by antagonist ABPs, e.g. ADFs, during key cellular processes such as cell division and elongation. Under such a scenario, GFP-LIM expressing plants would develop normally despite of an abnormal level of actin bundling in mature, non-dividing, cells. This hypothesis implies that plant cells possess a highly efficient cytoskeleton regulatory machinery able, when necessary, to overcome an abnormal elevation of the content of important ABPs such as LIMs. It is worthy noting that, as GFP-LIM expressing plants, single T-DNA-insertion mutants of *Arabidopsis* LIM do not exhibit an obvious developmental phenotype either (Dieterle et al., unpublished data). However, this is less surprising since a significant degree of functional redundancy between LIMs can be expected from their overlapping expression patterns (Papuga and Hoffman et al., 2010) and identical range of activities.

In conclusion, all the six *Arabidopsis* LIMs function as “true” actin-binding proteins able to stabilise and to crosslink actin filaments into thick bundles. Interestingly, in the tested conditions, WLIM subfamily members had a higher affinity for actin filaments than PLIMs subfamily members, and exhibited therefore a higher level of activity. These observations strongly suggest that WLIM and PLIM subfamilies have moderately but significantly diverged to achieve their specific functions in vegetative and pollen tissues, respectively. Pollen tube elongation is one of the best-characterised tip (asymmetrical)-growth system (Gibbon et al., 1999; Hepler et al., 2001; Vidali et al., 2001; Vidali et al (b), 2001; Chen et al., 2002; Hepler et al., 2006; Ren et al., 2007; Cheung et al., 2008; Chen et al., 2009; Vidali et al., 2009). Although the importance of actin bundles in pollen tube growth has been established, how these bundles are induced, and spatially and temporally maintained is not clearly understood yet. Taking into account of the high expression level of

PLIMs in pollen (Eliasson et al., 2000; Papuga and Hoffmann et al., 2010), we strongly suspect that they play important roles during pollen tube growth. Importantly, the actin cytoskeleton organisation and dynamics in growing pollen tubes have been shown to be regulated by pH and $[Ca^{2+}]$ gradients (Pierson et al., 1996; Holdaway-Clarke et al., 1997; Feijo et al., 1999; Hepler et al., 2001; Vidali et al., 2001; Lovy-Wheeler et al., 2006, 2007). Consequently, we have decided to address the potential regulation of *Arabidopsis* LIM actin-regulatory activity by these two factors. These data are presented in the next chapter.

Chapter 3

Regulation of *Arabidopsis* WLIM1 and PLIM2c activities by pH and Ca²⁺

Chapter 3: Regulation of *Arabidopsis* WLIM1 and PLIM2c activities by pH and Ca²⁺

I. Introduction

In the previous chapter, we provided evidence that the six *Arabidopsis* LIMs function as actin-binding proteins able to stabilise actin filaments and to promote the formation of actin bundles. Expression studies have revealed that the corresponding genes define two subfamilies: the *WLIM* subfamily, whose members exhibit a wide expression pattern in vegetative and reproductive tissues but are not or only weakly expressed in pollen grains, and the pollen *PLIM* subfamily, whose members exhibit a strong and predominant expression in pollen grains (Papuga and Hoffmann et al., 2010). Therefore, it is highly possible that WLIM and PLIM activities are specifically (not identically) regulated in order to generate the proper cytoskeleton structures in the different types of tissues. For instance, the actin cytoskeleton exhibits a very specific organisation in growing pollen tubes and plays central roles in the tube elongation process (Gibbon et al., 1999; Vidali et al., 2001; Chen et al., 2002; Cole and Fowler, 2006). In the shank of the tube, actin filaments organise into long and thick actin bundles, which are assumed to serve as the main tracks for the transport of secretory vesicles towards the subapical region. Within the latter region, actin filaments reorganise into a very dynamic structure commonly referred to as actin fringe, which consists in cortical arrays of short actin filaments and bundles (Hepler et al., 2001; Lovy-Wheeler et al., 2005; Chen et al., 2009). The actin fringe remains at a constant distance from the growing tip region and has been suggested to be involved in the delivery of vesicles to the precise sites of growth, although the exact underlying mechanism remains a matter of debate (Staiger et al., 2010). The tight regulation of the actin cytoskeleton organisation and dynamics in pollen tubes implies a fine regulation at the spatial level of the activities of pollen ABPs including PLIMs. Both pH and Ca²⁺ have been previously suggested to play key roles in these processes (Vidali and Hepler, 2001; Hepler et al., 2006; Cardenas et al., 2008; Iwano et al., 2009). On the one hand, physiological analyses have revealed that an increase in pH,

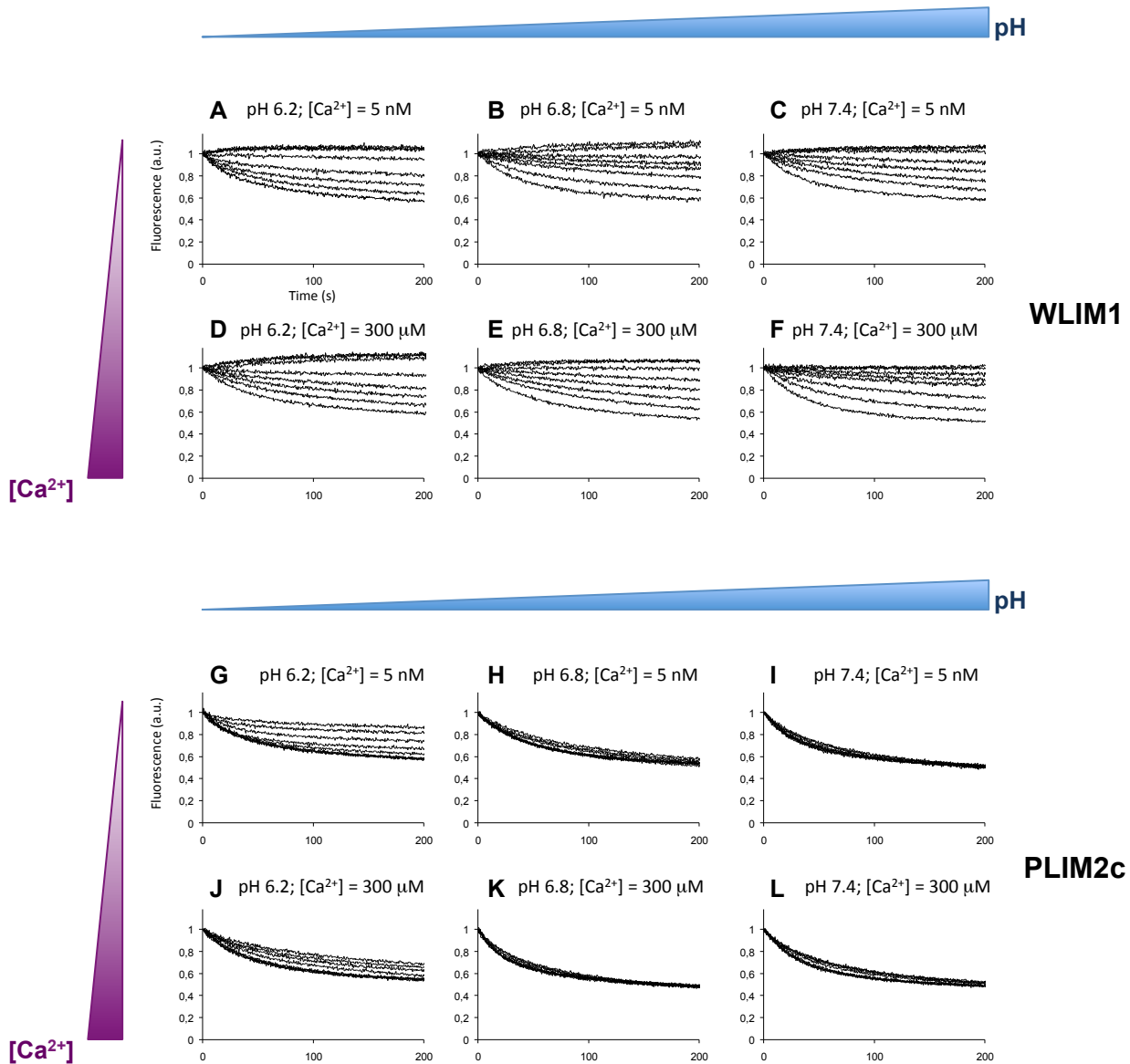


Figure 30: Comparison of WLIM and PLIM2c actin-stabilising activity in different combinations of pH and $[Ca^{2+}]$.

Depolymerisation assays. Pyrene- labelled actin filaments ($4 \mu\text{M}$) were co-polymerised in the presence of increasing concentrations of WLIM1 (A-F) or PLIM2c (G-L) (0, 1, 2, 4, 8, 16, 20 μM , from bottom to top curves) at different pH (6.2, 6.8 and 7.4) and $[Ca^{2+}]$ (5 nM and 300 μM). Subsequently, actin filaments were induced to depolymerise by dilution below the critical concentration (i.e. 0.2 μM). Initial fluorescence was set to 1.

the so-called alkaline band of the subapical region, occurs in anticipation of an increase in growth (Lovy-Wheeler et al., 2006). It is worth noting that the alkaline band is located in the vicinity of the actin fringe and might therefore play a central role in its formation. On the other hand, $[Ca^{2+}]$ oscillations have been correlated with pollen tube growth as well (Messerli et al., 1997). In addition, Ca^{2+} has been shown to regulate the activities of several ABPs (Fan et al., 2004; Yokota et al., 2005; Xiang et al., 2007; Wang et al., 2008b; Zhang et al., 2010). For the above-mentioned reasons, pH and Ca^{2+} appear as excellent candidates for regulatory factors of the pollen PLIM activities.

The following sections address the regulation of PLIM2c and WLIM1 by pH and Ca^{2+} using both *in vitro* and *in vivo* approaches. Data revealed that PLIM2c activities are directly regulated by pH and Ca^{2+} whereas those of WLIM1 would only be indirectly regulated by yet unidentified Ca^{2+} -dependent cellular factors. By a domain analysis, we identified the amino acid domain that confers direct pH and Ca^{2+} -responsiveness to PLIM2c. A model of the underlying molecular mechanism as well as a model for the role of PLIMs during pollen tube elongation is presented.

II. Differential regulation of WLIM1 and PLIM2c activities by pH and Ca^{2+}

1. Actin filament stabilisation by WLIM1 and PLIM2c at different pH and $[Ca^{2+}]$

In order to assess the direct regulation of WLIM1 and PLIM2c activities by pH and Ca^{2+} , we evaluated the ability of both proteins to stabilise actin filaments in different conditions of pH and $[Ca^{2+}]$. Bacterially-produced recombinant proteins were subjected to a series of actin depolymerisation assays conducted at three pH conditions (6.2, 6.8 and 7.4) and in the presence of low or high amounts of free Ca^{2+} (5 nM and 300 μ M, respectively). For each pH and $[Ca^{2+}]$ condition, different concentrations of WLIM1 and PLIM2c (ranging from 1 to 20 μ M, concentrations before sample dilution) have been tested, whereas the concentration of actin before dilution was set at 4 μ M (Figure 30). Under low pH and low $[Ca^{2+}]$, both WLIM1 and PLIM2c stabilised actin filaments in a concentration-dependant manner (Figure 30A and 30G). These data also confirmed the higher stabilising capability of WLIM1.

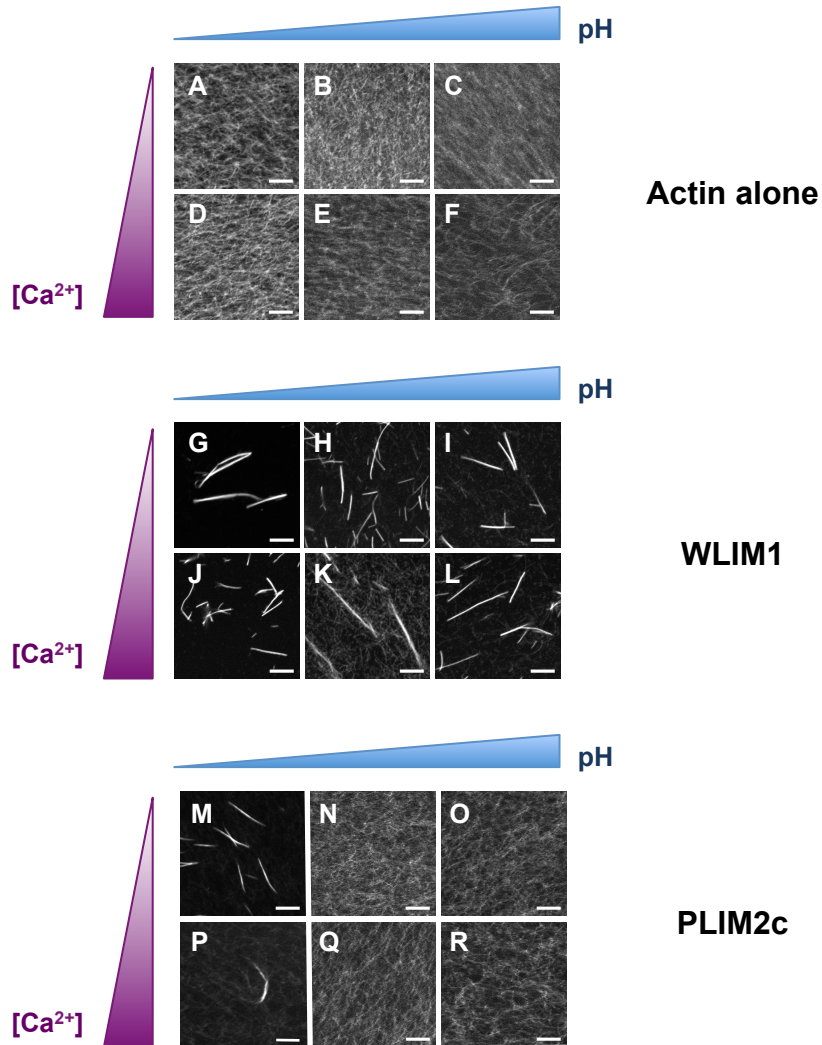


Figure 31: Comparison of WLIM1 and PLIM2c actin-bundling activity in different combinations of pH and $[Ca^{2+}]$.

Actin (4 μM) was co-polymerised in the absence (A-F) or in the presence of WLIM1 (6 μM , G-L) or PLIM2c (6 μM , M-R) at different pH (6.2, 6.8 and 7.4) and $[Ca^{2+}]$ (5 nM and 300 μM). The resulting actin structures were labelled with rhodamine-phalloidin and analysed by confocal microscopy.

Bars = 5 μm

Indeed, 1 μM of WLIM1 was sufficient to slow down the actin filament depolymerisation rate, whereas 3 μM of PLIM2c were required to produce a significant effect. In addition, full stabilisation of actin filaments was achieved for WLIM1 concentrations $\geq 6 \mu\text{M}$, whereas it required $\geq 10 \mu\text{M}$ for PLIM2c (Figure 30).

Increasing the pH from 6.2 to 6.8 or 7.4 caused the loss of PLIM2c stabilising activity, as indicated by depolymerisation curves similar to those obtained for actin filaments alone (Figure 30G-I). At higher pH, even the highest PLIM2c concentration failed to slow down actin filament depolymerisation, indicating a strong pH-dependent inhibition. By contrast, WLIM1 preserved prominent activity at both intermediate and high pH values (Figure 30A-C). Furthermore, its stabilising efficiency appeared unmodified by pH increase since maximal actin filament stabilisation was observed for WLIM1 concentrations $\geq 6 \mu\text{M}$ in all pH conditions. Additional depolymerisation experiments were performed at high $[\text{Ca}^{2+}]$ (Figure 30D, E, F, J, K, L). At pH 6.2, the high $[\text{Ca}^{2+}]$ significantly reduced the actin-stabilising capability of PLIM2c (Figure 30J). However, the weak but significant levels of stabilisation observed for the highest concentrations of PLIM2c indicated that the inhibition was not as strong as for pH (Figure 30J versus 30H-I). In higher pH conditions (i.e. pH 6.8 and 7.4), high $[\text{Ca}^{2+}]$ showed no visible effect, since PLIM2c activity remained turned off (Figure 30K-L). The depolymerisation curves obtained for WLIM1 were similar to those obtained at low $[\text{Ca}^{2+}]$, indicating that WLIM1 was not responsive to Ca^{2+} (Figure 30A, B, C versus 30D, E, F).

2. Actin filament bundling by WLIM1 and PLIM2c at different pH and $[\text{Ca}^{2+}]$

LIM-induced stabilisation most likely results from the crosslinking of actin filaments. Thus, from the above data, one might anticipate that PLIM2c actin bundling activity is negatively regulated by high pH and/or $[\text{Ca}^{2+}]$, whereas the one of WLIM1 is not. To confirm these assumptions, we directly observed by confocal microscopy actin filaments polymerised alone (4 μM , Figure 31A-F) or in the presence of WLIM1 (6 μM , Figure 31G-L) or PLIM2c (6 μM , Figure 31M-R). WLIM1 promoted the formation of actin bundles in an efficient manner in all the combinations of pH (6.2, 6.8 and 7.4) and $[\text{Ca}^{2+}]$ (5 nM and 300 μM) tested (Figure

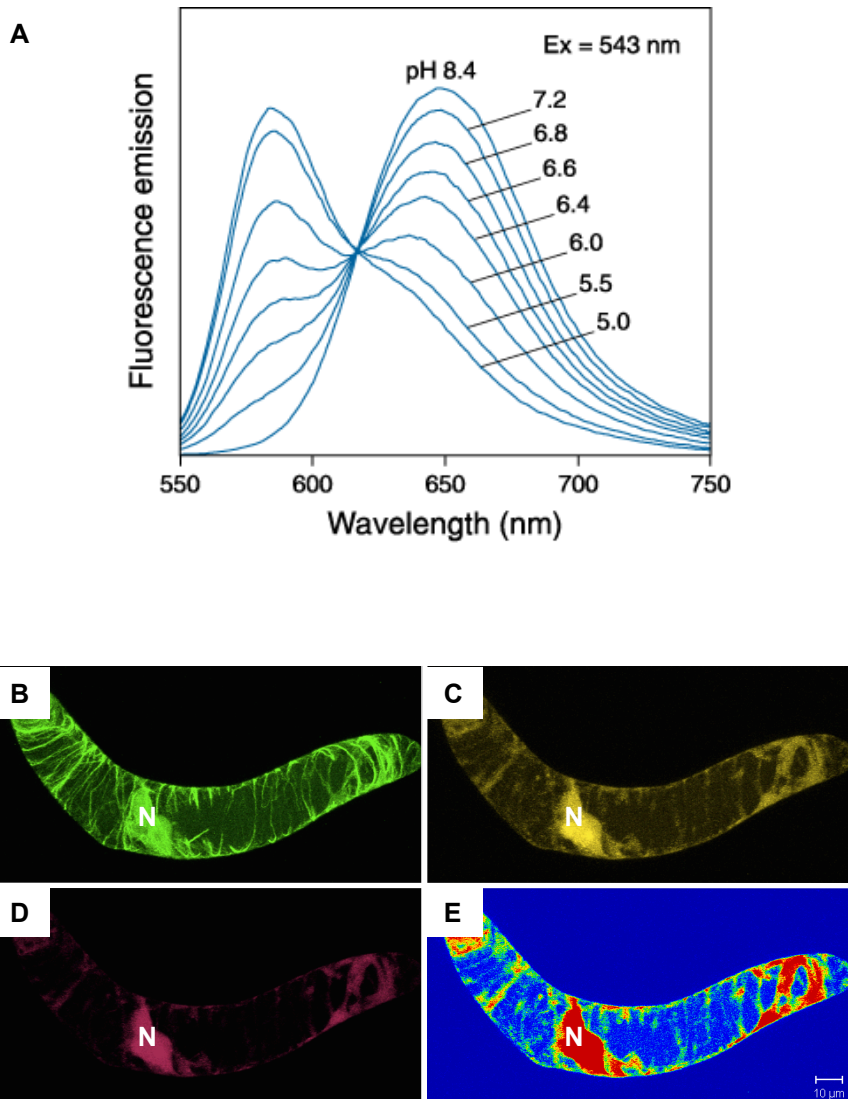


Figure 32: The ratiometric pH-sensitive SNARF5F dye.

(A) Fluorescence emission spectrum of SNARF5F as a function (taken from Invitrogen, USA).

(B-D) Typical fluorescence patterns of GFP-LIM (B) and SNARF5F (C and D) in a SNARF5F-loaded transgenic *Arabidopsis* cell. SNARF5F is excited at 543 nm and emission recorded at 580 nm (C) and 640 nm (D). The emission ratio $R_{640/580}$ (E) = (D)/(C) is shown with pseudocolours using the LSM510 rainbow mode.

Bars = 10 μ m. N: nucleus

31G-L). In contrast, PLIM2c induced the formation of actin bundles only under low pH and low $[Ca^{2+}]$ conditions (Figure 31M). Its actin-bundling activity was fully inhibited by $pH \geq 6.8$ (Figure 31N and 31O). In agreement with data from depolymerisation assays, Ca^{2+} only partially inhibited PLIM2c actin bundling activity. Indeed, a few actin bundles could be observed at pH 6.2 and 300 μM Ca^{2+} (Figure 31P). These results indicate that only the actin bundling activity of PLIM2c is negatively regulated by increase in pH and $[Ca^{2+}]$ *in vitro*.

Together our data indicate that WLIM1 and PLIM2c respond differently to pH and $[Ca^{2+}]$ *in vitro*. WLIM1 actin-stabilising and -bundling activities are not regulated by pH and $[Ca^{2+}]$, whereas those of PLIM2c are down-regulated by relatively high pH values and/or high $[Ca^{2+}]$.

III. *In vivo* pH- and Ca^{2+} -dependent regulation of WLIM1 and PLIM2c activities

The above biochemical data strongly suggest that pH and Ca^{2+} act as specific regulators of PLIM activities. To test this assumption, we analysed and compared the ability of PLIM2c and WLIM1 to localise to the actin cytoskeleton in different pH_{cyt} and $[Ca^{2+}]_{cyt}$ conditions. We used both “artificial” systems allowing the modifications of pH_{cyt} (§ III.1.) and $[Ca^{2+}]_{cyt}$ (§ III.2.) in *Arabidopsis* cell cultures derived from the transgenic plants previously described in chapter 1, and a more “natural” system (§ III.3.), i.e. the growing lily pollen tube, which possess “natural” pH_{cyt} and $[Ca^{2+}]_{cyt}$ gradients.

1. Subcellular localisation of WLIM1 and PLIM2c in *Arabidopsis* cells submitted to artificially induced modification of pH_{cyt}

To determine whether the actin-binding activity of *Arabidopsis* WLIM1 and PLIM2c is regulated by pH, a series of experiments were conducted using *Arabidopsis* cell cultures generated from GFP-WLIM1, GFP-PLIM2c and GFP-ABD2-GFP (control) expressing plants.

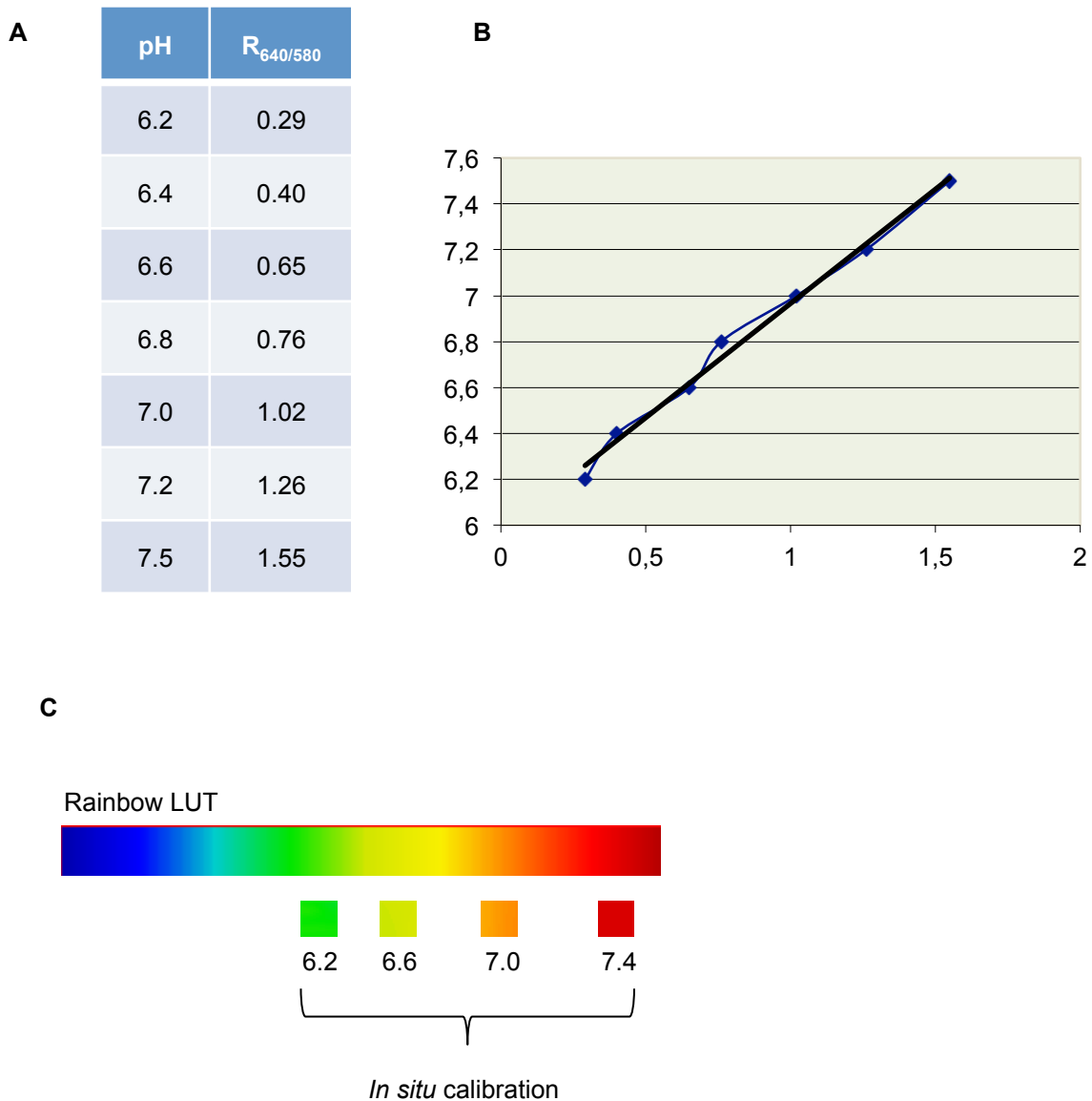


Figure 33: *In situ* pH calibration using SNARF5F.

(A) *Arabidopsis* cells were loaded with SNARF5F and subsequently incubated with reference buffers (pH 6.2-7.5). Ratios $R_{640/580}$ were calculated from the fluorescence intensities of $50 \mu\text{m}^3$ cytoplasmic cubes. (B) *In situ* calibration curve was generated by plotting pH against $R_{640/580}$ values. (C) The calibration curve has been fitted with the rainbow colour scale. LUT: lookup table.

1.1. Design and validation of the experimental procedure to modify the cytoplasmic pH in *Arabidopsis* cells

We selected a pH-sensitive dye allowing us to monitor pH_{cyt} variations in the range of 6.2 to 7.4: the ratiometric dye SNARF5F (SNARF®-5F 5-(and-6)-carboxylic acid, acetoxymethyl ester). SNARF5F exhibits a significant pH-dependent emission shift from orange yellow to deep red under acidic and basic conditions, respectively (Figure 32A). This pH dependence allows the use of the ratio of the fluorescence intensities from SNARF5F at two emission wavelengths (typically 580 nm and 640 nm, Figure 32C and 32D, respectively) to estimate pH (pseudocoloured image, Figure 32E). Importantly, the emission wavelengths do not overlap with the emission of GFP, which peaks at 509 nm (Figure 32B). In order to load SNARF5F without the need of microinjection, we used a cell-permeant version of the dye named acetoxymethyl ester (Kuchitsu et al., 2002). Modification of carboxylic acids with acetoxymethyl ester groups results in an uncharged molecule that permeates cell membranes. Once inside the cell, the lipophilic blocking groups are cleaved by non-specific esterases, resulting in a charged form, which does not diffuse back through the plasma membrane.

In order to use the pseudocolored ratio images as cytoplasmic pH_{cyt} indicators, *in situ* calibration was performed as recommended by Feijo et al. (1999) using a combination of two ionophores, namely nigericin (5 μM) and valinomycin (2 μM), in the presence of high concentration of potassium ions. Reference pH buffers adjusted to final pH values ranging from 6.2 to 7.5 were incubated with the SNARF5F dye and observed by confocal microscopy. The ratio $R_{640/580}$ was calculated for each pH value from the fluorescence intensities in 50- μm^3 cytoplasmic volumes (Figure 33A) and an *in situ*-obtained calibration curve was generated (Figure 33B, C). Using the latter calibration curve, we estimated that non-treated cells display an average pH_{cyt} of 7.06 ± 0.06 ($n = 10$, Figure 34).

Prior to pH treatment, cells overexpressing GFP-WLIM1, GFP-PLIM2c and GFP-ABD2-GFP (control) were incubated in standard culture medium supplemented with SNARF5F. Both the concentration and the incubation time of SNARF5F were optimised for *Arabidopsis* transgenic cells to 5 μM and 30 min, respectively. SNARF5F most frequently diffused in a relatively homogenous manner into the

$R_{640/580}$	pH
1.08	7.049964
1.1	7.06663
1.05	7.024965
1.2	7.14996
1.14	7.099962
0.95	6.941635
1.12	7.083296
1.099	7.065797
1.17	7.124961
Average	7.067463
SD	0.060588

Figure 34: Estimation of *Arabidopsis* cell cytoplasmic pH.

An average cytoplasmic pH value of 7.06 ± 0.06 has been calculated from 9 *Arabidopsis* cells using the previously described *in situ* calibration curve (Figure 35B). SD: Standard deviation..

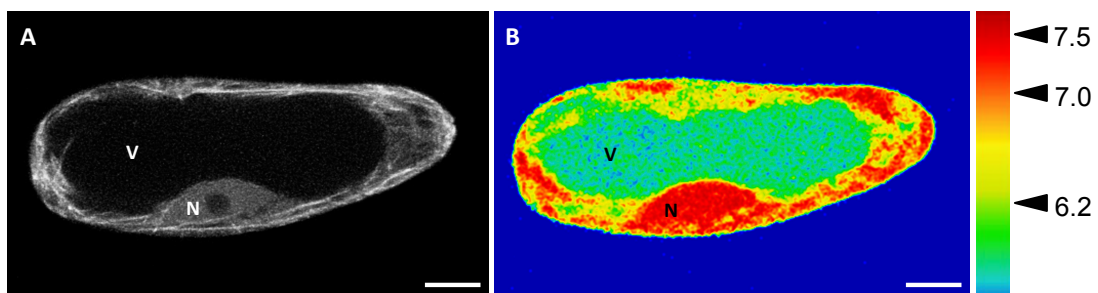


Figure 35: Imaging of SNARF5F in a GFP-PLIM2c-expressing *Arabidopsis* cell.

(A) Central confocal section of a transgenic *Arabidopsis* cell expressing the GFP-PLIM2c fusion protein. (B) Imaging of the pH-sensitive dye SNARF5F in the same section. Note that the vacuole is the most acidic compartment.

Bars = 10 μm . N: nucleus. V: vacuole.

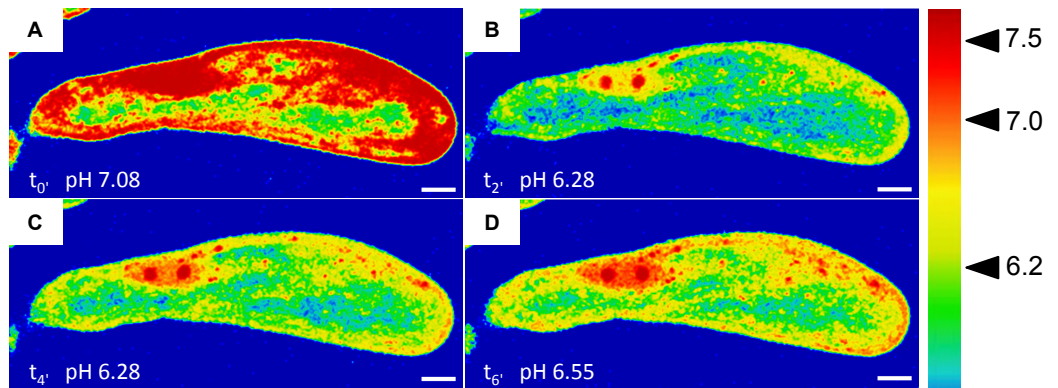


Figure 36: Recovery of pH_{cyt} after artificially induced acidification.

Arabidopsis cells were loaded with the ratiometric pH-sensitive dye SNARF5F and subsequently incubated in the acidifying buffer. Imaging of SNARF5F was performed before (A) and after 2 min (B), 4 min (C) and 6 min (D) of pH treatment. Mean cytoplasmic values were calculated from *in vivo* calibration and are indicated on each image. Note the slow but significant pH recovery occurring after the initial acidification.

Bars = 10 μm .

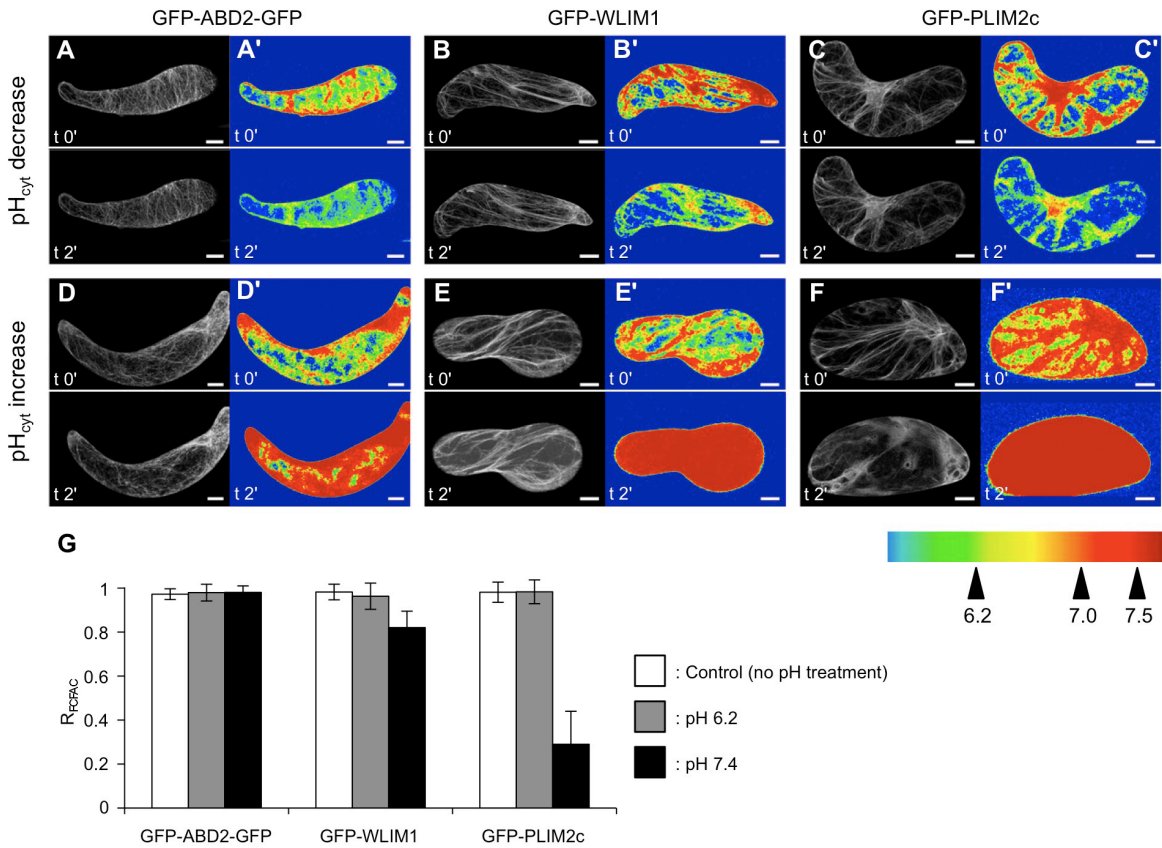


Figure 37: Increase in pH_{cyt} specifically impairs GFP-PLIM2c interaction with the actin cytoskeleton

(A) to (F') *Arabidopsis* cells expressing GFP-ABD2-GFP (A, A', D and D'), GFP-WLIM1 (B, B', E and E') and GFP-PLIM2c (C, C', F and F') were treated with acidifying (A-C and A'-C') or alkalinising buffers (D, F and D'-F'). Typical confocal images showing the localisation of GFP fusion proteins before (t0') and 2 min after pH treatment (t2') are presented on the left of each image panel (A-F). Modifications of cytoplasmic pH were controlled using the ratiometric SNARF-5F dye, and rainbow pH images are presented at the right of each image panel (A'-F'). Note the prominent diffuse cytoplasmic localisation of GFP-PLIM2c after increase in cytoplasmic pH (F and F').

(G) Quantitative analyses of the above experiments. The FCFAC was quantified for each GFP fusion protein before ($FCFAC_{t0'}$) and after pH treatment ($FCFAC_{t2'}$), and ratios were calculated ($R_{FCFAC} = FCFAC_{t2'} / FCFAC_{t0'}$). Grey and black bars indicate the R_{FCFAC} values calculated after a decrease and increase in cytoplasmic pH respectively ($n \geq 10$; error bars indicate SD). White bars indicate the R_{FCFAC} values calculated for control experiments in which cells have not been submitted to any pH treatment ($n \geq 10$; error bars indicate the SD). Note the low R_{FCFAC} value (0.29 +/- 0.15) calculated for GFP-PLIM2c upon increase in cytoplasmic pH indicating that GFP-PLIM2c has massively detached from the actin cytoskeleton.

Bars = 10 μ m.

cytoplasm and the nucleus (Figure 35). Occasionally, the dye also penetrated the central vacuole (Figure 35). As expected the vacuole was found to be the most acidic cellular compartment with pH values around 6.0 (Figure 35). To decrease or increase the pH_{cyt} , cells were incubated in pH-modifying buffers (PMB) containing the cell-permeant weak acid sodium propionate (pH adjusted to 6.2) or the cell-permeant weak base ammonium chloride (pH adjusted to 7.4; Parton et al., 1997). In order to determine the incubation time in PMB that was required to reach a maximum of pH_{cyt} modifications, we performed a time-lapse experiment to monitor the evolution of pH_{cyt} as a function of time. A picture was taken every 2 minutes after pH_{cyt} modifications for a total duration of two hours. We determined that confocal acquisitions of SNARF5F and the GFP-fused proteins have to be collected just before and 2 min after the application of PMB. It should be noted that, after longer incubation times in PMB, the evolution of pH frequently reversed although the recovery was much slower than the initial shift (Figure 36). The *in situ*-obtained calibration curve (Figure 33B) was used to control the pH_{cyt} modifications induced by the pH-modifying buffer. As expected, pH_{cyt} was found to reach values close to those of each pH-modifying buffer, i.e. 6.2 ± 0.1 and 7.4 ± 0.1 ($n > 10$).

1.2. An increase in cytoplasmic pH specifically inhibits the binding of GFP-PLIM2c to actin filaments

GFP-WLIM1, GFP-PLIM2c and GFP-ABD2-GFP (control) expressing cells were subjected to pH_{cyt} modifications and analysed by confocal microscopy. The effect of pH_{cyt} modifications on the ability of each GFP fusion protein to interact with the actin cytoskeleton was carefully analysed by quantifying the fraction of cytoplasmic fluorescence associated with the cytoskeleton (FCFAC) and by comparing this value before and after pH treatment ($R_{\text{FCFAC}} = \text{FCFAC}_{12} / \text{FCFAC}_{10}$). Figure 37 presents typical results obtained with the three cell lines of interest after 2 minutes of incubation in PMBs. Lowering the pH to 6.2 had no significant effects on the actin binding activity of GFP-WLIM1, GFP-PLIM2c, and GFP-ABD2-GFP, as indicated by direct comparison of confocal images (Figures 37A-C) and R_{FCFAC} values close to 1 (Figure 37G). By contrast, a pH increase dramatically weakened the binding of GFP-PLIM2c to the cytoskeleton, as shown by a prominent diffuse

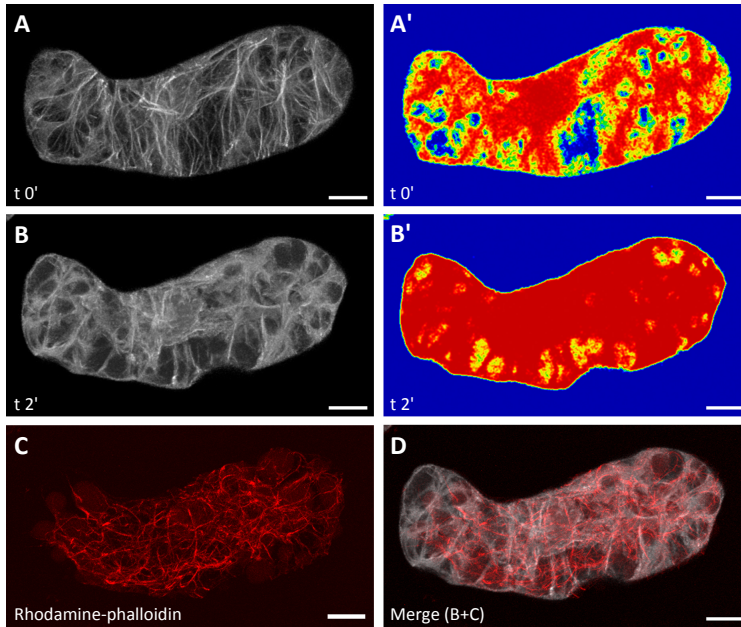


Figure 38: A prominent actin cytoskeleton persists after increase in pH_{cyt} in GFP-PLIM2c expressing *Arabidopsis* cells.

Typical localisation patterns of GFP-PLIM2c before (A) and 2 min after (B) artificial increase in cytoplasmic pH. (A' and B') corresponding rainbow images of the ratiometric SNARF5F dye showing the increase in pH_{cyt} . (C) Rhodamine-phalloidin labelling performed immediately after confocal acquisitions in B and B'. (D) Merge of (B) and (C).

Bars = 10 μm .

fluorescent signal (Figure 37F). Massive release of GFP-PLIM2c from the actin network upon pH elevation was supported by a R_{FCFAC} value of 0.29 ± 0.15 , indicating that $\sim 70\%$ of the fluorescence initially associated with the cytoskeleton has been displaced toward the cytoplasmic diffuse pool. Contrary to GFP-PLIM2c, GFP-ABD2-GFP and GFP-WLIM1 remained largely associated with the actin cytoskeleton upon cytoplasmic pH elevation (Figures 37D and 37E, respectively). However, quantitative analyses revealed a slight modification in the GFP-WLIM1 subcellular distribution (Figure 37G). Indeed, we calculated a R_{FCFAC} value of 0.82 ± 0.075 , indicating an 18% decrease of the cytoskeleton-bound GFP-WLIM1 population upon pH_{cyt} increase. By contrast, the subcellular distribution of GFP-ABD2-GFP was unaffected, as indicated by $R_{FCFAC} = 0.98 \pm 0.029$. However, considering the relatively weak effect of high pH on WLIM1 subcellular localisation, its biological significance remains uncertain. Importantly, rhodamine-phalloidin co-labelling experiments confirmed the persistence of a filamentous actin cytoskeleton after increase of pH_{cyt} in GFP-PLIM2-expressing cells (Figure 38). The reversibility of GFP-PLIM2c release was assessed by successive treatments of cells with the alkalizing and acidifying buffers. As shown in Figures 39A-D, GFP-PLIM2c efficiently dissociated and re-associated with the cytoskeleton, indicating that its actin-binding ability was not irreversibly damaged by elevated pH_{cyt} conditions. A control experiment conducted with GFP-ABD2-GFP-expressing cells confirmed that the predominant cytoskeletal localisation of GFP-ABD2-GFP is not significantly affected during similar pH treatment (Figures 39E-H).

Together these data are consistent with *in vitro* data and support the specific regulation of PLIM2c actin-binding activity by pH in the cellular context. Indeed, an increase in pH_{cyt} strongly inhibits the association of GFP-PLIM2c with the actin cytoskeleton, whereas it only slightly affects the subcellular localisation of GFP-WLIM1, which remains predominantly concentrated to the actin cytoskeleton.

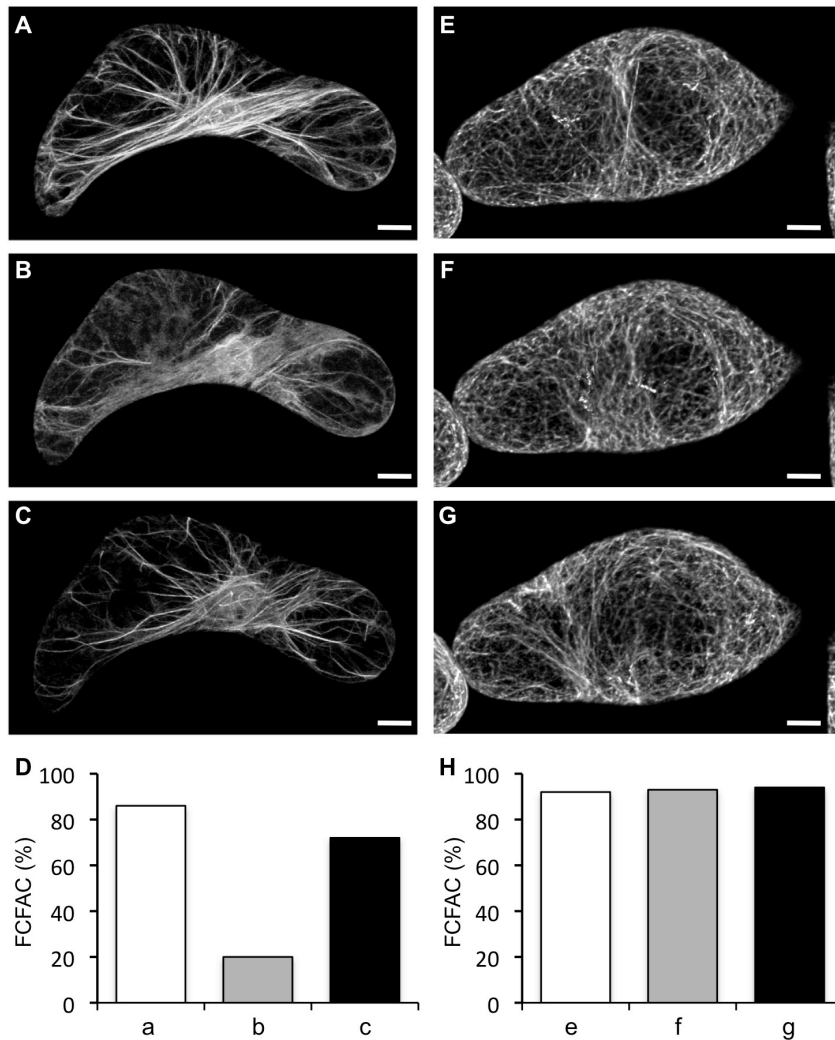


Figure 39: GFP-PLIM2c dissociates and re-associates with the actin cytoskeleton by successive increase and decrease in pH_{cyt} .

(A) To (C) Subcellular localisation of GFP-PLIM2c in a transgenic *Arabidopsis* cell before pH treatment (A), after 2 min of incubation in the alkalinising buffer (B) and after 2 min of subsequent incubation in the acidifying buffer (C). (D) Quantitative analysis of the fraction of cytoplasmic fluorescence associated with the actin cytoskeleton (FCFAC) in (A, white bar), (B, grey bar) and (C, black bar). (E-H) Corresponding control experiment conducted with the GFP-ABD2-GFP-expressing cell line. Note that GFP-ABD2-GFP is predominantly associated with the actin cytoskeleton before pH treatment (E and H, white bar), after 2 min of incubation in the alkalinising buffer (F and H, grey bar) and after 2 min of subsequent incubation in the acidifying buffer (G and H, black bar).

Bars = 10 μm .

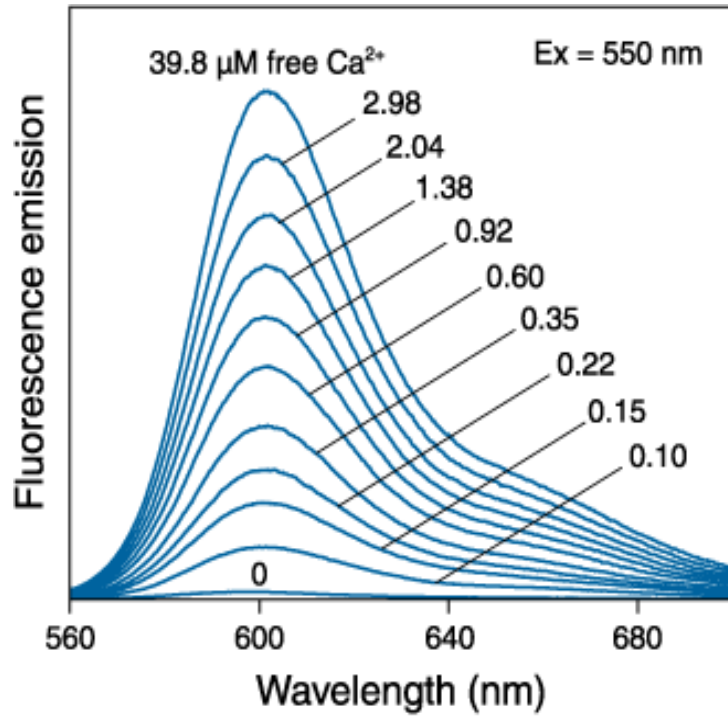


Figure 40: X-rhod-1 is a $[\text{Ca}^{2+}]$ -sensitive dye.

Fluorescence spectrum of X-rhod-1 as a function of free $[\text{Ca}^{2+}]$ (taken from Invitrogen, USA).

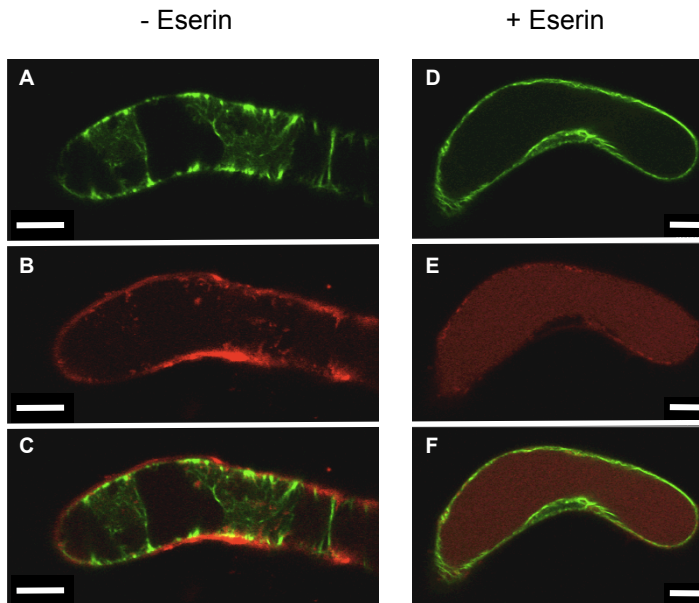


Figure 41: Eserin enhances loading of X-rhod-1 in transgenic *Arabidopsis* cells.

Imaging of X-rhod-1 in *Arabidopsis* cells expressing GFP-ABD2-GFP.

(A) and (D) Central confocal sections of GFP-ABD2-GFP expressing cells.

(B) and (E) Imaging of X-rhod-1 in the same section.

(C) and (F) Merges images of (A-B) and (D-E) respectively.

Note that the application of eserine strongly enhances loading of X-rhod-1 in the cytoplasm and the vacuole.

Bars = 10 μ m.

2. Subcellular localisation of WLIM1 and PLIM2c in *Arabidopsis* cells submitted to artificially induced modification of $[Ca^{2+}]_{cyt}$

One anticipates from the *in vitro* data that PLIM2c actin-regulatory activities are specifically down-regulated by an elevation of $[Ca^{2+}]_{cyt}$ as well. To test this assumption, we analysed and compared the ability of PLIM2c and WLIM1 to interact with the actin cytoskeleton at different $[Ca^{2+}]_{cyt}$.

2.1. Design and validation of the experimental procedure to modify the cytoplasmic calcium concentration of *Arabidopsis* cell

We selected a Ca^{2+} -sensitive dye allowing us to monitor $[Ca^{2+}]_{cyt}$ variations: X-rhod-1. X-rhod-1 is a high affinity Ca^{2+} indicator emitting in red (Figure 40), which is compatible with GFP. As for pH, in order to load X-rhod-1 without the need of microinjection, we used a cell-permeant version of the dye named acetoxymethyl ester (AM, Kuchitsu et al., 2002). Prior to $[Ca^{2+}]_{cyt}$ treatment, GFP-WLIM1, GFP-PLIM2c and GFP-ABD2-GFP (control) expressing cells were incubated in standard culture medium supplemented with X-rhod-1. First attempts using a standard protocol were not successful as X-rhod-1 only partially penetrated the cells. Since some acetoxymethyl esters are relatively insoluble in aqueous solutions, the low-toxicity dispersing agent Pluronic® F-127 (0.02%) was used to facilitate the loading of X-rhod-1 into the cells. In plant cells, extracellular esterases can severely reduce the loading of AM-esters into the cells (Kuchitsu et al., 2002). Therefore we applied eserine, also known as physostigmine (500 μ M, Sigma), an esterase inhibitor, to inhibit extracellular hydrolysis of the AM-ester. Indeed, eserine efficiently enhanced the X-rhod-1 loading as shown in Figure 41.

Both the concentration and the incubation time of X-rhod-1 were optimised for GFP-WLIM1, GFP-PLIM2c and GFP-ABD2-GFP expressing cells to 1 μ M and 2 hours, respectively. Before fluorescence measurements were performed, cells were washed in a dye-free buffer (fresh standard culture medium) in order to remove any traces of X-rhod-1, which could have remained associated with the cell surface, and incubated for 1 hour in the dye-free buffer. X-rhod-1 diffused in a homogenous manner into the cytoplasm as shown in Figure 42. The dye also penetrated the central

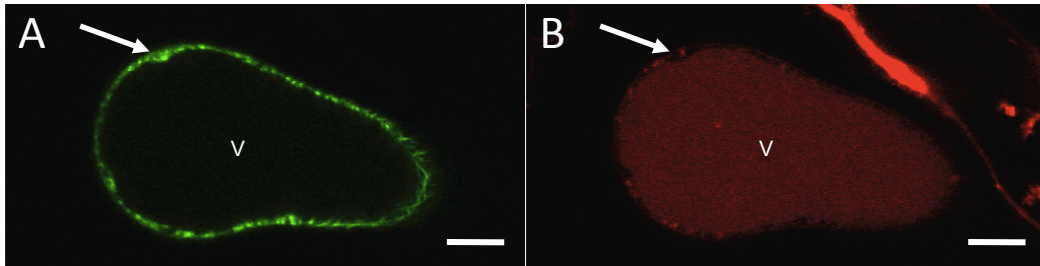


Figure 42: The vacuole contains high level of Ca^{2+} .

(A) Central confocal section of a GFP-ABD2-GFP expressing cell.

(B) Imaging of X-rhod-1 in the same section.

Note that the intensity of X-rhod-1 is much higher in the vacuole (V) than in the cytoplasm (arrow).

Bars = 10 μm . V: vacuole, Arrow: cytoplasm.

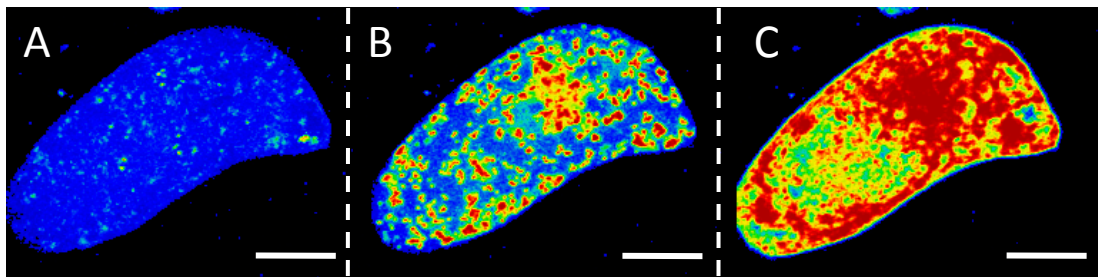


Figure 43: Strong increase in $[\text{Ca}^{2+}]_{\text{cyt}}$ induced by a prolonged exposure of *Arabidopsis* cell to the $[\text{Ca}^{2+}]_{\text{cyt}}$ increasing buffer.

Typical patterns of X-rhod-1 as visualised by pseudocolours before (A) and after 10 min (B) and 20 min (C) treatment with the $[\text{Ca}^{2+}]_{\text{cyt}}$ increasing buffer.

Bars = 10 μm .

vacuole (Figure 42), which is known to contain high levels of $[Ca^{2+}]$ (Allen et al., 1995; Rudd and Franklin-Tong, 1999). To increase or decrease $[Ca^{2+}]_{cyt}$, cells were incubated in buffers containing the A23187 ionophore and cyclopiazonic acid (CPA) or the cell-permeant Ca^{2+} -chelator BAPTA, respectively (Tsien, 1980; Deber et al., 1985; Busch and Sievers, 1993). In order to determine the optimised incubation time, we performed a time-lapse experiment to monitor the evolution of $[Ca^{2+}]_{cyt}$ as a function of time. A picture was taken every 3 minutes after $[Ca^{2+}]_{cyt}$ modifications for a total duration of 2 hours (data not shown). We determined that confocal acquisitions of X-rhod-1 and of GFP-fused proteins had to be collected just before and 6 min after the application of $[Ca^{2+}]$ -modifying buffers. It should be noticed that incubation times ≥ 9 min in $[Ca^{2+}]$ -increasing buffer frequently resulted in a cytotoxic Ca^{2+} burst (Figure 43).

2.2. An increase in $[Ca^{2+}]_{cyt}$ inhibits the binding of both GFP-PLIM2c and GFP-WLIM1 to actin filaments

To determine whether the subcellular localisations of *Arabidopsis* LIM proteins were regulated by Ca^{2+} , GFP-WLIM1, GFP-PLIM2c and GFP-ABD2-GFP (control) expressing cells were subjected to $[Ca^{2+}]_{cyt}$ modifications and analysed by confocal microscopy. The effect of $[Ca^{2+}]_{cyt}$ modifications on the ability of each GFP fusion protein to interact with the actin cytoskeleton was analysed by quantifying the FCFAC and by comparing this value before and after $[Ca^{2+}]_{cyt}$ treatment ($R_{FCFAC} = FCFAC_{t6}/FCFAC_{t0}$). Figure 44 shows typical results obtained with the three cell lines. Successful modifications of $[Ca^{2+}]_{cyt}$ were confirmed by comparing the relative $[Ca^{2+}]_{cyt}$ after and before the treatment (Figure 44O-Q, red curves). An increase in $[Ca^{2+}]_{cyt}$ dramatically weakened the binding of both GFP-WLIM1 and GFP-PLIM2c to the actin cytoskeleton, as shown by prominent diffuse fluorescent signal (Figure 44E-H and 44I-L, respectively). Massive release of both GFP-PLIM2c and GFP-WLIM1 from the actin network upon $[Ca^{2+}]_{cyt}$ elevation is confirmed by R_{FCFAC} values of 0.05 and 0.01, indicating that about 95% and 99% of the fluorescence initially associated with the cytoskeleton has been displaced toward the cytoplasmic diffuse pool after 6 min of treatment, respectively. Contrary to GFP-PLIM2c and GFP-WLIM1, GFP-ABD2-GFP remained predominantly associated with the actin

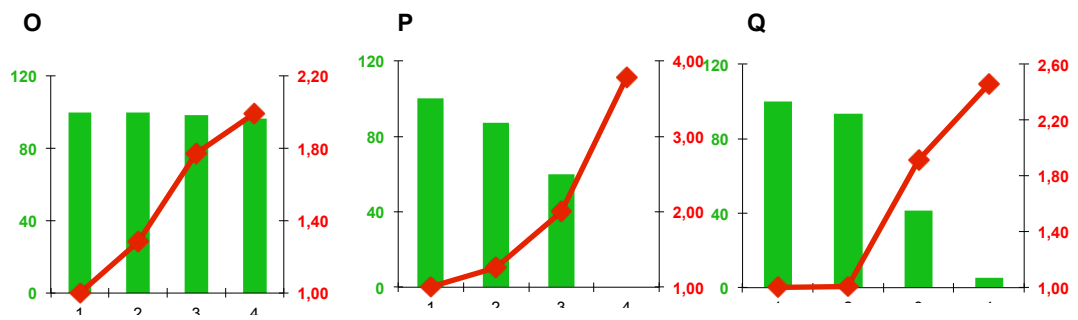
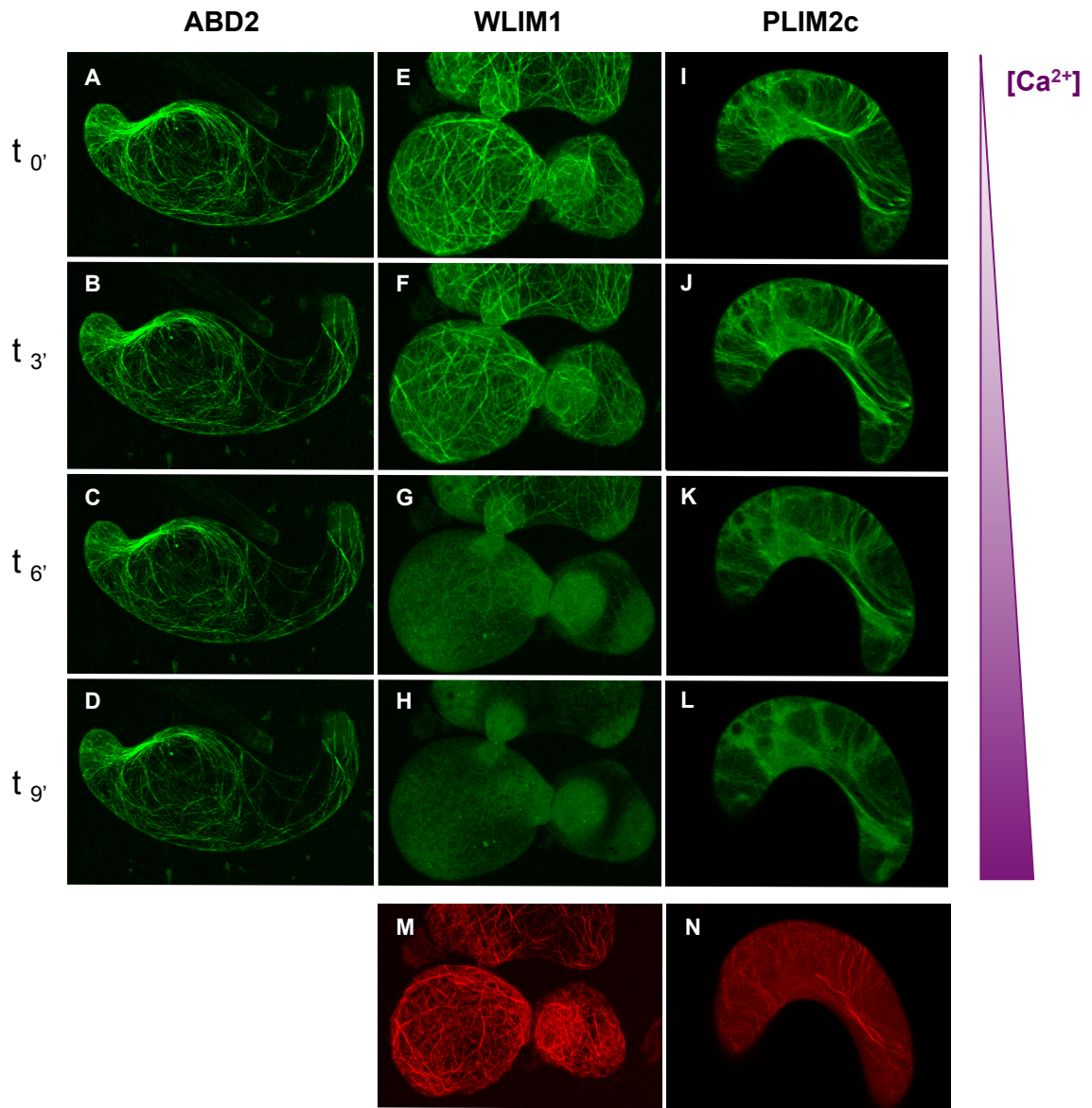


Figure 44: Increase in cytoplasmic $[Ca^{2+}]_{cyt}$ impairs GFP-WLIM1 and GFP-PLIM2c interaction with the actin cytoskeleton.

(A) to (L) *Arabidopsis* cells expressing GFP-ABD2-GFP (A-D), GFP-WLIM1 (E-H) and GFP-PLIM2c (I-L) treated with $[Ca^{2+}]_{cyt}$ increasing buffer.

Subcellular distribution patterns of GFP-fused proteins before (A,E,I) and 3 min (B,F,J), 6 min (C,G,K) and 9 min (D,H,L) after increase in $[Ca^{2+}]_{cyt}$.

Note the prominent diffuse cytoplasmic signal observed in GFP-WLIM1 and GFP-PLIM2c expressing cells 9 min after increase in $[Ca^{2+}]_{cyt}$ (G,H, K and L).

(M) and (N) Rhodamine-phalloidin labelling of GFP-WLIM1 and GFP-PLIM2c expressing cells 9 min increase in $[Ca^{2+}]_{cyt}$.

(O-Q) Determination of FCFAC (fraction of fluorescence associated with the cytoskeleton) values (green columns) for GFP-ABD2-GFP (O), GFP-WLIM1 (P) and GFP-PLIM2c (Q). Increase in $[Ca^{2+}]_{cyt}$ (red curves) were evaluated by comparing the fluorescence intensities (X-rhod-1) before and after treatments. Note the low FCFAC values calculated for GFP-WLIM1 and GFP-PLIM2c upon increase $[Ca^{2+}]_{cyt}$ increase.

Bars = 10 μ m.

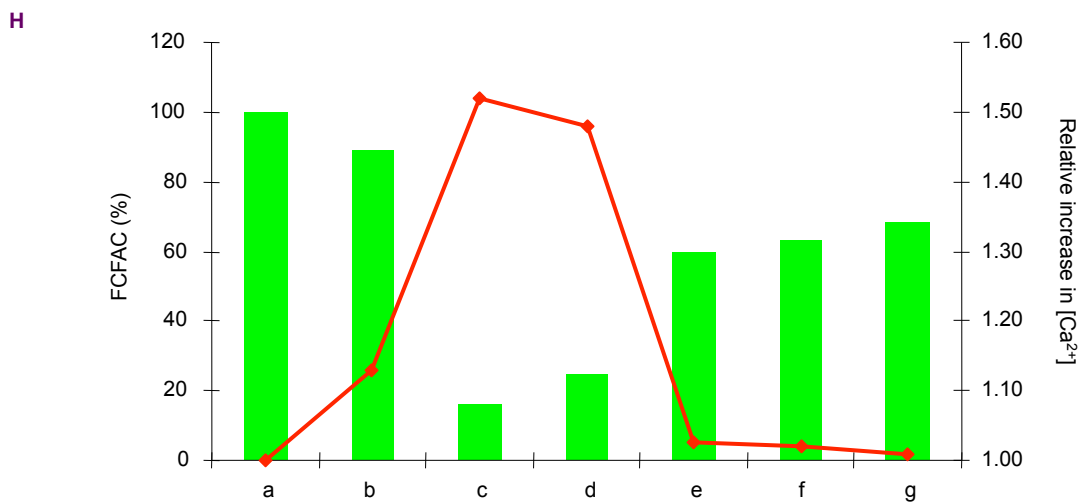
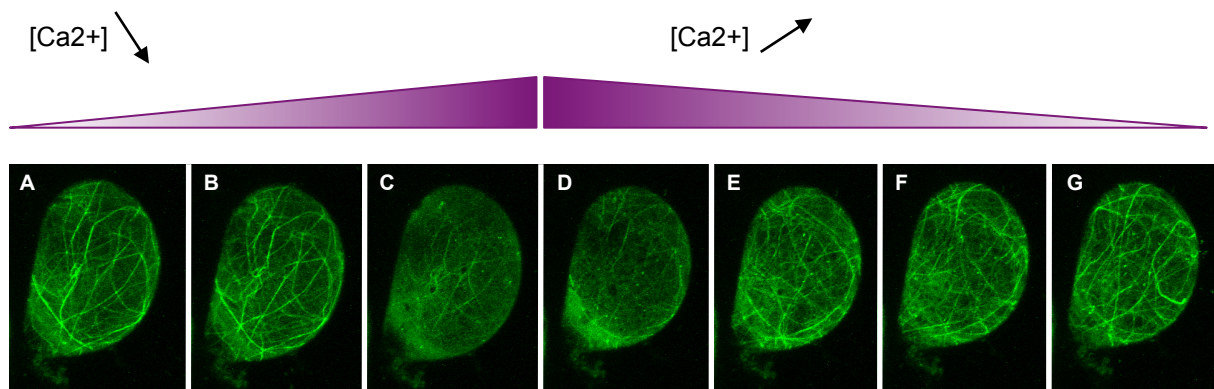


Figure 45: GFP-WLIM1 dissociates and re-associates with the actin cytoskeleton by successive increase and decrease in $[Ca^{2+}]_{\text{cyt}}$

Subcellular localisation of GFP-WLIM1 before (A) and after 3 and 6 min (B and C, respectively) of $[Ca^{2+}]_{\text{cyt}}$ increase and after 9, 19, 29 and 39 min (H, E, F and G, respectively) of incubation in a Ca^{2+} -chelator (BAPTA) buffer.

(H) FCFAC (fraction of cytoplasmic fluorescence associated with the cytoskeleton) values calculated from images A-G. The evolution in $[Ca^{2+}]_{\text{cyt}}$ (red curve) was monitored by comparing the fluorescence intensities (X-rhod-1) before and after each treatment. Note that GFP-WLIM1 is predominantly associated with the actin cytoskeleton before Ca^{2+} treatment (a), dissociates from the actin cytoskeleton upon $[Ca^{2+}]$ increase (b and c) and readily re-associates with the actin cytoskeleton upon $[Ca^{2+}]_{\text{cyt}}$ decrease (d-g).

Bars = 10 μm .

cytoskeleton upon cytoplasmic $[Ca^{2+}]_{cyt}$ elevation ($R_{FCFAC} = 0.96$; Figure 44A-D). Importantly, rhodamine-phalloidin co-labelling experiments confirmed the persistence of a filamentous actin cytoskeleton upon an increase in $[Ca^{2+}]_{cyt}$ in the GFP-PLIM2c and GFP-WLIM1-expressing cells (Figure 44N and 44M, respectively). As previously done for the pH, the reversibility of the process was checked by successive treatments of cells with $[Ca^{2+}]_{cyt}$ increasing and decreasing buffers. To perform this experiment, we had to adjust the pH to 7.0 in order to avoid a Ca^{2+} -burst that could not be compensated by the BAPTA-containing buffer. As exemplified for GFP-WLIM1, confocal images and corresponding FCFAC values indicate that WLIM1 could efficiently dissociate from and re-associate with the filamentous actin cytoskeleton (Figure 45). This demonstrates that WLIM1 actin-binding ability was not irreversibly damaged by high $[Ca^{2+}]_{cyt}$.

Together these data show that the subcellular localisation of both GFP-PLIM2c and GFP-WLIM1 is modified by Ca^{2+} . An increase in $[Ca^{2+}]_{cyt}$ induces a massive release of both GFP-WLIM1 and GFP-PLIM2c from the actin cytoskeleton. This is well consistent with the *in vitro* data obtained for PLIM2c but not for WLIM1 since the latter was found to be highly active in both low and high $[Ca^{2+}]$. This apparent inconsistency suggests that, contrary to PLIM2c, WLIM1 is not directly but indirectly regulated by Ca^{2+} . This will be further discussed in the discussion section (§ V).

3. Subcellular localisation of GFP-PLIM2c and GFP-WLIM1 in growing lily pollen tubes

The above *in vitro* and *in vivo* data indicate that pH and Ca^{2+} regulate the actin-regulatory activities of the pollen PLIM2c. This strongly suggests that PLIM2c plays central roles in the regulation of actin cytoskeleton organisation and dynamics during pollen tube growth since the latter process largely depends on pH and $[Ca^{2+}]$ gradients/oscillations. An additional step towards a clearer view of the role of PLIM2c in pollen consists in the examination of its subcellular localisation in live growing pollen tubes. We anticipate that PLIM2c should interact with long and thick actin bundles in the pollen tube shank where pH and $[Ca^{2+}]$ are maintained at

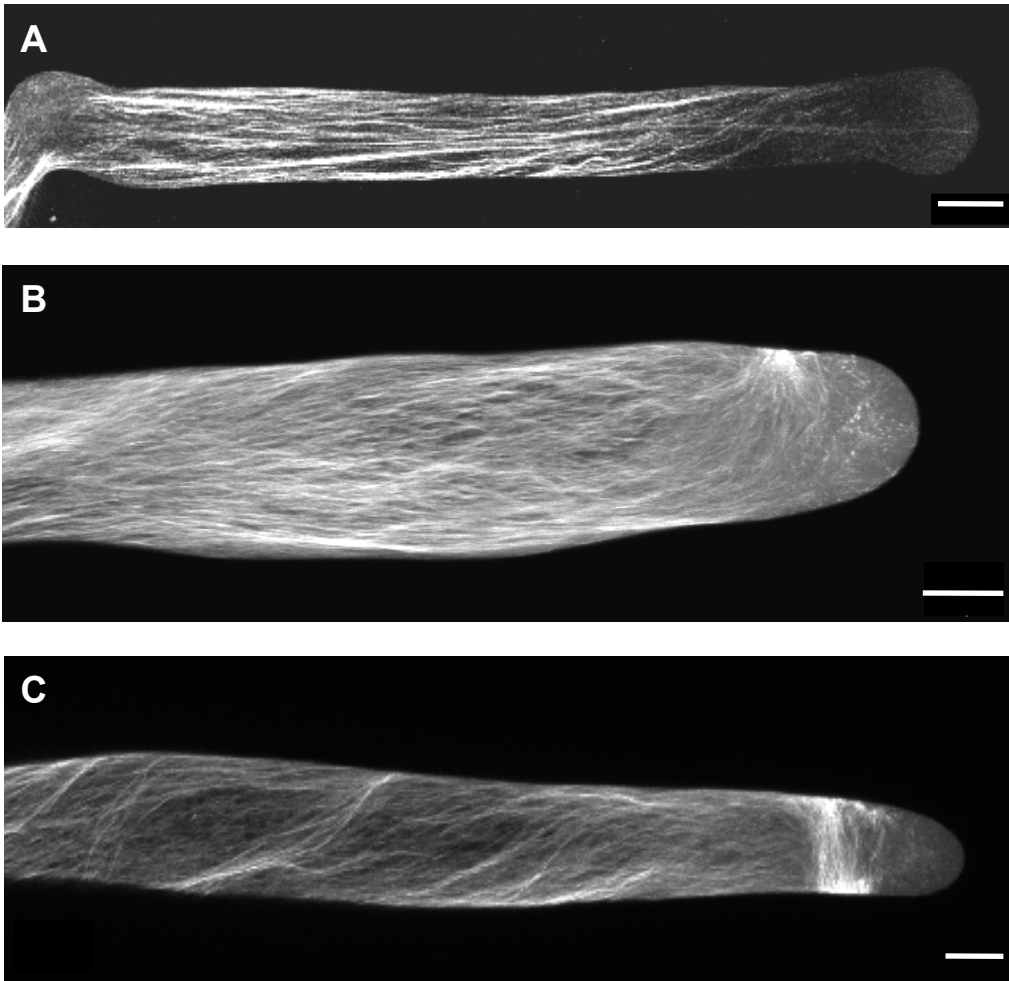


Figure 46: Most typical GFP-PLIM2c and GFP-WLIM1 subcellular localisation patterns in the lily growing pollen tube.

Green fluorescent patterns in GFP-PLIM2c (A) or GFP-WLIM1 (B and C) expressing growing pollen tubes. Observations were performed 4 to 6 h after the initiation of germination.

Bars = 10 μ m.

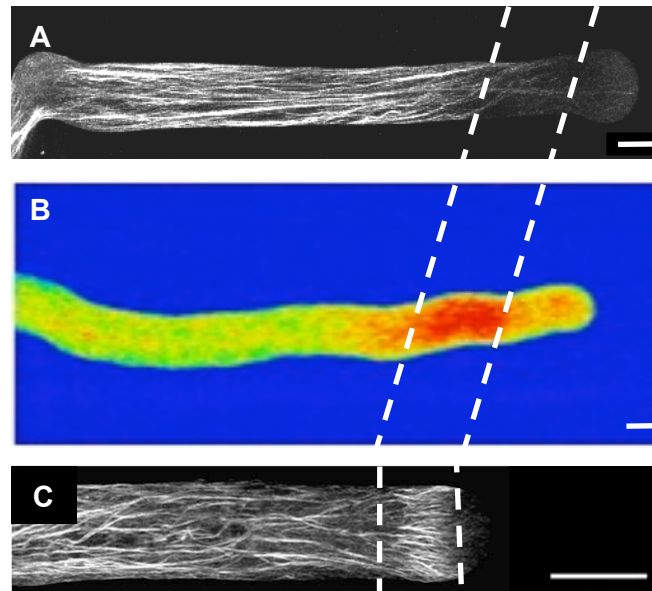


Figure 47: GFP-PLIM2c does not efficiently label with the actin cytoskeleton in the subapical region of growing pollen tubes.

(A) GFP-PLIM2c subcellular localisation in a growing pollen tube (same image as in Figure 46).

(B) Wild type lily pollen tube loaded with the pH-sensitive dye SNARF-5F. Note the prominent alkaline band in the subapical region.

(C) Lily pollen tube chemically fixed with EGS and stained with phalloidin (taken from Lovy-Wheeler et al., 2006). Note the prominent short actin bundles in the subapical region.

Bars = 10 μm .

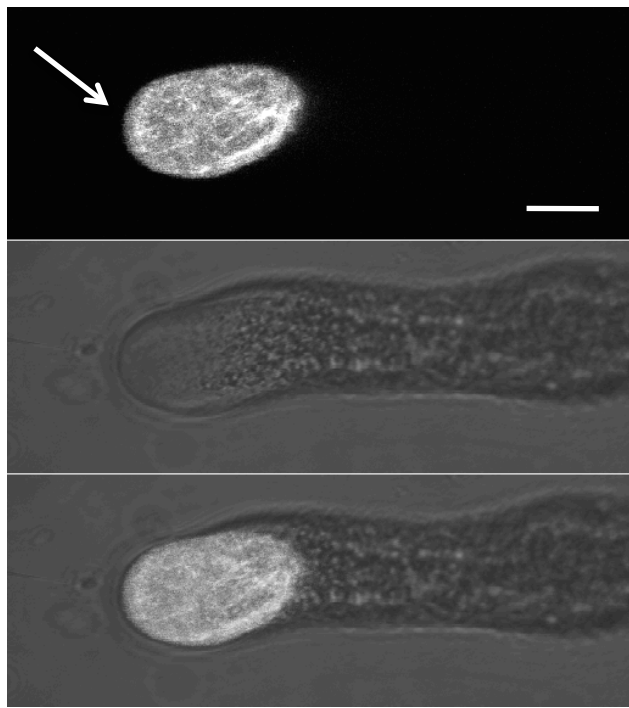


Figure 48: GFP-PLIM2c occasionally decorates cortical filamentous F-actin-like structures in the subapical region of growing pollen tubes.

Upper panel: cortical F-actin-like structures in the subapical region of growing pollen tubes (arrow) occasionally labelled by GFP-PLIM2c. Middle panel: corresponding phase contrast image. Lower panel: merge.
Bar = 10 μm .

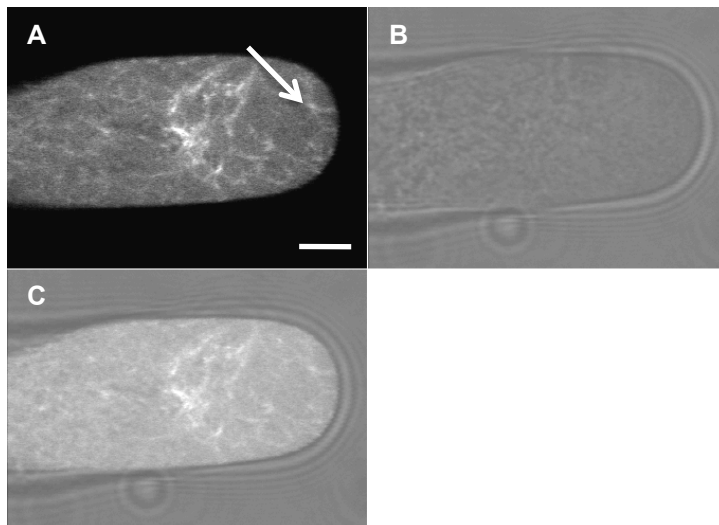


Figure 49: GFP-WLIM1 frequently decorates cortical filamentous F-actin-like structures in the subapical region of growing pollen tubes.

Upper left panel: cortical F-actin-like structures in the subapical and apical regions of growing pollen tubes (arrow) frequently labelled by GFP-WLIM1. Right panel: corresponding phase contrast image. Lower left panel: merge.
Bar = 10 μm .

relatively low values, whereas it should not robustly label the actin fringe in the subapical region where pH and $[Ca^{2+}]$ reach higher values. In parallel, the examination of the subcellular localisation in growing pollen tubes of an ectopically-expressed, non pollen and non pH-sensitive, LIM such as WLIM1 should yield valuable data that might help to build a solid model of PLIM function in pollen. Unfortunately, the constitutive CaMV 35S promoter does not trigger sufficient gene expression in pollen. Therefore the transgenic *Arabidopsis* lines previously described in this manuscript could not be used to examine the subcellular localisation of GFP-PLIM2c and GFP-WLIM1 in pollen tubes. Thus, we generated novel plasmids allowing the expression of GFP-PLIM2c and GFP-WLIM1 under the control of the maize pollen-specific promoter pZM13 (Hamilton et al., 1992). Using biolistic transformation, these plasmids were introduced into lily pollen grains. Consecutively to the transformation, lily pollen grains were germinated *in vitro* and the subcellular localisation of transiently-expressed GFP-fused LIMs was analysed by confocal microscopy. It should be mentioned that for time reasons, only preliminary results are presented here. Figure 46A shows typical localisation pattern observed for GFP-PLIM2c in most of the growing pollen tubes analysed. As expected, GFP-PLIM2c efficiently decorated the long actin bundles present in the pollen tube shank whereas no or only weak diffuse fluorescent signal was observed in the subapical and apical regions. Noticeably, imaging the pH_{cyt} gradients using the previously described SNARF5F dye shows that the inability of GFP-PLIM2c (Figure 47A) to label filamentous actin structures in the subapical region (see Figure 47C) is correlated with a local increase in pH_{cyt} most likely corresponding to the alkaline band (Figure 47B). It is however worth noting that in several pollen tubes, GFP-PLIM2c decorated not well defined cortical filamentous structures in the subapical region (Figure 48). This suggests that GFP-PLIM2c can occasionally interact with elements of the actin fringe, possibly when the oscillatory pH of the alkaline band reaches its lowest values.

The analysis of pollen tubes expressing GFP-WLIM1 pointed out a number of interesting differences with the above-described patterns. Although in most of the tubes, GFP-WLIM1 also decorated the longitudinal bundles in the pollen tube shank, these bundles were usually more abundant and thinner than those labelled by GFP-PLIM2c (Figure 46). In addition, within or in the vicinity of the subapical region, bundles occasionally concentrated at a discrete site of the cell cortex and changed

their orientation, i.e. they became perpendicular to the pollen tube axis (Figure 46B and C). In some cases, GFP-WLIM1-decorated bundles define an entire peripheral section of cortex, giving rise to a cortical “ring-like” actin structure (Figure 49). Noticeably, this “ring-like” structure obviously differed from the so-called actin fringe, which consists in a cortical array of longitudinal bundles. Finally, in some of the analysed tubes, bundles clearly penetrated the most apical region, including the very tip of the pollen tube which is unusual.

Together these data are in good agreement with the idea that GFP-PLIM2c actin regulatory activity is regulated by pH and Ca^{2+} during pollen tube growth. In addition, the cytoskeletal abnormalities induced by WLIM1 strongly support that the specific responsiveness of PLIM2c to pH_{cyt} and $[\text{Ca}^{2+}]_{\text{cyt}}$ gradients is of prime importance for proper regulation of the actin cytoskeleton organisation and dynamics during pollen tube elongation.

IV. *Arabidopsis* LIM C-terminal domain is involved in the direct responsiveness of PLIM activities to pH and Ca^{2+}

In order to determine which domain of PLIM2c is responsible for its direct responsiveness to pH and Ca^{2+} , we compared its amino acid sequence to the one of the pH and Ca^{2+} non-responsive WLIM1 (Figure 50). The most divergent domain in size and in amino acid composition is the C-terminal domain. Noticeably, this domain is longer and contains significantly more charged residues in PLIM2c than in WLIM1 (Figure 50). To test whether the C-terminal domain can be involved in the specific and direct responsiveness of PLIM2c to pH and Ca^{2+} , we generated C-terminal truncated versions of PLIM2c and WLIM1 (control), namely PLIM2c Δ Ct and WLIM1 Δ Ct, and evaluated the ability of these mutant proteins to stabilise and bundle actin filaments at different conditions of pH and Ca^{2+} .

Chimeric and wild type proteins were subjected to a series of actin depolymerisation assays conducted at two pH conditions (6.2 and 7.4) and in the presence of low or high amount of free Ca^{2+} (5 nM and 300 μM , respectively). Under low pH and low $[\text{Ca}^{2+}]$, both PLIM2c Δ Ct and WLIM1 Δ Ct stabilised actin filaments

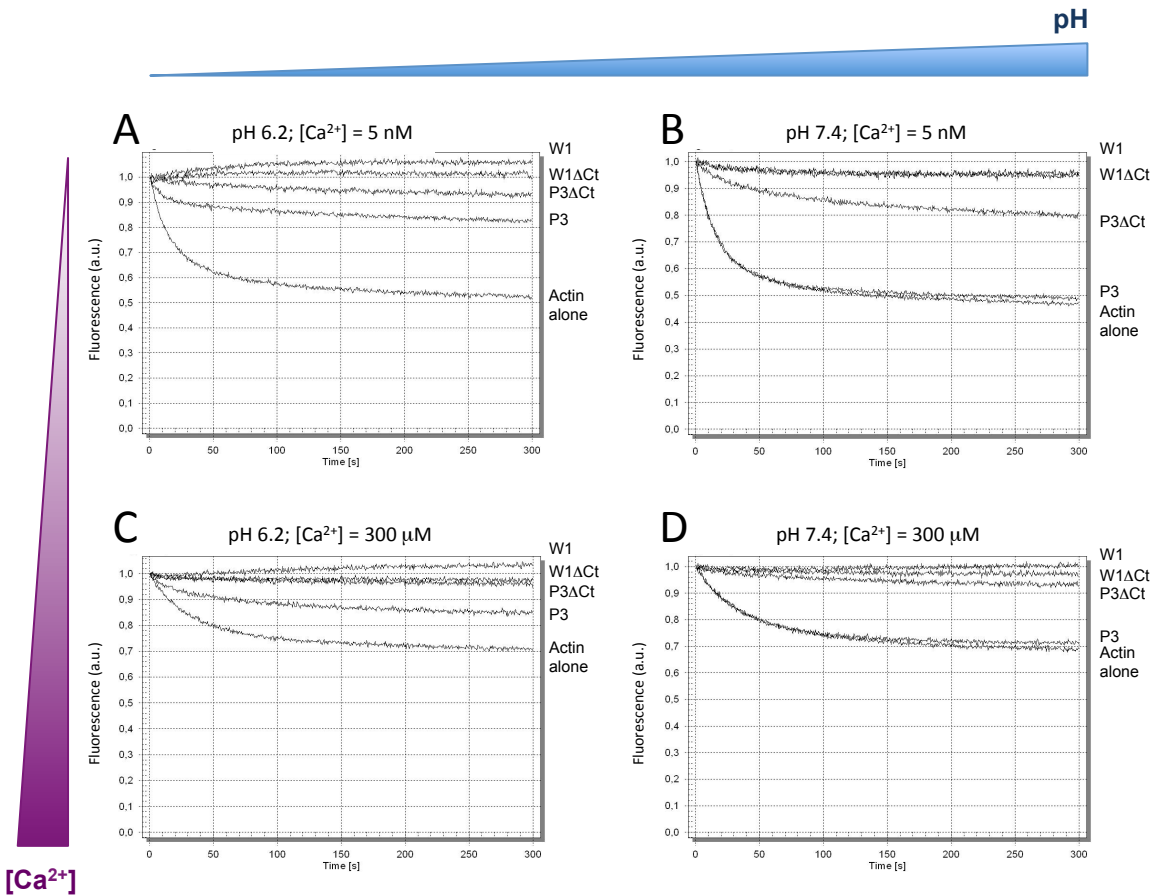


Figure 51: Comparison of the actin-stabilising activity of WLIM1, PLIM2c and their corresponding C-terminal deleted versions WLIM1ΔCt and PLIM2cΔCt at different pH and $[Ca^{2+}]$.

Depolymerisation assays. Pyrene-labelled actin filaments ($4 \mu\text{M}$) were co-polymerised in the presence of PLIM2c ($16 \mu\text{M}$), PLIM2cΔCt ($16 \mu\text{M}$), WLIM1 ($16 \mu\text{M}$) and WLIM1ΔCt ($16 \mu\text{M}$) in different combinations of pH (6.2 and 7.4) and $[Ca^{2+}]$ (5 nM and $300 \mu\text{M}$) and were induced to depolymerise by dilution below the critical concentration (i.e. $0.2 \mu\text{M}$). Initial fluorescence was set to 1.

with similar efficiencies as the corresponding full-length proteins (Figure 51A). As previously shown, increasing the pH from 6.2 to 7.4 caused an inhibition of the PLIM2c stabilising activity, as indicated by depolymerisation curves similar to the actin filaments alone (Figure 51B). By contrast, PLIM2c Δ Ct had prominent activity at both low and high pH values indicating that the deletion of the C-terminal domain has abolished the ability of PLIM2c to respond to pH (Figure 51A and 51B). As expected, at pH 6.2, an increase in [Ca²⁺] partially inhibited PLIM2c stabilising activity (Figure 51C). By contrast, in the same conditions, PLIM2c Δ Ct efficiently stabilised actin filaments indicating that the deletion of the C-terminal domain has abolished the ability of PLIM2c to respond to Ca²⁺ as well. In both high pH and high [Ca²⁺] conditions, PLIM2c Δ Ct remained fully active, supporting its non-responsiveness to pH and Ca²⁺ (Figure 51D). Both WLIM1 Δ Ct and WLIM1 efficiently stabilise actin filaments in all the tested conditions, indicating that the deletion of the C-terminal domain is not directly involved in WLIM1 actin-stabilising activity (Figure 51).

In parallel to the above experiments, we directly visualised by confocal microscopy the ability of PLIM2c, PLIM2c Δ Ct, WLIM1 and WLIM1 Δ Ct to crosslink actin filaments at different pH (6.2 and 7.4) and [Ca²⁺] (5 nM and 300 μ M; Figure 52). In agreement with the above data, both WLIM1 and WLIM1 Δ Ct efficiently bundled actin filaments in all the tested conditions (Figure 52 E-H and M-P) whereas PLIM2c was only active at low pH and low [Ca²⁺] (Figure 52A-D). Contrary to PLIM2c, PLIM2c Δ Ct promoted the formation of actin bundles in all the tested conditions (Figure 52I-L). These results confirm that PLIM2c Δ Ct is not directly regulated by pH and Ca²⁺ and is like WLIM1 “constitutively” active.

The above data point out a central role for the C-terminal domain of PLIM2c plays a central role in the specific direct responsiveness of PLIM2c to pH and Ca²⁺. We wondered whether the C-terminal domain was sufficient to confer this responsiveness to a normally non-responsive LIM protein. To address this issue, the C-terminal domains of PLIM2c and WLIM1 were swapped and the resulting chimeric proteins, namely PLIM2c Δ Ct-CtWLIM1 and WLIM1 Δ Ct-CtPLIM2c, were tested for their actin-bundling activities in different pH and [Ca²⁺] conditions.

Direct visualisation of actin filaments polymerised in the presence of chimeric proteins confirmed that WLIM1 Δ Ct-CtPLIM2c is partially deactivated by high [Ca²⁺]

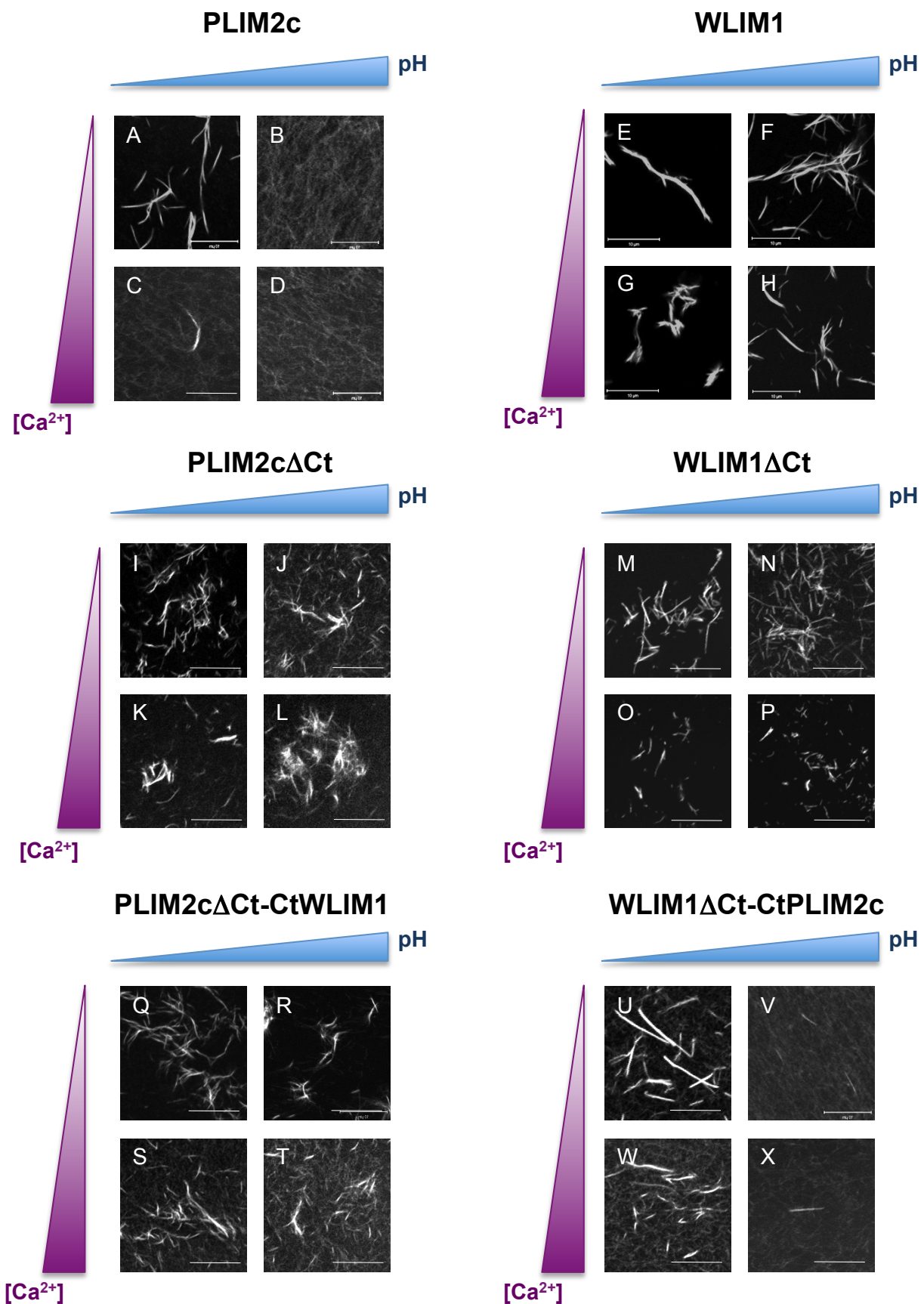


Figure 52: The C-terminal domain of PLIM2c is sufficient to confer pH and/or Ca^{2+} responsiveness to a normally pH and Ca^{2+} insensitive LIM protein.

Actin ($4 \mu\text{M}$) was polymerised the presence of $6 \mu\text{M}$ of PLIM2c (A-D), PLIM2c ΔCt (I-L), PLIM2c ΔCt -CtWLIM1 (Q-T), WLIM1 (E-H), WLIM1 ΔCt (M-P) and WLIM1 ΔCt -CtPLIM2c (U-X) in different pH (6.2 and 7.4) and $[\text{Ca}^{2+}]$ combinations (5 nM and $300 \mu\text{M}$). The induced actin structures were labelled with rhodamine-phalloin and analysed by confocal microscopy.
 Bars = $5 \mu\text{m}$

and fully inhibited by high pH values whereas PLIM2c Δ Ct-CtWLIM1 remains active in all pH and [Ca²⁺] combinations (Figure 52U-X and 52Q-T, respectively).

Together these data demonstrate that the C-terminal domain of PLIM2c is sufficient to confer pH and Ca²⁺ sensitivity to WLIM1. We conclude that the C-terminal domain of PLIM2c, possibly of all PLIMs, plays a central role in their specific and direct responsiveness to pH and Ca²⁺.

V. Discussion

pH is a major regulatory factor of PLIM activities

Plant *LIM* genes define two differentially expressed subfamilies: the *WLIM* subfamily, whose members are widely expressed in various types of tissues, and the *PLIM* subfamily, whose members are predominantly and strongly expressed in pollen (Eliasson et al., 2000; Mundel et al., 2000; Arnaud et al., 2007, Papuga and Hoffmann et al., 2010). Our biochemical data provide evidence that the PLIM2c actin-stabilising and -bundling activities are directly modulated by pH whereas those of WLIM1 are not. Noticeably, PLIM2c actin regulatory activities are turned off by pH values ≥ 6.8 . Similar results were obtained with the other members of each LIM subfamily (Papuga and Hoffmann et al., 2010). Indeed, PLIM2a and PLIM2b are deactivated by high pH values whereas WLIM2a and WLIM2b remain active at both low and high pH values. In addition, the pollen-enriched LIM1 from lily has also been reported to preferentially bind to actin filaments when pH is low (Wang et al., 2008b). Together these data support that direct pH responsiveness is a common and specific feature of most, possibly all, PLIM subfamily members. Importantly, our live-cell investigations demonstrate that *Arabidopsis* PLIM2c is effectively regulated by pH *in vivo*. Indeed, an increase in pH_{cyt} specifically disrupts the interaction between PLIM2c and the filamentous actin cytoskeleton. Surprisingly, the pH threshold above which PLIM2c is deactivated is apparently higher *in vivo* than *in vitro*. Indeed, when fused to GFP, PLIM2c still efficiently decorates the actin cytoskeleton of *Arabidopsis* cells whose average pH_{cyt} was estimated to be close to 7.0, whereas *in vitro* PLIM2c actin-

stabilising and -bundling activities are fully inhibited at pH 6.8 *in vitro*. This suggests that other factors than pH modulate PLIM2c activity in the cellular context. In agreement with the *in vitro* data, WLIM1 predominantly associates with the actin cytoskeleton of *Arabidopsis* cells independently of pH conditions. However, it should be noticed that a moderate reduction (~18 %) in the WLIM1 cytoskeletal fraction was observed upon an elevation of pH_{cyt}. On the one hand, the biological significance of this response is questionable considering its relative weakness. On the other hand, an indirect inhibition of WLIM1 activities by pH through de/activation of pH-dependent factors, such as pH-dependent kinases or phosphatases, cannot be ruled out. It is worth noting that several putative phosphorylation sites have been predicted in both WLIM and PLIM sequences (Arnaud et al., 2007) and that a vertebrate counterpart of plant LIMs, namely the rat CRP2, has been reported to be phosphorylated *in vivo* (Huber et al., 2000). In addition, a direct interaction between a PLIM and a NIMA-related kinase (serine/threonine) has been recently reported in rice (Fujii et al., 2009). Therefore, the possible regulation of WLIM and PLIM activities by phosphorylation is an important issue that should be addressed. Preliminary results of isoelectric focusing experiments support that *Arabidopsis* LIMs are post-translationally modified (S. Tholl, personal communication).

PLIMs, pH and pollen tube elongation

Many lines of evidence indicate that pH gradients occur in growing pollen tubes and that these gradients correlate with the position of distinct arrays of actin filaments (Messerli and Robinson, 1997; Feijo et al., 1999 and 2001; Lovy-Wheeler et al., 2006; Certal et al., 2008). A so-called alkaline band has been characterised in the subapical region of pollen tubes where the long actin bundles that run along the pollen tube shank (where pH is lower) are replaced by a cortical array of short bundles often referred to as the actin fringe (Kost et al., 1998; Hepler et al., 2001; Sheahan et al., 2004; Lovy-Wheeler et al., 2005; Hepler et al., 2006; Cheung et al., 2008; Cheung and Wu, 2009; Chen et al., 2009; Vidali et al., 2009). A number of studies have described the direct implication of this structure in pollen tube elongation and highlighted its high rate of turnover (Gibbon et al., 1999; Fu et al., 2001; Vidali et al., 2001). Based on our biochemical data and *in vivo* investigations in *Arabidopsis* cells,

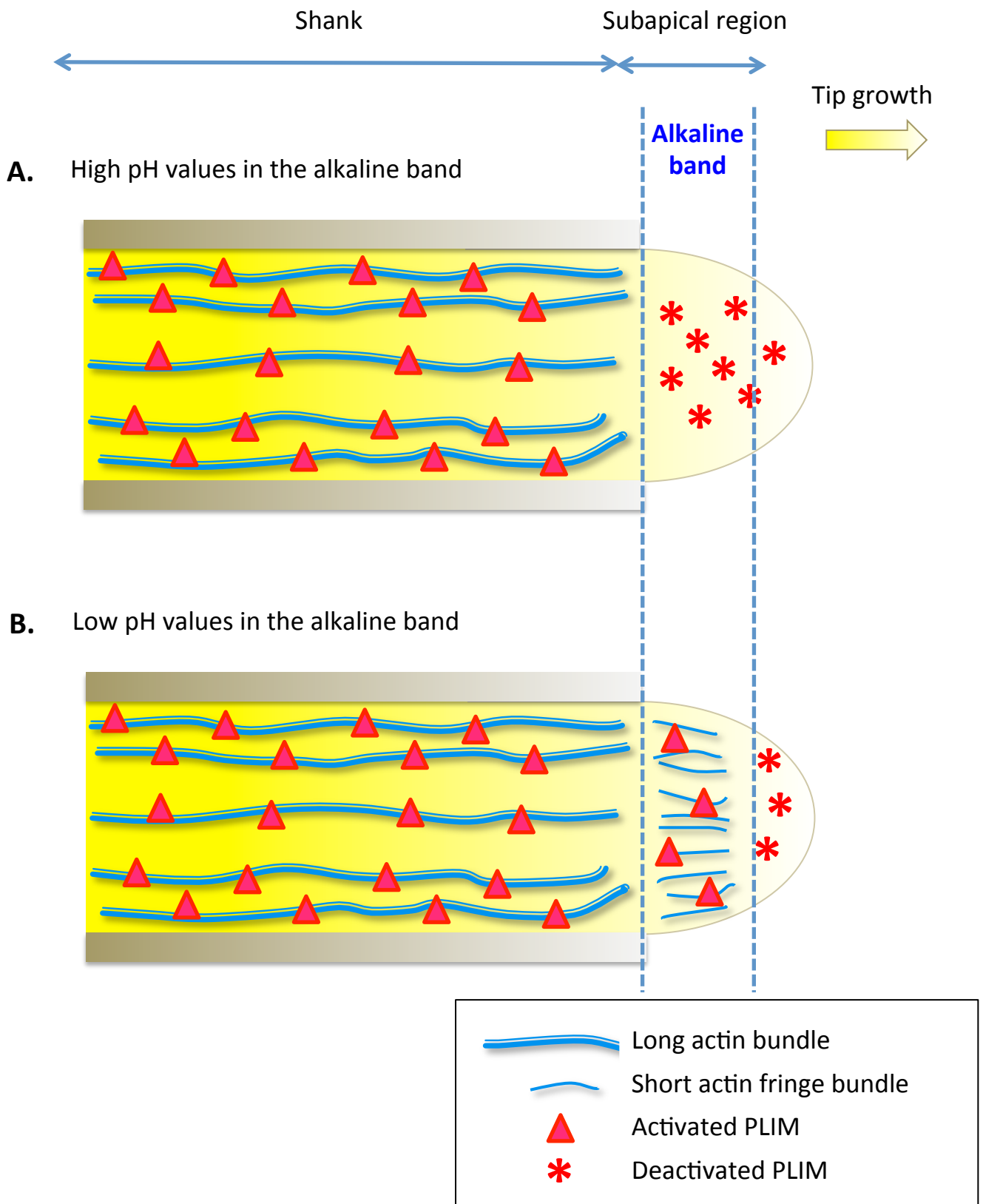


Figure 53: Model of the regulation of the actin cytoskeleton organisation and dynamics by PLIMs during pollen tube growth.

(A) The relatively low pH in the shank of the tube activates PLIMs (pink triangles) which promote the formation and stabilisation of long actin bundles. The high pH reached in the alkaline band inactivates PLIMs (pink stars). The actin fringe of the subapical region is not or only poorly stabilised.

(B) When the alkaline band reaches its lowest pH values, PLIMs are re-activated (pink triangle) and they transiently stabilise the actin fringe.

we propose a model describing the function and mode of regulation of PLIMs in pollen (Figure 53). In the shank of pollen tubes, the relatively low pH activates PLIMs which in turn promotes the formation and/or the maintenance of actin bundles. In the subapical region, the high pH values reached by the alkaline band down-regulate PLIM activity, allowing the actin cytoskeleton to remain in a highly dynamic state (Figure 53A). This dynamic state is required to keep the actin fringe at a constant distance from the growing tip (repeated cycles of assembly and disassembly). Our preliminary observations conducted in growing pollen tubes of lily are well consistent with our model. Indeed, GFP-PLIM2c predominantly decorates the long and thick actin bundles in the pollen tube shank (Figure 53) whereas it does not efficiently label the actin filaments/bundles in the subapical region, where pH was verified to reach the highest value. An important unsolved question is: how do the actin bundles of the actin fringe form? A seducing scenario is that PLIMs transiently crosslink and stabilise actin filaments of the actin fringe when the alkaline band reaches its lowest values (Figure 53B). Lovy-Wheeler et al. (2006) estimated that pH of the lily pollen alkaline band can briefly drop to 6.8, value allowing PLIM2c to interact efficiently with the actin cytoskeleton in *Arabidopsis* cells. Although GFP-PLIM2c did not efficiently decorate the actin fringe of transiently transformed lily pollen, it occasionally labelled not well-defined cortical structures in the subapical region, which could correspond to the actin fringe elements. In addition, more detailed and time-based analyses conducted in our laboratory with stably-transformed *Arabidopsis* lines revealed that GFP-PLIM2c intermittently labels an actin fringe-like structure in the subapical region of growing pollen tubes (Papuga and Hoffmann et al., 2010; see Figure 9). In conclusion, in addition to promoting actin-bundling in the pollen tube shank where pH is maintained at relatively low values, PLIMs likely participate in the formation and/or stabilisation of the actin fringe bundles in a transient, pH-dependent, manner.

Another ABP that has been proposed to play a central role in the regulation of the actin cytoskeleton dynamics in the subapical region of pollen tubes is the actin depolymerisation factor (ADF). Remarkably, ADF concentrates in the same area as the cortical actin fringe (Lovy-Wheeler et al., 2006), and its actin-severing activity is stimulated by alkaline pH conditions (Chen et al., 2002). Therefore, through their antagonistic actin regulatory activities, ADFs and PLIMs may orchestrate, in a pH-

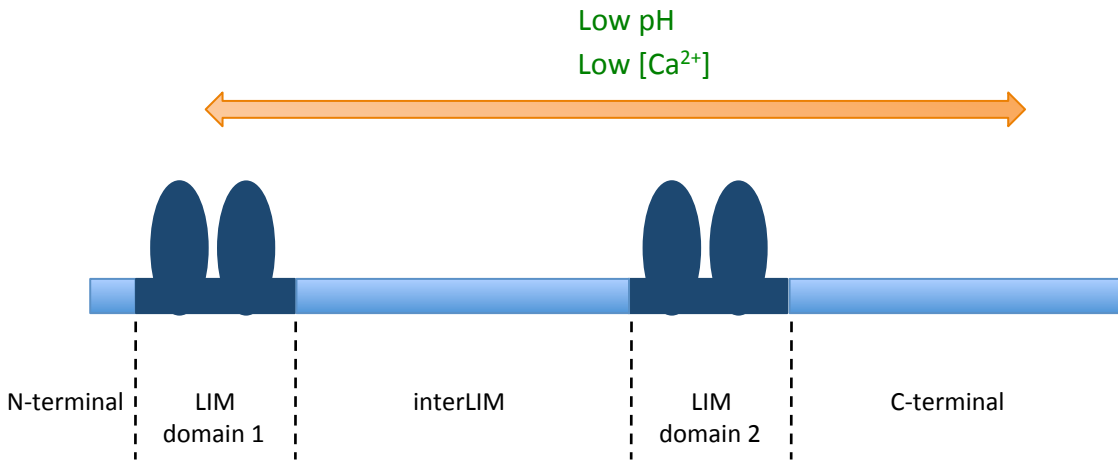
controlled manner and with other players, the successive cycles of disassembly and reassembly of the cortical fringe. Recently, the human CRP3 (or Muscle LIM Protein), a counterpart of plant LIMs, has been reported to directly interact with ADF/cofilin 2 in a pH-dependent manner (Papalouka et al., 2009). The possibility of a similar interaction between plant LIMs and ADFs as well as its potential effects on respective actin regulatory activities are important issues to be addressed by future work.

Calcium: another direct and indirect regulator of LIM activities

Calcium is another factor assumed to play crucial roles in the regulation of actin dynamics pollen tube elongation. Noticeably, a high tip oscillatory $[Ca^{2+}]_{\text{cyt}}$ gradient (Pierson et al., 1996; Holdaway-Clarke et al., 1997; Messerli and Robinson, 1997; Iwano et al., 2009) has been suggested to locally increase the rate of actin filament turnover through the activation of Ca^{2+} -dependent ABPs, such as profilins and villins/gelsolins (Fan et al., 2004; Huang et al., 2004, Yokota et al., 2005; Xiang et al., 2007; Khurana et al., 2010; Zhang et al., 2010). Consistent with this view, the down-regulation of PLIM2c actin-stabilising and -bundling activities by high $[Ca^{2+}]$ might participate in maintaining the actin cytoskeleton in a highly dynamic state in the subapical/apical region of growing pollen tubes.

Contrary to pH-responsiveness, direct Ca^{2+} -responsiveness is not a typical feature of PLIM subfamily members. Indeed, PLIM2a and PLIM2b do not respond to Ca^{2+} *in vitro* (Papuga and Hoffmann et al., 2010). However, we should be cautious not to rule out that these proteins can be (indirectly) regulated by Ca^{2+} *in vivo*. For instance, our *in vivo* investigations strongly support that WLIM1 binding to the actin cytoskeleton is Ca^{2+} -dependent, although WLIM1 was insensitive to pH and $[Ca^{2+}]$ variations *in vitro*. Plant calcium-dependent protein kinases (CDPKs) are the main contributors to Ca^{2+} -stimulated protein phosphorylation in plants, and form one of the largest protein kinase families (more than 30 genes encoding CDPKs have been identified in *Arabidopsis*). Several ABPs such as ADFs, have been reported to be phosphorylated by CDPKs (Smertenko et al., 1998; Allwood et al., 2001). Plant LIMs might be additional CDPK targets. As previously stated, post-translational modifications, which could correspond to phosphorylation events, of *Arabidopsis*

A. Open conformation



B. Closed conformation

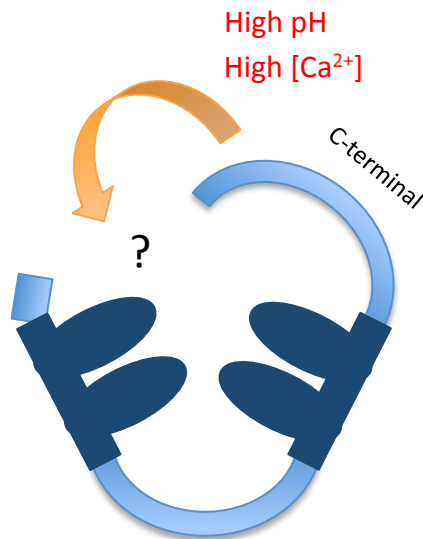


Figure 54: Model of the regulation of PLIM2c actin-regulatory activities by pH and Ca²⁺

(A) At low pH and low [Ca²⁺], PLIM2c adopt an open conformation allowing the two LIM domains to interact with the actin filaments.

(B) At high pH and high [Ca²⁺], the C-terminal domain of PLIM2c folds back by interacting with a yet unknown distant region and PLIM2c adopts a close conformation preventing its interaction with actin filaments.

LIMs are indicated by isoelectric focusing experiments (S. Tholl, unpublished data). We are currently characterising these modifications.

The C-terminal domain, a regulatory domain of LIM activities

A previous domain analysis conducted in the laboratory has demonstrated that both N- and C-terminal LIM domain function as autonomous actin-binding, and possibly -stabilising and -bundling, modules (Thomas et al., 2007b and 2008). Although no plant LIM structure has been published to date, the 3-dimensional conformation of vertebrate CRPs has been obtained by nuclear magnetic resonance (NMR; Perez-Alvarado et al., 1994; Konrat et al., 1997; Kontaxis et al., 1998; Yao et al., 1999; Schallus et al., 2007, 2009). These data indicate that the two LIM domains are two independent folding units that are connected by a very flexible linker region, i.e. the interLIM domain. Based on the above data and our findings that the C-terminal domain of PLIM2c plays a central role in pH and Ca^{2+} responsiveness, we propose a model for the molecular mechanism underlying the regulation of PLIM activity (Figure 54). At low pH and low $[\text{Ca}^{2+}]$, PLIM2c would adopt an open conformation, which allows the two LIM domains to interact with and to bundle actin filaments (Figure 54A). At high pH and/or high $[\text{Ca}^{2+}]$, the C-terminal domain would fold back by interacting with a distant region, e.g. the N-terminal or the interLIM domain, thereby masking one, possibly all, actin-binding sites and lowering or inhibiting the PLIM-actin filament interaction (Figure 54B). This hypothesis will be soon tested by NMR in collaboration with the laboratory of Prof. R. Konrat (University of Vienna, Institute of Biomolecular Structural Chemistry).

In conclusion, we propose that plant LIMs represent a highly specialised family of actin-bundling proteins that are present in virtually all plant cells. We propose that PLIM2c and possibly other PLIM subfamily members play central roles in the control of actin cytoskeleton organization and dynamics in pollen and are themselves under the control of oscillatory pH and $[\text{Ca}^{2+}]$ gradients.

Chapter 4

Conclusion and Perspectives

Chapter 4: Conclusion and Perspectives

Our laboratory was the first to report that plant LIMs are involved in the regulation of actin cytoskeleton organisation and dynamics. It demonstrated that the tobacco WLIM1 functions as an ABP that stabilises and promotes the formation of parallel actin bundles (Thomas et al., 2006, 2007). Afterwards, similar data were obtained with the lily LIM1 (Wang et al., 2008b). Plants genomes encode several *LIM* genes and it was therefore important to assess whether they all display similar actin regulatory activities/functions as tobacco WLIM1 and lily LIM1. Our data show that all six *Arabidopsis* LIMs display similar actin-binding, -stabilising and -bundling activities. According to their expression pattern, *Arabidopsis* LIMs respond differently to important cellular factors. Indeed, only the pollen-enriched PLIMs are deactivated by elevated pH and/or $[Ca^{2+}]$. This is highly consistent with a role for PLIMs in the formation and positioning of actin bundles in the growing pollen tube. Importantly, we could identify the C-terminal domain as the domain responsible for the pH and Ca^{2+} responsiveness of PLIMs. In addition to answering our initial questions, the present study also raises a number of novel questions which are listed below.

First, it will be important to extend *in vivo* studies regarding the pH and Ca^{2+} responsiveness to the rest of the *Arabidopsis* LIM family in order to validate our predictions and refine our model of PLIM functions in pollen tube growth. The subcellular localisation of all the six *Arabidopsis* LIMs will be assessed in cell suspension cultures whose pH_{cyt} and $[Ca^{2+}]_{\text{cyt}}$ will be artificially modified and in *in vitro* growing pollen tubes. In addition, we hope to succeed in immunolocalising endogenous LIM proteins in different cell types.

Although the involvement of the C-terminal domain in PLIM2c responsiveness to pH and/or Ca^{2+} has been clearly established, the underlying molecular mechanism remains speculative. Using NMR (in collaboration with Prof. R. Konrat, University of Vienna, Institute of Biomolecular Structural Chemistry), we will determine the spatial arrangement of WLIMs, PLIMs and of the respective C-terminal domain truncated variants in different conditions of pH and Ca^{2+} .

As discussed, *in vitro* and *in vivo* data argue against actin-severing or -nucleating activities for plant LIMs. However, other potential accessory activities including G-actin-binding, actin polymerisation facilitation and capping activities should be carefully assessed using fluorimetric and light scattering assays (e.g. Michelot et al., 2005). In addition, our confocal microscope will be soon equipped with a TIRF module and this will allow us to more directly and carefully study the mechanisms underlying plant LIM actin regulatory activities (e.g. Michelot et al., 2006).

We failed to efficiently decorate LIM-induced actin bundles using myosin S1-based assays. As an alternative, dual labelling profilin-based assays (Harris et al., 2006) will be used to characterise the relative orientation of actin filaments in LIM-induced bundles.

Possible dimerisation of LIMs will be assessed in live cells using Bimolecular Fluorescence Complementation (BiFC) and Fluorescence Lifetime Imaging Microscopy (FLIM).

Detailed studies of homozygous GFP-LIM expressing plants as well as analysis of multiple T-DNA insertion mutants should give insight into the function of actin-bundling by LIMs during plant development, e.g. in pollen tube growth.

Additional important aspect of our research is the elucidation of the nuclear functions of plant LIMs. Microarray experiments will reveal the genetic pathway possibly regulated by LIMs. The mechanism(s) of the cytoplasmic-nuclear LIM shuttling will be investigated by Fluorescence Recovery After Photobleaching (FRAP) experiments and the specific involved domain will be characterised.

Finally, yeast two-hybrid screening will possibly identify novel LIM partners.

Chapter 5

Materials and Methods

Materials and Methods

I. Microscopy

1. Confocal microscopy and imaging

Sample preparation

Leaves and roots of transgenic plants were cut from 4 to 5 day old seedlings and mounted between slide and coverslip in water for immediate observations.

Arabidopsis cells were fixed on poly-L-lysine coated slides and mounted in an open incubation chamber allowing an easy exchange of the medium which facilitated the treatment with actin depolymerisation medium and pH_{cyt} or $[\text{Ca}^{2+}]_{\text{cyt}}$ modification buffers.

For confocal analyses conducted with transiently transformed lily pollen, pollen grains were placed in microscope slides by embedding *in vitro* germinated pollen tubes in 1.4 % (w/v) low-melting agarose (Duchefa) re-suspended in pollen germination medium and observing them after 4 to 6 h.

Settings

Plants and cells expressing the GFP fusion proteins were imaged using a Zeiss LSM510 META confocal laser scanning microscope equipped with a 340 Plan-NeoFluar oil immersion objective (numerical aperture 1.3). GFP was detected by exciting samples at a wavelength of 488 nm and using a 505- to 530-nm band-pass emission filter. For rhodamine-phalloidin labelling experiments, a 543-nm excitation wavelength and a 560- to 615-nm band-pass emission filter were used. Confocal images were deconvolved using Huygens Essential image processing software package (Scientific Volume Imaging) and are shown as stacks of neighbouring sections reconstructed in ImageJ (National Institutes of Health).

SNARF5F (pH-sensitive dye) ratio imaging was used in the META channel using a 543-nm excitation wavelength and a laser power of 7%. Emitted light was simultaneously collected with a dual channel of 560- to 600-nm (Ch1) and 625- to 665-nm (Ch2) bandwidth. To optimize signal detection, the photomultiplier gain was

set over the range 60 to 70%. Ratio images were generated by dividing Ch2/Ch1 using the physiology module of LSM510 acquisition software. A 3 X 3 pixel median filter was applied to improve image quality, and final images were displayed with a rainbow look-up table.

Image treatment

Confocal images were deconvolved using Huygens Essential image processing software package (Scientific Volume Imaging) and are shown as stacks of neighbouring sections reconstructed in ImageJ (National Institutes of Health) or in Imaris (Bitplane).

For pH imaging with SNARF5F dye, ratio images were generated by dividing Ch2/Ch1 using the physiology module of LSM510 acquisition software. A 3 X 3 pixel median filter was applied to improve image quality, and final images were displayed with a rainbow look-up table.

Quantification of the FCFAC in GFP-LIM- and GFP-ABD2-GFP- expressing cells was performed using Metamorph software (Molecular Devices) by adjusting the image threshold to eliminate most of the diffuse cytoplasmic fluorescence. The threshold has to be adjusted for each cell because the actin cytoskeleton organisation and the associated intensity of fluorescence can slightly vary from one cell to another. The remaining integrated fluorescent signal was quantified and expressed as a percentage of the total cellular fluorescence (the nucleus was excluded). To estimate how artificial modifications of pH_{cyt} influence GFP-LIM and GFP-ABD2-GFP interaction with the actin cytoskeleton, FCFAC (fraction of fluorescence associated with the cytoskeleton) values were measured before (t_0') and after 2min (t_2') pH treatment, and FCFAC ratios ($R_{\text{FCFAC}} = \text{FCFAC}_{t_2'}/\text{FCFAC}_{t_0'}$) were calculated.

Relative quantity of calcium was measured in Metamorph (Molecular Devices). Fluorescence intensities corresponding to X-rhod-1 were measured at each timepoints (in a $50 \mu\text{m}^2$ square in the cytosol of the cell), compared to the intensity at t_0 and plotted on a graph.

Bundle density was measured with a home-made macro written for ImageJ (by Jérôme Mutterer, Plateforme de microscopie et d'imagerie, IBMP, Strasbourg). Briefly the macro will create a perpendicular section to the cell axis of a Z-stack projection (a $15 \mu\text{m}$ line corresponding to the cell width). The picture of this line will

be analysed with the “find maxima function” of ImageJ to count the number of intensity maxima. Each intensity maximum corresponds to an actin bundle.

2. Transmission electron microscopy (TEM)

We used the high-voltage TEM LEO 922 OMEGA (in collaboration with Jean-Christophe Lambrechts, Science and Analysis of Materials department, CRP-Gabriel Lippmann, Luxembourg).

One micromolar actin was polymerised with or without 1 μ M WLIM1 or PLIM2c protein on EM-grids (Carbon Fom on 150 square mesh nickel grids, Electron Microscopy Sciences) coated with poly-L-Lysine. After 20 min grids were washed 3 times in water and stained 1 min with uranyl acetate 1%.

II. Plant, cell and pollen material

1. Arabidopsis plants and plant growth

All transgenic *Arabidopsis thaliana* plants are in Columbia-0 background. For propagation, plants were greenhouse cultivated and propagated on soil under 16-h-light/8-h-dark cycles. For *in vitro* growth experiments seeds were surface sterilized by incubation for 5 min in 70% Ethanol, 0.05 % TritonX-100, washed for 3 times in 99% ethanol, dried in a laminar flow cabinet and transferred onto agar plates Half-strength Murashige and Skoog agar medium (MS255; Duchefa), pH 5.8, supplemented with 2% sucrose was used standard *Arabidopsis* growth medium. After 3-d stratification at 4°C in the dark, seeds were incubated in a growth chamber at 23°C under 12-h-light/12-h-dark cycles.

Generation of GFP-LIM-expressing transgenic *Arabidopsis thaliana* plants is described in Papuga et al., 2010. T1 generations have been provided by M. Dieterle. Transgenic *Arabidopsis thaliana* overexpressing GFP-ABD2-GFP were a kind gift of Dr. Blancaflor (Wang et al., 2008).

For selection, seeds were plated onto standard growth medium supplemented with 50 μ g/L of kanamycin (for GFP-ABD2-GFP) or 15 μ g/L of hygromycin (for GFP-LIMs).

2. Production of transgenic cell suspension cultures

2.1. Production of transgenic *Arabidopsis* cell suspension cultures expressing GFP-fused proteins

Arabidopsis cell suspension cultures were generated by transferring 10-d-old seedlings (GFP-WLIM1; GFP-PLIM2c and GFP-ABD2-GFP) onto a callus-inducing medium (Figure 18; Murashige and Skoog agar medium, 200 mg/L KH₂PO₄, 1 mg/L thiamine, 0.05 g/L myo-inositol, 20 g/L sucrose, and 1 mg/L 2,4-D, pH 5.7 supplemented with 8 g/L Plant Agar). Plates were wrapped in foil and kept in the dark at 22°C for 4 to 6 weeks. Calli were transferred to 40 mL liquid callus-inducing medium and maintained in the dark at 22°C with gentle agitation (100 rpm). Cells were propagated once a week by transferring 30 mL of 7-d-old suspension to 60 mL of fresh medium.

2.2. Production of transgenic tobacco BY-2 cell suspension cultures stably overexpressing GFP-PLIM2c

Agrobacterium tumefaciens (new scientific name: *Rhizobium radiobacter*) strain GV3101::pMP90 was transformed using the freeze/thaw shock method (Jyothishwaran et al., 2007). One ug of pMDC43/PLIM2c (Papuga et al., 2010) is added to 100 µL of chemically competent *Agrobacterium*, the suspension is flash frozen in liquid nitrogen for 30 sec, and afterwards thawed at 37°C for 5 min. Agrobacteria are subsequently added to 1 mL LB, incubated at 28°C with shaking for 3 h and finally plated on LB-agar medium supplemented with 50 µg/mL rifampicin, 25 µg/ml gentamycin and 50 µg/mL kanamycin and incubated at 28°C for 3 days. The presence of the plasmid in the selected agrobacteria was verified by colony PCR with primers MD400 and MD184.

Two mL LB were inoculated with a single agrobacteria colony transformed with pMDC43/PLIM2c and incubated at 28°C under shaking for 2 days. One day before co-cultivation agrobacteria were pelleted and resuspended 100 µL LB supplemented with 50 µg/mL rifampicin, 25 µg/ml gentamycin and 50 µg/mL

kanamycin. After 16 h of culture, agrobacteria were centrifuged 5 min at 3000 rpm. The supernatant were discarded and the bacterial pellet was resuspended in 1.5 mL LB supplemented with 200 μ M acetosyringone (3,5-dimethoxy-4-hydroxyacetophenon). For the co-culture, 4 mL of 3-day-old BY-2 cells were mixed with 100 μ L of agrobacteria in a 5-cm diameter petri dish. The petri dishes were incubated in the dark at 21°C under gentle shaking (50 rpm) for 3 days. After 72 h, BY-2 cells were transferred in a 50 mL tube and washed 3 times with fresh BY-2 culture medium. Between 2 washes, cells are centrifuged 10 mn at 800 rpm and the supernatants were discarded. After the last wash, 8 mL of BY-2 cells are conserved and mixed with 8 mL of BY-2 medium supplemented with 2 % low-melting agar (maintained at 40°C in the water bath). The sample is immediately plated on petri dishes containing solid BY-2 medium supplemented with 500 μ g/mL carbenicillin and 40 μ g/mL hygromycin and incubated at 28°C. Calli obtained after 3 to 6 weeks are transferred to liquid BY-2 culture medium and screened by confocal microscopy for GFP fluorescence.

3. Lily pollen grains

Lily (*Lilium longiflorum* White Europe) flowers were purchased in a local flower shop. Pollen was collected from freshly dehisced anthers and either directly used for experiments or flash-frozen in liquid nitrogen and conserved at -80°C.

III. Modifications of pH_{cyt}

Approximately 200 μ L of Arabidopsis cell suspension culture is plated on a poly-L-lysine-coated cover slip. After removing the culture medium, cells are incubated in 1 mL of 5 μ M ratiometric pH-sensitive dye SNARF-5F 5-(and-6)-carboxylic acid, acetoxymethyl ester, acetate (5 mM stock solution; Invitrogen) callus inducing medium for 30 min in the dark at 22°C. Modification of the pH_{cyt} is achieved by incubating cells afterwards with pH-modifying buffers (PMB) consisting in 1 mL of callus-inducing medium supplemented with 30 mM ammonium chloride and 10 mM HEPES, pH 7.4 (alkalizing buffer) or with 30 mM sodium propionate and 10 mM MES, pH 6.2 (acidifying buffer). Confocal microscopy observations are performed

just before pH buffer application and after 2, 4, and 6 min of treatment.

In situ calibration was performed as recommended by Feijo et al. (1999) using a combination of nigericin (5 μM) and valinomycin (2 μM) and in the presence of a high concentration of potassium ions. Reference pH buffers (half-strength Murashige and Skoog medium, 150 mM KCl, 30 mM NaCl, 25 mM HEPES, and 25 mM MES) were adjusted to a final pH of 6.2, 6.8, 7.0, 7.2, and 7.5. Cells were incubated 15 min in each pH buffer before imaging the SNARF-5F probe. A calibration curve was generated by calculating ratio values in cytoplasmic volumes of 50 μm^3 using Metamorph Software (Molecular Devices). This curve was used to estimate the pH in nontreated cells and to control pH modifications induced by the alkalizing and acidifying buffers ($n > 10$).

To visualize the pH_{cyt} in lily pollen tubes 1 mL liquid pollen germination medium (1.27 mM CaCl_2 , 0.162 mM H_3BO_3 , 0.99 mM KNO_3 , and 290 mM Sucrose, pH 5.2) supplemented with 10 μM SNARF-5F 5-(and-6)-carboxylic acid, acetoxymethyl ester, acetate was added on the semisolid PGM. After 1 h the liquid PGM was removed and the sample washed once with 1ml PGM. Images were taken after a further incubation of 30 min.

Approximately 200 μL of *Arabidopsis* cell suspension culture was plated on a poly-L-lysine-coated cover slip. After removing the culture medium, cells were incubated in 1 mL of diluted Ca^{2+} -sensitive dye X-rhod-1, acetoxymethyl ester, acetate (1 mM; Invitrogen) supplemented with eserine (500 μM) and 0.02% pluronic acid (Invitrogen) for 2 h in the dark at 22°C and washed with fresh culture medium for 1 h. Modifications of the $[\text{Ca}^{2+}]_{\text{cyt}}$ were achieved by incubating cells with $[\text{Ca}^{2+}]_{\text{cyt}}$ -modifying buffers consisting in 1 mL of callus-inducing medium supplemented with 20 μM cyclopiazonic acid (Sigma) and 10 μM ionophore A23187 (Invitrogen) ($[\text{Ca}^{2+}]_{\text{cyt}}$ increasing buffer) or 100 μM BAPTA (Invitrogen), 30 mM ammonium chloride HEPES, pH 7 ($[\text{Ca}^{2+}]_{\text{cyt}}$ decreasing buffer). Confocal microscopy observations were performed just before Ca^{2+} buffer application and after 3, 6, and 9 min treatment for $[\text{Ca}^{2+}]_{\text{cyt}}$ -increase. For Ca^{2+} decrease you image just before application and 10, 20, and 30 min after addition of ($[\text{Ca}^{2+}]_{\text{cyt}}$ decreasing buffer,

IV. F-actin labelling

In order to visualise the filamentous actin cytoskeleton, cells were labelled with high-affinity F-actin probe, named phalloidin, conjugated with a fluorescent dye. Approximately 200 μL of *Arabidopsis* or tobacco BY-2 cell suspension culture was plated on a poly-L-lysine-coated cover slip. Cells were incubated in PME buffer (50 mM PIPES, 20 mM MgCl_2 , and 50 mM EGTA) supplemented with 1 μM rhodamine-phalloidin or AlexaFluor®488-phalloidin (Molecular Probes) for 30 min and observed by confocal microscopy.

V. Latrunculin B treatment

Approximately 200 μL of *Arabidopsis* or tobacco BY-2 cell suspension culture was plated on a poly-L-lysine-coated cover slip. Cells were incubated in 1 mL of fresh culture medium supplemented with various concentrations of the F-actin disrupting drug latrunculin B (Sigma) and for various time periods (indicated in figures) and observed by confocal microscopy.

VI. Microprojectile transformation of pollen and pollen tube growth

1. Preparation of pollen grains

Pollen grains from dehisced anthers were isolated from anthers using the isolation medium (IsoMed; 680mM mannitol, 5mM CaCl_2 , 10 mM KCl, 0.5 mM ascorbic acid and 10 mM 2-morpholino-ethanesulfonic acid (MES) adjusted to pH 6.0). Two anthers are necessary for one experiment. Pollen grains were incubated in IsoMed on a rotary shaker at room temperature for 30 min. Resulting pollen grains were washed three times with freshly prepared pollen germination medium (PGM: 1.27 mM CaCl_2 , 0.162 mM, H_3BO_3 , 0.99 mM KNO_3 , and 290 mM Sucrose, pH 5.2) and spread evenly onto a filter paper positioned in a petri dish containing PGM supplemented with 1.4 % low-melting agarose.

2. Preparation of microprojectiles (Charest et al., 2004)

One mL 100 % ethanol is added to 60 mg of gold particle (Sigma-Aldrich 326585) in a 1.5 mL reaction tube, the suspension is vortexed for 3 minutes, centrifuged 1 minute at 10,000 g and the supernatant is removed. 1mL of sterile distilled water is added to the gold pellet. The pellet is re-suspended by vortexing for 1 minute, centrifuged for 1 minute and the supernatant is removed. The washing step with water is repeated once. The gold particles are re-suspended in 500 μ L sterile 50 % (v/v) glycerine. The gold particles can be used immediately or stored for up to 3 month at 4°C for short-term storage or -20°C for long-term storage.

25-50 μ L of homogenized gold particle solution is mixed with 10 μ g of plasmid, mixed for 3 minutes. 25 μ L of CaCl₂ 2.5 M (storage at -20°C) is added and the suspension is mixed for another 3 minutes. 10 μ L of spermidine 0.1 M is added (storage at -20°C). The suspension is mixed for 3 minutes, afterwards 1 mL of 100 % ethanol is added, mixed for 1 more minute and centrifuged for 10 sec at 10,000g. The pellet is washed once with 1mL of 70 % ethanol. Finally, the DNA-coated gold particles are re-suspended in 40 μ L of 100 % ethanol. The particles can be used immediately for bombardment or stored at 4°C for up to 1 month.

3. Microprojectile transformation of pollen grains

Microprojectile bombardment of pollen grains was adapted from Chen et al. (2002). Briefly, 5 mg of pollen grains (approximately corresponding to the pollen of two anthers) was prepared as above described and spread in a 60-mm petri dish. For each experiment, three consecutive bombardments were performed using the PDS-100/He Biolistic Particle Delivery System (BioRad) under the following settings: 1100 p.s.i.; 29-mm Hg vacuum; 1-cm gap distance and 9 cm particle flight distance.

4. Pollen tube growth

Bombarded pollen grains were immediately washed from the filter paper with 2 mL of PGM, transferred into a 3-cm diameter petri dish and incubated at 30°C with constant shaking at 60 rpm in the dark for 30 min. One hundred μ L of pollen grains

Name	Sequence	Purpose
MD172	GATCGGATCC AT GGCGTTCGCAGGAACAACC	<i>WLIM1</i> cds forw. BamHI/NcoI
MD173	GATCGGATCC ATG TCGTTTACAGGAACTCAG	<i>WLIM2a</i> cds forw. BamHI
MD174	GATCGGATCC ATG TCTTTTACAGGAACTCAAC	<i>WLIM2b</i> cds forw. BamHI
MD175	GATCGGATCC ATG TCTTTCACAGGAACTCTC	<i>PLIM2b</i> cds forw. BamHI
MD176	GATCGGATCC ATG TCGTTTACAGGAACATTG	<i>PLIM2a</i> cds forw. BamHI
MD178	GATCGGATCC ATG GCGGCGTTTACAGGGACA	<i>PLIM2c</i> cds forw. BamHI /NcoI
MD179	GATCGAATTC T TAAGCAGCGACGACTTTGTC	<i>WLIM1</i> cds rev. EcoRI
MD180	GATCGAATTC T CAAGATTCGGAACGGCTGC	<i>WLIM2a</i> cds rev. EcoRI
MD181	GATCGAATTC T TAAGATTCAGGAACGGAGG	<i>WLIM2b</i> cds rev. EcoRI
MD182	GATCGAATTC T CAAGACTCTGAAACGCCATTC	<i>PLIM2b</i> cds rev. EcoRI
MD183	GATCGAATTC T CAAGACTCAACGACCGGCTC	<i>PLIM2a</i> cds rev. EcoRI
MD184	GATCGAATTC T TAGGATTCATGTTCTTCAGC	<i>PLIM2c</i> cds rev. EcoRI
MD369	GATCGAGCTC T TAAGCAGCGACGACTTTGTC	<i>WLIM1</i> cds rev. SacI
JPzm12	GATCGAGCTC T TAGGATTCATGTTCTTCAGC	<i>PLIM2c</i> cds rev. SacI
CTAT1F2	GATTC CA TGGCGTTCGCAGGAACAACCCAG	<i>WLIM1ΔCt</i> cds forw. NcoI
CT65	TATGAC CA TGGCAGCTTTTACTGGTACTACC	<i>PLIM2cΔCt</i> cds forw. NcoI
CT80	ATGAGGATCCGAAGTGGACTTTGCAGTACAGACC	<i>PLIM2cΔCt</i> cds rev. BamHI
CT101	ATGATGGATCCAATATGATGATGCTTGCAATATAGC	<i>WLIM1ΔCt</i> cds rev. BamHI

Table 2: Oligonucleotides used in this study.

Restriction sites are underlined and Start and Stop codon are highlighted by bold letters. “rev.” indicates reverse primer and “forw.” Indicates forward primer.

were mixed with 100 μ L of PGM supplemented with 1.4 % low-melting agarose in order to immobilise them on a poly-L-lysine-coated cover slip. The pollen-containing cover slip was incubated at 4°C for 15 sec to facilitate the solidification. One mL of PGM was added on the embedded pollen grains, which were subsequently incubated at 30°C in the dark for 4 to 6 h and observed by confocal microscopy.

VII. Cloning methods

Standard plasmid cloning procedures were essentially performed as described in Sutcliffe, J.G., and Frederick M. Ausubel (1978). The correct sequence of inserts was verified by sequencing of plasmids with appropriate primers (Table 2) at SeqLab (Göttingen, Germany). For pollen bombardments large preparation of plasmid DNA have been obtained with the JETSTAR Plasmid Purification Kit (Genomed).

1. Plasmids used in this study

The pMDC43 plasmids containing the AtLIM CDSs (Papuga et al., 2010) have been provided by M. Dieterle. The pQE60 plasmids containing the AtLIM CDSs (Papuga et al., 2010) have been supplied by Qiagen. The pZM13 plasmid was kindly gifter by Dr Co-Shine Wang.

Briefly, *Arabidopsis* LIM coding DNA sequences (CDS, table 3) were sub-cloned into the bacterial expression vector pQE-60 (Qiagen) via NcoI and BamHI restriction enzyme sites. Due to the relatively low levels of expression in bacteria, *Escherichia coli* codon-optimised sequences have been generated for the three PLIMs (DNA2.0). The primers shown in Table 2 were used. This did not result in any modification of the predicted amino acid sequences for PLIMs. The deletion of the C-terminal domain of WLIM1 and PLIM2c for production of WLIM1 Δ Ct and PLIM2c Δ Ct recombinant proteins has been achieved by PCR using the specific primers CTAT1F2 + CT101 (WLIM1 Δ Ct) and CT65 + CT80 (PLIM2c Δ Ct) (Table 2).

Codon-optimised sequences for chimeric WLIM1 Δ Ct-CtPLIM2c and PLIM2c Δ Ct-CtWLIM1 coding sequences have been ordered from DNA2.0.

Name	AGI code
WLIM1	At1g10200
WLIM2a	At2g39900
WLIM2b	At3g55770
PLIM2a	At2g45800
PLIM2b	At1g01780
PLIM2c	At3g61230

Table 3: Accession numbers.

Sequence data from this article can be found in *Arabidopsis* Genome Initiative databases under the following accession number.

Arabidopsis LIM CDS were sub-cloned into pZM13 via BamHI and SacI restriction sites. The primers shown in Table 3 were used.

VIII. Protein related methods and protocols

1. Expression and purification of recombinant *Arabidopsis* LIMs in M15 [pREP4] *E.coli* bacteria

M15 [pREP4] *E.coli* bacteria (40 uL) are transformed with 1 ug of pQE-60 vector containing the CDS of *Arabidopsis* LIMs by electroporation (as described in the above section). Transformed bacteria are plated on selective LB medium supplemented with carbenicilline (100 ug/mL) and kanamycine (25 ug/mL) and incubated overnight at 37°C.

A pre-culture of 40 mL LB supplemented with carbenicilline and kanamycine is inoculated with a positively selected transformed bacteria and cultured overnight at 37°C. The obtained pre-culture inoculates an 800 mL LB culture supplemented with carbenicilline and kanamycine incubated at 37°C under shaking until the OD_{600 nm} raises 0.5 to 0.8. The addition of isopropyl β-D-1-thiogalactopyranoside (IPTG) to a final concentration of 1 mM induces the expression of recombinant *Arabidopsis* LIMs. To optimise the folding of the zinc finger motif-containing proteins, ZnCl₂ is added to a final concentration of 1 mM. This expression step is performed at 34°C and lasts 2 hours. Bacteria are pelleted by centrifugation (10 min, 4000 g, 4°C) and directly used for protein purification or fast-frozen in liquid nitrogen for a longer conservation.

His6-tagged *Arabidopsis* LIMs are purified using a Ni-NTA resin following procedures described by the manufacturer (QIAexpressionist kit, Qiagen). The bacterial pellet is resuspended in 5 mL lysis buffer B (10 mM Tris; 100 mM NaH₂PO₄, 8 M urea, pH 8) per g of pellet. Bacteria are lysed by 3 cycles of sonication (3 cycles of 20 sec, interval of 5 sec, Dynatech Sonic Dismembrator, relative output = 0.9). Afterwards the suspension is centrifuge for 30 min at 5000 g, 4°C and the supernatant is loaded onto 1 mL Ni-NTA agarose (Invitrogen, #R9101-15) equilibrated in lysis buffer B in 5 mL polypropylene columns (Qiagen). The matrix is washed 2 times with 6 mL buffer C (10 mM Tris, 100 mM NaH₂PO₄, 8 M urea, pH 6.3), 2 times with 2

mL buffer D (10 mM Tris, 100 mM NaH₂PO₄, 8 M urea, pH 5.9). The His-tagged protein is eluted with 2 times 2 mL buffer E (10 mM Tris, 100 mM NaH₂PO₄, 8 M urea, pH 4.5). Purified proteins were dialysed several times using 3-12 mL dialysis cassettes (Slide-A-Lyser 7,000 MWCO, Thermo Scientific) against dialysis buffer (10 mM Tris, 50 mM NaCl, 1 mM DTT, 50 µM ZnCl₂) containing decreasing urea concentrations and increasing pH:

- 1) Dialysis buffer supplemented with 6 M urea at pH 5.6 for 2 h
- 2) Dialysis buffer supplemented with 4 M urea at pH 6.3 for 2 h
- 3) Dialysis buffer supplemented with 2 M urea at pH 6.9 overnight at 4°C
- 4) Dialysis buffer supplemented with 2 M urea at pH 6.9 for 2 h

If necessary, purified proteins were concentrated in a centrifugal filter (Amicon), and stored on ice. Prior to an experiment, proteins were pre-clarified at 150 000g for 30 min at 4°C and checked for correct molecular weight by SDS-PAGE analysis, and their concentration was determined by Bradford assay (Bio-Rad) using BSA as standard.

2. Preparation of total protein extracts from *Arabidopsis* seedlings and organs

Seedlings are transferred to 1.5 ml reaction tubes supplemented with 10-15 glassbeads (diameter 1.25-1.5, Roth) and flash frozen in liquid nitrogen. Seedlings were disrupted by mixing for .2 times 15 sec with a Silmat shaker (Ivoclar vivadent). Plant organs are flash frozen in liquid nitrogen and ground to a fine powder with mortar and pestle. SDS-sample buffer (125 mM Tris pH6.8, 20%(v/v) Glycerol, 4 % (w/v) SDS, 3% (v/v) β-Mercaptoethanol) preheated to 95°C is added to the ground frozen plant material (approximately 200µl of buffer for 100 mg of plant material) and mixed until the plant material is completely thawed. The sample is incubated for 5 min at 95°C and afterwards centrifuged at 12.000 g for 10 min. The supernatant is transferred to a new tube. The protein concentration of the extract is determined by the Amidoblack method (Popov et al., 1975) using BSA as a standard

3. SDS-Polyacrylamide gel electrophoresis (Lämmli, 1970)

Prior to their loading on the polyacrylamide gel, proteins were solubilised in the loading buffer (125 mM Tris pH6.8, 20%(v/v) Glycerol, 4 % (w/v) SDS, 3% (v/v) β -Mercaptoethanol), boiled for 5 min and centrifuged 5 min at 10 000 g. 16% SDS-PAGE gels were used for protein separation using a Miniprotein3 cell (Bioradd). Electrophoresis was performed at constant voltage (150 V) in the Laemmli migration buffer (25 mM Tris, 190 mM glycine, 0.1 % SDS).

4. Western blot

After separation on SDS-PAGE, proteins were transferred to an Immobilon membrane (0.2 μ M, BioRad). Prior to its use, the membrane was rinsed in 100 % ethanol, rinsed with water and equilibrated in transfer buffer (25 mM Tris, 190 mM glycine, 20 % ethanol). The transfer was performed at 300 mA for 2 h in a Mini Trans-Blot®Electrophoretic Transfer Cell (Biorad) according to the instructions of the manufacturer.

After the transfer, the membrane was rinsed briefly in 1 x PBS-T (150 mM NaCl, 3 mM KH_2PO_4 , 10 mM Na_2HPO_4 pH 7.4, 0,1% tween-20) and afterwards incubated for 1 h in blocking buffer (1 x PBS-T supplemented with 5% (w/v) non-fat dry milk) under shaking. Afterward the membrane was incubated with the primary antibody diluted in the blocking buffer overnight at 4°C. After three washes in 1 x PBS-T for 10 min the membrane was incubated with the secondary peroxidase conjugated antibody directed against the primary antibody diluted in the blocking buffer for 2 h. The membrane was washed three times for 10 min in 1 x PBS-T. The detection was performed using the SuperSignal West Femto Substrate (Thermo Scientific) according to the instructions of the manufacturer. The chemiluminescent signal was detected by exposure of the membrane to a film (CL-XPosure, Thermo Scientific).

For GFP detection we used the anti-GFP rabbit IgG fraction (A11122, Invitrogen) diluted 1:2.500 as first antibody and affinity purified peroxidase conjugated anti-rabbit IgG (H+L) antibody (111-035-003, Jackson Immuno research) diluted 1:20,000 as secondary antibody. The polyclonal affinity-purified anti WLIM1

pH	[Ca ²⁺] _{free}		
6.2	Low (~ 5 nM)	MES	7 mM
		PIPES	10 mM
		Tris	-
		EGTA	10 mM
		CaCl ₂	-
	High (~ 300 μM)	MES	7 mM
		PIPES	10 mM
		Tris	-
		EGTA	-
		CaCl ₂	300 μM
6.8	Low (~ 5 nM)	MES	-
		PIPES	7 mM
		Tris	10 mM
		EGTA	5 mM
		CaCl ₂	-
	High (~300 μM)	MES	-
		PIPES	7 mM
		Tris	10 mM
		EGTA	-
		CaCl ₂	300 μM
7.4	Low (~ 5 nM)	MES	-
		PIPES	7 mM
		Tris	10 mM
		EGTA	0.5 mM
		CaCl ₂	-
	High (~300 μM)	MES	-
		PIPES	7 mM
		Tris	10 mM
		EGTA	-
		CaCl ₂	300 μM

Table 4: Concentrations of MES, PIPES, Tris, EGTA and CaCl₂ used in the different *in vitro* assays.

The concentration of EGTA required in each pH condition was determined using the EGTA calculator software (<http://brneurosci.org/egta.html>). The final pH within reaction tubes was measured using a pH microélectrode.

antibody from mouse was provided by F. Moreau and used at a 1:250 dilution. As secondary antibody a peroxidase conjugated anti mouse IgG antibody (A4416, Sigma) was used at a 1:10,000 dilution.

To stain the proteins on the membrane the membrane was incubated for 5min with Amidoblack solution (10 % (v/v) acetic acid, 90 % (v/v) Methanol, 0.05 % (w/v) Amidoblack), rinsed three times with water und air-dried.

5. *In vitro* biochemical assays

4.1. High- and low-speed co-sedimentation assays

High- and low-speed co-sedimentation assays were used to assess the actin binding and -crosslinking activities of *Arabidopsis* LIMs, respectively. In both cases, rabbit muscle actin (Cytoskeleton; concentration indicated in figures) was co-polymerised with various concentrations of individual LIMs for 1 h in 50 mM KCl, 2 mM MgCl₂, 1 mM ATP, and 0.5 mM DTT. Depending on the pH and [Ca²⁺] conditions tested, the reaction medium was buffered with MES and PIPES, pH 6.2, or PIPES and Tris, pH 6.8 and 7.4, and was supplemented with either EGTA (low [Ca²⁺] conditions) or CaCl₂ (high [Ca²⁺] conditions). Table 4 indicates the concentration of MES, PIPES, Tris, EGTA, and CaCl₂ for each of the co-polymerisation conditions used.

In high-speed experiments, samples were centrifuged at 100,000g for 30 min to pellet AFs. The presence of LIM in the resulting supernatants (F-actin unbound fraction) and pellets (F-actin bound fraction) was analysed by SDS-PAGE and Coomassie Brilliant Blue R (Sigma-Aldrich) staining.

In low-speed experiments, samples were centrifuged at 12,500g for 30 min in a microcentrifuge to pellet high-order F-actin structures. The presence of actin in the resulting supernatants (noncross-linked AFs) and pellets (cross-linked AFs) was analyzed by SDS-PAGE and Coomassie Brilliant Blue R (Sigma-Aldrich) staining.

The respective amounts of actin in pellet and supernatant fractions is quantified using ImageJ software. The concentration of free LIM (X-axis) is plotted against the ratio of the concentration of bound LIM to the concentration of actin (y-axis). The ligand binding function of Sigma Plot ($y=B_{max} \cdot x / (K_d + x)$) was used to

calculated K_d and B_{max} .

x = concentration [LIM free]

y = [LIM bound]/[actin]

The presence of actin bundles in samples was checked by direct visualization using fluorescence microscopy. An aliquot of the copolymerized actin samples was labelled with 1 μM rhodamine-phalloidin (Sigma-Aldrich). Images were recorded via confocal microscope using a pinhole set to produce thick ($\sim 2 \mu\text{m}$) optical sections.

4.2. F-actin depolymerisation assay

Pyrene-labeled actin (4 μM , 30% pyrene-labeled; Cytoskeleton) was copolymerised with individual *Arabidopsis* LIMs in the same conditions as in co-sedimentation assays. Depolymerisation was induced by diluting samples to a final actin concentration of 0.2 μM . The decrease in pyrene fluorescence accompanying actin depolymerisation was recorded over 200 to 300 sec using a PTI QM-4 QuantaMaster fluorimeter.

Chapter 6

References

References

- Allen, T.J., and Chapman, R.A.** (1995). The effect of a chemical phosphatase on single calcium channels and the inactivation of whole-cell calcium current from isolated guinea-pig ventricular myocytes. *Pflugers Arch* **430**, 68-80.
- Allwood, E.G., Smertenko, A.P., and Hussey, P.J.** (2001). Phosphorylation of plant actin-depolymerising factor by calmodulin-like domain protein kinase. *FEBS Lett* **499**, 97-100.
- Amann, K.J., and Pollard, T.D.** (2001). The Arp2/3 complex nucleates actin filament branches from the sides of pre-existing filaments. *Nat Cell Biol* **3**, 306-310.
- An, Y.Q., Huang, S., McDowell, J.M., McKinney, E.C., and Meagher, R.B.** (1996a). Conserved expression of the Arabidopsis ACT1 and ACT 3 actin subclass in organ primordia and mature pollen. *Plant Cell* **8**, 15-30.
- An, Y.Q., McDowell, J.M., Huang, S., McKinney, E.C., Chambliss, S., and Meagher, R.B.** (1996b). Strong, constitutive expression of the Arabidopsis ACT2/ACT8 actin subclass in vegetative tissues. *Plant J* **10**, 107-121.
- Andrianantoandro, E., and Pollard, T.D.** (2006). Mechanism of actin filament turnover by severing and nucleation at different concentrations of ADF/cofilin. *Mol Cell* **24**, 13-23.
- Arber, S., and Caroni, P.** (1996). Specificity of single LIM motifs in targeting and LIM/LIM interactions in situ. *Genes Dev* **10**, 289-300.
- Arber, S., Hunter, J.J., Ross, J. Jr., Hongo, M., Sansig, G., Borg, J., Perriard, J.C., Chien, K.R., and Caroni, P.** (1997). MLP-deficient mice exhibit a disruption of cardiac cytoarchitectural organization, dilated cardiomyopathy, and heart failure. *Cell* **88**, 393-403.
- Arnaud, D., Dejardin, A., Leple, J.C., Lesage-Descauses, M.C., and Pilate, G.** (2007). Genome-wide analysis of LIM gene family in *Populus trichocarpa*, *Arabidopsis thaliana*, and *Oryza sativa*. *DNA Res* **14**, 103-116.
- Augustine, R.C., Vidali, L., Kleinman, K.P., and Bezanilla, M.** (2008). Actin depolymerizing factor is essential for viability in plants, and its phosphoregulation is important for tip growth. *Plant J* **54**, 863-875.
- Bartles, J.R.** (2000). Parallel bundles and their multiple actin bundling proteins. *Curr Opin Cell Biol* **12**, 72-78.
- Baltz, R., Evrard, J.L., Domon, C., and Steinmetz, A.** (1992a). A LIM motif is present in a pollen-specific protein. *Plant Cell* **4**, 1465-1466.

- Baltz, R., Domon, C., Pillay, D.T., and Steinmetz, A.** (1992b). Characterization of a pollen-specific cDNA from sunflower encoding a zinc finger protein. *Plant J* **2**, 713-721.
- Baltz, R., Schmit, A.C., Kohnen, M., Hentges, F., Steinmetz, A.** (1999). Differential localization of the LIM domain protein PLIM-1 in microspores and mature pollen grains from sunflower. *Sex Plant Reprod* **12**, 60-65.
- Bernstein, B.W., and Bamburg, J.R.** (2010). ADF/cofilin: a functional node in cell biology. *Trends Cell Biol* **20**, 187-195.
- Blanchoin, L., and Pollard, T.D.** (1999). Mechanism of interaction of Acanthamoeba actophorin (ADF/Cofilin) with actin filaments. *J Biol Chem* **274**, 15538-15546.
- Blanchoin, L., Pollard, T.D., and Mullins, R.D.** (2000). Interactions of ADF/cofilin, Arp2/3 complex, capping protein and profilin in remodeling of branched actin filament networks. *Curr Biol* **10**, 1273-1282.
- Blanchoin, L., and Staiger, C.J.** (2010). Plant formins: diverse isoforms and unique molecular mechanism. *Biochim Biophys Acta* **1803**, 201-206.
- Blumenthal, S.S., Clark, G.B., and Roux, S.J.** (2004). Biochemical and immunological characterization of pea nuclear intermediate filament proteins. *Planta* **218**, 965-975.
- Boateng, S.Y., Senyo, S.E., Qi, L., Goldspink, P.H., and Russell, B.** (2009). Myocyte remodeling in response to hypertrophic stimuli requires nucleocytoplasmic shuttling of muscle LIM protein. *J Mol Cell Cardiol* **47**, 426-435.
- Bowman, G.D., Nodelman, I.M., Hong, Y., Chua, N.H., Lindberg, U., and Schutt, C.E.** (2000). A comparative structural analysis of the ADF/cofilin family. *Proteins* **41**, 374-384.
- Briere, C., Bordel, A.C., Barthou, H., Jauneau, A., Steinmetz, A., Alibert, G., and Petitprez, M.** (2003). Is the LIM-domain protein HaWLIM1 associated with cortical microtubules in sunflower protoplasts? *Plant Cell Physiol* **44**, 1055-1063.
- Bugyi, B., and Carlier, M.F.** (2010). Control of actin filament treadmilling in cell motility. *Annu Rev Biophys* **39**, 449-470.
- Caldwell, J.E., Heiss, S.G., Mermall, V., and Cooper, J.A.** (1989). Effects of CapZ, an actin capping protein of muscle, on the polymerization of actin. *Biochemistry* **28**, 8506-8514.

- Cardenas, L., Lovy-Wheeler, A., Kunkel, J.G., and Hepler, P.K.** (2008). Pollen tube growth oscillations and intracellular calcium levels are reversibly modulated by actin polymerization. *Plant Physiol* **146**, 1611-1621.
- Carlier, M.F., and Pantaloni, D.** (1997a). Control of actin dynamics in cell motility. *J Mol Biol* **269**, 459-467.
- Carlier, M.F., Laurent, V., Santolini, J., Melki, R., Didry, D., Xia, G.X., Hong, Y., Chua, N.H., and Pantaloni, D.** (1997b). Actin depolymerizing factor (ADF/cofilin) enhances the rate of filament turnover: implication in actin-based motility. *J Cell Biol* **136**, 1307-1322.
- Casella, J.F., Flanagan, M.D., and Lin, S.** (1981). Cytochalasin D inhibits actin polymerization and induces depolymerization of actin filaments formed during platelet shape change. *Nature* **293**, 302-305.
- Casella, J.F., Craig, S.W., Maack, D.J., and Brown, A.E.** (1987). Cap Z(36/32), a barbed end actin-capping protein, is a component of the Z-line of skeletal muscle. *J Cell Biol* **105**, 371-379.
- Certal, A.C., Almeida, R.B., Carvalho, L.M., Wong, E., Moreno, N., Michard, E., Carneiro, J., Rodriguez-Leon, J., Wu, H.M., Cheung, A.Y., and Feijo, J.A.** (2008). Exclusion of a proton ATPase from the apical membrane is associated with cell polarity and tip growth in *Nicotiana tabacum* pollen tubes. *Plant Cell* **20**, 614-634.
- Chan, C., Beltzner, C.C., and Pollard, T.D.** (2009). Cofilin dissociates Arp2/3 complex and branches from actin filaments. *Curr Biol* **19**, 537-545.
- Chang, D.F., Belaguli, N.S., Iyer, D., Roberts, W.B., Wu, S.P., Dong, X.R., Marx, J.G., Moore, M.S., Beckerle, M.C., Majesky, M.W., and Schwartz, R.J.** (2003). Cysteine-rich LIM-only proteins CRP1 and CRP2 are potent smooth muscle differentiation cofactors. *Dev Cell* **4**, 107-118.
- Chang, D.F., Belaguli, N.S., Chang, J., and Schwartz, R.J.** (2007). LIM-only protein, CRP2, switched on smooth muscle gene activity in adult cardiac myocytes. *Proc Natl Acad Sci U S A* **104**, 157-162.
- Chaudhry, F., Guerin, C., von Witsch, M., Blanchoin, L., and Staiger, C.J.** (2007). Identification of Arabidopsis cyclase-associated protein 1 as the first nucleotide exchange factor for plant actin. *Mol Biol Cell* **18**, 3002-3014.
- Chen, C.Y., Wong, E.I., Vidali, L., Estavillo, A., Hepler, P.K., Wu, H.M., and Cheung, A.Y.** (2002). The regulation of actin organization by actin-depolymerizing factor in elongating pollen tubes. *Plant Cell* **14**, 2175-2190.
- Chen, H., Bernstein, B.W., Sneider, J.M., Boyle, J.A., Minamide, L.S., and Bamburg, J.R.** (2004). In vitro activity differences between proteins of the

- ADF/cofilin family define two distinct subgroups. *Biochemistry* **43**, 7127-7142.
- Chen, N., Qu, X., Wu, Y., and Huang, S.** (2009). Regulation of actin dynamics in pollen tubes: control of actin polymer level. *J Integr Plant Biol* **51**, 740-750.
- Cheung, A. Y., and Wu, H.M.** (2004). Overexpression of an *Arabidopsis* formin stimulates supernumerary actin cable formation from pollen tube cell membrane. *Mol Plant* **1**, 686-702.
- Cheung, A.Y., and Wu, H.M.** (2008a). Structural and signaling networks for the polar cell growth machinery in pollen tubes. *Annu Rev Plant Biol* **59**, 547-572.
- Cheung, A.Y., Duan, Q.H., Costa, S.S., de Graaf, B.H., Di Stilio, V.S., Feijo, J., and Wu, H.M.** (2008b). The dynamic pollen tube cytoskeleton: live cell studies using actin-binding and microtubule-binding reporter proteins. *Mol Plant* **1**, 686-702.
- Cheung, A.Y., Niroomand, S., Zou, Y., and Wu, H.M.** (2010). A transmembrane formin nucleates subapical actin assembly and controls tip-focused growth in pollen tubes. *Proc Natl Acad Sci U S A* **107**, 16390-16395.
- Clough, S.J., and Bent, A.F.** (1998). Floral dip: a simplified method for *Agrobacterium*-mediated transformation of *Arabidopsis thaliana*. *Plant J* **16**, 735-743.
- Cole, R.A., and Fowler, J.E.** (2006). Polarized growth: maintaining focus on the tip. *Curr Opin Plant Biol* **9**, 579-588.
- Crawford, A.W., Pino, J.D., and Beckerle, M.C.** (1994). Biochemical and molecular characterization of the chicken cysteine-rich protein, a developmentally regulated LIM-domain protein that is associated with the actin cytoskeleton. *J Cell Biol* **124**, 117-127.
- Dawson, P.J., Hulme, J.S., and Lloyd, C.W.** (1985). Monoclonal antibody to intermediate filament antigen cross-reacts with higher plant cells. *J Cell Biol* **100**, 1793-1798.
- Deeks, M.J., and Hussey, P.J.** (2005). Arp2/3 and SCAR: plants move to the fore. *Nat Rev Mol Cell Biol* **6**, 954-964.
- Deeks, M.J., Rodrigues, C., Dimmock, S., Ketelaar, T., Maciver, S.K., Malho, R., and Hussey, P.J.** (2007). *Arabidopsis* CAP1 - a key regulator of actin organisation and development. *J Cell Sci* **120**, 2609-2618.
- Deeks, M.J., Fendrych, M., Smertenko, A., Bell, K.S., Oparka, K., Cvrckova, F., Zarsky, V., and Hussey, P.J.** (2010). The plant formin AtFH4 interacts with

both actin and microtubules, and contains a newly identified microtubule-binding domain. *J Cell Sci* **123**, 1209-1215.

- Djakovic, S., Dyachok, J., Burke, M., Frank, M.J., and Smith, L.G.** (2006). BRICK1/HSPC300 functions with SCAR and the ARP2/3 complex to regulate epidermal cell shape in Arabidopsis. *Development* **133**, 1091-1100.
- Dong, C.H., Kost, B., Xia, G., and Chua, N.H.** (2001a). Molecular identification and characterization of the Arabidopsis AtADF1, AtADFS and AtADF6 genes. *Plant Mol Biol* **45**, 517-527.
- Dong, C.H., Xia, G.X., Hong, Y., Ramachandran, S., Kost, B., and Chua, N.H.** (2001b). ADF proteins are involved in the control of flowering and regulate F-actin organization, cell expansion, and organ growth in Arabidopsis. *Plant Cell* **13**, 1333-1346.
- dos Remedios, C.G., Chhabra, D., Kekic, M., Dedova, I.V., Tsubakihara, M., Berry, D.A., and Nosworthy, N.J.** (2003). Actin binding proteins: regulation of cytoskeletal microfilaments. *Physiol Rev* **83**, 433-473.
- Drobak, B.K., Franklin-Tong, V.E., and Staiger, C.J.** (2004). The role of the actin cytoskeleton in plant cell signalling. *New Phytol.* **163**, 13-30.
- Eddy, R.J., Han, J., Sauterer, R.A., and Condeelis, J.S.** (1996). A major agonist-regulated capping activity in Dictyostelium is due to the capping protein, cap32/34. *Biochim Biophys Acta* **1314**, 247-259.
- El-Din El-Assal, S., Le, J., Basu, D., Mallery, E.L., and Szymanski, D.B.** (2004). DISTORTED2 encodes an ARPC2 subunit of the putative Arabidopsis ARP2/3 complex. *Plant J* **38**, 526-538.
- Eliasson, A., Gass, N., Mundel, C., Baltz, R., Krauter, R., Evrard, J.L., and Steinmetz, A.** (2000). Molecular and expression analysis of a LIM protein gene family from flowering plants. *Mol Gen Genet* **264**, 257-267.
- Fan, X., Hou, J., Chen, X., Chaudhry, F., Staiger, C.J., and Ren, H.** (2004). Identification and characterization of a Ca²⁺-dependent actin filament-severing protein from lily pollen. *Plant Physiol* **136**, 3979-3989.
- Feijo, J.A., Sainhas, J., Hackett, G.R., Kunkel, J.G., and Hepler, P.K.** (1999). Growing pollen tubes possess a constitutive alkaline band in the clear zone and a growth-dependent acidic tip. *J Cell Biol* **144**, 483-496.
- Feijo, J.A., Sainhas, J., Holdaway-Clarke, T., Cordeiro, M.S., Kunkel, J.G., and Hepler, P.K.** (2001). Cellular oscillations and the regulation of growth: the pollen tube paradigm. *Bioessays* **23**, 86-94.
- Fox, J.E., and Phillips, D.R.** (1981). Inhibition of actin polymerization in blood platelets by cytochalasins. *Nature* **292**, 650-652.

- Fu, Y.** (2010). The actin cytoskeleton and signaling network during pollen tube tip growth. *J Integr Plant Biol* **52**, 131-137.
- Fujii, S., Yamada, M., and Toriyama, K.** (2009). Cytoplasmic male sterility-related protein kinase, OsNek3, is regulated downstream of mitochondrial protein phosphatase 2C, DCW11. *Plant Cell Physiol* **50**, 828-837.
- Gehmlich, K., Geier, C., Milting, H., Furst, D., and Ehler, E.** (2008). Back to square one: what do we know about the functions of muscle LIM protein in the heart? *J Muscle Res Cell Motil* **29**, 155-158.
- Gibbon, B.C., Ren, H., and Staiger, C.J.** (1997). Characterization of maize (*Zea mays*) pollen profilin function in vitro and in live cells. *Biochem J* **327 (Pt 3)**, 909-915.
- Gibbon, B.C., Zonia, L.E., Kovar, D.R., Hussey, P.J., and Staiger, C.J.** (1998). Pollen profilin function depends on interaction with proline-rich motifs. *Plant Cell* **10**, 981-993.
- Gibbon, B.C., Kovar, D.R., and Staiger, C.J.** (1999). Latrunculin B has different effects on pollen germination and tube growth. *Plant Cell* **11**, 2349-2363.
- Grubinger, M., and Gimona, M.** (2004). CRP2 is an autonomous actin-binding protein. *FEBS Lett* **557**, 88-92.
- Grunt, M., Zarsky, V., and Cvrckova, F.** (2008). Roots of angiosperm formins: the evolutionary history of plant FH2 domain-containing proteins. *BMC Evol Biol* **8**, 115.
- Guo, H., Li, L., Ye, H., Yu, X., Algreen, A., and Yin, Y.** (2009). Three related receptor-like kinases are required for optimal cell elongation in *Arabidopsis thaliana*. *Proc Natl Acad Sci U S A* **106**, 7648-7653.
- Hamilton, D.A., Roy, M., Rueda, J., Sindhu, R.K., Sanford, J., and Mascarenhas, J.P.** (1992). Dissection of a pollen-specific promoter from maize by transient transformation assays. *Plant Mol Biol* **18**, 211-218.
- Hammarstrom, A., Berndt, K.D., Sillard, R., Adermann, K., and Otting, G.** (1996). Solution structure of a naturally-occurring zinc-peptide complex demonstrates that the N-terminal zinc-binding module of the Lasp-1 LIM domain is an independent folding unit. *Biochemistry* **35**, 12723-12732.
- Hargreaves, A.J., Goodbody, K.C., and Lloyd, C.W.** (1989). Reconstitution of intermediate filaments from a higher plant. *Biochem J* **261**, 679-682.
- Haus, U., Hartmann, H., Trommler, P., Noegel, A.A., and Schleicher, M.** (1991). F-actin capping by cap32/34 requires heterodimeric conformation and can be inhibited with PIP2. *Biochem Biophys Res Commun* **181**, 833-839.

- Henderson, J.R., Macalma, T., Brown, D., Richardson, J.A., Olson, E.N., and Beckerle, M.C.** (1999). The LIM protein, CRP1, is a smooth muscle marker. *Dev Dyn* **214**, 229-238.
- Hepler, P.K., Vidali, L., and Cheung, A.Y.** (2001). Polarized cell growth in higher plants. *Annu Rev Cell Dev Biol* **17**, 159-187.
- Hepler, P.K., Lovy-Wheeler, A., McKenna, S.T., and Kunkel, J.G.** (2006). Ions and pollen tube growth. *Plant Cell Monogr* **3**, 47-69.
- Holdaway-Clarke, T.L., Feijo, J.A., Hackett, G.R., Kunkel, J.G., and Hepler, P.K.** (1997). Pollen Tube Growth and the Intracellular Cytosolic Calcium Gradient Oscillate in Phase while Extracellular Calcium Influx Is Delayed. *Plant Cell* **9**, 1999-2010.
- Holmes, K.C., Popp, D., Gebhard, W., and Kabsch, W.** (1990). Atomic model of the actin filament. *Nature* **347**, 44-49.
- Huang, S., An, Y.Q., McDowell, J.M., McKinney, E.C., and Meagher, R.B.** (1996). The *Arabidopsis thaliana* ACT4/ACT12 actin gene subclass is strongly expressed throughout pollen development. *Plant J* **10**, 189-202.
- Huang, S., Blanchoin, L., Kovar, D.R., and Staiger, C.J.** (2003). *Arabidopsis* capping protein (AtCP) is a heterodimer that regulates assembly at the barbed ends of actin filaments. *J Biol Chem* **278**, 44832-44842.
- Huang, S., Blanchoin, L., Chaudhry, F., Franklin-Tong, V.E., and Staiger, C.J.** (2004). A gelsolin-like protein from *Papaver rhoeas* pollen (PrABP80) stimulates calcium-regulated severing and depolymerization of actin filaments. *J Biol Chem* **279**, 23364-23375.
- Huang, S., Gao, L., Blanchoin, L., and Staiger, C.J.** (2006). Heterodimeric capping protein from *Arabidopsis* is regulated by phosphatidic acid. *Mol Biol Cell* **17**, 1946-1958.
- Huber, A., Neuhuber, W.L., Klugbauer, N., Ruth, P., and Allescher, H.D.** (2000). Cysteine-rich protein 2, a novel substrate for cGMP kinase I in enteric neurons and intestinal smooth muscle. *J Biol Chem* **275**, 5504-5511.
- Hussey, P.J., Allwood, E.G., and Smertenko, A.P.** (2002). Actin binding proteins in the *Arabidopsis* genome database: Properties of functional distinct plant actin-depolymerising factors/cofilins. *Philos Trans R Soc Lond B Biol Sci* **357**, 791-798.
- Hulskamp, M., Misra, S., and Jurgens, G.** (1994). Genetic dissection of trichome cell development in *Arabidopsis*. *Cell* **76**, 555-566.

- Iwano, M., Entani, T., Shiba, H., Kakita, M., Nagai, T., Mizuno, H., Miyawaki, A., Shoji, T., Kubo, K., Isogai, A., and Takayama, S.** (2009). Fine-tuning of the cytoplasmic Ca²⁺ concentration is essential for pollen tube growth. *Plant Physiol* **150**, 1322-1334.
- Jang, H.S., and Greenwood, J.A.** (2009). Glycine-rich region regulates cysteine-rich protein 1 binding to actin cytoskeleton. *Biochem Biophys Res Commun* **380**, 484-488.
- Kabsch, W., Mannherz, H.G., Suck, D., Pai, E.F., and Holmes, K.C.** (1990). Atomic structure of the actin:DNase I complex. *Nature* **347**, 37-44.
- Kadmas, J.L., and Beckerle, M.C.** (2004). The LIM domain: from the cytoskeleton to the nucleus. *Nat Rev Mol Cell Biol* **5**, 920-931.
- Kandasamy, M.K., McKinney, E.C., and Meagher, R.B.** (2002a) Functional nonequivalency of actin isovariants in *Arabidopsis*. *Mol Biol Cell* **13**, 251-261.
- Kandasamy, M.K., McKinney, E.C., and Meagher, R.B.** (2002b). Plant profilin isovariants are distinctly regulated in vegetative and reproductive tissues. *Cell Motil Cytoskeleton* **52**, 22-32.
- Kandasamy, M.K., Burgos-Rivera, B., McKinney, E.C., Ruzicka, D.R., and Meagher, R.B.** (2007). Class-specific interaction of profilin and ADF isovariants with actin in the regulation of plant development. *Plant Cell* **19**, 3111-3126.
- Karlsson, O., Thor, S., Norberg, T., Ohlsson, H., and Edlund, T.** (1990). Insulin gene enhancer binding protein Isl-1 is a member of a novel class of proteins containing both a homeo- and a Cys-His domain. *Nature* **344**, 879-882.
- Kawaoka, A., Kaothien, P., Yoshida, K., Endo, S., Yamada, K., and Ebinuma, H.** (2000). Functional analysis of tobacco LIM protein Ntlm1 involved in lignin biosynthesis. *Plant J* **22**, 289-301.
- Khurana, T., Khurana, B., and Noegel, A.A.** (2002). LIM proteins: association with the actin cytoskeleton. *Protoplasma* **219**, 1-12.
- Khurana, P., Henty, J.L., Huang, S., Staiger, A.M., Blanchoin, L., and Staiger, C.J.** (2010). *Arabidopsis* VILLIN1 and VILLIN3 have overlapping and distinct activities in actin bundle formation and turnover. *Plant Cell* **22**, 2727-2748.
- Kinosian, H.J., Selden, L.A., Estes, J.E., and Gershman, L.C.** (1993). Nucleotide binding to actin. Cation dependence of nucleotide dissociation and exchange rates. *J Biol Chem* **268**, 8683-8691.

- Klahre, U., and Chua, N.H.** (1999). The Arabidopsis actin-related protein 2 (AtARP2) promoter directs expression in xylem precursor cells and pollen. *Plant Mol Biol* **41**, 65-73.
- Kong, Y., Flick, M.J., Kudla, A.J., and Konieczny, S.F.** (1997). Muscle LIM protein promotes myogenesis by enhancing the activity of MyoD. *Mol Cell Biol* **17**, 4750-4760.
- Konrat, R., Krautler, B., Weiskirchen, R., and Bister, K.** (1998). Structure of cysteine- and glycine-rich protein CRP2. Backbone dynamics reveal motional freedom and independent spatial orientation of the lim domains. *J Biol Chem* **273**, 23233-23240.
- Kontaxis, G., Konrat, R., Krautler, B., Weiskirchen, R., and Bister, K.** (1998). Structure and intramolecular dynamics of the amino-terminal LIM domain from quail cysteine- and glycine-rich protein CRP2. *Biochemistry* **37**, 7127-7134.
- Korn, E.D., Carlier, M.F., and Pantaloni, D.** (1987). Actin polymerization and ATP hydrolysis. *Science* **238**, 638-644.
- Kost, B., Spielhofer, P., and Chua, N.H.** (1998). A GFP-mouse talin fusion protein labels plant actin filaments in vivo and visualizes the actin cytoskeleton in growing pollen tubes. *Plant J* **16**, 393-401.
- Kost, B., Mathur, J., and Chua, N.H.** (1999). Cytoskeleton in plant development. *Curr Opin Plant Biol* **2**, 462-470.
- Kovar, D.R., Drobak, B.K., and Staiger, C.J.** (2000a). Maize profilin isoforms are functionally distinct. *Plant Cell* **12**, 583-598.
- Kovar, D.R., Staiger, C.J., Weaver, E.A., and McCurdy, D.W.** (2000b). AtFim1 is an actin filament crosslinking protein from Arabidopsis thaliana. *Plant J* **24**, 625-636.
- Kuchitsu, K., Ward, J.M., Allen, G., Schelle, I., and Schroeder, J.I.** (2002). Loadind acetoxymethyl ester fluorescent dyes into the cytoplasm of *Arabidopsis* and *Commelina* guard cells. *New Phytol* **153**, 527-533.
- Le, J., El-Assal Sel, D., Basu, D., Saad, M.E., and Szymanski, D.B.** (2003). Requirements for Arabidopsis ATARP2 and ATARP3 during epidermal development. *Curr Biol* **13**, 1341-1347.
- Li, Y., Zheng, L., Corke, F., Smith, C., and Bevan, M.W.** (2008). Control of final seed and organ size by the DA1 gene family in *Arabidopsis thaliana*. *Genes Dev* **15**, 1331-1336
- Li, Y., Shen, Y., Cai, C., Zhong, C., Zhu, L., Yuan, M., and Ren, H.** (2010). The type II Arabidopsis formin14 interacts with microtubules and microfilaments to regulate cell division. *Plant Cell* **22**, 2710-2726.

- Louis, H.A., Pino, J.D., Schmeichel, K.L., Pomies, P., and Beckerle, M.C.** (1997). Comparison of three members of the cysteine-rich protein family reveals functional conservation and divergent patterns of gene expression. *J Biol Chem* **272**, 27484-27491.
- Lovy-Wheeler, A., Wilsen, K.L., Baskin, T.I., and Hepler, P.K.** (2005). Enhanced fixation reveals the apical cortical fringe of actin filaments as a consistent feature of the pollen tube. *Planta* **221**, 95-104.
- Lovy-Wheeler, A., Kunkel, J.G., Allwood, E.G., Hussey, P.J., and Hepler, P.K.** (2006). Oscillatory increases in alkalinity anticipate growth and may regulate actin dynamics in pollen tubes of lily. *Plant Cell* **18**, 2182-2193.
- Lovy-Wheeler, A., Cardenas, L., Kunkel, J.G., and Hepler, P.K.** (2007). Differential organelle movement on the actin cytoskeleton in lily pollen tubes. *Cell Motil Cytoskeleton* **64**, 217-232.
- Machesky, L.M., and Gould, K.L.** (1999). The Arp2/3 complex: a multifunctional actin organizer. *Curr Opin Cell Biol* **11**, 117-121.
- Maciver, S.K.** (1998). How ADF/cofilin depolymerizes actin filaments. *Curr Opin Cell Biol* **10**, 140-144.
- Maciver, S.K., and Hussey, P.J.** (2002). The ADF/cofilin family: actin-remodeling proteins. *Genome Biol* **3**, reviews3007.
- Martiniere, A., Gayral, P., Hawes, C., and Runions, J.** (2011). Building bridges: FORMIN1 of Arabidopsis forms a connection between the cell wall and the actin cytoskeleton. *Plant J*.
- Maruyama, K., Kurokawa, H., Oosawa, M., Shimaoka, S., Yamamoto, H., and Ito, M.** (1990). Beta-actinin is equivalent to Cap Z protein. *J Biol Chem* **265**, 8712-8715.
- Mathur, J., Mathur, N., Kernebeck, B., and Hulskamp, M.** (2003a). Mutations in actin-related proteins 2 and 3 affect cell shape development in Arabidopsis. *Plant Cell* **15**, 1632-1645.
- Mathur, J., Mathur, N., Kirik, V., Kernebeck, B., Srinivas, B.P., and Hulskamp, M.** (2003b). Arabidopsis CROOKED encodes for the smallest subunit of the ARP2/3 complex and controls cell shape by region specific fine F-actin formation. *Development* **130**, 3137-3146.
- Mathur, J.** (2005). The ARP2/3 complex: giving plant cells a leading edge. *Bioessays* **27**, 377-387.
- McDowell, J.M., Huang, S., McKinney, E.C., An, Y.Q., and Meagher, R.B.** (1996a). Structure and evolution of the actin gene family in Arabidopsis thaliana. *Genetics* **142**, 587-602.

- McDowell, J.M., An, Y.Q., Huang, S., McKinney, E.C., and Meagher, R.B.** (1996b). The arabidopsis ACT7 actin gene is expressed in rapidly developing tissues and responds to several external stimuli. *Plant Physiol* **111**, 699-711.
- McKinney, E.C., Kandasamy, M.K., and Meagher, R.B.** (2002). Arabidopsis contains ancient classes of differentially expressed actin-related protein genes. *Plant Physiol* **128**, 997-1007.
- Meagher, R.B., McKinney, E.C., and Kandasamy, M.K.** (1999). Isovariant dynamics expand and buffer the responses of complex systems: the diverse plant actin gene family. *Plant Cell* **11**, 995-1006.
- Messerli, M., and Robinson, K.R.** (1997). Tip localized Ca²⁺ pulses are coincident with peak pulsatile growth rates in pollen tubes of *Lilium longiflorum*. *J Cell Sci* **110** (Pt 11), 1269-1278.
- Messerli, M., and Robinson, K.R.** (1998). Cytoplasmic acidification and current flux follow growth pulses of *Lilium longiflorum* pollen tubes. *Plant J* **16**, 87-91.
- Michelot, A., Guerin, C., Huang, S., Ingouff, M., Richard, S., Rodiuc, N., Staiger, C.J., and Blanchoin, L.** (2005). The formin homology 1 domain modulates the actin nucleation and bundling activity of Arabidopsis FORMIN1. *Plant Cell* **17**, 2296-2313.
- Michelot, A., Derivery, E., Paterski-Boujemaa, R., Guerin, C., Huang, S., Parcy, F., Staiger, C.J., and Blanchoin, L.** (2006). A novel mechanism for the formation of actin-filament bundles by a nonprocessive formin. *Curr Biol* **16**, 1924-1930.
- Michelot, A., Berro, J., Guerin, C., Boujemaa-Paterski, R., Staiger, C.J., Martiel, J.L., and Blanchoin, L.** (2007). Actin-filament stochastic dynamics mediated by ADF/cofilin. *Curr Biol* **17**, 825-833.
- Mullins, R.D., Heuser, J.A., and Pollard, T.D.** (1998). The interaction of Arp2/3 complex with actin: nucleation, high affinity pointed end capping, and formation of branching networks of filaments. *Proc Natl Acad Sci U S A* **95**, 6181-6186.
- Mundel, C., Baltz, R., Eliasson, A., Bronner, R., Grass, N., Krauter, R., Evrard, J.L., and Steinmetz, A.** (2000). A LIM-domain protein from sunflower is localized to the cytoplasm and/or nucleus in a wide variety of tissues and is associated with the phragmoplast in dividing cells. *Plant Mol Biol* **42**, 291-302.
- Narita, A., Takeda, S., Yamashita, A., and Maeda, Y.** (2006). Structural basis of actin filament capping at the barbed-end: a cryo-electron microscopy study. *EMBO J* **25**, 5626-5633.

- Navrot, N., Collin, V., Gualberto, J., Gelhaye, E., Hirasawa, M., Rey, P., Knaff, D.B., Issakidis, E., Jacquot, J.P., and Rouhier, N.** (2006). Plant glutathione peroxidases are functional peroxiredoxins distributed in several subcellular compartments and regulated during biotic and abiotic stresses. *Plant Physiol* **142**, 1364-1379.
- Oda, T., Iwasa, M., Aihara, T., Maeda, Y., and Narita, A.** (2009). The nature of the globular- to fibrous-actin transition. *Nature* **457**, 441-445.
- Pantaloni, D., Le Clainche, C., and Carlier, M.F.** (2001). Mechanism of actin-based motility. *Science* **292**, 1502-1506.
- Papalouka, V., Arvanitis, D.A., Vafiadaki, E., Mavroidis, M., Papadodima, S.A., Spiliopoulou, C.A., Kremastinos, D.T., Kranias, E.G., and Sanoudou, D.** (2009). Muscle LIM protein interacts with cofilin 2 and regulates F-actin dynamics in cardiac and skeletal muscle. *Mol Cell Biol* **29**, 6046-6058.
- Papuga, J., Hoffmann, C., Dieterle, M., Moes, D., Moreau, F., Tholl, S., Steinmetz, A., and Thomas, C.** (2010). Arabidopsis LIM proteins: a family of actin bundlers with distinct expression patterns and modes of regulation. *Plant Cell* **22**, 3034-3052.
- Parke, J.M., Miller, C.C., Cowell, I., Dodson, A., Dowding, A., Downes, M., Duckett, J.G., and Anderton, B.J.** (1987). Monoclonal antibodies against plant proteins recognise animal intermediate filaments. *Cell Motil Cytoskeleton* **8**, 312-323.
- Parton, R.M., Fischer, S., Malho, R., Pappasoulitis, O., Jelitto, T.C., Leonard, T., and Read, N.D.** (1997). Pronounced cytoplasmic pH gradients are not required for tip growth in plant and fungal cells. *J Cell Sci* **110**, 1187-1198.
- Perez-Alvarado, G.C., Miles, C., Michelsen, J.W., Louis, H.A., Winge, D.R., Beckerle, M.C., and Summers, M.F.** (1994). Structure of the carboxy-terminal LIM domain from the cysteine rich protein CRP. *Nat Struct Biol* **1**, 388-398.
- Perez-Alvarado, G.C., Kosa, J.L., Louis, H.A., Beckerle, M.C., Winge, D.R., and Summers, M.F.** (1996). Structure of the cysteine-rich intestinal protein, CRIP. *J Mol Biol* **257**, 153-174.
- Petrasek, J., and Schwarzerova, K.** (2009). Actin and microtubule cytoskeleton interactions. *Curr Opin Plant Biol* **12**, 728-734.
- Pierson, E.S., Miller, D.D., Callahan, D.A., van Aken, J., Hackett, G., and Hepler, P.K.** (1996). Tip-localized calcium entry fluctuates during pollen tube growth. *Dev Biol* **174**, 160-173.
- Pollard, T.D., and Cooper, J.A.** (1986). Actin and actin-binding proteins. A critical evaluation of mechanisms and functions. *Annu Rev Biochem* **55**, 987-1035.

- Pollard, T.D., and Beltzner, C.C.** (2002). Structure and function of the Arp2/3 complex. *Curr Opin Struct Biol* **12**, 768-774.
- Pomies, P., Louis, H.A., and Beckerle, M.C.** (1997). CRP1, a LIM domain protein implicated in muscle differentiation, interacts with alpha-actinin. *J Cell Biol* **139**, 157-168.
- Pope, B.J., Gonsior, S.M., Yeoh, S., McGough, A., and Weeds, A.G.** (2000). Uncoupling actin filament fragmentation by cofilin from increased subunit turnover. *J Mol Biol* **298**, 649-661.
- Redmond, T., Tardif, M., and Zigmond, S.H.** (1994). Induction of actin polymerization in permeabilized neutrophils. Role of ATP. *J Biol Chem* **269**, 21657-21663.
- Ren, H., and Xiang, Y.** (2007). The function of actin-binding proteins in pollen tube growth. *Protoplasma* **230**, 171-182.
- Ressad, F., Didry, D., Xia, G.X., Hong, Y., Chua, N.H., Pantaloni, D., and Carlier, M.F.** (1998). Kinetic analysis of the interaction of actin-depolymerizing factor (ADF)/cofilin with G- and F-actins. Comparison of plant and human ADFs and effect of phosphorylation. *J Biol Chem* **273**, 20894-20902.
- Ruzicka, D.R., Kandasamy, M.K., McKinney, E.C., Burgos-Rivera, B., and Meagher, R.B.** (2007). The ancient subclasses of Arabidopsis Actin Depolymerizing Factor genes exhibit novel and differential expression. *Plant J* **52**, 460-472.
- Sadler, I., Crawford, A.W., Michelsen, J.W., and Beckerle, M.C.** (1992). Zyxin and cCRP: two interactive LIM domain proteins associated with the cytoskeleton. *J Cell Biol* **119**, 1573-1587.
- Saedler, R., Mathur, N., Srinivas, B.P., Kernebeck, B., Hulskamp, M., and Mathur, J.** (2004). Actin control over microtubules suggested by DISTORTED2 encoding the Arabidopsis ARPC2 subunit homolog. *Plant Cell Physiol* **45**, 813-822.
- Sagave, J.F., Moser, M., Ehler, E., Weiskirchen, S., Stoll, D., Gunther, K., Buttner, R., and Weiskirchen, R.** (2008). Targeted disruption of the mouse *Csrp2* gene encoding the cysteine- and glycine-rich LIM domain protein CRP2 result in subtle alteration of cardiac ultrastructure. *BMC Dev Biol* **8**, 80.
- Schallus, T., Edlich, C., Stier, G., and Muhle-Goll, C.** (2007). ¹H, ¹³C, and ¹⁵N assignment of the muscular LIM protein MLP/CRP3. *Biomol NMR Assign* **1**, 41-43.

- Schallus, T., Feher, K., Ulrich, A.S., Stier, G., and Muhle-Goll, C.** (2009). Structure and dynamics of the human muscle LIM protein. *FEBS Lett* **583**, 1017-1022.
- Schmeichel, K.L., and Beckerle, M.C.** (1997). Molecular dissection of a LIM domain. *Mol Biol Cell* **8**, 219-230.
- Schmit, A.C.** (2000). Actin during mitosis and cytokinesis. In *Actin: A Dynamic Framework for Multiple Plant Cell Functions*, C.J. Staiger, F. Baluska, D. Volkmann, and Barlow, eds (Dordrecht, The Netherlands: Kluwer Academic Publishers), pp. 437-456
- Sheahan, M.B., Rose, R.J., and McCurdy, D.W.** (2007). Actin-filament-dependent remodeling of the vacuole in cultured mesophyll protoplasts. *Protoplasma* **230**, 141-152.
- Sheterline, P., Clayton, J., and Sparrow, J.** (1998). *Actin*. Oxford: Oxford University Press.
- Smertenko, A.P., Jiang, C.J., Simmons, N.J., Weeds, A.G., Davies, D.R., and Hussey, P.J.** (1998). Ser6 in the maize actin-depolymerizing factor, ZmADF3, is phosphorylated by a calcium-stimulated protein kinase and is essential for the control of functional activity. *Plant J* **14**, 187-193.
- Staiger, C.J., Goodbody, K.C., Hussey, P.J., Valenta, R., Drobak, B.K., and Lloyd, C.W.** (1993). The profilin multigene family of maize: differential expression of three isoforms. *Plant J* **4**, 631-641.
- Staiger, C.J., and Blanchoin, L.** (2006). Actin dynamics: old friends with new stories. *Curr Opin Plant Biol* **9**, 554-562.
- Staiger, C.J., Poulter, N.S., Henty, J.L., Franklin-Tong, V.E., and Blanchoin, L.** (2010). Regulation of actin dynamics by actin-binding proteins in pollen. *J Exp Bot* **61**, 1969-1986.
- Stronach, B.E., Siegrist, S.E., and Beckerle, M.C.** (1996). Two muscle-specific LIM proteins in *Drosophila*. *J Cell Biol* **134**, 1179-1195.
- Symons, M.H., and Mitchison, T.J.** (1991). Control of actin polymerization in live and permeabilized fibroblasts. *J Cell Biol* **114**, 503-513.
- Szymanski, D.B.** (2005). Breaking the WAVE complex: the point of Arabidopsis trichomes. *Curr Opin Plant Biol* **8**, 103-112.
- Tellam, R., and Frieden, C.** (1982). Cytochalasin D and platelet gelsolin accelerate actin polymer formation. A model for regulation of the extent of actin polymer formation in vivo. *Biochemistry* **21**, 3207-3214.

- Thomas, C., Hoffmann, C., Dieterle, M., Van Troys, M., Ampe, C., and Steinmetz, A.** (2006). Tobacco WLIM1 is a novel F-actin binding protein involved in actin cytoskeleton remodeling. *Plant Cell* **18**, 2194-2206.
- Thomas, C., Moreau, F., Dieterle, M., Hoffmann, C., Gatti, S., Hofmann, C., Van Troys, M., Ampe, C., and Steinmetz, A.** (2007). The LIM domains of WLIM1 define a new class of actin bundling modules. *J Biol Chem* **282**, 33599-33608.
- Thomas, C., Diterle, M., Gatti, S., Hoffmann, C., Moreau, F., Papuga, J., and Steinmetz, A.** (2008) Actin bundling via LIM domains. *Plant Signal Behav* **3**, 320-321
- Thomas, C., Tholl, S., Moes, D., Dieterle, M., Papuga, J., Moreau, F., and Steinmetz, A.** (2009) Actin bundling in plants. *Cell Motil Cytoskeleton* **66**, 940-957.
- Tran, T.C., Singleton, C., Fraley, T.S., and Greenwood, J.A.** (2005). Cysteine-rich protein 1 (CRP1) regulates actin filament bundling. *BMC Cell Biol* **6**, 45.
- Tsien, R.Y.** (1980). New calcium indicators and buffers with high selectivity against magnesium and protons: design, synthesis, and properties of prototype structures. *Biochemistry* **19**, 2396-2404.
- Valenta, R., Ferreira, F., Grote, M., Swoboda, I., Vrtala, S., Duchene, M., Deviller, P., Meagher, R.B., McKinney, E., Heberle-Bors, E., and et al.** (1993). Identification of profilin as an actin-binding protein in higher plants. *J Biol Chem* **268**, 22777-22781.
- Van Troys, M., Huyck, L., Leyman, S., Dhaese, S., Vandekerkhove, J., and Ampe, C.** (2008). Ins and outs of ADF/cofilin activity and regulation. *Eur J Cell Biol* **87**, 649-667.
- Velyvis, A., Yang, Y., Wu, C., and Qin, J.** (2001). Solution structure of the focal adhesion adaptor PINCH LIM1 domain and characterization of its interaction with the integrin-linked kinase ankyrin repeat domain. *J Biol Chem* **276**, 4932-4939.
- Vidali, L., and Hepler, P.K.** (1997). Characterization and localization of profilin in pollen grains and tubes of *Lilium longiflorum*. *Cell Motil Cytoskeleton* **36**, 323-338.
- Vidali, L., and Hepler, P.K.** (2001a). Actin and pollen tube growth. *Protoplasma* **215**, 64-76.
- Vidali, L., McKenna, S.T., and Hepler, P.K.** (2001b). Actin polymerization is essential for pollen tube growth. *Mol Biol Cell* **12**, 2534-2545.

- Vidali, L., van Gisbergen, P.A., Guerin, C., Franco, P., Li, M., Burkart, G.M., Augustine, R.C., Blanchoin, L., and Bezanilla, M.** (2009). Rapid formin-mediated actin-filament elongation is essential for polarized plant cell growth. *Proc Natl Acad Sci U S A* **106**, 13341-13346.
- Vitha, S., Baluska, F., Braun, M., Samaj, J., Volkmann, D., and Barlow, P.W.** (2000). Comparison of cryofixation and aldehyde fixation for plant actin immunocytochemistry: aldehydes do not destroy F-actin. *Histochem J* **32**, 457-466.
- Volkmann, N., Amann, K.J., Stoilova-McPhie, S., Egile, C., Winter, D.C., Hazelwood, L., Heuser, J.E., Li, R., Pollard, T.D., and Hanein, D.** (2001). Structure of Arp2/3 complex in its activated state and in actin filament branch junctions. *Science* **293**, 2456-2459.
- Vrtala, S., Wiedemann, P., Mittermann, I., Eichler, H.G., Sperr, W.R., Valent, P., Kraft, D., and Valenta, R.** (1996). High-level expression in *Escherichia coli* and purification of recombinant plant profilins: comparison of IgE-binding capacity and allergenic activity. *Biochem Biophys Res Commun* **226**, 42-50.
- Wang, Y.S., Yoo, C.M., and Blancaflor, E.B.** (2008a). Improved imaging of actin filaments in transgenic *Arabidopsis* plants expressing a green fluorescent protein fusion to the C- and N-termini of the fimbrin actin-binding domain 2. *New Phytol* **177**, 525-536.
- Wang, H.J., Wan, A.R., and Jauh, G.Y.** (2008b). An actin-binding protein, LILIM1, mediates calcium and hydrogen regulation of actin dynamics in pollen tubes. *Plant Physiol* **147**, 1619-1636.
- Wang, F., Jing, Y., Wang, Z., Mao, T., Samaj, J., Yuan, M., and Ren, H.** (2009). *Arabidopsis* profilin isoforms, PRF1 and PRF2 show distinctive binding activities and subcellular distributions. *J Integr Plant Biol* **51**, 113-121.
- Way, J.C., and Chalfie, M.** (1988). *mec-3*, a homeobox-containing gene that specifies differentiation of the touch receptor neurons in *C. elegans*. *Cell* **54**, 5-16.
- Wegner, A.** (1982). Treadmilling of actin at physiological salt concentrations. An analysis of the critical concentrations of actin filaments. *J Mol Biol* **161**, 607-615.
- Weiskirchen, R., and Gunther, K.** (2003). The CRP/MLP/TLP family of LIM domain proteins: acting by connecting. *Bioessays* **25**, 152-162.
- Winder, S.J., and Ayscough, K.R.** (2005). Actin-binding proteins. *J Cell Sci* **118**, 651-654.

- Whippo, C.W., Khurana, P., Davis, P.A., Deblasio, S.L., Desloover, D., Staiger, C.J., and Hangarter, R.P.** (2011). THRUMIN1 Is a Light-Regulated Actin-Bundling Protein Involved in Chloroplast Motility. *Curr Biol* **21**, 59-64.
- Wu, Y., Yan, J., Zhang, R., Qu, X., Ren, S., Chen, N., and Huang, S.** (2010). Arabidopsis FIMBRIN5, an actin bundling factor, is required for pollen germination and pollen tube growth. *Plant Cell* **22**, 3745-3763.
- Xiang, Y., Huang, X., Wang, T., Zhang, Y., Liu, Q., Hussey, P.J., and Ren, H.** (2007). ACTIN BINDING PROTEIN 29 from *Lilium* pollen plays an important role in dynamic actin remodeling. *Plant Cell* **19**, 1930-1946.
- Yahara, I.** (1982). [Cytoskeletal proteins--actin, tubulin, and their organizations (author's transl)]. *Tanpakushitsu Kakusan Koso* **27**, 1005-1020.
- Yamashita, A., Maeda, K., and Maeda, Y.** (2003). Crystal structure of CapZ: structural basis for actin filament barbed end capping. *EMBO J* **22**, 1529-1538.
- Yao, X., Perez-Alvarado, G.C., Louis, H.A., Pomies, P., Hatt, C., Summers, M.F., and Beckerle, M.C.** (1999). Solution structure of the chicken cysteine-rich protein, CRP1, a double-LIM protein implicated in muscle differentiation. *Biochemistry* **38**, 5701-5713.
- Ye, J., Zheng, Y., Yan, A., Chen, N., Wang, Z., Huang, S., and Yang, Z.** (2009). Arabidopsis formin3 directs the formation of actin cables and polarized growth in pollen tubes. *Plant Cell* **21**, 3868-3884.
- Yeoh, S., Pope, B., Mannherz, H.G., and Weeds, A.** (2002). Determining the differences in actin binding by human ADF and cofilin. *J Mol Biol* **315**, 911-925.
- Yokota, E., Tominaga, M., Mabuchi, I., Tsuji, Y., Staiger, C.J., Oiwa, K., and Shimmen, T.** (2005). Plant villin, lily P-135-ABP, possesses G-actin binding activity and accelerates the polymerization and depolymerization of actin in a Ca²⁺-sensitive manner. *Plant Cell Physiol* **46**, 1690-1703.
- Zhang, H., Qu, X., Bao, C., Khurana, P., Wang, Q., Xie, Y., Zheng, Y., Chen, N., Blanchoin, L., Staiger, C.J., and Huang, S.** (2010). Arabidopsis VILLIN5, an actin filament bundling and severing protein, is necessary for normal pollen tube growth. *Plant Cell* **22**, 2749-2767.

Chapter 7

Appendix

***Arabidopsis* LIM Proteins: A Family of Actin Bundlers with Distinct Expression Patterns and Modes of Regulation**

Jessica Papuga,¹ Céline Hoffmann,¹ Monika Dieterle, Danièle Moes, Flora Moreau, Stéphane Tholl, André Steinmetz, and Clément Thomas²

Centre de Recherche Public-Santé, L-1526 Luxembourg, Luxembourg

Recently, a number of two LIM-domain containing proteins (LIMs) have been reported to trigger the formation of actin bundles, a major higher-order cytoskeletal assembly. Here, we analyzed the six *Arabidopsis thaliana* LIM proteins. Promoter- β -glucuronidase reporter studies revealed that *WLIM1*, *WLIM2a*, and *WLIM2b* are widely expressed, whereas *PLIM2a*, *PLIM2b*, and *PLIM2c* are predominantly expressed in pollen. LIM-green fluorescent protein (GFP) fusions all decorated the actin cytoskeleton and increased actin bundle thickness in transgenic plants and in vitro, although with different affinities and efficiencies. Remarkably, the activities of WLIMs were calcium and pH independent, whereas those of PLIMs were inhibited by high pH and, in the case of PLIM2c, by high $[Ca^{2+}]$. Domain analysis showed that the C-terminal domain is key for the responsiveness of PLIM2c to pH and calcium. Regulation of LIM by pH was further analyzed in vivo by tracking GFP-WLIM1 and GFP-PLIM2c during intracellular pH modifications. Cytoplasmic alkalization specifically promoted release of GFP-PLIM2c but not GFP-WLIM1, from filamentous actin. Consistent with these data, GFP-PLIM2c decorated long actin bundles in the pollen tube shank, a region of relatively low pH. Together, our data support a prominent role of *Arabidopsis* LIM proteins in the regulation of actin cytoskeleton organization and dynamics in sporophytic tissues and pollen.

INTRODUCTION

Actin is one of the most abundant and highly conserved proteins in eukaryotes. In the cytoplasm, actin monomers polymerize into actin filaments (AFs), which constitute the core elements of the actin cytoskeleton, providing mechanical support to the cytoplasm and serving as tracks for myosin-dependent intracellular transport (Hepler et al., 2001; Shimmen, 2007). In animal cells, AF-myosin interactions power cell division, cell contraction, and cell migration. AF polymerization itself is used as a driving force that directs the growth of membrane protrusions and enables cells to alter their shape and to move. In plant cells, AFs are essential for the establishment and maintenance of cell polarity (Vidali and Hepler, 2001) as well as for the formation of plant-specific cytoskeletal structures, such as the phragmoplast and the preprophase band (Schmit, 2000). In addition to its direct functions, the actin cytoskeleton is a key target of many signaling events and acts itself as a transducer of signals in both animal and plant cells (Drobak et al., 2004). To fulfill its various roles, the actin cytoskeleton requires a sophisticated regulatory system to control its organization and dynamics at both spatial and temporal levels. Primary components of this system are the actin binding proteins (ABPs) that directly interact with monomeric and/or polymerized actin to promote AF nucleation, polymerization, depolymerization, stabilization, severing, capping, and cross-linking (Winder and Ayscough, 2005). ABP activities themselves are tightly regulated by many cellular parameters, includ-

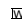
ing Ca^{2+} , pH, phosphoinositides, phosphorylation, and protein-protein interactions. The coordinated regulation of ABP activities ultimately defines AF positioning, turnover, and supraorganization in orthogonal networks or parallel bundles.

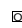
ABPs have been categorized into different classes according to the main or the historically first function attributed to them. Each class subdivides into several ABP families, which differ in their domain composition and/or organization and usually comprise several members. However, many ABPs display multiple actin regulatory activities. In addition, all the members belonging to one given ABP family do not necessarily retain the full range of possible activities, neither do they respond similarly to regulatory signals. A typical example is the villin family whose members exhibit distinct features. Indeed, the *Arabidopsis thaliana* VLIN1 generates actin bundles in an unusual Ca^{2+} /CaM-independent manner and lacks the nucleating, severing, and capping activities that are predicted (although not yet experimentally confirmed) for other *Arabidopsis* villins (Huang et al., 2005). Other villins, such as the lily (*Lilium longiflorum*) villin P-135-ABP, have been biochemically demonstrated to bundle and cap AFs as well as to accelerate the rate of AF depolymerization in a Ca^{2+} /CaM-sensitive manner (Yokota et al., 2005). Another functionally heterogeneous ABP family is the formin family. In *Arabidopsis*, it comprises >20 members that significantly differ in their domain organization, suggesting disparities in activities and modes of regulation (Blanchoin and Staiger, 2008; Grunt et al., 2008). Hence, the biological functions of one given ABP family cannot be fully appreciated by examining a limited number of its members.

Recently, a number of vertebrate LIM domain proteins belonging to the Cys-rich protein (CRP) family and several structurally related plant proteins (hereafter referred as to plant LIMs)

¹ These authors contributed equally to this work.

² Address correspondence to clement.thomas@crp-sante.lu.

 Online version contains Web-only data.

 Open Access articles can be viewed online without a subscription.
www.plantcell.org/cgi/doi/10.1105/tpc.110.075960

have been shown to function as ABPs (Grubinger and Gimona, 2004; Tran et al., 2005; Thomas et al., 2006; Wang et al., 2008a). CRPs and plant LIMs define a subset of relatively short (~200 amino acids) proteins that are characterized by two LIM domains and an unusually long interLIM spacer (40 to 50 amino acids; Weiskirchen and Gunther, 2003). In vitro, both chicken CRP1 and tobacco (*Nicotiana tabacum*) WLIM1 directly bind to AFs and trigger the formation of thick actin bundles. Importantly, overexpression of CRP1 and WLIM1 proteins was sufficient to significantly increase the bundling of AFs in rat fibroblasts and tobacco cells, respectively (Tran et al., 2005; Thomas et al., 2006, 2008). Similar results have been reported for the pollen-enriched *Lilium* LIM1 protein (Wang et al., 2008a), suggesting that actin bundling is a prevalent, rather than an accessory, activity among plant LIMs. However, this remains to be confirmed by the analysis of additional plant LIMs.

Interestingly, LIM1 overexpression induced an oscillatory formation of asterisk-shaped AF aggregates in the subapical region of growing pollen tubes (Wang et al., 2008a). In vitro investigations have suggested that the interaction of LIM1 and AFs is regulated by pH and Ca^{2+} , two central regulators of pollen tube oscillatory growth that are assumed to function through the activation/deactivation of several ABPs (Cheung and Wu, 2008; Staiger et al., 2010). Therefore, LIM1 has been proposed, along with pH and Ca^{2+} , to be part of the central oscillatory mechanism that regulates actin cytoskeleton remodeling during pollen tube elongation (Wang et al., 2008a). However, evidence of pH- and/or Ca^{2+} -dependent regulation of *Lilium* LIM1 or other plant LIMs in the context of live cells is still lacking.

Plants possess multimember LIM gene families, with six members in *Arabidopsis* and rice (*Oryza sativa*) and up to 12 members in poplar (*Populus* spp; Arnaud et al., 2007). Earlier studies have suggested the existence of two main LIM gene subfamilies that differ in their expression patterns (Eliasson et al., 2000). The WLIM subfamily includes genes that exhibit a wide expression pattern throughout the sporophytic plant tissues, whereas the PLIM subfamily includes genes with exclusive or preferential expression in pollen. A more complex classification of LIM genes has been recently proposed based on the phylogenetic analysis of 149 LIMs and the comparison of available expression data (Arnaud et al., 2007). According to this classification, the *Arabidopsis* LIM gene family comprises three vegetative (WLIM1 and WLIM2a and b) and three reproductive (PLIM2a-c) isoforms, one of which, PLIM2a, has been shown to be expressed in flowers (Alves-Ferreira et al., 2007).

By conducting a detailed analysis of the entire LIM gene/protein family in *Arabidopsis*, we addressed a number of central issues regarding the functions and modes of action of plant LIMs. Organ- and tissue-specific expression patterns of the six *Arabidopsis* LIMs were characterized in transgenic plants expressing a β -glucuronidase (GUS) reporter gene under the control of individual LIM regulatory sequences. Our data demonstrate the existence of two differentially expressed LIM subfamilies, although not always with a strict separation between vegetative and reproductive patterns. Both in vitro and in vivo investigations provide evidence that all six *Arabidopsis* LIMs display actin binding, -stabilizing, and -bundling activities, although with different efficiencies. By contrast, all LIMs did not respond similarly

to pH and [Ca^{2+}] variations. Most strikingly, the three pollen-enriched PLIMs were inactivated by relatively high pH values (≥ 6.8), whereas the three WLIMs remained fully active in the range of conditions tested. PLIM2c exhibited additional responsiveness to calcium. A domain analysis pointed out a central role of the C-terminal domain in the regulation of PLIM activities. Specific pH-dependent regulation of PLIMs was confirmed in live *Arabidopsis* cells whose pH was artificially modified. Finally, a green fluorescent protein (GFP)-fused PLIM2c fusion protein expressed in pollen interacted with the long actin bundles in the shank of elongating pollen tubes and occasionally decorated a subapical actin fringe-like structure. Together, our data strongly support that plant LIMs define a highly specialized ABP family, which contributes to the regulation of actin bundling in virtually all plant cells. Specific control of PLIM actin regulatory activities by pH is particularly relevant with regard to the potential biological functions of these proteins in tip-growing pollen tubes.

RESULTS

Tissue-Specific Expression of *Arabidopsis* LIM Genes Reveals Two Differentially Expressed Subfamilies

According to a recent wide-range phylogenetic analysis, the six *Arabidopsis* LIM genes have been renamed WLIM1 (*At1g10200*), WLIM2a (*At2g39900*), WLIM2b (*At3g55770*), PLIM2a (*At2g45800*), PLIM2b (*At1g01780*), and PLIM2c (*At3g61230*) (Arnaud et al., 2007). The possibility that individual *Arabidopsis* LIMs have specific functions in specific tissues or cell types due to nonoverlapping expression patterns was examined in *Arabidopsis* plants expressing the GUS reporter gene under the control of individual LIM gene 5' upstream sequences (*ProLIM*).

Preliminary RNA gel blot analysis shows expression of all three WLIMs in a wide range of organs, including roots, leaves, stem, flowers, and siliques (see Supplemental Figure 1A online). By contrast, PLIM transcripts were predominantly detected in flowers. GUS histochemical assays confirmed and refined these data (Figure 1). Indeed, *ProWLIM1-GUS* and *ProWLIM2b-GUS* expression was high in virtually all organs and tissues, including root, stem, leaf, and apical bud tissues (Figures 1A to 1D and 1I to 1L). WLIM2a promoter activity was also strong in roots and leaf vasculature but resulted in rather weak staining in other leaf tissues (Figures 1E to 1H). Significant expression of the three *ProWLIM-GUS* fusions was detected in floral tissues, including peduncle, pedicels, pistils, and stamen filaments (Figures 1C, 1D, 1G, 1H, 1K, and 1L). However, no (*ProWLIM1*) or only a faint signal (*ProWLIM2a* and *ProWLIM2b*) could be detected in pollen grains, even after long staining periods (>15 h; Figures 1D, 1H, and 1L). By contrast, the three *ProPLIM-GUS* fusions exhibited prominent expression in pollen grains (Figures 1O, 1P, 1S, 1T, 1W, and 1X). Particularly high expression levels of PLIMs were indicated by a fast (<30 min) and intense staining. *ProPLIM2c-GUS* expression exclusively appeared in pollen (Figures 1U to 1X). A weak GUS staining was sometimes (four out of nine lines) observed in leaves for *Pro-PLIM2a* (Figure 1M), and PLIM2b promoter activity was regularly detected in roots and leaf

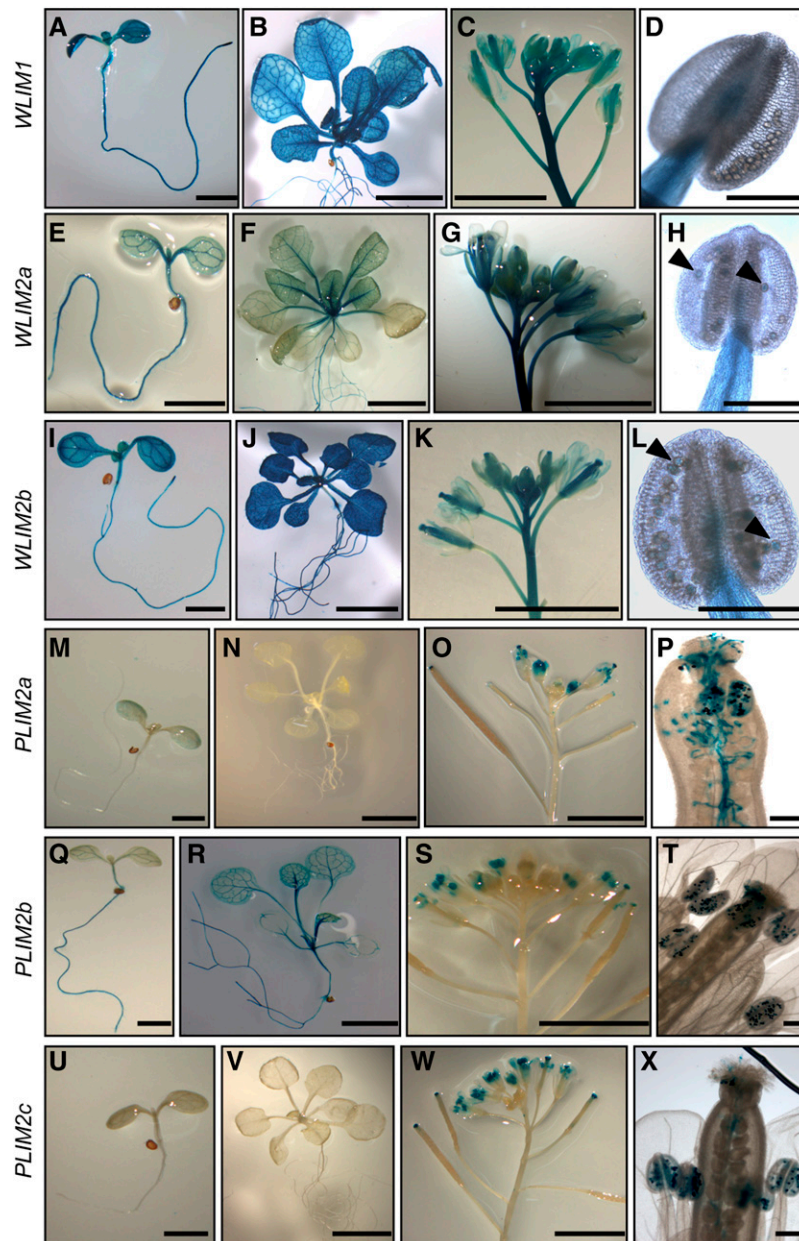


Figure 1. *Arabidopsis* LIM Gene Expression Patterns in Transgenic Plants Expressing Fusions of LIM Regulatory Sequences with the GUS Reporter Gene.

(A) to (D) ProWLM1-GUS expression.

(E) to (H) ProWLM2a-GUS expression.

(I) to (L) ProWLM2b-GUS expression.

(M) to (P) ProPLIM2a-GUS expression.

(Q) to (T) ProPLIM2b-GUS expression.

(U) to (X) ProPLIM2c-GUS expression.

Histological GUS assays were performed on 7-d-old seedlings ([A], [E], [I], [M], [Q], and [U]; bars = 2 mm), 4-week-old plantlets ([B], [F], [J], [N], [R], and [V]; bars = 5 mm), inflorescences ([C], [G], [K], [O], [S], and [W]; bars = 5 mm), anthers ([D], [H], and [L]), pistil with pollen tubes ([P]), and single flowers ([T] and [X]). Bars in (D), (H), (L), (P), (T), and (X) = 200 μ m. Arrows in (H) and (L) indicate faint-blue staining in pollen grains.

vasculature (Figures 1Q and 1R). Together, these results are in good agreement with the analysis of publicly available microarray data (see Supplemental Figures 1B and 1C online). Indeed, much higher signal intensities were detected for *WLIMs* than for *PLIMs* in vegetative tissues (see Supplemental Figure 1B online), whereas the situation was inverted in pollen (see Supplemental Figure 1C online). In addition, *PLIM2b* was the *PLIM* subfamily member exhibiting the highest expression level in vegetative tissues (see Supplemental Figure 1B online). The strong upregulation of the three *PLIMs* in tricellular and mature pollen grains suggests that *PLIM* activity is required during the late stages of pollen development and during pollen germination.

In conclusion, our data provide strong evidence for the separation of *Arabidopsis LIMs* into two subfamilies with different, to some extent complementary, expression patterns. *WLIM1*, *WLIM2a*, and *WLIM2b* are widely expressed in most sporophytic tissues with no or very weak expression in pollen, whereas *PLIM2a*, *PLIM2b*, and *PLIM2c* are predominantly and abundantly expressed in pollen grains.

The Six *Arabidopsis* LIM Proteins Interact with the Actin Cytoskeleton in Different Cell Types

Two tobacco and one lily LIM have been previously reported to interact with the actin cytoskeleton in live cells (Thomas et al., 2006; Cheung et al., 2008; Wang et al., 2008a). The possibility that all six members of the *Arabidopsis* LIM family display a similar activity was examined in transgenic *Arabidopsis* plants that constitutively express individual LIMs fused to GFP (GFP-LIMs). Figure 2 shows typical confocal microscopy images obtained for different cell types, including leaf epidermal, root, and root hair cells. All six GFP-LIMs associated with a cytoplasmic filamentous network (Figures 2A to 2R) similar to the one revealed by the fimbrin-derived actin cytoskeleton marker GFP-ABD2-GFP (Wang et al., 2008b; Figures 2S to 2U). This network was confirmed to be the actin cytoskeleton by both rhodamine-phalloidin colabeling and latrunculin B depolymerizing experiments (see Supplemental Figure 2 online). Comparison of confocal images suggested that *PLIMs* interact less efficiently with the cytoskeleton than *WLIMs*. Indeed, most of GFP-*PLIM*-expressing cells exhibited a relatively high level of diffuse cytoplasmic fluorescence, whereas GFP-*WLIMs* more sharply decorated the cytoskeleton (cf. Figures 2A to 2C to 2D to 2F, 2G to 2I to 2J to 2L, and 2M to 2O to 2P to 2R). Differences in the subcellular distribution of GFP-*PLIMs* and GFP-*WLIMs* were further characterized by quantifying the fraction of cytoplasmic fluorescence associated with the cytoskeleton (FCFAC) in GFP-*PLIM2c*, GFP-*WLIM1*, and GFP-ABD2-GFP (control) expressing cells (see Supplemental Figure 3A online). In primary root cells, $\sim 53\% \pm 5\%$ of the fluorescent signal due to GFP-*PLIM2c* concentrated on the cytoskeleton. In root hairs, the FCFAC dropped to $31\% \pm 5\%$, indicating that roughly 70% of the GFP-*PLIM2c* population was unbound in the cytoplasm. By contrast, GFP-*WLIM1* and GFP-ABD2-GFP predominantly associated with the cytoskeleton, as indicated by FCFAC values of roughly 70 and 90% in both types of cells, respectively. Immunoblot analysis performed with an anti-GFP antibody confirmed that GFP-*WLIM1* and GFP-*PLIM2c* were expressed at similar levels in the *Arabidopsis* lines

used in the above analyses, ruling out that results were due to differences in transgene expression levels (see Supplemental Figure 3B online).

Remarkably, no obvious developmental or morphological phenotype was noticed in LIM-overexpressing transgenic plants. However, confocal microscopy images revealed substantial modifications of the actin cytoskeleton organization. Indeed, actin bundles were usually thicker and less abundant than in control cells (cf. Figures 2A to 2R to 2S to 2U). These observations are consistent with those previously reported in the case of tobacco *WLIM1* overexpression (Thomas et al., 2006, 2008) and support that all six LIMs promote cross-linking of AFs into thick bundles.

Although this study focuses on the cytoplasmic functions of plant LIMs, it is noteworthy that, contrary to GFP-ABD2-GFP, GFP-LIMs also accumulated within the nucleus, suggesting potential nuclear functions for LIMs.

The Six *Arabidopsis* LIM Proteins Display Actin Binding, -Stabilizing, and -Bundling Activities

To date, actin regulatory activities have been biochemically demonstrated for only two plant LIMs (i.e., tobacco *WLIM1* [Thomas et al., 2006, 2007] and lily *LIM1* [Wang et al., 2008a]). Here, we assessed the actin binding, -stabilizing, and -bundling activities of the whole *Arabidopsis* LIM family. Wang et al. (2008a) recently reported that *LIM1* preferentially binds AFs under low pH and low $[Ca^{2+}]$. We therefore initiated biochemical investigations using similar conditions.

The ability of LIMs to directly bind to AFs was evaluated by high-speed cosedimentation assays. Recombinant LIMs were produced in *Escherichia coli* and purified by affinity chromatography. AFs (4 μ M) were copolymerized with individual LIMs (4 μ M) and centrifuged at 100,000g, and the resulting pellet and supernatant fractions were analyzed by SDS-PAGE (Figure 3A). Control experiments showed that recombinant LIMs do not sediment significantly when centrifuged alone (Figure 3A, top gel series). In the presence of AFs, the six LIMs accumulated in the pellet fraction, indicating that they directly interact with AFs (Figure 3A, bottom gel series). However, the relative amount of pelleted LIM was slightly lower in the case of the three *PLIMs*, suggesting differences in affinity for AFs. This possibility was further investigated by conducting additional high-speed cosedimentation assays with increasing concentrations of LIM proteins and calculating apparent equilibrium dissociation constant (K_d) values as previously described by Thomas et al. (2006, 2007) (Table 1; see Supplemental Figure 4 online). In the conditions used (pH 6.2 and 100 nM Ca^{2+}), the three *WLIMs* displayed relatively high and similar affinities for AFs as indicated by apparent K_d values of $0.4 \pm 0.2 \mu$ M (*WLIM1*), $0.4 \pm 0.2 \mu$ M (*WLIM2a*), and 0.5 ± 0.3 ($n = 3$). Noticeably, these values were significantly lower than those calculated for *PLIMs*, which ranged from $1.3 \pm 0.2 \mu$ M (*PLIM2a*) to $1.7 \pm 0.9 \mu$ M (*PLIM2b*).

The effect of LIM binding on AF stability was examined in depolymerization assays. Pyrene-labeled AFs (4 μ M) were copolymerized with individual LIMs (6 μ M) and subsequently subjected to depolymerization by diluting the samples to an actin concentration below the critical concentration (i.e., 0.2 μ M).

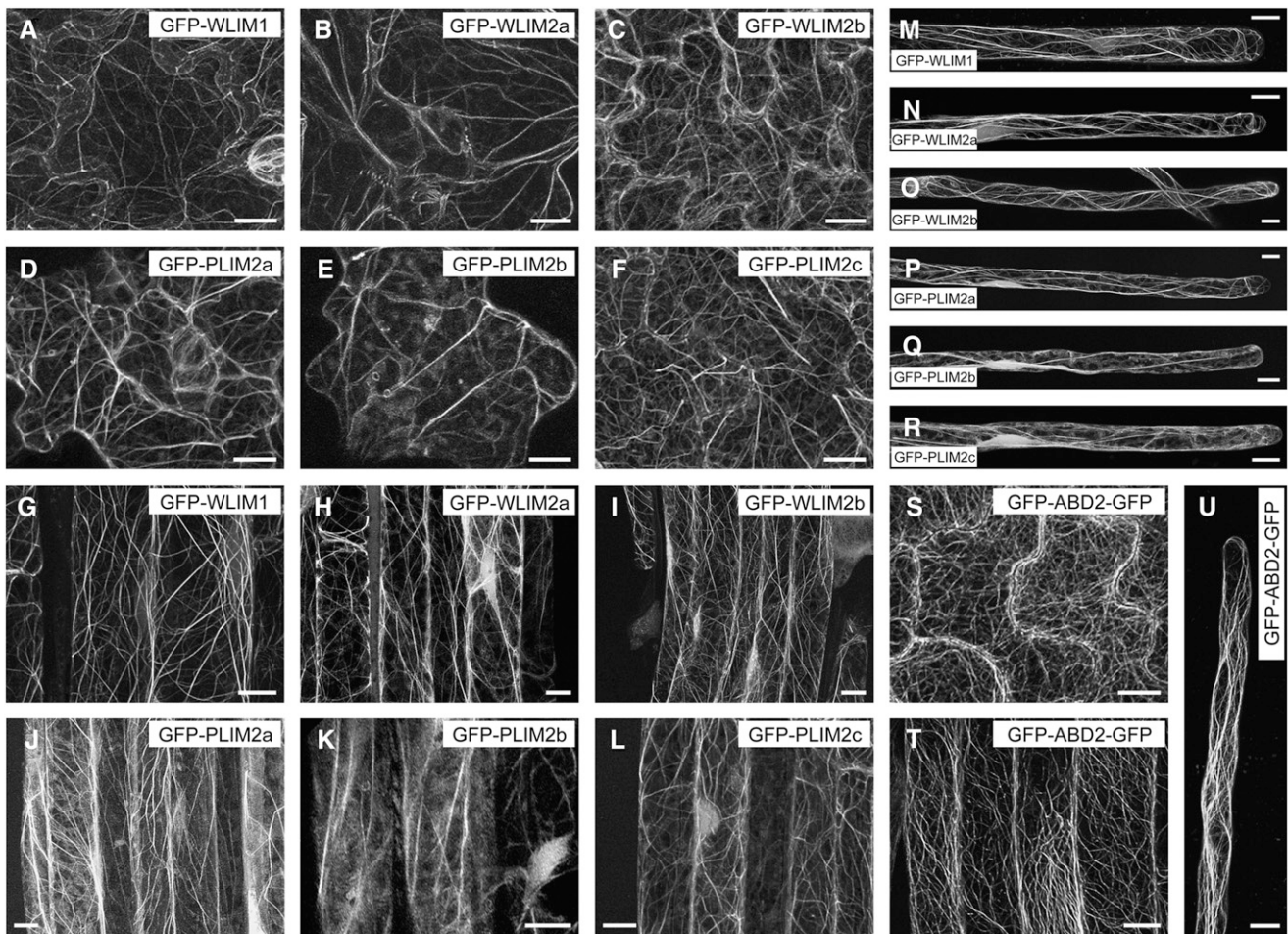


Figure 2. Localization of GFP-Fused LIMs in Different Tissues of Transgenic *Arabidopsis* Seedlings.

Typical fluorescent patterns observed for GFP-WLIM1 ([A], [G], and [M]), GFP-WLIM2a ([B], [H], and [N]), GFP-WLIM2b ([C], [I], and [O]), GFP-PLIM2a ([D], [J], and [P]), GFP-PLIM2b ([E], [K], and [Q]), GFP-PLIM2c ([F], [L], and [R]), and the actin cytoskeleton marker GFP-ABD2-GFP ([S] to [U]) in epidermal leaf cells ([A] to [F] and [S]), main root cells ([G] to [L] and [T]), and root hairs ([M] to [R] and [U]). Bars = 10 μ m.

Depolymerization kinetics were recorded by monitoring fluorescence intensity over time (Figure 3B). In the absence of LIMs (actin alone), AFs promptly depolymerized, as shown by the rapid decline of fluorescence. By contrast, in the presence of individual LIMs, the AF depolymerization rate was markedly decreased. Consistent with the K_d values calculated above, the two LIM subfamilies exhibited different stabilization capabilities. Whereas WLIMs fully stabilized AFs, as indicated by stable fluorescence curves, PLIMs only reduced the AF depolymerization rate. Remarkably, the three members of each LIM subfamily displayed roughly identical stabilizing capabilities.

Finally, the ability of each LIM to cross-link AFs was assessed using low-speed cosedimentation assays. AFs (4 μ M) were copolymerized with individual LIMs (6 μ M) and centrifuged at 12,500g, and the resulting pellet and supernatant fractions were analyzed by SDS-PAGE (Figure 3C). In the absence of LIM (actin alone), most of the actin was detected in the supernatant fraction. By contrast, in the presence of individual LIMs, actin

massively sedimented, indicating the presence of high-order actin structures. The latter were directly examined by fluorescence light microscopy after rhodamine-phalloidin labeling and identified as actin bundles (Figure 3D).

In conclusion, all six *Arabidopsis* LIMs function as true ABPs (i.e., they directly interact with AFs). In addition, they display autonomous actin-stabilizing and -bundling activities. However, differences are also pointed out by data (the three WLIMs exhibiting a higher affinity for AFs than the three PLIMs).

WLIM1 and PLIM2c Activities Are Differently Regulated by pH and Ca^{2+}

The potential regulation of LIM activities by pH and Ca^{2+} were assessed by focusing on one member of each LIM subfamily, namely, WLIM1 and PLIM2c. Both proteins were first subjected to a series of actin depolymerization assays conducted at three different pH conditions, 6.2, 6.8, and 7.4, and in the presence of

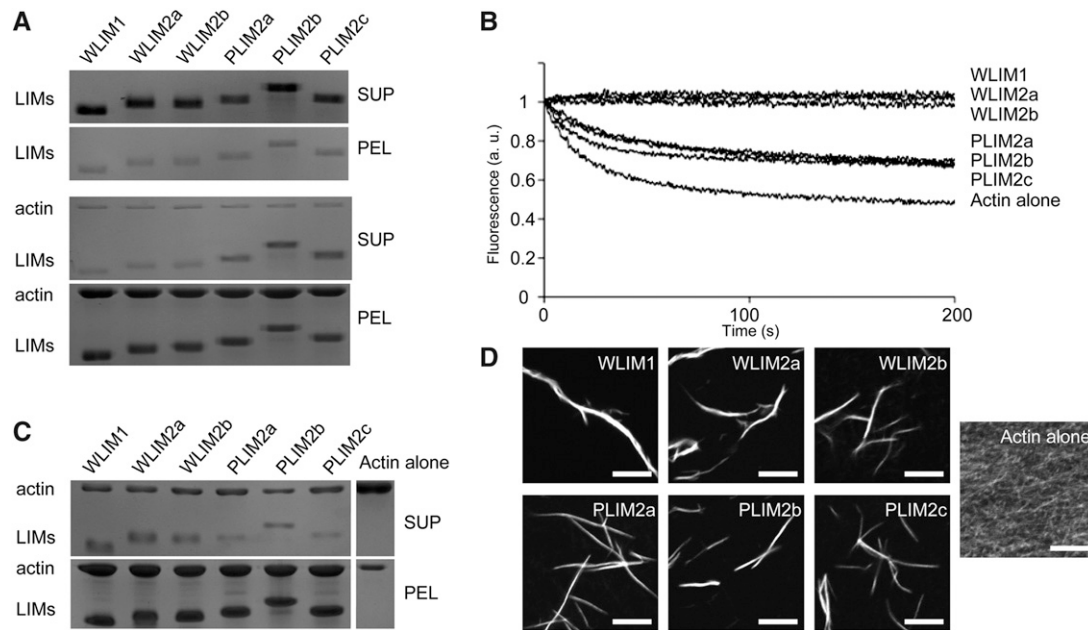


Figure 3. *Arabidopsis* LIMs Bind to, Stabilize, and Bundle AFs.

(A) High-speed cosedimentation assay. After centrifugation at 100,000g, LIMs (4 μM) accumulate in the pellet fraction in the presence (bottom gel panel) but not in the absence of AFs (4 μM ; top gel panel).

(B) Depolymerization assay. Time course of AF (4 μM) depolymerization in the absence and in the presence of individual LIMs (6 μM) was monitored by pyrene fluorescence. Initial fluorescence was set to 1. Note that WLIMs stabilize AFs more efficiently than PLIMs.

(C) Low-speed cosedimentation assay. After centrifugation at 12,500g, AFs (4 μM) sediment in the presence but not in the absence of LIMs (6 μM).

(D) Direct visualization of actin bundles induced by LIMs. After polymerization in the absence (actin alone) or in the presence of individual LIMs (6 μM), AFs (4 μM) were labeled with rhodamine-phalloidin and examined by light fluorescence microscopy. Bars = 5 μm . All above assays were conducted at pH 6.2 and in low $[\text{Ca}^{2+}]$ (~ 5 nM free Ca^{2+}). SUP, supernatant fraction; PEL, pellet fraction.

low or high amounts of free Ca^{2+} , corresponding to ~ 100 nM and ~ 5 μM , respectively. For each pH and $[\text{Ca}^{2+}]$ condition, different concentrations of WLIM1 and PLIM2c (ranging from 1 to 10 μM , concentrations before sample dilution) have been tested, whereas the concentration of actin before dilution was set at 4 μM (Figures 4A to 4L). Under low pH and low $[\text{Ca}^{2+}]$, both WLIM1 and PLIM2c stabilized AFs in a concentration-dependent manner (Figures 4A and 4G). Data confirmed the higher stabilizing capability of WLIM1. Indeed, 1 μM of WLIM1 was sufficient to slow down the AF depolymerization rate, whereas 3 μM of PLIM2c were required to produce a significant effect. In addition, full stabilization of AFs was achieved for WLIM1 concentrations ≥ 6 μM , whereas it required >10 μM of PLIM2c.

Increasing pH from 6.2 to 6.8 or 7.4 caused the loss of PLIM2c stabilizing activity, as indicated by depolymerization curves similar to the controls (AFs alone; Figures 4H and 4I). At higher pH, even the highest PLIM2c concentrations failed to slow down AF depolymerization, indicating a strong pH-dependent inhibition. By contrast, WLIM1 preserved prominent activity at both intermediate and high pH values (Figures 4B and 4C). Furthermore, its stabilizing efficiency appeared unmodified by pH increase since, in all pH conditions, maximal AF stabilization was observed for WLIM1 concentrations ≥ 6 μM . To check whether high pH values can also inhibit the actin-stabilizing activity of AF-bound PLIM2c, AFs (4 μM) were first copolymerized with

PLIM2c (8 μM) in optimal conditions (i.e., pH 6.0 and 100 nM of free Ca^{2+}), and the pH was subsequently shifted by the addition of alkalinizing buffers of increasing strength (final pH 6.0, 6.2, 6.4, 6.8, and 7.4). Supplemental Figure 5A online shows that the rate of depolymerization increased proportionally to the shift of pH applied, indicating that pH can inactivate PLIM2c when the latter is associated with AFs. By contrast, the ability of WLIM1 to stabilize AFs was preserved whatever the shift of pH applied (see Supplemental Figure 5B online).

Additional depolymerization experiments were performed at high $[\text{Ca}^{2+}]$ levels (Figures 4D to 4F and 4J to 4L). At pH 6.2, the

Table 1. Affinities of the Six *Arabidopsis* LIM Proteins for AFs

Protein	K_d (μM)	B_{max}
WLIM1	0.4 ± 0.2	1.4 ± 0.2
WLIM2a	0.4 ± 0.2	1.1 ± 0.2
WLIM2b	0.5 ± 0.3	1.5 ± 0.2
PLIM2a	1.3 ± 0.2	1.5 ± 0.1
PLIM2b	1.7 ± 0.9	1.5 ± 0.1
PLIM2c	1.5 ± 1.1	1.8 ± 0.2

Apparent equilibrium dissociation constants (K_d) values (\pm SD) were calculated from three independent high-speed cosedimentation assay experiments after fitting the data (bound protein plotted against free protein; see Supplemental Figure 4 online) with a hyperbolic function.

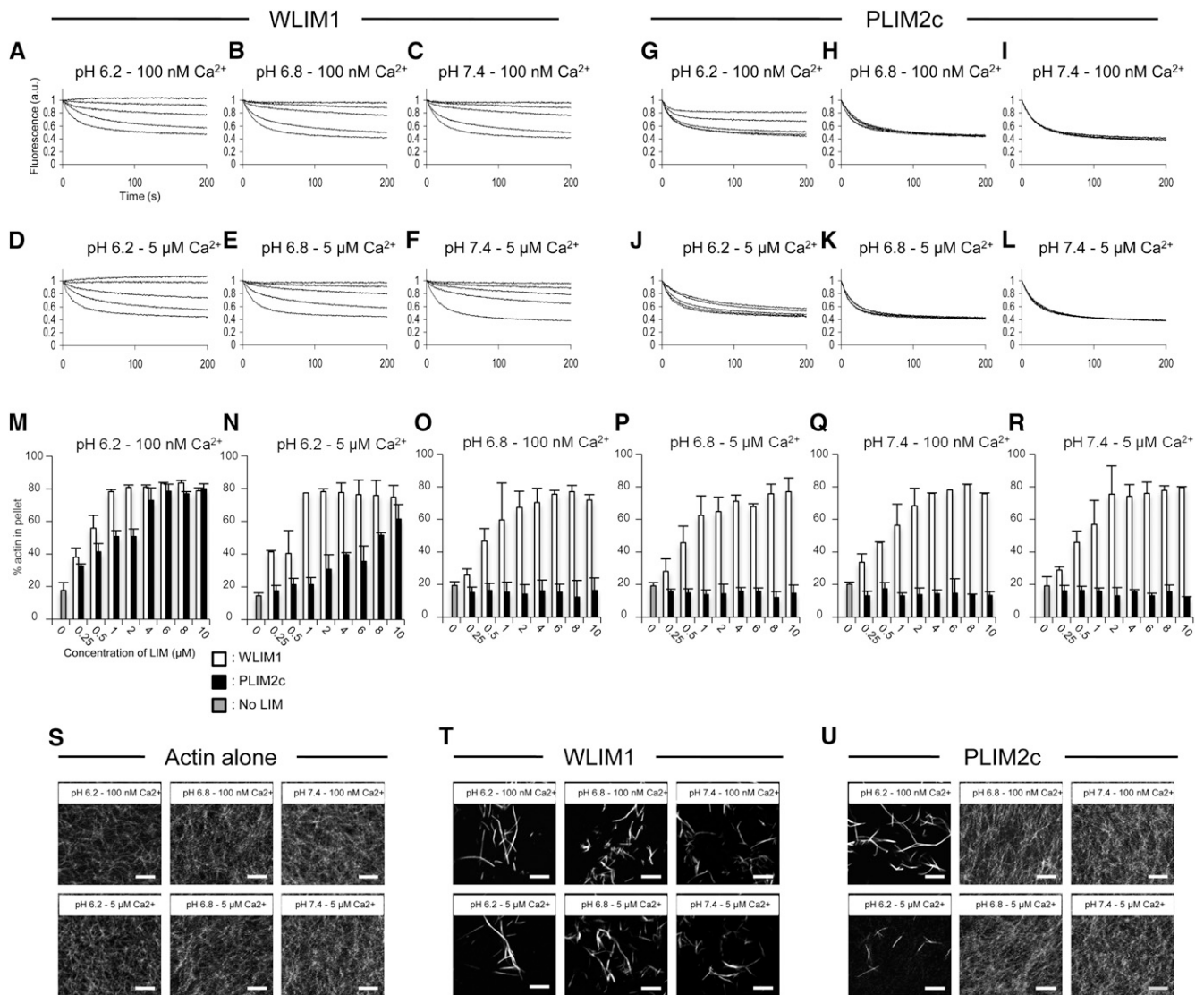


Figure 4. Detailed Comparison of WLIM1 and PLIM2c Actin Regulatory Activities in Different Combinations of pH and $[Ca^{2+}]$.

(A) to (L) Depolymerization assays. Pyrene-labeled AFs (4 μ M) were copolymerized in the presence of increasing concentrations of WLIM1 or PLIM2c (0, 1, 3, 6, and 10 μ M from bottom to top curves) and were induced to depolymerize by dilution below the critical concentration (i.e., 0.2 μ M). Initial fluorescence was set to 1.

(M) to (R) Low-speed cosedimentation assays. AFs (4 μ M) were copolymerized in the presence of increasing concentrations of WLIM1 or PLIM2c (0 to 10 μ M) and centrifuged at 12,500g. The amount of actin in the pellet and supernatant fractions was quantified. Results are expressed as the percentage of total actin in the pellet as a function of LIM concentration ($n = 3$; error bars indicate SD).

(S) to (U) Direct visualization of AFs (4 μ M) that were polymerized alone (left panel) or in the presence of WLIM1 (6 μ M; middle panel) or PLIM2c (6 μ M; left panel) using rhodamine-phalloidin labeling. Bars = 5 μ m.

high $[Ca^{2+}]$ significantly reduced the actin-stabilizing capability of PLIM2c (Figure 4J). However, this inhibition was less strong than that of pH, as indicated by the weak but significant levels of stabilization observed for the highest concentrations of PLIM2c (Figure 4J versus 4G). In higher pH conditions (i.e., pH 6.8 and 7.4), high $[Ca^{2+}]$ showed no visible effect, since PLIM2c activity remained turned off (Figures 4K and 4L). The depolymerization curves obtained for WLIM1 were similar to those obtained at low

$[Ca^{2+}]$, indicating that WLIM1 was not responsive to Ca^{2+} (Figures 4D to 4F versus 4A to 4C).

LIM-induced stabilization most likely results from the cross-linking of AFs. Thus, from the above data, one might anticipate that PLIM2c bundling activity is negatively regulated by high pH and/or high $[Ca^{2+}]$, whereas the one of WLIM1 is not. To confirm these assumptions, low-speed (12,500g) cosedimentation assays were conducted in different pH and $[Ca^{2+}]$ conditions using

a fixed concentration of actin (4 μM) and increasing concentrations of LIM (0.5 to 10 μM ; Figures 4M to 4R). To make comparisons easier, SDS-PAGE gels were scanned after staining, and the respective amounts of actin in the pellet and in supernatant fractions were quantified using ImageJ software. As expected, WLIM1 induced actin sedimentation in a concentration-dependent manner in all tested pH and $[\text{Ca}^{2+}]$ combinations (Figures 4M to 4R, white bars). Lack of responsiveness to pH and Ca^{2+} was further demonstrated by the fact that maximal sedimentation (75 to 80% of total actin in the pellet fraction) was invariably achieved for WLIM1 concentrations $\geq 2 \mu\text{M}$. PLIM2c also induced efficient cross-linking of AFs under low pH and $[\text{Ca}^{2+}]$ conditions (Figures 4M to 4R, black bars). However, maximal sedimentation required $\sim 6 \mu\text{M}$ of PLIM2c, confirming its weaker activity compared with WLIM1 (Figure 4M, black versus white bars). Higher pH values (i.e., 6.8 and 7.4) fully inhibited PLIM2c cross-linking activity, as shown by the relative amounts of actin in the pellet similar to those measured in controls (actin alone, $\sim 20\%$; Figures 4O to 4R, black bars). Consistent with the depolymerization data, high $[\text{Ca}^{2+}]$ partially inhibited PLIM2c activity at pH 6.2, as shown by the reduced but significant amounts of actin sedimented in the presence of high PLIM2c concentrations (Figure 4N, black bars).

Direct observation of AFs polymerized alone (Figure 4S) or in the presence of WLIM1 (Figure 4T) or PLIM2c (Figure 4U) confirmed the above data. Indeed, WLIM1 triggered the formation of actin bundles in all pH and $[\text{Ca}^{2+}]$ combinations tested (Figure 4S versus 4T), whereas PLIM2c only induced similar structures under both low pH and low $[\text{Ca}^{2+}]$ (Figure 4S versus 4U). As expected, PLIM2c bundling activity was partially inhibited by high $[\text{Ca}^{2+}]$, as shown by the rare bundles observed at pH 6.2 and 5 μM Ca^{2+} (Figure 4U, bottom left image).

In conclusion, WLIM1 and PLIM2c respond differently to pH and $[\text{Ca}^{2+}]$ in vitro. WLIM1 actin regulatory activities are not

regulated by pH and $[\text{Ca}^{2+}]$, whereas those of PLIM2c are inhibited by pH values ≥ 6.8 and/or high $[\text{Ca}^{2+}]$.

LIM Subfamily-Specific Modes of pH- and Ca^{2+} -Dependent Regulation

To test whether responsiveness to pH and Ca^{2+} is a specific property of *Arabidopsis* PLIM subfamily members, additional low-speed cosedimentation assays were performed using 4 μM actin and 6 μM each *Arabidopsis* LIM (Figure 5). Similarly to WLIM1, WLIM2a and WLIM2b induced actin sedimentation in a pH- and Ca^{2+} -independent manner. Indeed, $\sim 80\%$ of actin were pelleted in all the combinations of pH and $[\text{Ca}^{2+}]$ tested (Figures 5A to 5F). Similarly to PLIM2c, PLIM2a and PLIM2b were unable to promote actin sedimentation at relatively high pH values (i.e., pH 6.8 and pH 7.4) (Figures 5C to 5F). However, both PLIM2a and PLIM2b efficiently cross-linked AFs at low pH (6.2) whatever the $[\text{Ca}^{2+}]$, indicating that they are not responsive to Ca^{2+} (Figures 5A and 5B).

In summary, the three WLIM subfamily members cross-link AFs in a pH- and Ca^{2+} -independent manner. By contrast, the cross-linking activity of the three PLIM subfamily members is inhibited by pH values ≥ 6.8 . Finally, PLIM2c is the only *Arabidopsis* LIM to clearly respond to Ca^{2+} , its activity being down-regulated by high $[\text{Ca}^{2+}]$.

Deletion of the C-Terminal Domain Abolishes PLIM2c Responsiveness to pH and Calcium

The most divergent domain in size and in amino acid sequence between WLIM and PLIM family members is the C-terminal domain (see Supplemental Figure 6 online). Noticeably, this domain is longer and contains a significantly higher number of acidic residues in PLIMs than in WLIMs. To test whether the

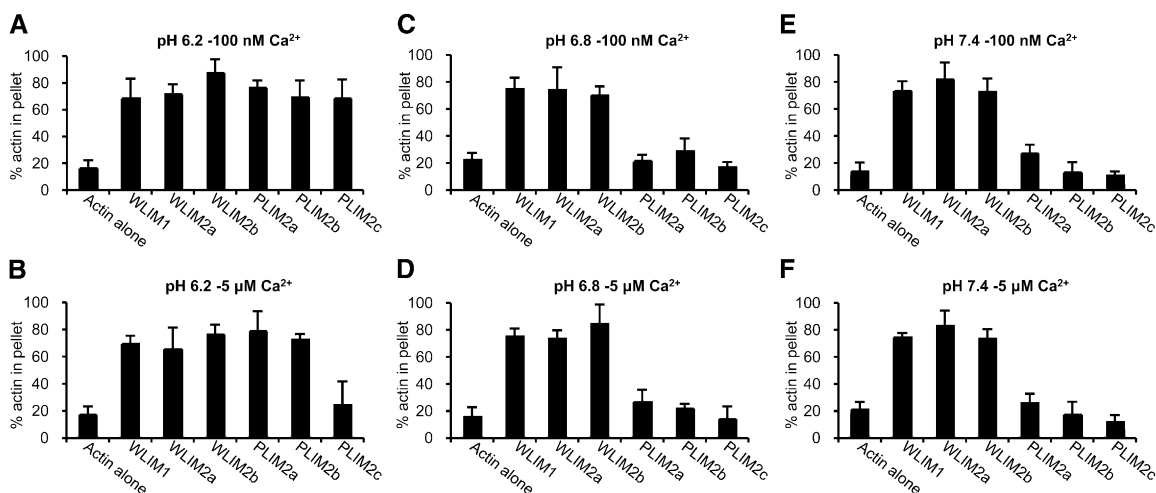


Figure 5. Actin Cross-Linking Activity of the Six *Arabidopsis* LIMs in Different Combinations of pH and $[\text{Ca}^{2+}]$.

Low-speed (12,500g) cosedimentation assays were performed after copolymerization of AFs (4 μM) with individual LIM proteins (6 μM) at pH 6.2 (**A**) and (**B**), pH 6.8 (**C**) and (**D**), or pH 7.4 (**E**) and (**F**) and in the presence of low $[\text{Ca}^{2+}]_{\text{free}}$ ($\sim 100 \text{ nM}$; **A**, **C**), and (**E**) or high $[\text{Ca}^{2+}]_{\text{free}}$ (5 μM ; **B**, **D**), and (**F**). The relative amount of actin in the pellet and supernatant fractions was quantified, and results are expressed as the percentage of total actin in the pellet for each of the *Arabidopsis* LIM tested ($n = 3$; error bars indicate SD).

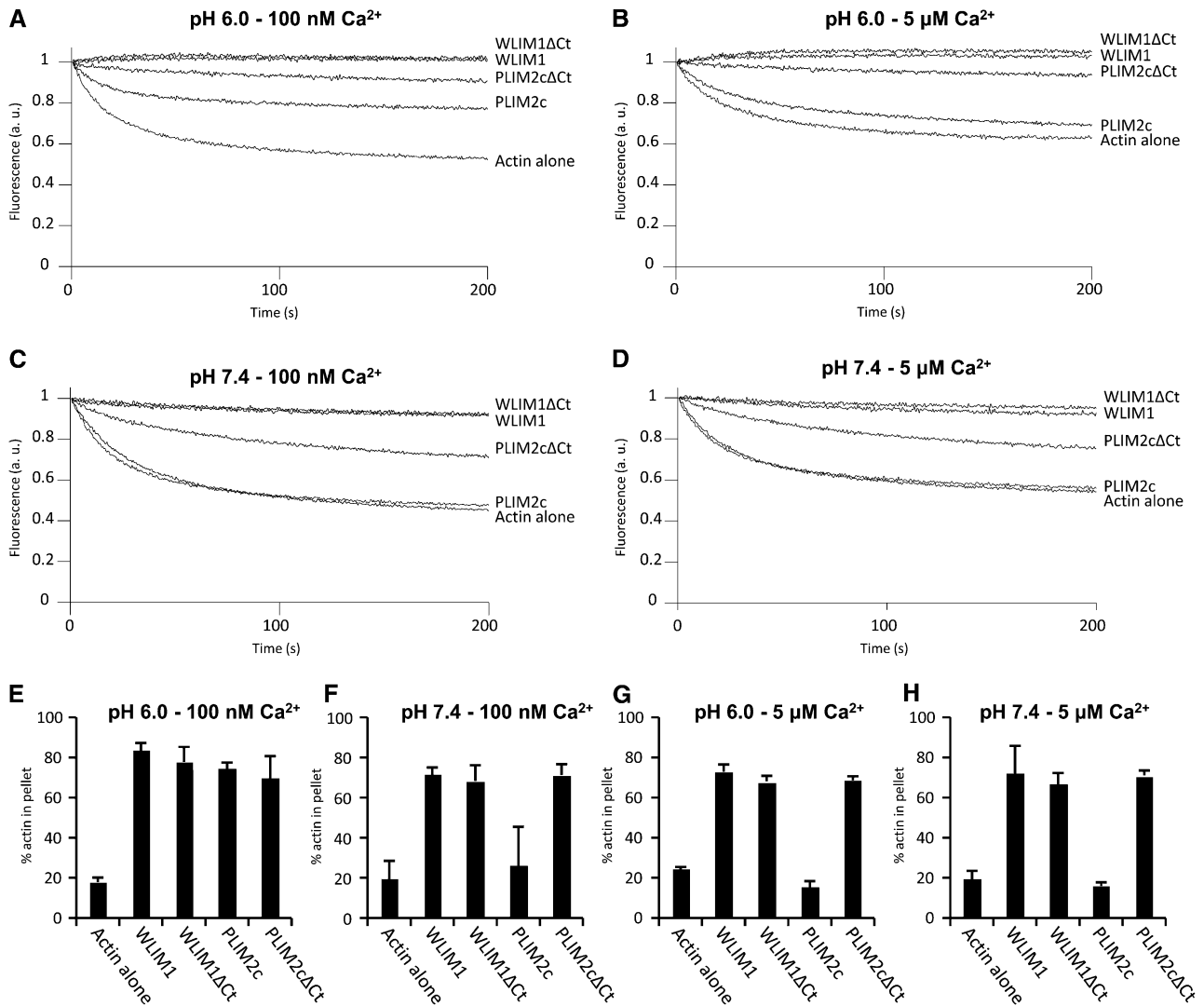


Figure 6. Comparison of the Actin-Stabilizing and -Bundling Activities of WLIM1, PLIM2c, and Their Corresponding C-Terminal Deleted Versions WLIM1ΔCt and PLIM2cΔCt in Different pH and [Ca²⁺] Conditions.

(A) to (D) Depolymerization assays. Pyrene-labeled AFs (4 μM) were copolymerized with PLIM2c, WLIM1, PLIM2cΔCt, or WLIM1ΔCt (10 μM) in different combinations of pH and [Ca²⁺] and were induced to depolymerize by dilution. Initial fluorescence was set to 1.

(E) to (H) Low-speed cosedimentation assays. AFs (4 μM) were copolymerized with PLIM2c, WLIM1, PLIM2cΔCt, or WLIM1ΔCt (6 μM) and centrifuged at 12,500g. The relative amount of actin in the pellet and supernatant fractions was quantified and results are expressed as the percentage of total actin in the pellet as a function of the LIM or LIM variant tested ($n \geq 4$; error bars indicate SD).

C-terminal domain is involved in the specific responsiveness of PLIMs to pH (and calcium in the case of PLIM2c), we generated C-terminal deleted versions of PLIM2c and WLIM1 (control), namely, PLIM2cΔCt and WLIM1ΔCt, and studied their actin-stabilizing and -bundling activities in different conditions of pH (6.2 and 7.4) and Ca²⁺ (100 nM and 5 μM). Our data indicate that, in contrast with PLIM2c, whose activities are inhibited by high pH and/or high [Ca²⁺], PLIM2cΔCt efficiently stabilized and cross-linked AFs in all the conditions tested (Figure 6). Indeed, the deletion of the C-terminal domain is sufficient to abolish the ability of PLIM2c to respond to pH and calcium variations. In addition, WLIM1 and WLIM1ΔCt displayed strong and nearly

identical activities whatever the pH and [Ca²⁺], supporting that the deletion of the C-terminal domain is not detrimental to the basal activity of LIM proteins.

In Vivo pH-Dependent Regulation *Arabidopsis* LIM Proteins

The above biochemical data strongly suggest that cytoplasmic pH acts as a regulator of PLIM activities. This hypothesis is consistent with the existence of intracellular pH gradients in growing pollen tubes and the concept that pH variations regulate the actin cytoskeleton organization and dynamics through the in/activation of different classes of ABPs (Feijo et al., 1999; Hepler

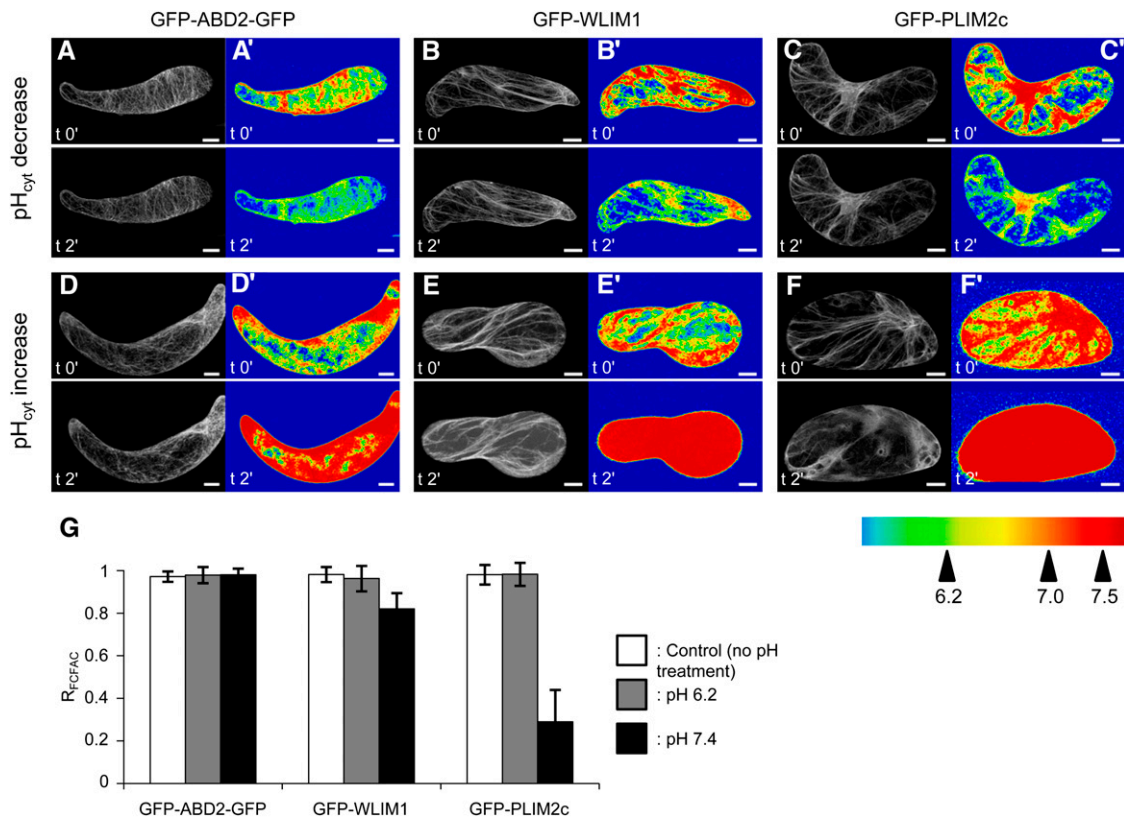


Figure 7. Increase of Cytoplasmic pH Specifically Impairs PLIM2c Interaction with the Actin Cytoskeleton.

(A) to (F) *Arabidopsis* cells expressing GFP-ABD2-GFP (A), (A'), (D), and (D)'), GFP-WLIM1 (B), (B'), (E), and (E)'), and GFP-PLIM2c (C), (C'), (F), and (F')) were treated with acidifying (A) to (C) and (A') to (C') or alkalinizing buffers (D) to (F) and (D') to (F')). Typical confocal images showing the localization of GFP fusion proteins before (t_0) and 2 min after pH treatment (t_2) are presented on the left of each image panel (A) to (F). Modifications of cytoplasmic pH were controlled using the ratiometric SNARF-5F dye, and rainbow pH images are presented at the right of each image panel (A') to (F')). Note the prominent diffuse cytoplasmic localization of GFP-PLIM2c after increase of cytoplasmic pH (F) and (F')).

(G) Quantitative analyses of the above experiments. The FCFAC was quantified for each GFP fusion protein before ($FCFAC_{t_0}$) and after pH treatment ($FCFAC_{t_2}$), and ratios were calculated ($R_{FCFAC} = FCFAC_{t_2} / FCFAC_{t_0}$). Gray and black bars indicate the R_{FCFAC} values calculated after a decrease and increase of cytoplasmic pH respectively ($n \geq 10$; errors bars indicate SD). White bars indicate the R_{FCFAC} values calculated for control experiments in which cells have not been submitted to any pH treatment ($n \geq 10$; errors bars indicate SD). Note the low R_{FCFAC} value (0.29 ± 0.15) calculated for GFP-PLIM2c upon increase of cytoplasmic pH indicating that GFP-PLIM2c has massively detached from the actin cytoskeleton. Bars = 10 μ m.

et al., 2006; Lovy-Wheeler et al., 2006). However, pH-specific monitoring of PLIM actin regulatory activities in the context of live cells requires direct demonstration. In that attempt, we artificially modulated the cytoplasmic pH of *Arabidopsis* cells and analyzed the resulting effect of such manipulations on the ability of GFP-WLIM1 and GFP-PLIM2c fusion proteins to interact with the actin cytoskeleton.

Briefly, cell culture lines were produced from transgenic *Arabidopsis* plants expressing GFP-WLIM1, GFP-PLIM2c, and the actin cytoskeleton marker GFP-ABD2-GFP (control). Prior to pH treatment, cells were immobilized on polylysine-coated cover slips and incubated in standard culture medium supplemented with the ratiometric pH-sensitive dye SNARF-5F. Both concentration and incubation time of the dye were optimized for *Arabidopsis* cells to 5 μ M and 30 min, respectively. The pH dye most frequently diffused in a relatively homogenous manner into the cytoplasm and the nucleus (Figures 7A to 7F). The average

cytoplasmic pH was estimated to be 7.06 ± 0.06 ($n = 15$). Occasionally, the dye also penetrated the central vacuole. As expected, the vacuole was found to be the most acidic cellular compartment, with pH values ≤ 6.0 (see Supplemental Figure 7 online). To decrease or increase the cytoplasmic pH, cells were incubated in buffers containing the cell-permeant weak acid sodium propionate (pH adjusted to 6.2) or the cell-permeant weak base ammonium chloride (pH adjusted to 7.4; Parton et al., 1997). Confocal acquisitions of the pH-sensitive dye and of the GFP-fused proteins were collected just before and 2 min after the application of pH buffers. It should be noted that, after longer incubation times in pH buffers, the evolution of pH frequently reversed, although the recovery was much slower than the initial shift (see Supplemental Figure 8 online). Figure 7 presents typical results obtained with the three cell lines of interest. Successful modifications of pH were confirmed by pseudocolored ratio images, and the cytoplasmic pH was found to reach values close

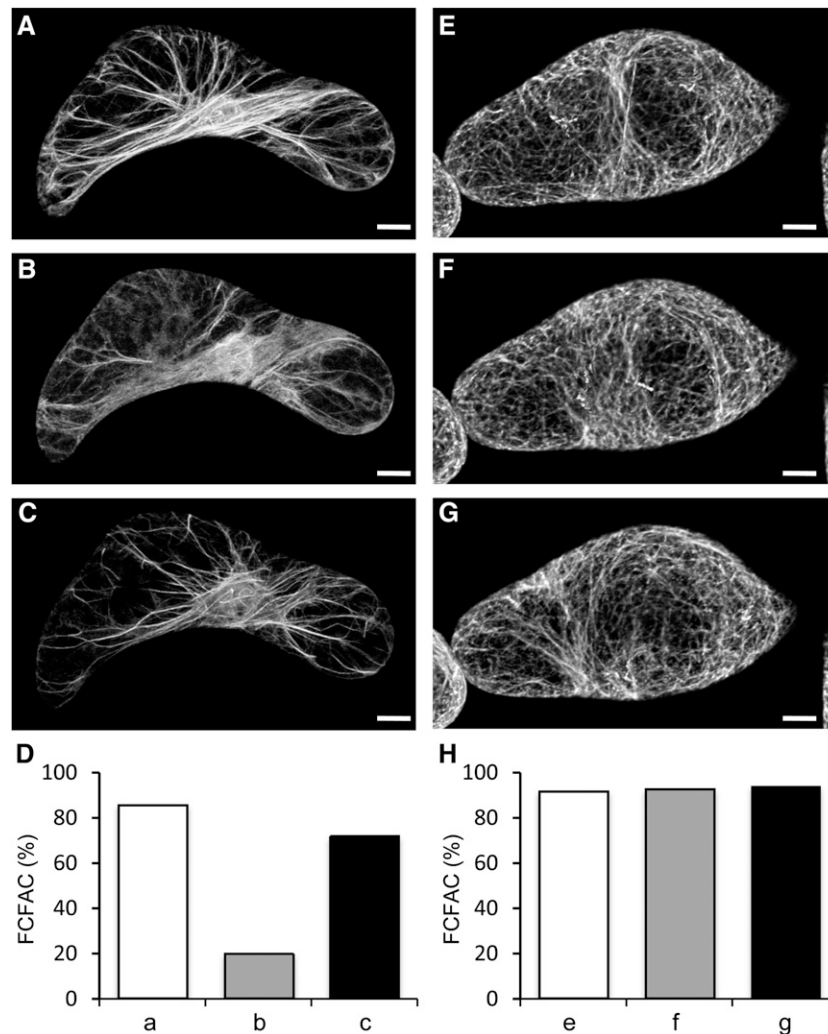


Figure 8. Specific Dissociation and Reassociation of GFP-PLIM2c with the Actin Cytoskeleton Induced by Successive Increase and Decrease of Cytoplasmic pH.

(A) to (C) Subcellular localization of GFP-PLIM2c in a transgenic *Arabidopsis* cell before pH treatment (A), after 2 min of incubation in the alkalinizing buffer (B), and after 2 min of subsequent incubation in the acidifying buffer (C).

(D) Quantitative analysis of the FCFAC in (A) (white bar), (B) (gray bar), and (C) (black bar).

(E) to (H) Corresponding control experiment conducted with the GFP-ABD2-GFP-expressing cell line. Note that GFP-ABD2-GFP is predominantly associated with the actin cytoskeleton before pH treatment (E) and (H), white bar), after 2 min of incubation in the alkalinizing buffer (F) and (H), gray bar), and after 2 min of subsequent incubation in the acidifying buffer (G) and (H), black bar). Bars = 10 μ m.

to those of pH buffers (i.e., 6.2 ± 0.1 or 7.4 ± 0.1). The effect of pH modifications on the ability of each GFP fusion protein to interact with the actin cytoskeleton was carefully analyzed by quantifying the FCFAC and by comparing this value before and after pH treatment ($R_{\text{FCFAC}} = \text{FCFAC}_{t2} / \text{FCFAC}_{t0}$). Lowering the pH had no significant effects on the actin binding activity of GFP-WLIM1, GFP-PLIM2c, and GFP-ABD2-GFP, as indicated by direct comparison of confocal images (Figures 7A to 7C) and R_{FCFAC} values close to 1 (Figure 7G). By contrast, pH increase dramatically weakened the binding of GFP-PLIM2c to the cytoskeleton, as shown by prominent diffuse fluorescent signal (Figure 7F). Massive release of GFP-PLIM2c from the actin

network upon pH elevation is supported by a calculated R_{FCFAC} value of 0.29 ± 0.15 , indicating that $\sim 70\%$ of the fluorescence initially associated with the cytoskeleton has been displaced toward the cytoplasmic diffuse pool. Contrary to GFP-PLIM2c, GFP-ABD2-GFP and GFP-WLIM1 remained largely associated with the actin cytoskeleton upon cytoplasmic pH elevation (Figures 7D and 7E). However, quantitative analyses revealed a slight modification in the GFP-WLIM1 subcellular distribution (Figure 7G). Indeed, we calculated a R_{FCFAC} value of 0.82 ± 0.075 , indicating an 18% decrease of the cytoskeleton-bound GFP-WLIM1 population upon pH elevation. By contrast, the subcellular distribution of GFP-ABD2-GFP was unaffected, as

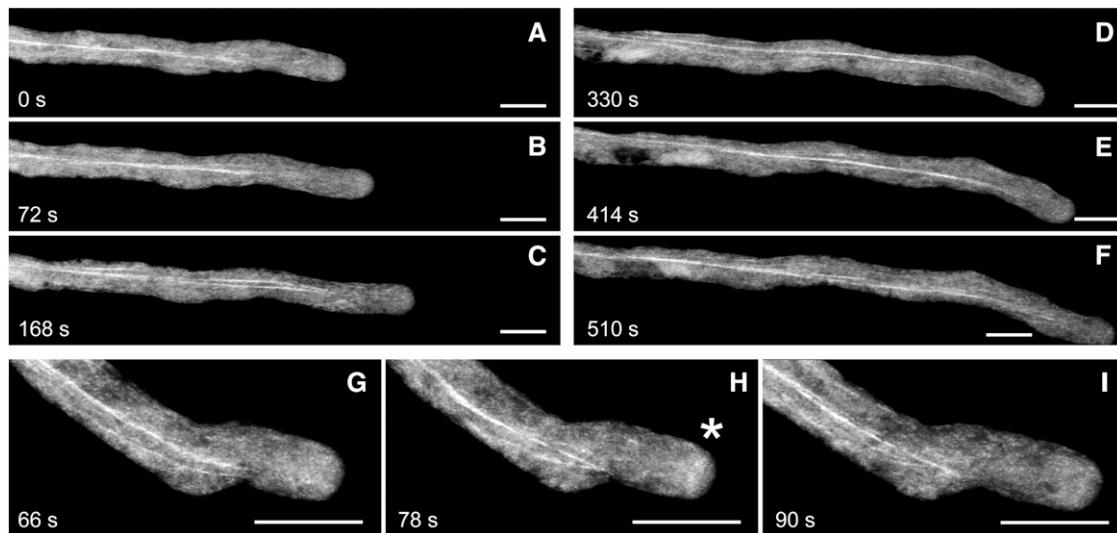


Figure 9. Localization of GFP-PLIM2c in Growing Pollen Tubes.

(A) to (F) Selected confocal stack images in a time series of a GFP-PLIM2c-expressing pollen tube.

A movie for this time series (see Supplemental Movie 1 online) shows that the PLIM2c-decorated actin bundles are dynamic.

(G) to (I) Selected confocal stack images in a time series of a GFP-PLIM2c-expressing pollen tube showing the decoration of an actin fringe-like structure in the subapical region (indicated by an asterisk). A movie for this time series (see Supplemental Movie 2 online) shows the morphological changes of this structure during growth. Bars = 10 μM .

indicated by $R_{\text{FCFAC}} = 0.98 \pm 0.029$. However, considering the relatively weak effect of high pH on WLIM1 subcellular localization, its biological significance remains uncertain. Importantly, rhodamine-phalloidin colabeling experiments confirmed the persistence of a filamentous actin cytoskeleton after increase of cytoplasmic pH in GFP-PLIM2-expressing cells (see Supplemental Figure 9 online). The reversibility of the process was assessed by successive treatments of cells with the alkalinizing and acidifying buffers. As shown in Figures 8A to 8D, GFP-PLIM2c efficiently dissociated and reassociated with the cytoskeleton, indicating that its actin binding ability was not irreversibly damaged by elevated pH conditions. A control experiment conducted with GFP-ABD2-GFP-expressing cells confirmed that the predominant cytoskeletal localization of GFP-ABD2-GFP is not significantly affected during similar pH treatment (Figures 8E to 8H).

GFP-PLIM2c Predominantly Associates with Long and Dynamic Actin Bundles in the Shank of Growing Pollen Tubes

To examine the cellular distribution of PLIM2c in live growing pollen tubes of *Arabidopsis*, we produced transgenic plants expressing a GFP-PLIM2c fusion protein under the control of the PLIM2c promoter. Analyses performed on heterozygous plants revealed that transgenic and wild-type nonfluorescent pollen grains germinate and elongate with very similar rates (i.e., $3.56 \pm 0.65 \mu\text{m}\cdot\text{s}^{-1}$ and $3.41 \pm 0.76 \mu\text{m}\cdot\text{s}^{-1}$, respectively; $n \geq 10$), indicating that the recombinant protein does not significantly disturb pollen tube physiology. Figure 9A shows that GFP-PLIM2c interacted with a population of long actin bundles

running along the pollen tube shank. Time-lapse imaging revealed that these bundles are highly dynamic and do not penetrate subapical and apical regions (see Supplemental Movie 1 online). Interestingly, GFP-PLIM2c occasionally decorates a structure in the subapical region resembling the cortical actin fringe, which has been described by several studies (e.g., Kost et al., 1998; Sheahan et al., 2004; Lovy-Wheeler et al., 2005; Cheung et al., 2008; Vidali et al., 2009; Figure 9B; see Supplemental Movie 2 online).

DISCUSSION

Actin bundles are key structural components in eukaryotes (Bartles, 2000; Thomas et al., 2009). In plant cells, they are required to stabilize the strands that cross the vacuole to connect distant cytoplasmic regions (Shimmen et al., 1995; Tominaga et al., 2000). In addition, actin bundles represent the main long-distance tracks for (myosin-dependent) vesicle and organelle transport and are therefore particularly important for cytoplasmic streaming and during tip growth processes, such as pollen tube and root hair growth (Tominaga et al., 2000; Vidali and Hepler, 2001). Four families of ABPs are commonly assumed to be involved in the formation and/or the maintenance of actin bundles in plants: the villin (Vidali et al., 1999; Tominaga et al., 2000; Huang et al., 2005), the fimbrin (McCurdy and Kim, 1998; Kovar et al., 2000; Klein et al., 2004), the formin (Cheung and Wu, 2004; Michelot et al., 2005, 2006; Ye et al., 2009), and the two LIM domain-containing protein (LIM) families (Thomas et al., 2006, 2007; Wang et al., 2008a). However, their exact contribution in actin bundling remains difficult to appreciate because only a few of their members have been closely studied so far.

Two plant LIMs, namely, tobacco WLIM1 and lily LIM1, were reported to bind to AFs and trigger the formation of actin bundles (Thomas et al., 2006, 2007; Wang et al., 2008a). Our data provide evidence that the six *Arabidopsis* LIMs display direct actin binding activity, indicating that most and possibly all plant LIMs function as ABPs. Interestingly, the mammalian counterparts of plant LIMs, namely, the CRPs, were initially suggested to interact only indirectly with AFs via ABPs, such as zyxin and α -actinin (Sadler et al., 1992; Louis et al., 1997; Pomies et al., 1997). However, recently, two out of the three mammalian CRPs have been reported to bind AFs autonomously (Grubinger and Gimona, 2004; Tran et al., 2005; Jang and Greenwood, 2009). This strongly suggests that direct actin binding activity is a common feature to all CRPs and CRP-like proteins, such as the plant LIMs.

Remarkably, the six *Arabidopsis* LIMs not only bind to AFs but also cross-link them into bundles, suggesting that actin bundling is a major actin regulatory function of LIMs rather than an accessory function displayed by only few family members. Fluorimetric data ruled out a cofilin-like severing activity, which would have been identified by faster actin depolymerization rates in the presence of LIMs. Additional evidence that actin bundling is a predominant function of LIMs is provided by the increase of actin bundle thickness and the concurrent decrease of the number of bundles observed in most LIM overexpressing cells (Figure 2; Thomas et al., 2006, 2008). Interestingly, such cytoskeletal rearrangements differ from those resulting from the overexpression of *Arabidopsis* FH1, an *Arabidopsis* formin that has been reported to bundle AFs in vitro (Michelot et al., 2005, 2006). Indeed, FH1 overexpression increases the number of actin bundles in pollen tubes (Cheung and Wu, 2004). Opposite effects on bundle population induced by the two classes of actin-bundling proteins may be explained by the fact that only FH1 displays actin-nucleating activity. Mechanistic studies have suggested that FH1 functions as a nonprocessive nucleating factor that detaches from the barbed end after nucleation and moves to the side of the growing filament to promote the assembly of a novel filament, thereby facilitating the formation of actin bundles (Michelot et al., 2006; Blanchoin and Staiger, 2008). Therefore, FH1, in addition to its bundling activity, promotes de novo formation of actin bundles, whereas LIMs only cross-link existing filaments, thereby reducing the number of individual filaments and small bundles. A recent loss-of-function study has provided evidence of the central role played by another formin, namely, AFH3, in the nucleation of longitudinal actin bundles in *Arabidopsis* pollen tubes (Ye et al., 2009). However, in vitro analyses failed to reveal autonomous cross-linking activity, suggesting that, in vivo, the bundling of AFH3-nucleated AFs requires the action of other ABPs (e.g., villins or LIMs). Noticeably, the supernumerary actin bundles induced by AFH3 overexpression were abnormally thin (Ye et al., 2009). This possibly results from insufficient levels of actin-bundling proteins to assemble bundles of normal thickness.

The expression pattern of a number of plant LIM genes has been previously examined to some extent (Eliasson et al., 2000; Mundel et al., 2000; Arnaud et al., 2007). Here, we show that, like actin and most ABP genes, including *ADFs* and *profilins* (McDowell et al., 1996; Hussey et al., 2002; Kandasamy et al., 2002; Ruzicka et al., 2007), *Arabidopsis* LIM genes can be

categorized into two major groups according to their expression pattern. Indeed, *WLIM1*, *WLIM2a*, and *WLIM2b* are widely expressed throughout sporophytic tissues but are not or only very weakly expressed in pollen. By contrast, *PLIM2a*, *PLIM2b*, and *PLIM2c* are predominantly and abundantly expressed in pollen. As already reported for cytoskeletal gene families (e.g., Ruzicka et al., 2007), the separation between vegetative and reproductive patterns is not always clear. Most noteworthy are the relatively high expression levels of *PLIM2b* observed in vasculature and roots. The expression of the various LIM gene family members considerably overlaps in plant tissues with at least two, usually three, members coexpressed at significant levels. On the one hand, this supports the high degree of functional redundancy suggested by the lack of clear phenotypes in single insertion mutants (M. Dieterle, unpublished data). On the other hand, the expression of multiple actin or ABP isoforms in the same cells has been proposed to be a key element of the extreme flexibility in dynamic behavior of the cytoskeleton (Meagher et al., 1999). Interestingly, the wide expression of *LIMs* in plant tissues contrasts with the more restricted expression patterns of mammalian CRPs. Indeed, CRPs are predominantly expressed in muscle tissues (Louis et al., 1997; Yet et al., 1998; Henderson et al., 1999) where they are assumed to participate in the organization of contractile fibers (Arber et al., 1997; Kim-Kaneyama et al., 2005; Tran et al., 2005; Sagave et al., 2008). Similarly, villins, another important class of actin-bundling proteins, exhibit wide expression patterns in plants, whereas mammalian villin expression is limited to microvilli of brush border cells, indicating a higher degree of functional specialization (Klahre et al., 2000). The high overall level of actin bundling in plant cells (Thomas et al., 2009) supports the idea that actin bundles and associated bundling proteins are involved in ubiquitous plant-specific processes (e.g., the formation and/or the maintenance of the transvacuolar cytoplasmic strand network) (Shimmen et al., 1995; Tominaga et al., 2000; Yokota et al., 2005).

This study shows a remarkable correlation between the expression pattern of *Arabidopsis* LIM genes and the pH responsiveness of the corresponding proteins. Indeed, the in vitro activities of the three PLIMs are virtually turned off by pH values above 6.8, whereas those of the three WLIMs remain optimal in all pH conditions tested. Consistent with these data, the pollen LIM1 protein from *Lilium*, which belongs to another phylogenetical subgroup than *Arabidopsis* PLIMs (Arnaud et al., 2007), has been shown to preferentially bind to AFs under low pH conditions (Wang et al., 2008a). Therefore, pH responsiveness appears to be a feature common to pollen LIMs. Importantly, in vivo pH-dependent regulation of pollen LIM activities is strongly supported by our live-cell investigations showing that an increase in cytoplasmic pH specifically disrupts the interaction between PLIM2c and the actin cytoskeleton. Interestingly, the pH threshold above which PLIM2c activities are inhibited is apparently higher in vivo than in vitro. Indeed, when fused to GFP, PLIM2c efficiently decorates the actin cytoskeleton in cells whose average cytoplasmic pH is estimated to be close to 7.0 (Figures 2 and 7), whereas it is already deactivated at pH 6.8 in vitro biochemical assays. This suggests that other factors than pH might regulate LIM protein activities in the context of a live cell. In contrast with PLIM2c, WLIM1 remains predominantly associated

with AFs in both low and high intracellular pH conditions. However, a moderate reduction (~18%) in the WLIM1 cytoskeletal fraction was noticed after an increase in cytoplasmic pH. On the one hand, the biological significance of this response is questionable considering its relative weakness. On the other hand, an indirect regulation of WLIM1 activities by pH through de/activation of pH-dependent factors, such as pH-dependent kinases or phosphatases, cannot be ruled out. It is worth noting that several putative phosphorylation sites have been predicted in both WLIM and PLIM sequences (Arnaud et al., 2007) and that an animal CRP is phosphorylated in vivo (Huber et al., 2000). Possible regulation of plant LIM functions by phosphorylation is therefore an important issue to address in future work. PLIM2c is the only *Arabidopsis* LIM to obviously respond to Ca^{2+} in our in vitro assays, its activities being downregulated by high, physiologically relevant, $[\text{Ca}^{2+}]$. This corroborates the previous observation that optimal binding of lily LIM1 to F-actin requires both low pH and $[\text{Ca}^{2+}]$ conditions (Wang et al., 2008a). However, inactivation of PLIM2c and lily LIM1 by high cytoplasmic $[\text{Ca}^{2+}]$ remains to be experimentally confirmed in vivo. Interestingly, a PLIM2c variant from which the C-terminal domain has been deleted is fully active but is no longer able to respond to variations of pH and/or $[\text{Ca}^{2+}]$. Therefore, the C terminus appears as a candidate of choice for a regulatory domain of PLIMs. Whether this domain is involved in the regulation of WLIMs by other factors than pH and calcium has to be investigated.

Under favorable conditions (i.e., pH 6.2 and 100 nM Ca^{2+}), PLIMs exhibited a lower affinity for AFs than WLIMs, as indicated by 2 to 3 times higher apparent K_d values. Consistent with these data, maximal actin stabilization and sedimentation required significantly higher amounts of PLIM2c than WLIM1 (Figures 4A, 4G, and 4M). Moreover, the three members of each subfamily exhibit similar affinities for AFs as well as similar stabilizing and bundling efficiencies (e.g., Figure 3B). These observations suggest that WLIMs and PLIMs have coevolved with vegetative and reproductive actin isoforms, respectively, so that they exhibit dissimilar, subfamily-specific affinities for a given source of actin. The hypothesis regarding functional specificity and class-specific interaction of actin and ABP isoforms is strongly supported by elegant studies showing that the toxic effect of a misexpressed reproductive actin in vegetative tissues can be neutralized only by coexpression of a reproductive but not a vegetative profilin or ADF isoform (Kandasamy et al., 2007).

Many lines of evidence indicate that pH gradients are present in growing pollen tubes (Messerli and Robinson, 1998; Feijo et al., 2001; Certal et al., 2008). A so-called alkaline band has been characterized in the subapical region of lily pollen tubes (Feijo et al., 1999; Lovy-Wheeler et al., 2006). Within this band, the pH oscillates relative to the oscillatory growth and reaches values above 7.5. Strikingly, the alkaline band is located in the vicinity of the clear zone, a region where the actin cytoskeleton is subjected to profound remodeling. Indeed, in the subapical region, a dense collar of cortical AFs, also referred to as a cortical fringe, replaces the prominent longitudinal bundles that run along the pollen tube shank (e.g., Kost et al., 1998; Sheahan et al., 2004; Lovy-Wheeler et al., 2005; Cheung et al., 2008; Vidali et al., 2009). A number of studies have described the direct implication of this structure in pollen tube elongation and highlighted its high

rate of turnover (Gibbon et al., 1999; Fu et al., 2001; Vidali et al., 2001). Therefore, our data regarding the regulation of PLIM activities by pH are consistent with pH and actin cytoskeleton patterns in growing pollen tubes. The relatively low pH in the shank of the tube would activate PLIMs, which in turn would enhance the formation of long actin bundles. By contrast, the cyclic increases of pH in the alkaline band would downregulate PLIM activity, thereby maintaining the actin cytoskeleton in a highly dynamic state. However, it is not excluded that PLIMs transiently protect the cytoskeletal structures forming in the subapical region. Indeed, when the alkaline band reaches its lowest pH values, down to 6.8 (Lovy-Wheeler et al., 2006), PLIMs may reactivate and stabilize the short actin bundles of the cortical fringe until the next pH increase. Our observations conducted in growing pollen strongly support this view. Indeed, as fused to GFP, PLIM2c predominantly associates with long and dynamic actin bundles in the pollen tube shank. Careful analysis revealed that it also occasionally faintly labels a subapical structure resembling the actin cortical fringe. It should be noticed that the latter is expected to be rather difficult to image in live growing pollen, as it is highly dynamic.

Another ABP that has been proposed to play a central role in the regulation of the actin cytoskeleton dynamics in the subapical region of pollen tubes is the actin depolymerization factor (ADF). Remarkably, ADF concentrates in the same area as the cortical actin fringe (Lovy-Wheeler et al., 2006), and its F-actin severing activity is stimulated by alkaline pH conditions (Chen et al., 2002). Therefore, through their antagonist actin regulatory activities, ADF and PLIMs may orchestrate, in a pH-controlled manner and with other players, the successive cycles of disassembly and reassembly of the cortical fringe. Recently, the human CRP3 (or Muscle LIM Protein), a counterpart of plant LIMs, has been reported to directly interact with ADF/cofilin 2 in a pH-dependent manner (Papalouka et al., 2009). The possibility of a similar interaction between plant LIMs and ADFs as well as its potential effects on respective actin regulatory activities are important issues to be addressed by future work.

Calcium is another factor assumed to play crucial roles in the regulation of actin dynamics during pollen tube elongation. Noticeably, a tip-high oscillatory cytosolic Ca^{2+} gradient (Holdaway-Clarke et al., 1997; Messerli and Robinson, 1997; Pierson et al., 1996; Iwano et al., 2009) is assumed to locally increase the rate of AF turnover through the activation of Ca^{2+} -dependent ABPs, such as profilins and villins/gelsolins (Fan et al., 2004; Huang et al., 2004; Yokota et al., 2005; Xiang et al., 2007; Wang et al., 2008a). Therefore, the downregulation of PLIM2c activity by high $[\text{Ca}^{2+}]$ suggested by in vitro data might also contribute to maintain the cytoskeleton in a highly dynamic state in the apex of growing pollen tubes.

In conclusion, we propose that plant LIMs represent a highly specialized family of actin-bundling proteins that is present in virtually all plant cells. Interestingly, the two differentially expressed WLIM and PLIM subsets exhibit similar but not identical activities, suggesting that they have been optimized for vegetative and pollen tissues, respectively. We provide clear evidence for the in vivo regulation of PLIM subfamily members by pH as well as for the involvement of the C-terminal domain in this process. Importantly, our data are highly consistent with the

cellular distribution of a GFP-PLIM2c fusion protein in elongating pollen tubes and support a central role of PLIM proteins in the regulation of AF organization and dynamics during pollen tube growth. An aspect that has not been covered here is the nuclear function of plant LIMs. *Arabidopsis* LIMs accumulate in the nucleus, and this has been found not to be a consequence of passive diffusion (C. Thomas, unpublished data). Therefore, they represent attractive candidates as signal integrating factors connecting the nucleus and the actin cytoskeleton.

METHODS

Plant Material and Generation of Transgenic Lines

Transgenic *Arabidopsis thaliana* lines described in this study were produced in Landsberg *erecta* for *ProPLIM2c*-eGFP-PLIM2c and in Columbia-0 ecotype for all other lines. Plants were greenhouse cultivated and propagated on soil under 16-h-light/8-h-dark cycles. Transformations were performed with *Agrobacterium tumefaciens* strain GV3101 using the floral dip method (Clough, 2005). For selection, seeds were surface sterilized and plated onto half-strength Murashige and Skoog agar medium (MS255; Duchefa), pH 5.8, supplemented with 1% sucrose and with 50 mg/L of kanamycin or 15 mg/L of hygromycin. After a 3-d stratification at 4°C in the dark, seeds were incubated in a growth chamber at 22°C under 12-h-light/12-h-dark cycles. *Arabidopsis* cell suspension cultures were generated by transferring 10-d-old seedlings onto a callus-inducing medium (Murashige and Skoog agar medium, 200 mg/L KH_2PO_4 , 1 mg/L thiamine, 0.05 g/L myo-inositol, 20 g/L sucrose, and 1 mg/L 2,4-D, pH 5.7). Plates were wrapped in foil and kept in the dark at 22°C for 4 to 6 weeks. Calli were transferred to 40 mL liquid callus-inducing medium and maintained in the dark at 22°C with gentle agitation (100 rpm). Cells were propagated once a week by transferring 30 mL of 7-d-old suspension to 60 mL of fresh medium.

Arabidopsis LIM coding sequences (cds) were amplified from clones obtained from the ABRC (pUNI clones U18145 for At3g55770 and U50754 for At2g45800; Yamada et al., 2003) and Institut National de la Recherche Agronomique—Centre National de Ressources Génomiques Végétales (BX817923 for At1g01780 and BX825681 for At3g61230) or from a homemade seedling cDNA library (At1g10200 and At2g39900) and cloned in the pENTR vector. Binary vectors harboring *pro35S*-GFP-LIM fusions were constructed by transferring LIM cds from pENTR-LIM vectors by Gateway cloning (Invitrogen) into pMDC43 (Curtis and Grossniklaus, 2003).

For each *Arabidopsis* LIM gene, a promoter region consisting of a minimal sequence of 900 bp upstream the translational start site was amplified from *Arabidopsis* genomic DNA and subsequently cloned into the binary vector pGPTVII.Kan (Walter et al., 2004) to obtain *proLIM*-GUS. LIM coding sequences were cloned into pMDC43 (Curtis and Grossniklaus, 2003) to obtain *proCaMV35S*-GFP-LIM. A *ProPLIM2c*-eGFP-PLIM2c-TermNos cassette was assembled in pUC18 and transferred in the binary vector pGPTVII.bar (Walter et al., 2004). Detailed cloning procedures and primer sequences can be found in Supplemental Methods online and Table 1, respectively.

The F-actin reporter line, expressing the actin binding domain 2 of *Arabidopsis* fimbrin 1 fused to GFP at both C and N termini with GFP (GFP-ABD2-GFP; Wang et al., 2008b), was kindly provided by the group of Elison Blancaflor (The Samuel Roberts Noble Foundation).

GUS Histochemical Analyses

GUS histochemical analyses of each reporter gene were performed on at least nine independent transgenic lines. Staining for GUS activity was

performed for 12 to 15 h according to Marrocco et al. (2003) and on samples of various stages of development, including 7-d-old seedlings and 4-week-old seedlings and inflorescences. In the case of inflorescences, additional shorter staining periods (30 min to 1 h) were applied to confirm the high expression level of PLIM genes. After staining, samples were dehydrated by a series of ethanol washes and stored in 70% ethanol until observation at the binocular and light microscope (Leica DMI 6000B).

Confocal Microscopy and Imaging

Plants and cells expressing the GFP fusion proteins were imaged using a Zeiss LSM510 META confocal laser scanning microscope equipped with a $\times 40$ Plan-Neofluar oil immersion objective (numerical aperture 1.3). GFP was detected by exciting samples at a wavelength of 488 nm and using a 505- to 530-nm band-pass emission filter. For rhodamine-phalloidin labeling experiments, a 543-nm excitation wavelength and a 560- to 615-nm band-pass emission filter were used. Confocal images were deconvolved using Huygens Essential image processing software package (Scientific Volume Imaging) and are shown as stacks of neighboring sections reconstructed in ImageJ (National Institutes of Health).

SNARF-5F ratio imaging was performed in the META channel using a 543-nm excitation wavelength and a laser power of 7%. Emitted light was simultaneously collected with a dual channel of 560- to 600-nm (Ch1) and 625- to 665-nm (Ch2) bandwidth. To optimize signal detection, the photomultiplier gain was set over the range 60 to 70%. Ratio images were generated by dividing Ch2/Ch1 using the physiology module of LSM510 acquisition software. A 3×3 pixel median filter was applied to improve image quality, and final images were displayed with a rainbow look-up table.

Quantification of the FCFAC in GFP-LIM- and GFP-ABD2-GFP-expressing cells was performed using Metamorph software (Molecular Devices) by adjusting the image threshold to eliminate most of the diffuse cytoplasmic fluorescence. The threshold has to be adjusted for each cell (in the range of $\pm 10\%$) because the actin cytoskeleton organization and the associated intensity of fluorescence can slightly vary from one cell to another. The remaining integrated fluorescent signal was quantified and expressed as a percentage of the total cellular fluorescence (the nucleus was excluded). To avoid under- or overexposure problem during acquisition, the image intensity histogram was systematically checked, and acquisition settings were adjusted so that the fluorescent signal distributes within the 0 to 255 range (8-bit grayscale image). To estimate how artificial modifications of cytoplasmic pH influence GFP-LIM and GFP-ABD2-GFP interaction with the actin cytoskeleton, FCFAC values were measured before (t_0) and after 2 min (t_2) pH treatment, and FCFAC ratios ($R_{\text{FCFAC}} = \text{FCFAC}_{t_2} / \text{FCFAC}_{t_0}$) were calculated.

In the *in vivo* actin depolymerization experiments, *Arabidopsis* cells were mounted in an open observation chamber and imaged before and 1 h after addition of 100 μM cytoskeletal inhibitor latrunculin B (Sigma-Aldrich). Rhodamine-phalloidin labeling was performed in PME buffer (50 mM PIPES, 20 mM MgCl_2 , and 50 mM EGTA).

For confocal analyses conducted with pollen, pollen grains were placed on microscope slides by dipping freshly dehiscent anthers onto pollen germination medium solidified with 0.5% (w/v) low-melting agarose (Duchefa). Pollen germination medium was modified from Li et al. (1999) and consisted of 0.01% boric acid, 5 mM CaCl_2 , 5 mM $\text{Ca}(\text{NO}_3)_2$, 5 mM MgSO_4 , 5 mM KCl, and 18% (w/v) sucrose, pH 6.8 to 7.0. Pollen of T1 plants were used for pollen germination studies.

pH Treatments

Approximately 200 μL of *Arabidopsis* cell suspension culture was plated on a poly-L-lysine-coated cover slip. After removing the culture medium, cells were incubated in 1 mL of diluted ratiometric pH-sensitive dye SNARF-5F 5-(and-6)-carboxylic acid, acetoxymethyl ester, acetate (5

mM; Invitrogen) for 30 min in the dark at 22°C. Modification of the intracellular pH was achieved by incubating cells in 1 mL of callus-inducing medium supplemented with 30 mM ammonium chloride and 10 mM HEPES, pH 7.4 (alkalizing buffer), or with 30 mM sodium propionate and 10 mM MES, pH 6.2 (acidifying buffer). Confocal microscopy observations were performed just before pH buffer application and after 2, 4, and 6 min of treatment.

In situ calibration was performed as recommended by Feijo et al. (1999) using a combination of nigericin (5 μ M) and valinomycin (2 μ M) and in the presence of a high concentration of potassium ions. Reference pH buffers (half-strength Murashige and Skoog medium, 150 mM KCl, 30 mM NaCl, 25 mM HEPES, and 25 mM MES) were adjusted to a final pH of 6.2, 6.8, 7.0, 7.2, and 7.5. Cells were incubated 15 min in each pH buffer before imaging the SNARF-5F probe. A calibration curve was generated by calculating ratio values in cytoplasmic volumes of 50 μ m³ using MetaMorph Software (Molecular Devices). This curve was used to estimate the pH in nontreated cells and to control pH modifications induced by the alkalizing and acidifying buffers ($n \geq 10$).

Expression and Purification of Recombinant *Arabidopsis* LIMs

Arabidopsis LIM cds were subcloned into the bacterial expression vector pQE-60 (Qiagen). Due to relatively low levels of expression in bacteria, *Escherichia coli* codon-optimized sequences have been generated for the three PLIMs (DNA2.0). This did not result in any modification of the predicted amino acid sequences for PLIMs. The deletion of the C-terminal domain of WLIM1 and PLIM2c for production of WLIM1 Δ Ct and PLIM2c Δ Ct recombinant proteins has been achieved by PCR using the specific primers CTAT1F2 + CT101 (WLIM1 Δ Ct) and CT65 + CT80 (PLIM2c Δ Ct) (see Supplemental Table 1 online). His₆-tagged LIMs were expressed in M15[pREP4] bacteria and purified using a Ni-NTA resin following procedures described by the manufacturer (Qiagen). Purified proteins were concentrated in a centrifugal filter (Amicon), buffer exchanged (10 mM Tris-Cl, 50 mM NaCl, 1 mM DTT, 50 μ M ZnCl₂, and 2 M urea, pH 6.9) using a 7 K molecular weight cutoff dialysis cassette (Pierce), and stored on ice. Prior to an experiment, proteins were preclarified at 150 000g and checked for correct molecular weight by SDS-PAGE analysis, and their concentration was determined by Bradford assay (Bio-Rad) using BSA as standard.

High- and Low-Speed Cosedimentation Assays

High- and low-speed cosedimentation assays were used to assess the actin binding and -crosslinking activities of *Arabidopsis* LIMs, respectively. In both cases, rabbit muscle actin (Cytoskeleton; concentration indicated in figures) was copolymerized with various concentrations of individual LIMs for 1 h in 50 mM KCl, 2 mM MgCl₂, 1 mM ATP, and 0.5 mM DTT. Depending on the pH and [Ca²⁺] conditions tested, the reaction medium was buffered with either MES and PIPES, pH 6.2, or PIPES and Tris, pH 6.8 and 7.4, and was supplemented with either EGTA (low [Ca²⁺] conditions) or CaCl₂ (high [Ca²⁺] conditions). Supplemental Table 2 online indicates the concentration of MES, PIPES, Tris, EGTA, and CaCl₂ for each of the copolymerization conditions used.

In high-speed experiments, samples were centrifuged at 100,000g for 30 min to pellet AFs. The presence of LIM in the resulting supernatants (F-actin unbound fraction) and pellets (F-actin bound fraction) was analyzed by SDS-PAGE and Coomassie Brilliant Blue R (Sigma-Aldrich) staining.

In low-speed experiments, samples were centrifuged at 12,500g for 30 min in a microcentrifuge to pellet high-order F-actin structures. The presence of actin in the resulting supernatants (noncross-linked AFs) and pellets (cross-linked AFs) was analyzed by SDS-PAGE and Coomassie Brilliant Blue R (Sigma-Aldrich) staining. In some experiments, the respective amounts of actin in pellet and supernatant fractions were

quantified using ImageJ software. The presence of actin bundles in samples was checked by direct visualization using fluorescence microscopy. An aliquot of the copolymerized actin samples was labeled with 4 μ M rhodamine-phalloidin (Sigma-Aldrich). One micromolar of sample was diluted in one drop of cityfluor (Agar Scientific) and applied to a cover slip coated with poly-L-lysine (0.01%). Images were recorded via confocal microscope using a pinhole set to produce thick (~2 μ m) optical sections.

F-Actin Depolymerization Assay

Pyrene-labeled actin (4 μ M, 30% pyrene-labeled; Cytoskeleton) was copolymerized with individual *Arabidopsis* LIMs in the same conditions as in cosedimentation assays. Depolymerization was induced by diluting samples to a final actin concentration of 0.2 μ M. The decrease in pyrene fluorescence accompanying actin depolymerization was recorded over 200 s using a PTI QM-4 QuantaMaster fluorimeter.

Accession Numbers

Sequence data from this article can be found in the GenBank/EMBL or *Arabidopsis* Genome Initiative databases under the following accession numbers: WLIM1 NM_100894.3 (At1g10200), WLIM2a NM_129548.3 (At2g39900), WLIM2b NM_001035791.1 (At3g55770), PLIM2a NM_001036468.2 (At2g45800), PLIM2b NM_100061.3 (At1g01780), and PLIM2c NM_115987.3 (At3g61230).

Supplemental Data

The following materials are available in the online version of this article.

Supplemental Figure 1. RNA Gel Blot and Microarray Analyses of LIM Gene Expression in *Arabidopsis*.

Supplemental Figure 2. *Arabidopsis* LIMs Interact with the Actin Cytoskeleton in *Arabidopsis* Cells.

Supplemental Figure 3. Fraction of Cytoplasmic Fluorescence Associated with the Actin Cytoskeleton in GFP-ABD2-GFP-, GFP-WLIM1-, and GFP-PLIM2c-Expressing Root and Root Hair Cells.

Supplemental Figure 4. Examples of Data Used to Calculate the Apparent Equilibrium Dissociation Constant (K_d) Values Shown in Table 1.

Supplemental Figure 5. Inactivation by pH of the Stabilizing Activity of AF-Bound PLIM2c.

Supplemental Figure 6. Alignment of *Arabidopsis* LIM Protein Sequences.

Supplemental Figure 7. Imaging of SNARF-5F in a GFP-PLIM2c-Expressing *Arabidopsis* Cell.

Supplemental Figure 8. Cytoplasmic pH Recovery after Artificially Induced Acidification.

Supplemental Figure 9. Persistence of a Prominent Actin Cytoskeleton after Increase of Cytoplasmic pH in GFP-PLIM2c-Expressing Cells.

Supplemental Table 1. Oligonucleotides Used in the Study.

Supplemental Table 2. Concentrations of MES, PIPES, Tris, EGTA, and CaCl₂ Used in the Different *In Vitro* Assays.

Supplemental Movie 1. Time-Lapse Confocal Scanning Microscopy of a Growing *Arabidopsis* Pollen Tube Expressing GFP-PLIM2c under the Control of the PLIM2c Promoter.

Supplemental Movie 2. Time-Lapse Confocal Scanning Microscopy of a Growing Pollen Tube Showing the Interaction of GFP-PLIM2c with a Subapical Actin Fringe-Like Structure.

Supplemental Methods. Detailed Cloning Procedures.

Supplementary References.

ACKNOWLEDGMENTS

We thank Elison B. Blancaflor (The Samuel Roberts Noble Foundation, OK) who kindly provided *Arabidopsis* GFP-ABD2-GFP-expressing seeds. We also thank the gardeners of the Institut de Biologie Moléculaire des Plantes (Centre National de la Recherche Scientifique and University of Strasbourg, France) for excellent plant care and Esther Lechner and Katia Marocco for logistic support of plant-related experiments. This work was supported by the Ministry of Culture, Higher Education, and Research and by the National Research Fund (Luxembourg).

Received April 26, 2010; revised July 4, 2010; accepted August 19, 2010; published September 3, 2010.

REFERENCES

- Alves-Ferreira, M., Wellmer, F., Banhara, A., Kumar, V., Riechmann, J.L., and Meyerowitz, E.M. (2007). Global expression profiling applied to the analysis of *Arabidopsis* stamen development. *Plant Physiol.* **145**: 747–762.
- Arber, S., Hunter, J.J., Ross, J., Jr., Hongo, M., Sansig, G., Borg, J., Perriard, J.C., Chien, K.R., and Caroni, P. (1997). MLP-deficient mice exhibit a disruption of cardiac cytoarchitectural organization, dilated cardiomyopathy, and heart failure. *Cell* **88**: 393–403.
- Arnaud, D., Dejardin, A., Leple, J.C., Lesage-Descauses, M.C., and Pilate, G. (2007). Genome-wide analysis of LIM gene family in *Populus trichocarpa*, *Arabidopsis thaliana*, and *Oryza sativa*. *DNA Res.* **14**: 103–116.
- Bartles, J.R. (2000). Parallel actin bundles and their multiple actin-bundling proteins. *Curr. Opin. Cell Biol.* **12**: 72–78.
- Blanchain, L., and Staiger, C.J. (2008). Plant formins: Diverse isoforms and unique molecular mechanism. *Biochim. Biophys. Acta* **1803**: 201–206.
- Certal, A.C., Almeida, R.B., Carvalho, L.M., Wong, E., Moreno, N., Michard, E., Carneiro, J., Rodriguez-Leon, J., Wu, H.M., Cheung, A.Y., and Feijo, J.A. (2008). Exclusion of a proton ATPase from the apical membrane is associated with cell polarity and tip growth in *Nicotiana tabacum* pollen tubes. *Plant Cell* **20**: 614–634.
- Chen, C.Y., Wong, E.I., Vidali, L., Estavillo, A., Hepler, P.K., Wu, H.M., and Cheung, A.Y. (2002). The regulation of actin organization by actin-depolymerizing factor in elongating pollen tubes. *Plant Cell* **14**: 2175–2190.
- Cheung, A.Y., Duan, Q.H., Costa, S.S., de Graaf, B.H., Di Stilio, V.S., Feijo, J., and Wu, H.M. (2008). The dynamic pollen tube cytoskeleton: live cell studies using actin-binding and microtubule-binding reporter proteins. *Mol. Plant* **1**: 686–702.
- Cheung, A.Y., and Wu, H.M. (2004). Overexpression of an *Arabidopsis* formin stimulates supernumerary actin cable formation from pollen tube cell membrane. *Plant Cell* **16**: 257–269.
- Cheung, A.Y., and Wu, H.M. (2008). Structural and signaling networks for the polar cell growth machinery in pollen tubes. *Annu. Rev. Plant Biol.* **59**: 547–572.
- Clough, S.J. (2005). Floral dip: Agrobacterium-mediated germ line transformation. *Methods Mol. Biol.* **286**: 91–102.
- Curtis, M.D., and Grossniklaus, U. (2003). A Gateway cloning vector set for high-throughput functional analysis of genes in plants. *Plant Physiol.* **133**: 462–469.
- Drobak, B.K., Franklin-Tong, V.E., and Staiger, C.J. (2004). The role of the actin cytoskeleton in plant cell signaling. *New Phytol.* **163**: 13–30.
- Eliasson, A., Gass, N., Mundel, C., Baltz, R., Kräuter, R., Evrard, J.L., and Steinmetz, A. (2000). Molecular and expression analysis of a LIM protein gene family from flowering plants. *Mol. Gen. Genet.* **264**: 257–267.
- Fan, X., Hou, J., Chen, X., Chaudhry, F., Staiger, C.J., and Ren, H. (2004). Identification and characterization of a Ca²⁺-dependent actin filament-severing protein from lily pollen. *Plant Physiol.* **136**: 3979–3989.
- Feijo, J.A., Sainhas, J., Hackett, G.R., Kunkel, J.G., and Hepler, P.K. (1999). Growing pollen tubes possess a constitutive alkaline band in the clear zone and a growth-dependent acidic tip. *J. Cell Biol.* **144**: 483–496.
- Feijo, J.A., Sainhas, J., Holdaway-Clarke, T., Cordeiro, M.S., Kunkel, J.G., and Hepler, P.K. (2001). Cellular oscillations and the regulation of growth: the pollen tube paradigm. *Bioessays* **23**: 86–94.
- Fu, Y., Wu, G., and Yang, Z. (2001). Rop GTPase-dependent dynamics of tip-localized F-actin controls tip growth in pollen tubes. *J. Cell Biol.* **152**: 1019–1032.
- Gibbon, B.C., Kovar, D.R., and Staiger, C.J. (1999). Latrunculin B has different effects on pollen germination and tube growth. *Plant Cell* **11**: 2349–2363.
- Grubinger, M., and Gimona, M. (2004). CRP2 is an autonomous actin-binding protein. *FEBS Lett.* **557**: 88–92.
- Grunt, M., Zarsky, V., and Cvrckova, F. (2008). Roots of angiosperm formins: the evolutionary history of plant FH2 domain-containing proteins. *BMC Evol. Biol.* **8**: 115.
- Henderson, J.R., Macalma, T., Brown, D., Richardson, J.A., Olson, E.N., and Beckerle, M.C. (1999). The LIM protein, CRP1, is a smooth muscle marker. *Dev. Dyn.* **214**: 229–238.
- Hepler, P.K., Lovy-Wheeler, A., McKenna, S.T., and Kunkel, J.G. (2006). Ions and pollen tube growth. *Plant Cell Monogr.* **3**: 47–69.
- Hepler, P.K., Vidali, L., and Cheung, A.Y. (2001). Polarized cell growth in higher plants. *Annu. Rev. Cell Dev. Biol.* **17**: 159–187.
- Holdaway-Clarke, T.L., Feijo, J.A., Hackett, G.R., Kunkel, J.G., and Hepler, P.K. (1997). Pollen tube growth and the intracellular cytosolic calcium gradient oscillate in phase while extracellular calcium influx is delayed. *Plant Cell* **9**: 1999–2010.
- Huang, S., Blanchain, L., Chaudhry, F., Franklin-Tong, V.E., and Staiger, C.J. (2004). A gelsolin-like protein from *Papaver rhoeas* pollen (PrABP80) stimulates calcium-regulated severing and depolymerization of actin filaments. *J. Biol. Chem.* **279**: 23364–23375.
- Huang, S., Robinson, R.C., Gao, L.Y., Matsumoto, T., Brunet, A., Blanchain, L., and Staiger, C.J. (2005). Arabidopsis VILLIN1 generates actin filament cables that are resistant to depolymerization. *Plant Cell* **17**: 486–501.
- Huber, A., Neuhuber, W.L., Klugbauer, N., Ruth, P., and Allescher, H.D. (2000). Cysteine-rich protein 2, a novel substrate for cGMP kinase I in enteric neurons and intestinal smooth muscle. *J. Biol. Chem.* **275**: 5504–5511.
- Hussey, P.J., Allwood, E.G., and Smertenko, A.P. (2002). Actin-binding proteins in the *Arabidopsis* genome database: Properties of functionally distinct plant actin-depolymerizing factors/cofilins. *Philos. Trans. R. Soc. Lond. B Biol. Sci.* **357**: 791–798.
- Iwano, M., Entani, T., Shiba, H., Kakita, M., Nagai, T., Mizuno, H., Miyawaki, A., Shoji, T., Kubo, K., Isogai, A., and Takayama, S. (2009). Fine-tuning of the cytoplasmic Ca²⁺ concentration is essential for pollen tube growth. *Plant Physiol.* **150**: 1322–1334.
- Jang, H.S., and Greenwood, J.A. (2009). Glycine-rich region regulates

- cysteine-rich protein 1 binding to actin cytoskeleton. *Biochem. Biophys. Res. Commun.* **380**: 484–488.
- Kandasamy, M.K., Burgos-Rivera, B., McKinney, E.C., Ruzicka, D.R., and Meagher, R.B.** (2007). Class-specific interaction of profilin and ADF isoforms with actin in the regulation of plant development. *Plant Cell* **19**: 3111–3126.
- Kandasamy, M.K., McKinney, E.C., and Meagher, R.B.** (2002). Functional nonequivalency of actin isoforms in *Arabidopsis*. *Mol. Biol. Cell* **13**: 251–261.
- Kim-Kaneyama, J.R., Suzuki, W., Ichikawa, K., Ohki, T., Kohno, Y., Sata, M., Nose, K., and Shibamura, M.** (2005). Uni-axial stretching regulates intracellular localization of Hic-5 expressed in smooth-muscle cells *in vivo*. *J. Cell Sci.* **118**: 937–949.
- Klahre, U., Friederich, E., Kost, B., Louvard, D., and Chua, N.H.** (2000). Villin-like actin-binding proteins are expressed ubiquitously in *Arabidopsis*. *Plant Physiol.* **122**: 35–48.
- Klein, M.G., Shi, W., Ramagopal, U., Tseng, Y., Wirtz, D., Kovar, D.R., Staiger, C.J., and Almo, S.C.** (2004). Structure of the actin crosslinking core of fimbrin. *Structure* **12**: 999–1013.
- Kost, B., Spielhofer, P., and Chua, N.H.** (1998). A GFP-mouse talin fusion protein labels plant actin filaments *in vivo* and visualizes the actin cytoskeleton in growing pollen tubes. *Plant J.* **16**: 393–401.
- Kovar, D.R., Staiger, C.J., Weaver, E.A., and McCurdy, D.W.** (2000). AtFim1 is an actin filament crosslinking protein from *Arabidopsis thaliana*. *Plant J.* **24**: 625–636.
- Li, H., Lin, Y., Heath, R.M., Zhu, M.X., and Yang, Z.** (1999). Control of pollen tube tip growth by a Rop GTPase-dependent pathway that leads to tip-localized calcium influx. *Plant Cell* **11**: 1731–1742.
- Louis, H.A., Pino, J.D., Schmeichel, K.L., Pomies, P., and Beckerle, M.C.** (1997). Comparison of three members of the cysteine-rich protein family reveals functional conservation and divergent patterns of gene expression. *J. Biol. Chem.* **272**: 27484–27491.
- Lovy-Wheeler, A., Kunkel, J.G., Allwood, E.G., Hussey, P.J., and Hepler, P.K.** (2006). Oscillatory increases in alkalinity anticipate growth and may regulate actin dynamics in pollen tubes of lily. *Plant Cell* **18**: 2182–2193.
- Lovy-Wheeler, A., Wilsen, K.L., Baskin, T.I., and Hepler, P.K.** (2005). Enhanced fixation reveals the apical cortical fringe of actin filaments as a consistent feature of the pollen tube. *Planta* **221**: 95–104.
- Marrocco, K., Lecureuil, A., Nicolas, P., and Guerche, P.** (2003). The *Arabidopsis* SKP1-like genes present a spectrum of expression profiles. *Plant Mol. Biol.* **52**: 715–727.
- McCurdy, D.W., and Kim, M.** (1998). Molecular cloning of a novel fimbrin-like cDNA from *Arabidopsis thaliana*. *Plant Mol. Biol.* **36**: 23–31.
- McDowell, J.M., Huang, S., McKinney, E.C., An, Y.Q., and Meagher, R.B.** (1996). Structure and evolution of the actin gene family in *Arabidopsis thaliana*. *Genetics* **142**: 587–602.
- Meagher, R.B., McKinney, E.C., and Kandasamy, M.K.** (1999). Isovariant dynamics expand and buffer the responses of complex systems: The diverse plant actin gene family. *Plant Cell* **11**: 995–1006.
- Messerli, M., and Robinson, K.R.** (1997). Tip localized Ca^{2+} pulses are coincident with peak pulsatile growth rates in pollen tubes of *Lilium longiflorum*. *J. Cell Sci.* **110**: 1269–1278.
- Messerli, M., and Robinson, K.R.** (1998). Cytoplasmic acidification and current influx follow growth pulses of *Lilium longiflorum* pollen tubes. *Plant J.* **16**: 87–91.
- Michelot, A., Derivery, E., Paterski-Boujema, R., Guerin, C., Huang, S., Parcy, F., Staiger, C.J., and Blanchoin, L.** (2006). A novel mechanism for the formation of actin-filament bundles by a non-processive formin. *Curr. Biol.* **16**: 1924–1930.
- Michelot, A., Guerin, C., Huang, S., Ingouff, M., Richard, S., Rodiuc, N., Staiger, C.J., and Blanchoin, L.** (2005). The formin homology 1 domain modulates the actin nucleation and bundling activity of *Arabidopsis* FORMIN1. *Plant Cell* **17**: 2296–2313.
- Mundel, C., Baltz, R., Eliasson, A., Bronner, R., Grass, N., Krauter, R., Evrard, J.L., and Steinmetz, A.** (2000). A LIM-domain protein from sunflower is localized to the cytoplasm and/or nucleus in a wide variety of tissues and is associated with the phragmoplast in dividing cells. *Plant Mol. Biol.* **42**: 291–302.
- Papalouka, V., Arvanitis, D.A., Vafiadaki, E., Mavroidis, M., Papadodima, S.A., Spiliopoulou, C.A., Kremastinos, D.T., Kranias, E.G., and Sanoudou, D.** (2009). Muscle Lim Protein interacts with Cofilin 2 and regulates F-actin dynamics in cardiac and skeletal muscle. *Mol. Cell. Biol.* **29**: 6046–6058.
- Parton, R.M., Fischer, S., Malhó, R., Pappasoulitis, O., Jelitto, T.C., Leonard, T., and Read, N.D.** (1997). Pronounced cytoplasmic pH gradients are not required for tip growth in plant and fungal cells. *J. Cell Sci.* **110**: 1187–1198.
- Pierson, E.S., Miller, D.D., Callahan, D.A., van Aken, J., Hackett, G., and Hepler, P.K.** (1996). Tip-localized calcium entry fluctuates during pollen tube growth. *Dev. Biol.* **174**: 160–173.
- Pomies, P., Louis, H.A., and Beckerle, M.C.** (1997). CRP1, a LIM domain protein implicated in muscle differentiation, interacts with alpha-actinin. *J. Cell Biol.* **139**: 157–168.
- Ruzicka, D.R., Kandasamy, M.K., McKinney, E.C., Burgos-Rivera, B., and Meagher, R.B.** (2007). The ancient subclasses of *Arabidopsis* Actin Depolymerizing Factor genes exhibit novel and differential expression. *Plant J.* **52**: 460–472.
- Sadler, I., Crawford, A.W., Michelsen, J.W., and Beckerle, M.C.** (1992). Zyxin and cCRP: two interactive LIM domain proteins associated with the cytoskeleton. *J. Cell Biol.* **119**: 1573–1587.
- Sagave, J.F., Moser, M., Ehler, E., Weiskirchen, S., Stoll, D., Gunther, K., Buttner, R., and Weiskirchen, R.** (2008). Targeted disruption of the mouse *Csrp2* gene encoding the cysteine- and glycine-rich LIM domain protein CRP2 result in subtle alteration of cardiac ultrastructure. *BMC Dev. Biol.* **8**: 80.
- Schmit, A.C.** (2000). Actin during mitosis and cytokinesis. In *Actin: A Dynamic Framework for Multiple Plant Cell Functions*, C.J. Staiger, F. Baluska, D. Volkmann, and P.W. Barlow, eds (Dordrecht, The Netherlands: Kluwer Academic Publishers), pp. 437–456.
- Sheahan, M.B., Staiger, C.J., Rose, R.J., and McCurdy, D.W.** (2004). A green fluorescent protein fusion to actin-binding domain 2 of *Arabidopsis* fimbrin highlights new features of a dynamic actin cytoskeleton in live plant cells. *Plant Physiol.* **136**: 3968–3978.
- Shimmen, T.** (2007). The sliding theory of cytoplasmic streaming: Fifty years of progress. *J. Plant Res.* **120**: 31–43.
- Shimmen, T., Hamatani, M., Saito, S., Yokota, E., Mimura, T., Fusetani, N., and Karaki, H.** (1995). Roles of actin filaments in cytoplasmic streaming and organization of transvacuolar strands in root hair cells of *Hydrocharis*. *Protoplasma* **185**: 188–193.
- Staiger, C.J., Poulter, N.S., Henty, J.L., Franklin-Tong, V.E., and Blanchoin, L.** (2010). Regulation of actin dynamics by actin-binding proteins in pollen. *J. Exp. Bot.* **61**: 1969–1986.
- Thomas, C., Dieterle, M., Gatti, S., Hoffmann, C., Moreau, F., Papuga, J., and Steinmetz, A.** (2008). Actin bundling via LIM domains. *Plant Signal. Behav.* **3**: 320–321.
- Thomas, C., Hoffmann, C., Dieterle, M., Van Troys, M., Ampe, C., and Steinmetz, A.** (2006). Tobacco WLIM1 is a novel F-actin binding protein involved in actin cytoskeleton remodeling. *Plant Cell* **18**: 2194–2206.
- Thomas, C., Moreau, F., Dieterle, M., Hoffmann, C., Gatti, S., Hofmann, C., Van Troys, M., Ampe, C., and Steinmetz, A.** (2007). The LIM domains of WLIM1 define a new class of actin bundling modules. *J. Biol. Chem.* **282**: 33599–33608.
- Thomas, C., Tholl, S., Moes, D., Dieterle, M., Papuga, J., Moreau, F.,**

- and Steinmetz, A. (2009). Actin bundling in plants. *Cell Motil. Cytoskeleton* **66**: 940–957.
- Tominaga, M., Yokota, E., Vidali, L., Sonobe, S., Hepler, P.K., and Shimmen, T. (2000). The role of plant villin in the organization of the actin cytoskeleton, cytoplasmic streaming and the architecture of the transvacuolar strand in root hair cells of *Hydrocharis*. *Planta* **210**: 836–843.
- Tran, T.C., Singleton, C., Fraley, T.S., and Greenwood, J.A. (2005). Cysteine-rich protein 1 (CRP1) regulates actin filament bundling. *BMC Cell Biol.* **6**: 45.
- Vidali, L., and Hepler, P.K. (2001). Actin and pollen tube growth. *Protoplasma* **215**: 64–76.
- Vidali, L., McKenna, S.T., and Hepler, P.K. (2001). Actin polymerization is essential for pollen tube growth. *Mol. Biol. Cell* **12**: 2534–2545.
- Vidali, L., Rounds, C.M., Hepler, P.K., and Bezanilla, M. (2009). Lifeact-mEGFP reveals a dynamic apical F-actin network in tip growing plant cells. *PLoS ONE* **4**: e5744.
- Vidali, L., Yokota, E., Cheung, A.Y., Shimmen, T., and Hepler, P.K. (1999). The 135-kDa actin-bundling protein from *Lilium longiflorum* pollen is the plant homolog of villin. *Protoplasma* **209**: 283–291.
- Walter, M., Chaban, C., Schutze, K., Batistic, O., Weckermann, K., Nake, C., Blazevic, D., Grefen, C., Schumacher, K., Oecking, C., Harter, K., and Kudla, J. (2004). Visualization of protein interactions in living plant cells using bimolecular fluorescence complementation. *Plant J.* **40**: 428–438.
- Wang, H.J., Wan, A.R., and Jauh, G.Y. (2008a). An actin-binding protein, LILIM1, mediates calcium and hydrogen regulation of actin dynamics in pollen tubes. *Plant Physiol.* **147**: 1619–1636.
- Wang, Y.S., Yoo, C.M., and Blancaflor, E.B. (2008b). Improved imaging of actin filaments in transgenic *Arabidopsis* plants expressing a green fluorescent protein fusion to the C- and N-termini of the fimbrin actin-binding domain 2. *New Phytol.* **177**: 525–536.
- Weiskirchen, R., and Gunther, K. (2003). The CRP/MLP/TLP family of LIM domain proteins: acting by connecting. *Bioessays* **25**: 152–162.
- Winder, S.J., and Ayscough, K.R. (2005). Actin-binding proteins. *J. Cell Sci.* **118**: 651–654.
- Xiang, Y., Huang, X., Wang, T., Zhang, Y., Liu, Q., Hussey, P.J., and Ren, H. (2007). ACTIN BINDING PROTEIN 29 from *Lilium* pollen plays an important role in dynamic actin remodeling. *Plant Cell* **19**: 1930–1946.
- Yamada, K., et al. (2003). Empirical analysis of transcriptional activity in the *Arabidopsis* genome. *Science* **302**: 842–846.
- Ye, J., Zheng, Y., Yan, A., Chen, N., Wang, Z., Huang, S., and Yang, Z. (2009). *Arabidopsis* Formin3 directs the formation of actin cables and polarized growth in pollen tubes. *Plant Cell* **21**: 3868–3884.
- Yet, S.F., Folta, S.C., Jain, M.K., Hsieh, C.M., Maemura, K., Layne, M.D., Zhang, D., Marria, P.B., Yoshizumi, M., Chin, M.T., Perrella, M.A., and Lee, M.E. (1998). Molecular cloning, characterization, and promoter analysis of the mouse Crp2/SmLim gene. Preferential expression of its promoter in the vascular smooth muscle cells of transgenic mice. *J. Biol. Chem.* **273**: 10530–10537.
- Yokota, E., Tominaga, M., Mabuchi, I., Tsuji, Y., Staiger, C.J., Oiwa, K., and Shimmen, T. (2005). Plant villin, lily P-135-ABP, possesses G-actin binding activity and accelerates the polymerization and depolymerization of actin in a Ca²⁺-sensitive manner. *Plant Cell Physiol.* **46**: 1690–1703.

Article Addendum

Actin bundling via LIM domains

Clément Thomas,* Monika Dieterle, Sabrina Gatti, Céline Hoffmann, Flora Moreau, Jessica Papuga and André Steinmetz

Centre de Recherche Public-Santé; Val Fleuri 84; L-1526; Luxembourg

Key words: Actin-binding proteins, actin-bundling, cysteine-rich proteins, cytoskeleton, LIM domain.

The LIM domain is defined as a protein-protein interaction module involved in the regulation of diverse cellular processes including gene expression and cytoskeleton organization. We have recently shown that the tobacco WLIM1, a two LIM domain-containing protein, is able to bind to, stabilize and bundle actin filaments, suggesting that it participates to the regulation of actin cytoskeleton structure and dynamics. In the December issue of the *Journal of Biological Chemistry* we report a domain analysis that specifically ascribes the actin-related activities of WLIM1 to its two LIM domains. Results suggest that LIM domains function synergistically in the full-length protein to achieve optimal activities. Here we briefly summarize relevant data regarding the actin-related properties/functions of two LIM domain-containing proteins in plants and animals. In addition, we provide further evidence of cooperative effects between LIM domains by transiently expressing a chimeric multicopy WLIM1 protein in BY2 cells.

The LIM domain is a ≈ 55 amino acid peptide domain that was first identified in 1990 as a common cysteine-rich sequence found in the three homeodomain proteins LIN-11, Isl1 and MEC-3. It has since been found in a wide variety of eukaryotic proteins of diverse functions. Animals possess several families of LIM proteins, with members containing 1-5 LIM domains occasionally linked to other catalytic or protein-binding domains such as homeodomain, kinase and SH3 domains. In contrast, plants only possess two distinct sets of LIM proteins. One is plant-specific and has not been functionally characterized yet. The other one comprises proteins that exhibit the same overall structure as the animal cysteine rich proteins (CRPs), i.e., two very similar LIM domains separated by a ≈ 50 amino acid-long interLIM domain and a relatively short and variable C-terminal domain (Fig. 1A). The mouse CRP2 protein was the first CRP reported to interact directly with actin filaments (AF) and to stabilize the latter.¹ Identical observations were subsequently described for the chicken CRP1 and tobacco WLIM1 proteins.^{2,3} In addition, these two proteins were shown to arrange AF into cables both in vitro and in vivo and thus join the list of actin bundlers.

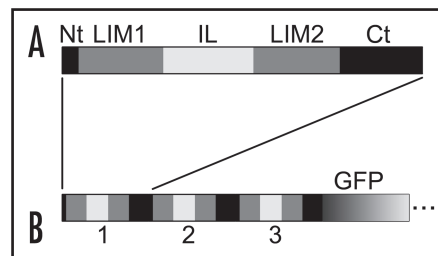


Figure 1. Domain maps for wild-type WLIM1 (A) and GFP-fused chimeric 3xWLIM1 (B). A. WLIM1 basically comprises a short N-terminal domain (Nt), two LIM domains (LIM1 and LIM2), an interLIM spacer (IL) and a C-terminal domain (Ct). B. 3xWLIM1 consists of three tandem WLIM1 copies. This chimeric protein has been fused in C-terminus to GFP and transiently expressed in tobacco BY2 cells.

To identify the peptide domains of WLIM1 responsible for its actin-related properties/activities, we generated domain-deleted and single domain variants and submitted them to a series of in vivo and in vitro assays.⁴ Localization experiments established that both LIM domains are required to efficiently target the actin cytoskeleton in tobacco BY2 cells. High-speed (200,000 g) cosedimentation data confirmed that the actin-binding activity of WLIM1 relies on its LIM domains. Indeed, the deletion of either the first or the second LIM domain respectively resulted in a 5-fold and 10-fold decrease of the protein affinity for AF. Importantly, each single LIM domain was found able to interact with AF in an autonomous manner, although with a reduced affinity compared to the wild-type WLIM1. Low-speed (12,500 g) cosedimentation data and electron microscopy observations revealed that the actin bundling activity of WLIM1 is also triggered by its LIM domains. Surprisingly each single LIM domain was able to bundle AF in an autonomous manner, suggesting that WLIM1 has two discrete actin-bundling sites. However, the bundles induced by the variants containing only one LIM domain, i.e., LIM domain-deleted mutants and single LIM domains, differed from those induced by the full-length WLIM1. They appeared more wavy and loosely packed and formed only at relatively high protein: actin ratios. Together these data suggest that LIM domains are autonomous actin-binding and -bundling modules that function in synergy in wild-type WLIM1 to achieve optimal activities.

To further assess the mechanism of cooperation between the LIM domains of plant CRP-related proteins, we generated a chimeric protein composed of three WLIM1 copies in tandem (3 x WLIM1, Fig. 1B), and transiently expressed it as a GFP-fusion in tobacco

*Correspondence to: Clément Thomas; Centre de Recherche Public-Santé; Val Fleuri 84; L-1526 Luxembourg; Email: clement.thomas@crp-sante.lu

Submitted: 11/14/07; Accepted: 11/19/07

Previously published online as a *Plant Signaling & Behavior* E-publication: www.landesbioscience.com/journals/psb/article/5310

Addendum to: Thomas C, Moreau F, Dieterle M, Hoffmann C, Gatti S, Hofmann C, Van Troys M, Ampe C, Steinmetz A. The LIM domains of WLIM1 define a new class of actin bundling modules. *J Biol Chem* 2007; 282:33599-608.

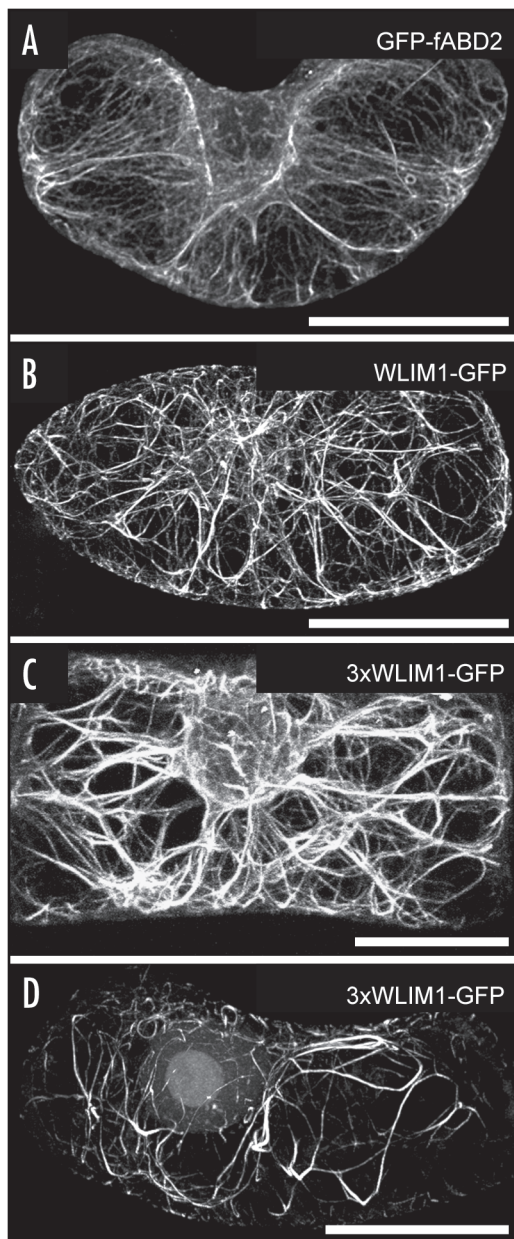


Figure 2. Typical actin cytoskeleton patterns in tobacco BY2 cells that have been transiently transformed, using a particle gun, with GFP-fABD2 (A), WLIM1-GFP (B), and 3xWLIM1-GFP (C and D). For each construct, more than 60 cells were analyzed by confocal microscopy. In the case of 3xWLIM1-GFP, two prevalent patterns have been observed (C and D). Bars = 20 μ m.

from the increase of cable stability and thickness induced by the 3xWLIM1-GFP protein, as these parameters are likely to determine, at least partially, the maximal length of actin bundles. Together the present observations support earlier data showing that LIM domains work in concert in LIM proteins to regulate actin bundling in plant cells. Strikingly, vertebrate and plant CRPs invariably contain two LIM domains. The lack, in these organisms, of CRP-related proteins combining more than two LIM domains may be explained by the fact that very thick cables, such as those induced by the artificial 3xWLIM1, may be too stable structures incompatible with the necessary high degree of actin cytoskeleton plasticity. As an exception, a muscle CRP-related protein with five LIM domains (Mlp84B) has been identified in *Drosophila*.⁶ However, rather than decorating actin filaments in an homogenous manner, this protein has been found to concentrate in a specialized region of the Z-discs where it stabilizes, in concert with D-titin, muscle sarcomeres.⁷

The relatively well conserved spacer length (\approx 50 amino acids) that separates the two LIM domains in vertebrate CRPs and related plant LIM proteins remains an intriguing feature the importance of which in actin cable organization remains to be established. Using electron microscopy we are currently evaluating the effects of the modification of the interLIM domain length on the structural properties of actin cables.

References

1. Grubinger M, Gimona M. CRP2 is an autonomous actin-binding protein. *FEBS Lett* 2004; 55:88-92.
2. Tran TC, Singleton C, Fraley TS, Greenwood JA. Cysteine-rich protein 1 (CRP1) regulates actin filament bundling. *BMC Cell Biol* 2005; 6:45.
3. Thomas C, Hoffmann C, Dieterle M, Van Troys M, Ampe C, Steinmetz A. Tobacco WLIM1 is a novel F-actin binding protein involved in actin cytoskeleton remodeling. *Plant Cell* 2006; 18:2194-206.
4. Thomas C, Moreau F, Dieterle M, Hoffmann C, Gatti S, Hofmann C, Van Troys M, Ampe C, Steinmetz A. The LIM Domains of WLIM1 define a new class of actin bundling modules. *J Biol Chem* 2007; 282:33599-608.
5. Sheahan MB, Staiger CJ, Rose RJ, McCurdy DW. A green fluorescent protein fusion to actin-binding domain 2 of *Arabidopsis* fimbrin highlights new features of a dynamic actin cytoskeleton in live plant cells. *Plant Physiol* 2004; 136:3968-78.
6. Stronach BE, Siegrist SE, Beckerle MC. Two muscle-specific LIM proteins in *Drosophila*. *J Cell Biol* 1996; 134:1179-95.
7. Clark KA, Bland JM, Beckerle MC. The *Drosophila* muscle LIM protein, Mlp84B, cooperates with D-titin to maintain muscle structural integrity. *J Cell Sci* 2007; 120:2066-77.

BY2 cells. We anticipated that such a six LIM domain-containing protein displays an even higher actin-bundling activity. (Fig. 2A) shows the typical actin cytoskeleton pattern in an expanding BY2 cell as visualized using the actin marker GFP-fABD2.⁵ As previously reported by Sheahan et al.,⁵ GFP-fABD2 decorated dense, transversely oriented, cortical networks as well as transvacuolar strands connecting the subcortical-perinuclear region to the cortex. Ectopic expression of WLIM1-GFP (BY2 cells normally do not express the WLIM1 gene) induced moderate but perceptible modifications of the actin cytoskeleton structure (Fig. 2B). Most AF are arranged in bundles thicker than those observed in GFP-fABD2 expressing cells and fine AF arrays are less frequently observed. As expected, this phenotype was significantly enhanced in cells transformed with the 3xWLIM1-GFP protein (Fig. 2C). Indeed, cells were almost devoided of fine AF arrays and exhibited very thick actin cables (Fig. 2C) that, at times (\approx 30 %), form atypical long looped structures (Fig. 2D). The appearance of such structures may result

Rôle des protéines LIM d'*Arabidopsis* dans la régulation de l'organisation et de la dynamique du cytosquelette d'actine.

Introduction

Le cytosquelette d'actine est un système complexe de filaments jouant un rôle central dans divers processus cellulaires tels que la division, la croissance, la contraction et la mobilité. Afin de remplir ses nombreuses fonctions, le cytosquelette d'actine requiert un système de régulation sophistiqué contrôlant son organisation et sa dynamique aux niveaux spatial et temporel. Les acteurs centraux de ce système sont les protéines de liaison à l'actine ou "actin-binding proteins" (ABPs). Les ABPs interagissent directement avec l'actine et induisent selon le cas la nucléation, la polymérisation, la dépolymérisation, la stabilisation, le découpage, la coiffe ou le pontage des filaments d'actine. Deux types majeurs de structures pontées sont présents dans les cellules: les réseaux orthogonaux de filaments et les câbles d'actine (faisceaux parallèles de filaments). Dans les cellules végétales, ces derniers stabilisent les travées cytoplasmiques traversant la vacuole et connectant les régions distantes. De plus, ils servent de supports aux transports intracellulaires (organites et vésicules) impliquant la myosine et sont impliqués dans le mouvement de cyclose (mouvement dirigé du cytoplasme et de ses éléments). Enfin, certaines observations suggèrent que les câbles d'actine sont également requis pour le mouvement et l'ancrage du noyau, l'optimisation du mouvement de la myosine et la génération de la force nécessaire à la formation de nouvelles travées cytoplasmiques. En dépit de l'importance biologique des câbles d'actine, les mécanismes moléculaires régulant leur formation restent mal connus. Notre laboratoire a récemment identifié une nouvelle famille d'ABP impliquées dans la formation des câbles d'actine dans les cellules végétales : les protéines à deux domaines LIM (LIM). En effet, des études fonctionnelles conduites sur la protéine WLIM1 de tabac ont montré que cette dernière possède la capacité de se lier directement aux filaments d'actine et d'induire la formation de câbles de manière autonome. Il est remarquable que les protéines LIM végétales forment de petites familles composées de plusieurs membres. On en dénombre six chez *Arabidopsis* qui peuvent se classer en deux sous-familles en fonction de leur expression : les WLIMs (WLIM1, WLIM2a et WLIM2b) qui sont exprimées dans la

plupart des tissus végétatifs, et les PLIMs (PLIM2a, PLIM2b et PLIM2c) qui sont exprimées quasi exclusivement dans le pollen. Il est donc légitime de se demander si ces protéines possèdent toutes une fonction similaire à celle identifiée pour la protéine WLIM1 de tabac ou si elles possèdent des spécificités d'activité et/ou de régulation.

Mon projet de thèse a consisté à identifier et comparer les activités des six membres de la famille de protéines LIM d'*Arabidopsis* et à étudier comment ces activités sont modulées par le pH et le Ca^{2+} , deux facteurs cellulaires fréquemment impliqués dans la régulation des ABPs.

Résultats

Pour chaque protéine LIM fusionnée à la Green Fluorescent Protein (GFP-LIM) surexprimée dans les plantes transgéniques, l'analyse a révélé une interaction avec un réseau filamenteux similaire au cytosquelette d'actine. La nature du réseau a pu être confirmée par co-localisation des protéines LIM avec des marqueurs spécifiques du cytosquelette d'actine et l'utilisation de drogues telles que la latrunculine B induisant la dépolymérisation des filaments d'actine. Par ailleurs, des investigations *in vitro* ont révélé l'habilité des six protéines LIM d'*Arabidopsis* à interagir de manière directe avec les filaments.

La fixation des protéines LIM aux filaments d'actine entraîne une stabilisation de ces derniers. Ainsi la résistance du cytosquelette d'actine de lignées cellulaires transgéniques sur-exprimant les protéines LIM à la latrunculine B est significativement plus élevée que celle de lignées témoin. Il est toutefois intéressant de noter que les protéines WLIM possèdent un pouvoir stabilisateur supérieur à celui des protéines PLIM.

L'analyse microscopique des filaments d'actine polymérisés en présence de protéines LIM recombinantes indique que les six protéines LIM d'*Arabidopsis* induisent la formation de câbles d'actine. Ce résultat corrobore l'épaississement des câbles d'actine observé dans les cellules des plantes transgéniques. En accord avec les résultats relatifs à la stabilisation, les protéines WLIM présentent un pouvoir de pontage significativement supérieur aux protéines PLIM (une plus faible quantité de protéine LIM est requise pour ponter une quantité donnée de filaments).

L'ensemble de ces données démontre que les six protéines LIM d'*Arabidopsis* fonctionnent comme de réelles ABPs induisant la stabilisation et le pontage des filaments d'actine. Les différences d'efficacité de stabilisation et de pontage observées entre les protéines des deux sous-familles suggèrent une adaptation de chaque sous-famille au type cellulaire dans lequel elle est exprimée (tissus végétatifs pour les WLIMs et pollen pour les PLIMs).

Mon attention s'est ensuite focalisée sur la régulation des activités des protéines d'*Arabidopsis* par le pH et le Ca^{2+} , deux facteurs fréquemment impliqués dans la régulation des ABPs. Les résultats indiquent qu'il existe des modes de régulation différents pour les membres des deux sous-familles. En conditions *in vitro*, seules les PLIMs présentent une sensibilité directe au pH (PLIM2a, b et c) et au Ca^{2+} (uniquement PLIM2c). En effet, leurs activités sont inhibées par une élévation de pH et $[\text{Ca}^{2+}]$ (PLIM2c). Afin de valider ces résultats dans un contexte cellulaire, j'ai mis au point un système permettant de faire varier le pH et $[\text{Ca}^{2+}]$ cytoplasmiques dans des suspensions cellulaires dérivées des plantes transgéniques d'*Arabidopsis* exprimant les protéines GFP-WLIM1 et GFP-PLIM2c. En accord avec les résultats *in vitro*, une diminution du pH cytoplasmique n'affecte pas significativement la capacité des protéines WLIM1 et PLIM2c à se lier au cytosquelette d'actine. A l'inverse, une augmentation de pH entraîne un détachement spécifique de la protéine PLIM2c alors que la protéine WLIM1 reste majoritairement associée avec les filaments d'actine. Enfin, une élévation de $[\text{Ca}^{2+}]$ cytoplasmique entraîne un détachement significatif des deux protéines LIM. Ce dernier résultat est en partie surprenant puisque les données *in vitro* ont indiqué une absence de sensibilité directe de la protéine WLIM1 au Ca^{2+} . La protéine WLIM1 serait donc régulée indirectement par le Ca^{2+} .

La régulation des protéines PLIM par le pH et le Ca^{2+} est parfaitement cohérente avec l'organisation du cytosquelette d'actine et les gradients de pH et $[\text{Ca}^{2+}]$ dans le tube pollinique en croissance. En effet, le manchon du tube, où le pH et la $[\text{Ca}^{2+}]$ sont relativement bas (protéines PLIM actives), contient de nombreux câbles d'actine impliqués dans l'acheminement des vésicules vers la partie apicale en croissance. La région subapicale, où le pH et la $[\text{Ca}^{2+}]$ oscillent (protéines PLIM successivement actives et inactives), contient une structure particulière composée de courts câbles corticaux qui subit des phases successives d'assemblage/désassemblage. Ceci suggère un rôle particulièrement important des protéines PLIM dans la

croissance du tube pollinique. Dans l'optique de vérifier nos hypothèses quant à l'importance de la régulation des activités des protéines PLIM par le pH et le Ca^{2+} , une étude comparative de la localisation des protéines WLIM1 (non régulée) et PLIM2c (régulée) dans le tube pollinique de *Lilium longiflorum* a été entreprise.

Afin de caractériser le domaine impliqué dans la sensibilité directe des protéines PLIMs au pH et Ca^{2+} , les séquences des six protéines LIM d'*Arabidopsis* ont été comparées. Les résultats indiquent que le domaine C-terminal présente le plus fort degré de variation en taille et en séquence entre les membres des sous-familles WLIMs et PLIMs. Une version de la protéine PLIM2c tronquée de son domaine C-terminal (PLIM2cDCt) a été produite et analysée par une série d'expériences *in vitro*. Les résultats montrent que la protéine PLIM2cDCt a perdu toute sensibilité au pH et Ca^{2+} indiquant que le domaine C-terminal joue un rôle central dans la régulation directe des activités des protéines PLIM par le pH et le Ca^{2+} . Dans l'optique de préciser le rôle du domaine C-terminal des protéines PLIM et de déterminer si ce domaine peut conférer une sensibilité directe au pH et Ca^{2+} à une protéine WLIM, une protéine chimère WLIM1CtPLIM2c (protéine WLIM1 dont le domaine C-terminal a été remplacé par celui de la protéine PLIM2c) a été produite. Des résultats préliminaires indiquent que la protéine WLIM1CtPLIM2c présente des activités et une sensibilité au pH et au Ca^{2+} similaires à celles de la protéine PLIM2c. Un modèle décrivant le mode de fonctionnement du domaine C-terminal est présenté.

Conclusion

L'ensemble des résultats me permet d'affirmer que la famille des protéines LIMs d'*Arabidopsis* représente une famille entière d'ABPs impliquée dans la stabilisation et le pontage en câbles des filaments d'actine. Compte tenu de son large profil d'expression (chaque cellule végétale exprime au moins deux, en général trois, protéines LIM), la famille des protéines LIM représente une famille majeure de protéine de pontage. Des lignées d'*Arabidopsis* dont les gènes *LIM* ont été inactivés sont en cours d'analyse afin de confirmer cette hypothèse.

Si les six protéines LIM d'*Arabidopsis* possèdent un panel d'activités identique, les membres de chaque sous-famille possèdent des efficacités et des modes de régulation distincts. Les activités des protéines PLIM sont régulées de façon

directe par le pH et le Ca^{2+} (dans le cas de PLIM2c) alors que les protéines WLIM ne présentent pas de sensibilité directe à ces facteurs. Une régulation indirecte des protéines WLIM par le Ca^{2+} est toutefois suggérée par les analyses *in vivo*.

J'ai pu mettre en évidence que le domaine C-terminal des protéines PLIM joue un rôle central dans leur régulation par le pH et le Ca^{2+} . Ceci ouvre de nombreuses perspectives pour caractériser le mécanisme moléculaire sous-jacent.

Résumé des principaux résultats

- 1) Les six protéines LIM d'*Arabidopsis* sont des "actin-binding proteins"
- 2) Les six protéines LIM d'*Arabidopsis* stabilisent les filaments d'actine et induisent la formation de câbles *in vitro* et *in vivo*
- 3) *In vitro*, seules les protéines PLIM présentent une sensibilité directe au pH et Ca^{2+} , leurs activités étant inhibées par une augmentation de pH et/ou de $[\text{Ca}^{2+}]$ (PLIM2c)
- 4) *In vivo*, une augmentation de pH entraîne l'inactivation de la protéine PLIM2c mais pas celle de la protéine WLIM1
- 5) *In vivo*, une augmentation de $[\text{Ca}^{2+}]$ entraîne l'inactivation des protéines PLIM2c et WLIM1, suggérant une régulation indirecte des activités de WLIM1 par le Ca^{2+}
- 6) Le domaine C-terminal est impliqué dans la régulation des activités des protéines PLIM par le pH et le Ca^{2+}